COARSE-GRAINED VADOSE ZONE IMPACTS ON MOUNTAIN BASIN GROUNDWATER RECHARGE

Page ii is for Water Research Foundation use only.

COARSE-GRAINED VADOSE ZONE IMPACTS ON MOUNTAIN BASIN GROUNDWATER RECHARGE

Prepared by:
William W. Woessner and James E. Swierc
Department of Geosciences
The University of Montana
32 Campus Drive,
Missoula, MT 59812

Sponsored by:
Water Research Foundation
6666 West Quincy Avenue,
Denver, CO 80235

Published by:
Water Research Foundation

DISCLAIMER

This study was funded by the Water Research Foundation (Foundation). The Foundation assumes no responsibility for the content of the research study reported in this publication or for the opinions or statements of fact expressed in the report. The mention of trade names for commercial products does not represent or imply the approval or endorsement of the Foundation. This report is presented solely for informational purposes.

ISBN xxx-x-xxxxx-xxx-x

Printed in the U.S.A.

CONTENTS

TABLES

LIST OF FIGURES

FOREWORD

The Water Research Foundation (Foundation) is a nonprofit corporation that is dedicated to the implementation of a research effort to help utilities respond to regulatory requirements and traditional high-priority concerns of the industry. The research agenda is developed through a process of consultation with subscribers and drinking water professionals. Under the umbrella of a Strategic Research Plan, the Research Advisory Council prioritizes the suggested projects based upon current and future needs, applicability, and past work; the recommendations are forwarded to the Board of Trustees for final selection. The Foundation also sponsors research projects through the unsolicited proposal process; the Collaborative Research, Research Applications, and Tailored Collaboration programs; and various joint research efforts with organizations such as the U.S. Environmental Protection Agency, the U.S. Bureau of Reclamation, and the Association of California Water Agencies.

This publication is a result of one of these sponsored studies, and it is hoped that its findings will be applied in communities throughout the world. The following report serves not only as a means of communicating the results of the water industry's centralized research program but also as a tool to enlist the further support of the nonmember utilities and individuals.

Projects are managed closely from their inception to the final report by the Foundation's staff and large cadre of volunteers who willingly contribute their time and expertise. The Foundation serves a planning and management function and awards contracts to other institutions such as water utilities, universities, and engineering firms. The funding for this research effort comes primarily from the Subscription Program, through which water utilities subscribe to the research program and make an annual payment proportionate to the volume of water they deliver and consultants and manufacturers subscribe based on their annual billings. The program offers a cost-effective and fair method for funding research in the public interest.

A broad spectrum of water supply issues is addressed by the Foundation's research agenda: resources, treatment and operations, distribution and storage, water quality and analysis, toxicology, economics, and management. The ultimate purpose of the coordinated effort is to assist water suppliers to provide the highest possible quality of water economically and reliably. The true benefits are realized when the results are implemented at the utility level. The Foundation's trustees are pleased to offer this publication as a contribution toward that end.

David E. Rager
Chair, Board of Trustees
Water Research Foundation

Robert C. Renner, P.E.
Executive Director
Water Research Foundation

ACKNOWLEDGMENTS

The important logistical and financial support of Mountain Water Company of Missoula Montana made this research effort possible. Their matching funds and in-kind contribution were greatly appreciated. The Water Research Foundation support and the guidance of the advisory committee: Ted Johnson, P.G., C.HG.; Bill Hutchison, Ph.D., P.E., P. G.; and John Ungvarsky, EPA Region 9 Water Division, were also highly valued. The contributions of Ms. Jennifer Warner of the Water Research Foundation who kept us organized and on track are recognized. Locally, a number of undergraduate and graduate students assisted the principal investigators with field and laboratory assistance; their help was indispensable. Geosciences staff member Donna Smith contributed to data collection in the field and oversaw much of the analytical work. The University of Montana provided needed facilities and support.

EXECUTIVE SUMMARY

OBJECTIVES

This work identified key processes controlling the rates of movement and water quality of infiltrating storm water as it percolates through thick sand and gravel, cobble and boulder dominated vadose zones found in intermountain basins of the Northern Rocky Mountains. The research program was designed to answer three primary research questions and one management question. These questions are:

1. What physical and hydrological factors in coarse grained intermountain basin vadose zones control the rates of storm water infiltration and percolation?
2. What geochemical processes impact the quality of infiltrating storm water passing through coarse-grained vadose zone materials?
3. What factors dominate the treatment/protection capacity of coarse-grained vadose zones?
4. What management approaches can preserve or extend the treatment/protection capacity of vadose zones receiving percolating storm water?

The approach used to meet the project goals and objectives involved instrumenting a vadose zone and an unconfined sole source aquifer receiving storm water injected by Class V Injection Wells (sumps) in Missoula, Montana. The key physical and geochemical processes that dominate the character and rates of percolating water were identified, and findings were extrapolated to other vadose zone settings using modeling.

BACKGROUND

Western intermountain valleys contain productive aquifer systems that support urban, agricultural and industrial activities. Shallow alluvial aquifers are often comprised of unconsolidated coarse-grained geologic deposits dominated by sand and gravel, cobbles and boulders. Storm water management in these settings is commonly handled by storm sewers or other collection and disposal mechanisms. When shallow soils in valleys are dominated by coarse-grained sediments and deep water tables, storm water disposal using street sumps and dry wells is viable. These Class V Injection Wells (sumps) deliver storm water either directly to the groundwater system or place the runoff into the vadose zone where it percolates to the local water table. Metropolitan areas such as Phoenix, Arizona; Modesto, California; Portland, Oregon; and Spokane, Washington, fully or partially utilize Class V Injection Wells as a means of storm water disposal. As regulations governing storm water disposal to streams and rivers become more restrictive, Class V Injection Well use for storm water management is likely to increase.

Unconfined aquifer systems recharged by storm water through sumps have been identified as highly susceptible to contamination from surface sources. Unfortunately the degree to which the vadose zone will positively or negatively impact recharge water quality is often unknown, as is the longevity of possible insitu vadose zone geochemical treatment processes. These data gaps exist in part because the gravel and cobble dominated sediments make

successful installation of traditional unsaturated zone monitoring instruments difficult. As a result, studies addressing the vadose zone soil aquifer treatment processes effecting ground water quality in these setting are limited.

This research was conducted in the Missoula, Montana intermountain valley setting where storm water is managed using over 7,000 Class V Injection Wells. Geological materials filling the upper part of the valley are dominated by high permeability course grained sediments derived from a fluvial depositional environment. The unconfined Missoula Aquifer is an EPA designated sole source aquifer.

APPROACH

Field and laboratory investigations focused on identifying processes controlling percolation rates and changes in recharge water quality during both "natural" storm water infiltration events and controlled tracer tests. Field methods were designed to characterize specific physical, hydrologic and geochemical processes occurring at five study sites during unsaturated flow events. The field study results were used to calibrate numerical models to test and refine conceptual models of observed processes.

Five study sites were selected for evaluation. Storm water volumes were determined using site mapping, precipitation gauges, pressure transducers installed in sumps, and infiltration temperature sensors. In addition, storm water quality was assessed from samples gathered via storm water event samplers and grab samples. Rotary sonic drilling was used to collect one or two continuous cores at each site; with three inch diameter monitoring wells constructed at four sites after completion of the coring. Standard descriptions of the vadose zone stratigraphy were completed. In addition supplemented with grain mineralogy and grain size distributions for representative core sample intervals were derived. Selected core intervals were placed in permeameter columns to determine hydrologic and physical properties including porosity, specific yield, field capacity, saturated hydraulic conductivity and bulk density. Site infiltration and percolation characteristics were generated using storm water ponding levels and sump dimensions. Artificial storm runoff and tracer tests were used along with natural event records to determine percolation rates.

Geochemical conditions within the vadose zone were examined by determining a number of sediment characteristics. X-ray diffraction was used to identify clay composition; other laboratory analysis established the concentrations of total organic carbon, ion exchange, sorption, and reaction capacities of grain surfaces. Groundwater was also sampled for water quality, while datalogging pressure transducers monitored water levels and temperatures. Physical and geochemical data sets were evaluated and used to calibrate conceptual and numerical vadose zone models. Study results suggested how water purveyors could use these findings to assess risks to groundwater systems receiving storm water recharge.

RESULTS/CONCLUSIONS

Storm water runoff contained the least dissolved constituents during the summer period (May through October), when 60% of total annual runoff occurred. Winter storm runoff (40% of the total annual storm water) resulted from both direct precipitation and thawing snow pack events. Water from winter storm runoff contained higher constituent concentrations and chemical components identified with winter street de-icers. Evaluations of the behavior of natural storm

water infiltrated at sump sites, and artificial runoff, and tracer experiments found percolation rates varied between a few feet per hour to over 9 ft/h. Percolation to the water table for some events was measured as less than 2 ft/h to 48 ft/h. Borehole geophysical tomography tracked wetting fronts through the vadose zone in the first 20 ft of transport, recording percolation rates of 6 to 7 ft/h.

Comparison of storm water runoff quality to that of percolating storm water found that, at one site, the vadose zone both reduced and enhanced different components of storm water runoff. Runoff dominated by low concentrations of constituents appears to have reacted with vadose zone sediment surfaces, increasing the dissolved constituent load in storm water percolating during the summer period. However, late winter to early spring storm water either already contained higher concentrations of sodium, magnesium and chloride or concentrations of these components increased during percolation.

Modeling of the physical and geochemical processes occurring during storm water percolation confirmed the rapid percolation rates observed in this geologic setting; the first arrival occurred after 1 h over a distance of 50 ft. It was also observed that the percolation and recharge rate to the water table decreases as the presence of lower hydraulic conductivity layers increases within the vadose zone stratigraphy. Conceptual geochemical models showed that the siliceous nature of the sediments, the low total organic carbon content, and the ion exchange capacity limited the ability of the vadose zone sediments to remove either winter or summer constituents found in storm runoff as the water percolated to the water table. Metal concentrations, however, were removed from infiltrating water and provided a mechanism by which de-icer sourced chloride was temporarily stored in the vadose zone. However, this chloride appears to be flushed from the vadose zone before the next winter groundwater sampling.

APPLICATIONS/RECOMMENDATIONS

Study results and conclusions are of importance to both local municipal water providers, and state and local governments as they strive to protect aquifers and manage storm water. Source water protection efforts require hydrogeological assessments and a characterization of barriers that may reduce the relative vulnerability of aquifers to contamination.

The results of this work suggest that storm water quality in an urban intermountain valley area (>60,000 population) generated during the summer period (May through October) is commonly characterized by low concentrations of major ions and minor constituents. In contrast, winter runoff (November through April) has significantly higher values of major and minor constituents; their composition reflects the composition of street de-icers. The percolation of storm water through a thick vadose zone dominated by sand, gravel, pebbles and boulders is rapid and has little measurable capacity to reduce major chemical components of infiltrating constituents.

Management strategies of potable unconfined aquifers receiving recharge through coarse grained vadose zones need to consider approaches that would limit the volumes and concentrations of storm water constituents that enter the aquifer. In addition, the nature of practical vadose zone barriers available to protect aquifer quality need to be assessed. It is recommended that this be accomplished using a range of approaches including:

1. Monitoring street de-icer use, including the variations in liquid deicer and salt compositions, locations and volumes of applications, and identification of which municipal wells are most likely to be impacted.
2. Evaluating the advantages and disadvantages of using multiple chambered storm drain systems to reduce the impact of storm water and spills on underlying groundwater systems.
3. Conducting further analyses of the spatial distribution of vadose zone properties, including mapping of vadose zone character, dominant geologic material, presence and nature of fine grained deposits, and overall treatment capacity.
4. Monitoring of sump stage, conductivity, and associated shallow groundwater stage; water quality monitoring at selected storm drain sites to further characterize timing and seasonal variations in water quality.

RESEARCH PARTNERS

This research was supported by the administration and staff of Mountain Water Company of Missoula, Montana and a number of undergraduate and graduate students of the Department of Geosciences of The University of Montana.

PARTICIPANTS

We recognize the support of the administration and technical staff of Mountain Water Company who provided direct funding, an in-kind commitment and technical staff assistance.

INTRODUCTION

In communities without integrated sanitary sewer and storm water management systems, storm water runoff is typically managed using surface water holding ponds, infiltration basins or injection systems. When soil conditions are favorable and water tables sufficiently deep, storm water management systems are frequently developed without networked drainage conduits to surface water. Storm water disposal in these systems is accomplished by allowing guttered storm water to directly infiltrate into the subsurface using rock filled sumps or cased injection wells. These disposal systems are typically located in parking lots, at street corners and in green spaces. In cities and developed areas these storm water disposal locations may number in the thousands. They provide a direct mechanism for storm water to recharge the underlying aquifer (EPA, 1999). This approach to storm water management is common in western cities and towns with low rainfall and permeable valley floor soils. The Federal EPA Underground Injection Control Program identifies these infiltration systems used for disposal of non-hazardous fluids in the subsurface as Class V Injection Wells (CVIW) (EPA, 1997). Source Water Protection assessment criteria require the identification of potential contaminant sources to each water supply source and aquifers (EPA, 1997). Aquifers receiving recharge from CVIW water have been identified as highly vulnerable to contamination from surface sources.

A number of studies addressing the water quality impact of storm water on groundwater have been completed across the United States (Pitt et al., 1996). These studies have generally focused on geochemical changes in storm water retention systems or the underlying groundwater chemistry with little detailed assessment of vadose zone geochemical processes. A few studies address the vadose zone processes directly. For example the fate of metals in storm water sedimentation basins was assessed by Wilde (1994). An analysis of the vadose zone mechanisms affecting the fate and transport of arsenic was reported by Lin and Puls (2003). Other studies evaluating managed aquifer recharge processes have focused on the geochemical interaction of reclaimed wastewater with vadose zone sediments (e.g. Johnson et al., 1999; Vanderzalm et al., 2004). Additional vadose zone geochemical studies have been focused on sediments reactions associated with releases of hazardous constituents at federal superfund sites, hazardous waste sites, mining areas, and other sites where toxic materials have been disposed of or released to the environment (e.g. Qafoku et al., 2004). Some of this work is directly applicable to understanding the fate of dissolved storm water constituents after infiltration.

Municipal water purveyors operating in aquifers recharged partially from injected storm water often do not have a clear understanding of the subsurface processes that control the water quality and percolation rates of infiltrating source water. It is often assumed that the vadose zone provides some level of water quality treatment and aquifer protection. As noted above, at some locations, however, groundwater was found to contain varying levels of contaminants linked to storm water runoff (Pitt et. al., 1996; EPA, 1986; 1999). Unfortunately the degree to which the vadose zone will positively impact recharge water quality is often unknown, as is the longevity of possible insitu vadose zone geochemical treatment processes.

This research will focus on determining the controlling factors influencing the rate of storm water flow through coarse grained vadose zones, and their influence on groundwater recharge quality. Geologic deposits dominated by sand and gravel, cobbles and boulders form productive aquifers and are common in the valley fill sequences of the intermontane basins of western North America (Kendy and Tresch, 1996). These settings often use CVIW to dispose of

storm water including the urban areas of Phoenix, Arizona; Modesto, California; Portland, Oregon, and Spokane, Washington (EPA, 1999; Wilson, 2003; Jenson and Eckart, 1989). Some localities in the mid west also use CVIW. These areas are dominated by highly conductive glacial outwash and fluvial sediment systems associated with buried valley aquifer systems (Gallagher and Price, 1966; Spieker, 1968).

Urbanization typically results in the development of large areas with impermeable surfaces, requiring management of storm water. Prior to urbanization, surface water runoff in rural landscapes was naturally controlled by soil properties and rainfall intensity; when precipitation rates exceed infiltration rates surface water runoff is instituted. In these systems, storm water either directly infiltrated at the site of precipitation impact, or collected in topographic depressions and entered the soil zone and groundwater system as depression focused recharge. However, when such sites are urbanized, the rainfall/runoff relationships and runoff chemistry change as flow over impermeable surfaces dominates landscapes. In these settings when this water enters Class V Injection Wells (CVIW or sumps), it bypasses the active soil zone and is injected into the native vadose zone material. The amount of runoff entering the CVIW is determined by the duration and intensity of a storm event and the catchment area and character of the land surface contributing to a CVIW site. Physical controls on the infiltration volume of injected water include sediment properties of the sump bottom, the nature and antecedent conditions of the vadose zone, and lastly, the thickness of the vadose zone sediments (Figure 1.1).

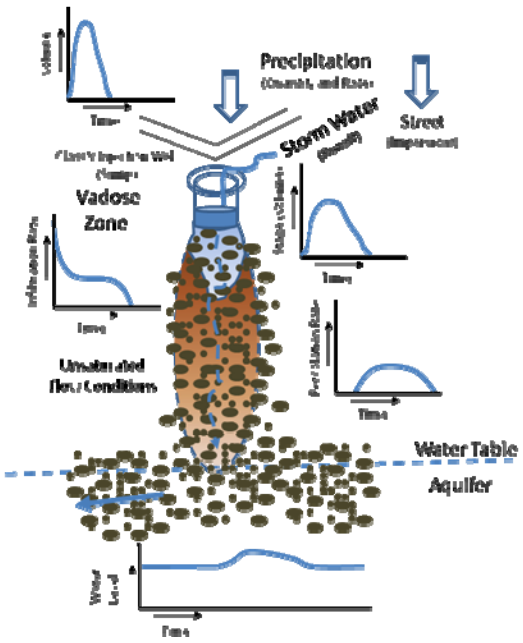

Figure 1.1 A conceptual model of the factors controlling the physical movement of water through the vadose zone from a Class Five Injection Well storm water runoff source. The stage in the sump is a function of the rate runoff water from a storm event enters the sump and the infiltration capacity of the bottom and immediately adjacent sediments. During an example storm event, water rapidly enters the CVIW (volume vs. time graph). Infiltration rates at the bottom of the CVIW (infiltration rate vs time) start out high as storm water first enters the CVIW then decreases to become stable as the water level in the sump stabilizes; it then decreases as the runoff ends. As water percolates through the vadose zone it will initially move under the influence of partial saturation. As time progresses the

vadose zone will either remain under unsaturated conditions or portions of the vadose zone will become fully saturated and higher percolation rates will prevail. Percolating water will initially enter the water table as diffuse flow. Depending on the hydraulic properties of the aquifer and groundwater flow system fluxes, the water table may rise, particularly when the percolation rates to the water table exceed the rate of groundwater transport away from the recharge point.

The water quality of the recharge water is controlled by source water chemistry, and reactions and attenuation processes that occur as the water moves through the percolation zone. The impact of recharge water on the overall water quality of the aquifer is a function of the water quality, volume, and flux rate of the percolating water associated with an individual storm event, and the degree of mixing with the receiving groundwater chemistry.

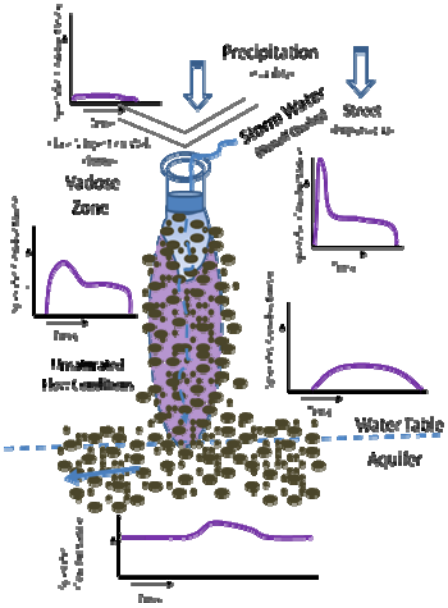

Figure 1.2 A conceptual model of the water quality changes (represented as specific conductance) in response to a single storm event assuming that the vadose zone provides processes that reduce constituents in a storm water source. Precipitation typically has a low specific conductance. When precipitation becomes storm water runoff it readily incorporates reactive elements from the land and pavement surfaces. Often the "first flush" has the highest concentrations of constituents. Once the water infiltrates into the vadose zone and interacts with the sediments under existing geochemical conditions, the percolating water will either become higher or lower in dissolved components (higher as shown here) as the water proceeds downward. Percolating water recharges the underlying aquifer, and depending on the volume and rate of recharge may influence the shallow groundwater chemistry.

MOVEMENT AND CONTROLS ON INFILTRATING STORM WATER

The unsaturated, or vadose zone, can be conceptualized as granular material where, depending on the pore size, a limited number of the pore spaces may be completely full of water. Simple infiltration/percolation models assume water enters the vadose zone as piston flow, with

percolating waters displacing pore waters (Green-Ampt 1911). The Richards equation, derived from Darcy's law (Richards 1931), provides a more complex and representative depiction of vadose zone flow:

$$C_w(\psi)\frac{\partial h}{\partial t} = \frac{\partial}{\partial x}\left[K_x(\psi)\frac{\partial h}{\partial x}\right] + \frac{\partial}{\partial y}\left[K_y(\psi)\frac{\partial h}{\partial y}\right] + \frac{\partial}{\partial z}\left[K_z(\psi)\frac{\partial h}{\partial z}\right] + q_s$$

Where: $C_w = \delta\theta_w/\delta\psi$; the slope of the soil characteristic curve of moisture content as a function of matric potential, ψ; $Kx\psi$, $Ky\psi$ and $Kz\psi$ represent the unsaturated hydraulic conductivity in the x, y and z directions; h is the head at a location in the unsaturated zone = position head plus the matrix potential; ψ is the matric potential equal to a negative value (soil suction); and q is a source or sink flux term.

Use of the Richards equations assumes that water is the fluid, the hydraulic conductivity is a function of moisture content, and that air is not entrapped in the system (Hillel 1998).

A critical component necessary to model unsaturated flow is the unsaturated hydraulic function, which is the relationship between water content, matrix potential and unsaturated hydraulic conductivity. As the unsaturated hydraulic conductivity increases with water content, the soil pore pressures or matric potential decrease. A number of studies have used laboratory experiments to develop empirical methods of estimating the unsaturated hydraulic function in soils based on the saturated hydraulic conductivity and moisture retention characteristics (e.g. van Genuchten 1980; Mualem 1976; Brooks and Corey 1964; Millington and Quirk 1961). In general, the unsaturated hydraulic conductivity and percolation rate increase with vadose zone moisture content. However, wetting rates differ from drainage rates resulting in hysteresis effects on parameters. Within large pores in coarse grained systems, pore pressures are generally low and gravity dominates flow processes over capillary forces (Tokunaga et al. 2002). The hysteretic effects on the hydraulic function decrease with increasing grain and pore size. As a result, the role of hysteresis is often not addressed in coarse gain dominated systems (Or 2007; Tokunaga et al. 2004). Under these conditions, macro pore flow will dominate, resulting in a greater vadose zone hydraulic conductivity than predicted for just pore flow (Schaap and Leij 2000: Schaap and van Genuchten 2005). A number of analytical solutions to estimated vadose zone water transport rates have been developed for specific vadose zone conditions or ranges of conditions (e.g. Marinoschi 2008; Menziani et al. 2007; Tracey 2007; Miller et al. 2006, Ross 2003, Chen et al. 2003, Chen et al. 2001, Hogarth & Parlange 2000, Basha 1999; Parlange et al. 1997; Tocci et al. 1997; Ross 1990). An alternative approach to modeling vadose zone transport has been to apply a stochastic approach, which provides a method of predicting contamination from the macroscopic characterization of vadose zone properties (Aquirre and Haghighi, 2003). Though useful in many vadose zone settings, these models generally do not address the observed rapid infiltration in coarse grained materials.

By definition, coarse grained materials include deposits with a significant percentage of sediments having a diameter exceeding 2 mm, the diameter of gravel (Wentworth 1922; Folk 1974). These deposits frequently include pebbles, cobbles and boulders of much larger grain sizes (Collinson 2006; Tucker 1981). Deposits with clast-supported gravel and larger grains with limited matrix materials are characterized as open framework gravels. Gravel dominated vadose zones are reported to lack uniform infiltration fronts and are often dominated by percolation along preferred flow paths (Bodvarsson et al., 2000; Bauters et al. 1999; Wang et al. 2003; Jury et al. 2003). It is reported that unsaturated flow systems may have an effective flux

through as little as half of the sediment volume, with flow pathways dominated by a few high-flow regimes (Tokunaga et al. 2005). Boulders within coarse grained deposits increase the spreading of the percolating waters (Bouwer and Rice 1984), where flow can occur primarily as film flow across clast surfaces (Tokunaga et al., 2002). The spreading from the preferred flow conduits results in a more uniform infiltration front with depth. This uniformity of the infiltration front increases when vertical flow enters lower permeability materials, where oversaturation of the sediments occurs, resulting in lateral spreading of the infiltration front (DiCarlo 2006). The presence of layers, or lenses, of finer material also slows the downward movement of percolating water and acts to spread out groundwater recharge over a longer time period and area (Figure 1.3). In very coarse grained vadose zones, the mix of both coarse and finer grained sediments creates a "dual porosity system" with characteristics similar to porous bedrock fracture flow systems.

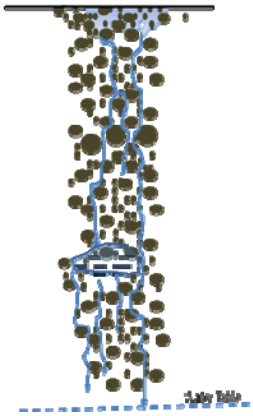

Figure 1.3 Cross section of a coarse-grained vadose zone receiving recharge at the land surface. Non-uniform infiltration and preferential flow paths are illustrated, along with dispersion (spreading) when large cobbles and bounders are encountered (large black dots). The buildup of water at a fine-grained lens (horizontal short lines) continues until the lens is saturated, resulting in further spreading. Overall the flow is dominated by vertical transport.

Monitoring the percolation process in the field, and quantifying dominant parameters necessary to model the physical movement of water in the vadose zone is challenging. Standard instruments used in shallow, finer grained vadose zone characterizations typically cannot be installed or will not maintain hydrologic continuity (Bouwer and Rice 1984; Tokunanga 2003, Tokunaga et al. 2004; Simunek et al. 2003). Sediment sampling of the vadose zone poses additional challenges as cobbles often exceed the diameter of standard coring or geotechnical sampling tools.

STORM WATER QUALITY

Storm water runoff is the source of water entering CVIW where they are used to manage storm water. Thus, it is important to understand the makeup of this source of recharge.

The quality of urban storm water runoff has been extensively characterized by the EPA National Urban Runoff Program, which included samples from approximately 2,300 storm events in 28 urban areas (USEPA, 1982, 1983). The United States Geological Survey has

expanded and updated this data base (Smullen et al. 1999). The most common types of contaminants in urban storm water are nutrients, pesticides and herbicides from residential areas, parks and golf courses (EPA, 1983; Pitt et al., 1996; EPA, 1999; Taebi and Droste, 2004); organic chemicals from industrial areas and incomplete combustion of fuels (Borden et al., 2002); pathogenic microorganisms (Pitt et al., 1996; EPA, 1999); heavy metals from roads and industrial areas (EPA, 1999; Gromaire-Mertz et al., 1999; Asaf et al., 2004; Taebi and Droste, 2004); and salts from road salts in northern climates (Pitt et al., 1996). The results of these studies indicate that, in general, heavy metals and salts are the most common constituents found in infiltrating storm waters (EPA, 1999; Pitt et al, 1996). In addition, major ions, nutrients and fecal coliforms could not be linked to specific urban land uses, whereas metals and organic constituents, including petroleum hydrocarbons, were attributed to industrial areas and road surfaces. It was further observed that storm water quality generally does not exceed drinking water standards, including volatile organic contaminant concentrations, unless a specific input of contamination is present. This nationwide sampling also documented "first-flush" effects, where the first water generated by a storm contains the highest levels of contaminants (Pitt et. al., 1996).

CONTROLS ON THE QUALITY OF INFILTRATING AND PERCOLATION OF STORM WATER

When the source water infiltrating into the vadose zone enters from the soil zone, the low specific conductance and slightly acidic water begins to react with the soils and underlying parental vadose zone material. This process often results in a removal of oxygen, an increase in the bicarbonate, incorporation of natural organic constituents and the addition of cations derived from the chemical weathering of the soil material to the infiltrating water. In settings with very limited precipitation percolating water may remain very near the land surface where it becomes attached to soil grains, used by plants, or directly evaporated. In areas with more precipitation that generates appropriate soil antecedent conditions, infiltrating water will pass through the soil zone and percolate downward. The chemistry of this water can be influenced by a number of geochemical and biological processes before it arrives at the water table. Geochemical interaction between constituents in the percolating water and the solid surfaces of the sediments through which the water is passing may either reduce the constituents in the percolating water or add constituents to it (Darty et al., 2006). Cations, anions, and some organic compounds present in the infiltrating water may attach to vadose zone sediment surfaces resulting in mass transfer by sorption between the water and mineral surfaces. The degree of sorption is controlled by the sediment surface charge character, the mass of the constituent present, and the amount of available grain surface area that acts as potential sorption sites (Horowitz and Elrick, 1987). Primary sorption surfaces available in the vadose zone also include organic matter and clay minerals. Sorption for some source water constituents is further enhanced by the diagenetic growth of iron and magnesium oxy-hydroxide minerals on grain surfaces.

Diagenetic minerals may also incorporate constituents from the percolating water into stable mineral structures immobilizing them from further geochemical processes. In many soils, carbonate precipitation occurs during percolation. The precipitated minerals may incorporate trace metals into the crystalline structure (Konigsberger et al. 1999), or the surface may adsorb dissolved ions (Stipp 1999).

The geochemical behavior of metals present in the percolating water has also been shown to have a strong relationship with local biological activity (Hutchins et al., 1986; Elder, 1988; Ainsworth et al., 2000). Under natural conditions, specific bacteria may utilize particular metals and nutrients for metabolic energy. The metabolic process changes the oxidation state of the metal, which may modify the mobility and toxicity of the metal (Haack and Warren, 2003). Mineral precipitation may also occur as a result of changing redox conditions directly, or from biologically mediated processes.

SIGNIFICANCE TO WATER UTILITIES

State and local governments and local municipal water providers have had to address water quality issues associated with storm water runoff. Storm water impacts to surface water have come under increasing scrutiny (Clear Water Act, the National Pollutant Discharge Elimination System (NPDES) Phase I and II; TMDL program; WHO, 1996; EPA 1997; Foster et al., 2002). In regions where subsurface conditions are appropriate, the use of CVIWs for storm water disposal is anticipated to increase as regulatory pressures restrict direct disposal in surface water (EPA 1999). Though the use of additional CVIWs will reduce urbanization costs, if complex storm water handling systems and water quality monitoring are not required, the wells may pose additional threats to water quality in receiving unconfined aquifer systems. As a result, Source Water Protection Planning for public water supply sources in these areas must incorporate detailed methods to respond to surface spills and other conditions that may negatively impact potable source water quality receiving recharge from storm water runoff.

The study results of this research will provide information needed to protect water supplies in areas with highly conductive aquifers and coarse grained vadose zone systems served by CVIWs. The approach, methodology, and results of this work will also provide support to operation and feasibility evaluations performed by water managers where groundwater supplies are recharged by natural and artificial methods.

RESEARCH GOALS AND PROJECT OBJECTIVES

The study goal is to identify, and generalize for geologic settings found in intermountain basins in the Northern Rocky mountains, key processes controlling source water percolation rates, and the quality of that water during percolation through sand and gravel, cobble and boulder dominated vadose zones. The research program is designed to answer three primary research questions and one management question. These questions are:

1. What physical and hydrologic factors in coarse grained intermountain basin vadose zones control the rates of storm water infiltration and percolation?

2. What geochemical processes impact the quality of infiltrating storm water passing through coarse-grained vadose zone materials?

3. What factors dominate the treatment/protection capacity of coarse-grained vadose zones?

4. What management approaches can preserve or extend the treatment/protection capacity of vadose zones receiving percolating storm water?

Project objectives formulated to address the research goal and questions included:

1. Selection of a number of research sites in an urbanized Northern Rocky Mountain basin containing a coarse grained vadose zone and a productive unconfined aquifer used for water supply;
2. Establish precipitation runoff relations and storm water source volumes and chemistry;
3. Determine infiltration rates at selected CVIWs;
4. Quantify the percolation rate of storm water through the vadose zone accounting for variable rates and quantities of storm water runoff:
5. Define the changes in chemistry of storm water sources as this water passes through the vadose zone;
6. Establish impacts of vadose flux on water levels and the quality of the receiving groundwater;
7. Develop a general conceptual model of the physical and geochemical processes controlling water movement and its quality through coarse grain vadose zones;
8. Using appropriate models, and project observations and results, assess the conceptual model by calibration and sensitivity analyses;
9. Based on field, lab, and modeling results, develop a generic set of models that vary key vadose zone parameters within reasonable values to establish how changes in physical conditions influence the efficiency of percolation and impact recharge quality;
10. Examine potential approaches to protecting groundwater resources from storm water recharge.

The approach used to meet the project goals and objectives involved instrumenting storm water injection sites in the Missoula, Montana valley, identifying the physical and geochemical processes that dominated percolation and vadose zone water quality, and modeling these processes to generalize findings.

PROJECT DEVELOPMENT

This project was funded as a cooperative effort with Mountain Water Company, the primary public water supply provider in Missoula, Montana area, and the Water Research Foundation (f/k/a American Water Works Association Research Foundation, AwwaRF). The project was developed to evaluate concerns raised by Mountain Water Company that the use of Class V Injection wells, used for storm water management across the Missoula urban area, impacts aquifer water quality. Storm water provides recharge to the unconfined Missoula Valley Aquifer, designated by USEPA in 1988 as a Sole Source aquifer for potable water use (MVWQD 1988). The general project design and rationale are presented in the project proposal, "Quantifying the Capacity of Coarse-Grained Vadose Zones to Treat Class V Well Injected Storm Water that Recharges Aquifers Managed for Water Supply,' prepared for AwwaRF and Mountain Water Company (Woessner and Swierc, 2006).

MISSOULA MONTANA STUDY AREA

The study area is the Missoula Valley, located in Missoula County in Western Montana, USA (Figure 2.1). Missoula has an estimated population of 68,000 within the city limits, and represents the major regional urban area for a population exceeding 100,000 (MDC 2009). The City of Missoula is located in the eastern part of the Missoula Valley, a northwest-southeast trending valley defined by several mountain ridgelines along the valley margins (Figure 2.1). The study area is the eastern part of the valley, coincident with the urban center of Missoula.

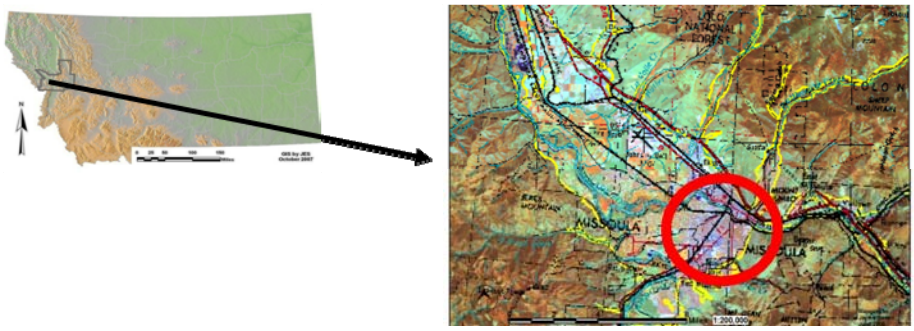

Figure 2.1 Location of Missoula County, Montana and the urban area containing the City of Missoula in the Missoula Valley (red circle).

The climate in the Missoula Valley is semi-arid, receiving 13 inches of rain per year in the central part of the valley, and more in the surrounding mountainous areas. A summary of the monthly average climate data for Missoula, measured at the Airport west of the study area in the central part of the valley, is presented in Table 2.1. The climate is dominated by somewhat rainy springs and falls, with dry summers and winters. Snow dominates the precipitation from late October through February each year.

Table 2.1 Missoula Weather Station Average Annual Climate Data

Airport Station	Jan	Feb	Mar	Apr	May	Jun	Jul	Aug	Sep	Oct	Nov	Dec	Annual
Avg Max Temp (°F)	30.1	37.0	46.4	57.1	66.0	73.9	84.6	83.2	71.5	57.0	40.5	31.1	56.5
Avg Min Temp (°F)	15.1	19.9	25.6	31.9	39.0	45.7	50.3	49.0	40.8	31.6	24.1	17.1	32.5
Avg Total Precip (in)	1.13	0.76	0.90	1.10	1.81	1.92	0.93	1.02	1.08	0.86	0.95	1.12	13.58
Avg Total Snow (in)	12.3	7.2	6.2	1.9	0.6	0.0	0.0	0.0	0.0	0.7	5.7	10.9	45.5
Avg Snow Depth (in)	4	3	1	0	0	0	0	0	0	0	0	2	1

Data from Western Regional Climate center, obtained September 7, 2009 (http://www.wrcc.dri.edu/Climsum.html). Period of Record is from7/1/1948 to 12/31/2008 for the Airport Station.

Surface water in the study area is dominated by the west flowing Clark Fork River that has a mean annual flow of about 3000 cfs (USGS station#12340500 above Missoula). Flows peak in the spring and early summer in response to spring snowmelt. A number of studies have shown that the river is an important recharge source for the underlying prolific groundwater system (e.g. Woessner 1988, LeFave 2003, Tallman 2006).

The geology and hydrogeology of the Missoula Valley have been studied by a number of researchers (McMurtrey et al., 1965; Geldon, 1979; Clark, 1986; Woessner, 1988; Wogsland, 1988; Miller, 1991; Stringer, 1992; LaFave, 2002; Morrow, 2002; Tallman, 2005; Cook, 2005; Patel, 2006). Finer grained older Tertiary valley fill sediments underlie the coarse fluvial sand, gravel, cobbles, and boulders that extend from land surface to between 100 and 150 ft below land surface. It is these coarse grained sediments that form the Missoula Aquifer and its vadose zone (Fields et al., 1985; Evans, 1998) (Figure 2.2).

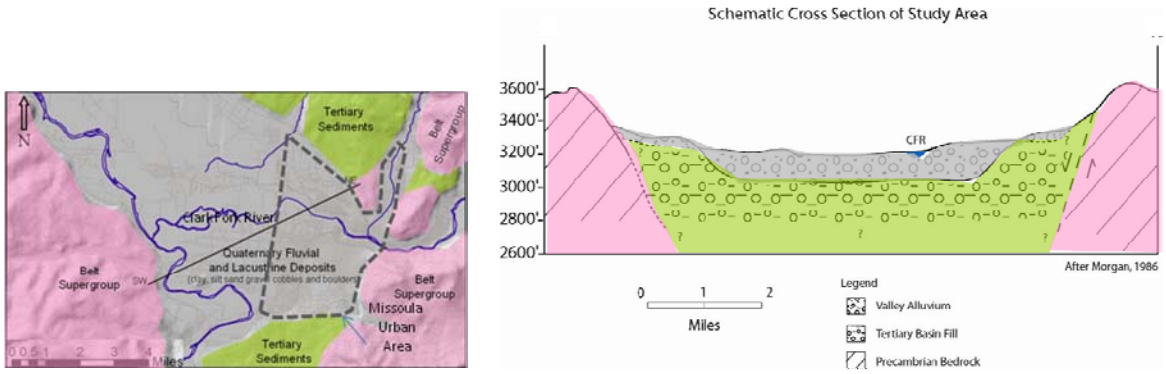

Figure 2.2. The alluvial valley floor is covered with valley alluvium (gray) with Tertiary (green) and Precambrian bedrock (pink) exposed on the hill and mountain sides. The cross section follows a southwest to northeast line through the valley (after Tallman, 2005).

The stratigraphy of the near-surface Missoula valley fill materials reflects a high energy fluvial depositional environment, including erosion and deposition from glacial flooding associated with Glacial Lake Missoula (Figure 2.3). The sediments are dominated by sand and gravel interspersed with cobbles and bounders deposited by waning large floods and river flows.

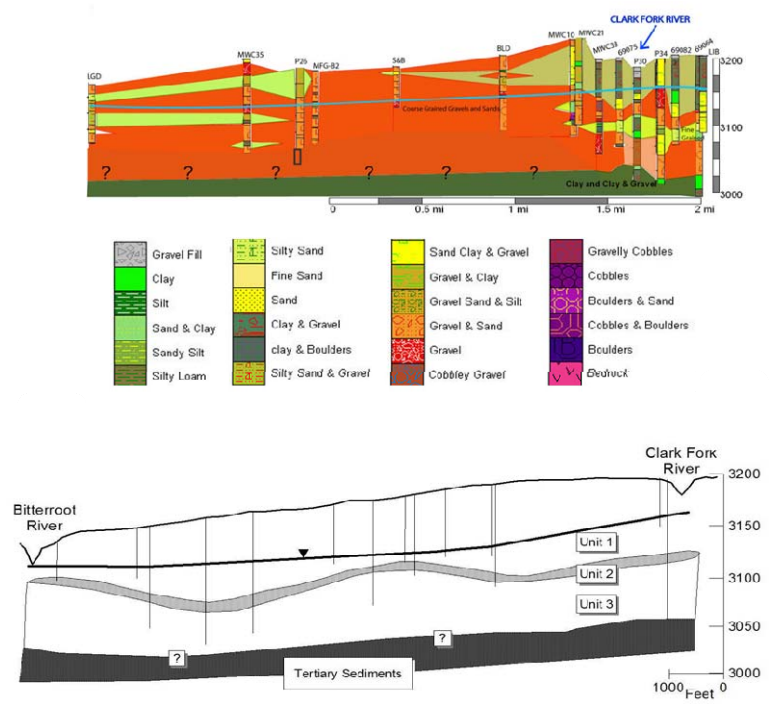

Figure 2.3. Geologic cross section of the upper sand, gravel, cobble and boulder dominated valley fill that forms the Missoula Aquifer and its vadose zone. The cross section follows the location shown in Figures 2.2. The bottom drawing is a representation of the hydrostratigraphy of the sediments that are roughly divided into three units (after Woessner, 1988; Tallman, 2005).

Hydrostratigraphic units include two coarse grained fluvial sequences (Units 1 and 3), separated by coarse material containing discontinuous fine-grained deposits (Unit 2) (Woessner, 1988; Land and Water, 2005). Sediments are dominated by Precambrian meta-sediments of the Belt Super Group and are composed of quartzites and argillites. Water supply wells are generally completed in Unit 3, located at the base of the coarse grained valley fill sequence above the Tertiary valley fill material (Land & Water, 2005). The unsaturated zone is mostly a component of Unit 1, as the water table commonly occurs between 30 and 70 ft below land surface in the eastern portion of the valley (Figure 2.4).

Groundwater levels vary annually from 10 to 15 ft, with the highest water table position occurring in late spring to early summer. Ground water flow in the Missoula valley is generally to the west (Figure 2.4). The aquifer receives an estimated 80% of recharge as stream leakage from the Clark Fork River (Tallman, 2005). The Bitterroot and Clark Fork rivers in the western part of the valley are discharge points for the groundwater system. Hydraulic conductivities range from a few thousand ft/d to greater than 18,000 ft/d. Groundwater velocities are over 60 ft/d in most portions of the aquifer. Groundwater in the valley is a calcium bicarbonate type with low concentrations of dissolved solids (MWC, 2006; Cook, 2005; Woessner, 1988).

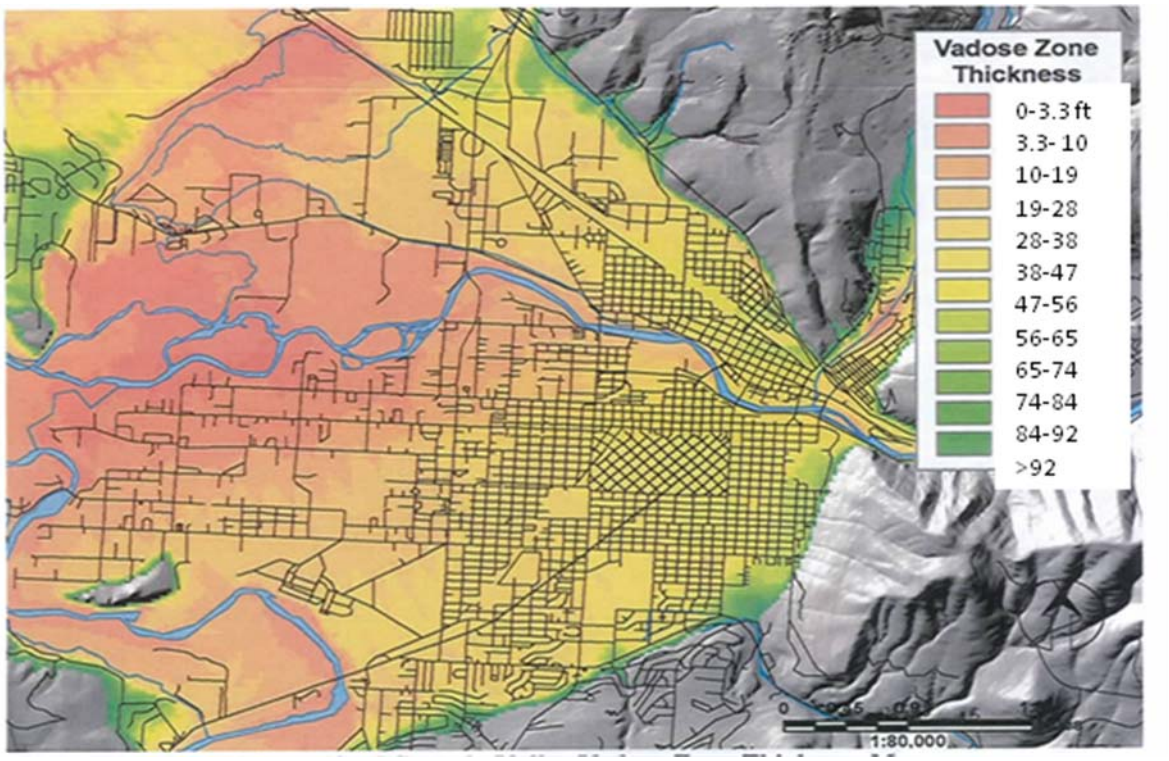

Figure 2.4. Thickness of the vadose zone derived by differencing land surface elevations and the average position of the water table (Swierc and Woessner, 2006). The vadose zone is thickest in the eastern portion of the valley and thins to the west.

There are over 40 public water supply wells in the urban Missoula area (Figure 2.5). Wells commonly pump at over several hundred gallons per minute (gpm) with one well producing over 6,000 gpm. There are also high capacity industrial wells in the town area. Potable water outside of the city is obtained from private wells.

This hydrogeologic setting is similar to many of the intermontane basins of western North America (Kendy and Tresch 1996; USEPA, 1997). These basins are often dominated by valley fill composed of sand and gravel. The characteristics of the Missoula valley sediment include, in addition to sand and gravel, cobbles and boulders that create zones of high hydraulic conductivity. In the Missoula valley the coarse grained vadose zone and shallow water table (Figure 2.4) allow infiltrating water to rapidly percolate to the water table. It is likely that only limited geochemical changes to the percolating water occur under these conditions. Where intermountane basins, and associated vadose zones and aquifers are composed of less transmissive sediments, percolation rates are slower, allowing for longer transport times and possibly additional geochemical processes to occur.

Storm water management in the Missoula urban area utilizes numerous in-street sumps, or French drains, which discharge surface water runoff into the vadose zone of the Missoula Aquifer system. The EPA classifies the sumps as Class V Injection Wells (CVIW), systems that dispose of wastewater by injecting it into the subsurface (EPA, 1999). The sumps are constructed using four-foot diameter concrete rings with an open grate at the surface (Figure 2.6). The base of the sump comprises a layer of course boulders, which over time may become filled with fine-grained materials washed into the sump. Currently, these storm water sumps are

exempt from state and local permitting requirements. Missoula has more than 6,000 sumps located along streets, at corners, and in parking lots (Figure 2.7). These valley conditions were used to evaluate the storm water infiltration process at a variety of both geological and land use settings.

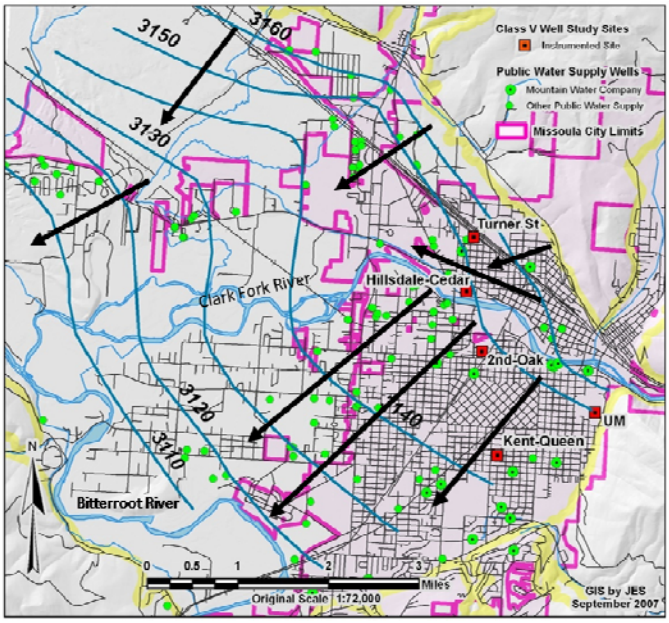

Figure 2.5. Map showing general groundwater flow direction (black arrows) in the Missoula Aquifer (data from LaFave 2002, Tallman 2005, and Patel 2006). Flow south of the Clark Fork River is generally to the southwest, discharging into the Bitterroot River. North of the river, the flow moves west to southwest, with the Clark Fork River acting as a hydrologic divide for about 3 mi., starting as the river enters the eastern side of the valley through Hellgate Canyon.

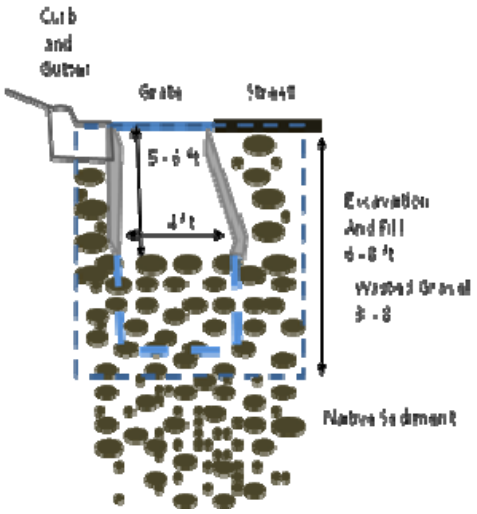

Figure 2.6. Schematic cross section of a storm drain located at a street corner. The gray is a cross section of the concrete tube creating the drain cavity. An excavation about 6 to 8 ft deep and 8 ft wide is created, the hole is partially backfilled with washed gravel, and the drain is installed. The thick blue dashed line represents that at some installations an additional 4 ft of concrete rings are added to extend the depth of the sump.

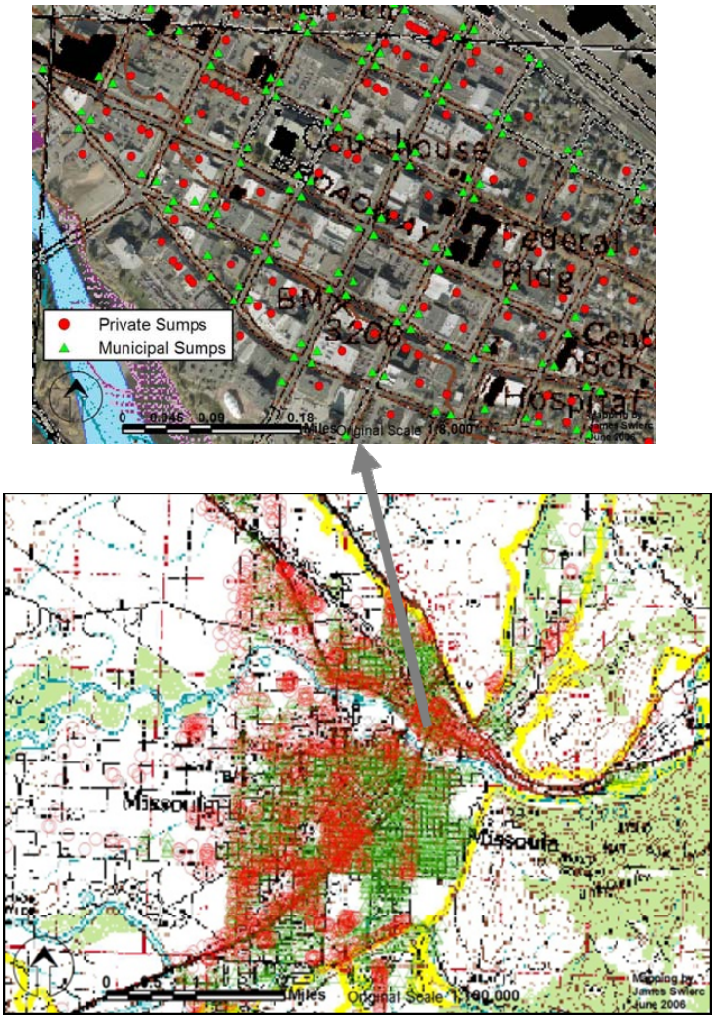

Figure 2.7. Bottom map with small red dots shows the overall distribution of storm drains (Class V Injection Wells) in the Missoula area. The upper map provides a detail of a portion of the valley in downtown Missoula, north of the Clark Fork River.

METHODS

Field and laboratory investigations focused on identifying key processes controlling percolation rates and changes in recharge water quality during both natural storm water infiltration events and controlled tracer tests. The field program collected site-specific data from several different locations across the study area to characterize the specific physical, hydrologic and geochemical processes occurring during unsaturated flow. The results of the field studies were used to test and revise conceptual models of observed processes (e.g. Figures 1.1 and 1.2). These revised conceptual models provided the basis for numerical model development, using field data for calibration. The numerical models provided a method to evaluate infiltration events of varying durations and magnitudes at a variety of observed or formulated subsurface conditions. The management recommendations founded on the results of this study reflect the high probability that vadose zone transport is rapid and only limited changes in percolating water quality occur. The general components of this research effort are summarized in Figure 3.1.

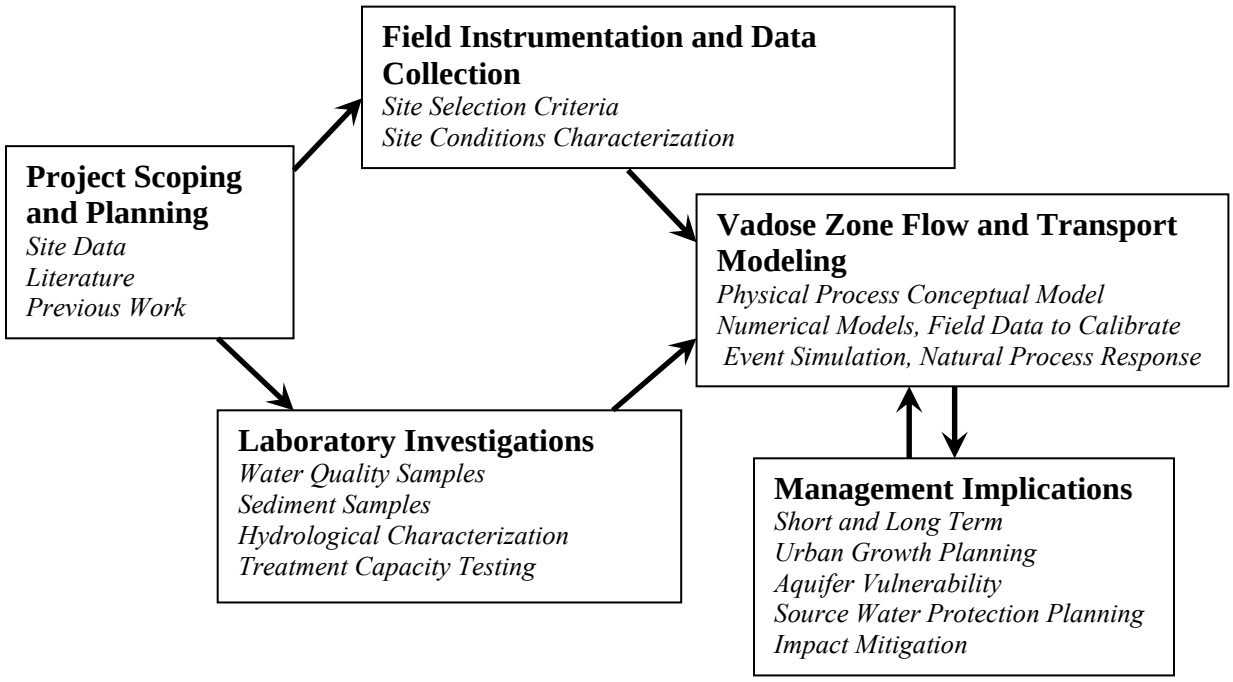

Figure 3.1. Flow chart of the research approach.

As required by the granting agency, the key components of the research were outlined in a project work plan. The work plan was organized by the tasks listed here for completeness. It should be noted that this report uses a more holistic approach to describing research methodology. The different tasks from the work plan document are summarized as follows:

PROJECT SCOPING AND PLANNING

Task 1: Collect, review and assess physical vadose zone characteristics by utilizing existing databases, including state, county, and unpublished data.

Task 2: Collect, review and assess the general treatment capacity of the vadose zone based on environmental site investigation reports, previous storm water investigations, and other literature.

Task 3: Consult with the Boise State surface Geophysical group to evaluate appropriate geophysical tools and borehole designs applicable to characterizing the physical properties of coarse grained vadose zones.

Task 4: Develop field site selection criteria and instrumentation matrices that address project goals. Meet with city officials to discuss limitations related to the locations and instrumentation of Class V wells in the urban area.

Task 5: Assess the value of establishing a dedicated specifically constructed Class V injection well research site (at a controlled location) in addition to instrumentation of existing Class V sites.

Task 6: Select field sites for various levels of instrumentation.

Field Instrumentation and Data Collection

Task 7: Develop site maps and establish storm water drainage areas.

Task 8: Develop a relationship between rainfall and snowmelt event intensities, durations and quality, and infiltration volumes and quality at individual Class V Injection Wells.

Task 9: Develop and implement a vadose zone and groundwater instrumentation plan.

Task 10: Spatially and temporally map the movement and quality of storm water and project-injected water and tracers through the vadose zone under a variety of physical settings.

Laboratory Investigations

Task 11: Describe and photograph cores, cuttings and Class V injection well sediment samples.

Task 12: Determine moisture content of selected portions of vadose zone cores.

Task 13: Establish the physical properties of the soil and sediment, including grain size, carbon content, and soil mineralogy.

Task 14: Conduct column percolation experiments to simulate physical and geochemical processes anticipated to impact vadose zone water quality.

Vadose Zone Flow and Transport Modeling

Task 15: Assimilate field and laboratory data, and develop calibrated site-specific vadose zone flow and transport models.

Task 16: Develop generalized basin vadose modeling tools and examine how identified key factors influence the character of percolating water and the likely consequence to the quality of the underlying groundwater system.

Management Implications

Task 17: Use both qualitative and quantitative study results to evaluate the consequence of regulatory, physical, and engineered methods on forecasted vadose zone water quality and treatment capacity.

In this report, the methodology and results are organized into four overarching sections: Characterization of the physical processes influencing storm water infiltration and movement through the vadose zone, characterization of the geochemical processes impacting percolating

water and groundwater recharge, approaches used to determine vadose zone treatment capacity and aquifer vulnerability, and management implications. The following sections describe the establishment of five specific research sites, the methods used to characterize the physical and geochemical vadose zone properties and conditions, processes used to formulate physical and geochemical conceptual models that define key factors influencing the treatment capacity of the vadose zone, and the development data to support management policy and actions.

Characterization tools, including vadose zone coring, temperature monitoring, and geophysical observations, were used in combination to examine the in-situ infiltration and percolation process in coarse-grained sediments. Storm water runoff was used as source water for the investigation. Research included sampling and laboratory analyses to determine storm water recharge timing, recharge rates, and source chemistry. Groundwater geochemistry and lab characterization of sediment geochemistries and sorption capacity were used to identify likely factors controlling the transport of source water constituents to the water table. These observations were then used to formulate models of the vadose zone flow and transport processes. Once these models were calibrated and tested with field observations, additional analyses were performed to examine how changes in the nature of the vadose zone and source water chemistry would likely impact underlying aquifers. These generalizations provided insight into the transferability of the site-specific results.

OVERVIEW OF RESEARCH SITES

The field program was implemented at five sites located in the eastern part of the Missoula Valley study area (Figure 3.2). The sites were positioned within the central urban area of the City of Missoula where the density of the CVIWs is highest (Figure 2.6).

Study Site Selection Criteria

The study sites were selected using a set of criteria organized as a matrix assessment (Table 3.1). Anticipated budget and field instrumentation requirements suggested that five sites could be instrumented. This approach allowed flexibility and spread out the risk of site loss through natural or anthropogenic factors. The matrix assessment evaluated nine different factors for a subgroup of 17 potential sites (Table 3.1). The sites were selected in the Missoula urban area at locations that were up groundwater gradient from the majority of the public water supply sources. This approach allowed for different geologic conditions to be evaluated, as the coarse grained stratigraphy of the vadose zone was anticipated to vary widely and locally yet be dominated by sand and gravel interspersed with cobbles and boulders. Geologic factors such as the thickness of the vadose zone and the potential presence of perched layers or fine-grained sand lenses were evaluated using the literature and local well logs from municipal and domestic wells (McMurtrey et al., 1965; Woessner, 1988; Miller, 1991; Stringer, 1992; Morrow, 2002; Tallman, 2005; Cook, 2005; Patel, 2006). Data from environmental assessment site reports containing descriptions of the vadose zone and behavior of contaminant releases above the water table were also reviewed (Swierc and Woessner 2006). In addition, historical land use and property development data sets were evaluated to identify areas with different land use patterns. The age of urbanization was determined using Sanborn Fire Insurance Company maps. Finally, the potential land ownership was evaluated to determine if site access was likely.

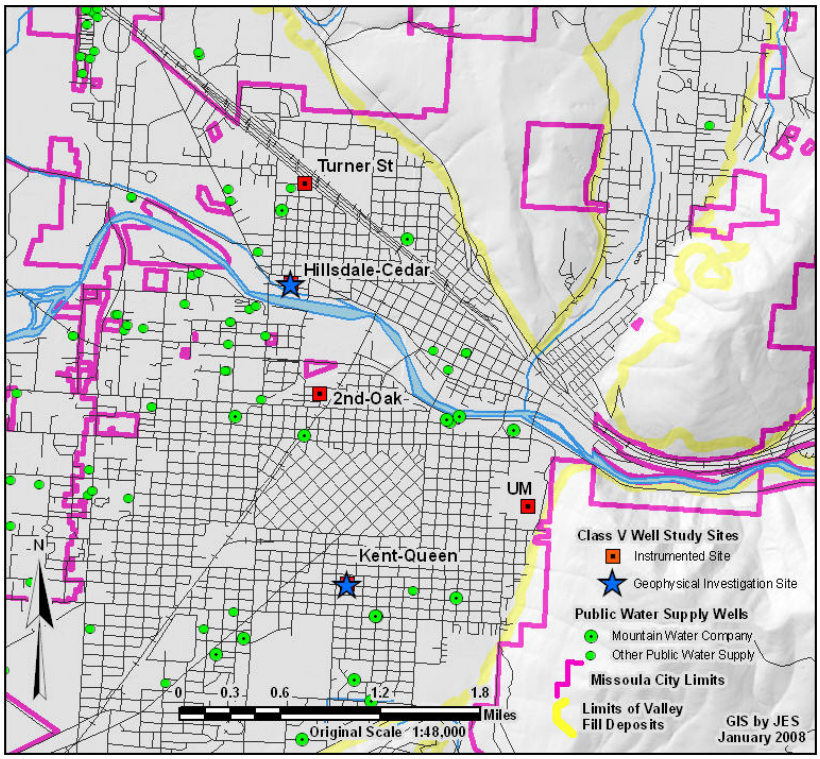

Figure 3.2 Location map of the five study sites (red squares), sites at which geophysical investigations were performed (blue stars), and Mountain Water Company and other public supply wells (green dots).

Table 3.1 Site Selection Matrix

Matrix Factor	Description	Missoula Valley Study Area Results
Spatial location in valley	Drilling locations are needed to evaluate different subsurface conditions across the study area.	The study area is focused on the urban area in the eastern Missoula Valley. The drilling and instrumentation sites include two sites north and three sites south of the Clark Fork River.
Vadose zone thickness	The potential treatment capacity of the vadose zone increases with vadose zone thickness. In the Missoula Valley, the vadose zone thickness increases from west to east.	Includes two sites with vadose zone thicknesses >50', two sites where the vadose zone is between 30'-50' thick, and one site with a vadose zone thickness <30' thick.
Presence of perching layers and/or fine-grained sand lenses	Fine-grained layers retard flow and laterally disperse percolating waters with an overall reduction in the percolation rate. The increased contact time between soil and slowly percolating waters allows for more geochemical processes to occur, potentially affecting percolating water quality.	A drilling and instrumentation site was installed in the north part of the valley study area where perching layers are known to exist. Based on the review of environmental site data and literature, no other perching layers are likely to be found in the study area. Drilling confirmed the absence of perching layers and provided stratigraphic data to correlate with environmental site data.
Flux of water from storm events	The infiltrating storm water volume is a function of the surface catchment recharge area and sump location. Larger catchment areas result in greater runoff volumes.	Sites were selected based on visual observation of runoff during storm events during project scoping. Three sites were selected with larger runoff contributing areas when compared to the two other sites selected.
Water table fluctuations	Water table surface fluctuations determine the thickness of the vadose zone. Both short and long term fluctuations can impact the physical and geochemical conditions at the interface	The water table surface annually fluctuates approximately 15 feet at the study site proximal to the Clark Fork River and the study site in the northern part of the valley. The annual amplitude of variation at the other three study sites is

	between the saturated zone and vadose zone.	approximately 10 feet.
Land use	Differences in urban land use (residential, commercial, or industrial) are likely to generate unique variations in associated storm water quality.	Instrumented sites were selected to represent all three urban land use types. The current selection of study sites includes one residential site, one mixed residential/commercial site and two mixed commercial/industrial sites. An additional site is located in a parking lot at the University of Montana.
Age of urban growth	Older urbanized areas have received storm water runoff over a longer period of time. The geochemical character of sediments in older urbanized areas may have different properties that affect water quality during percolation.	The selected drilling sites were urbanized at different times: one site was urbanized in the early 1900's, two sites were urbanized between 1900 and 1950, and two sites were urbanized after 1950.
Location proximal to environ-mental sites	Known releases of contaminants into a storm drain or the vadose zone may provide additional information about fate and transport contaminants in a geological setting.	The northern most site is located adjacent to a Montana State Superfund site. The two sites in the central part of the valley are separated by two environmental sites. The southern site is located near several Leaking Underground Storage Tank sites.
Land ownership	Instrumentation requires security at wellheads and permission for access.	Instrumented sumps are on property owned by the City of Missoula and the University of Montana

Properties of Selected Sites

The general properties of the five sites (Figure 3.2) selected for instrumentation are summarized in the following section.

The Kent-Queen (KQ) site is located in the central part of the valley and is the southernmost study area (Figure 3.3). The land use type is exclusively residential with the onset of urbanization dating to the mid-1950s. Based on the drilling results of this work, the vadose zone is dominated by very coarse gained sand, gravel and cobbles. A thin fine-grained layer of sediment is located approximately 45 feet beneath the surface that creates limited perching of percolating water. The water table depth and vadose zone thickness ranges from 60 to 70 feet below ground surface. The site is located approximately 0.67 miles east of a leaking underground storage tank site (Swierc and Woessner, 2006). The site is located within a City of Missoula street right-of-way.

Figure 3.3. Kent Queen study site (light blue circle) showing the street drainage area.

The Hillsdale-Cedar (HC) site is located on a river terrace of the Clark Fork River, approximately 500 feet north of the river in the north-central part of the valley (Figure 3.4). The land use type is a mixed commercial/industrial and residential area that was developed during the

early to mid 1900s. Based on drilling results of this work the vadose zone is dominated by very coarse gained sand, gravel and cobbles with a fine-grained layer within 4 to 10 ft below the sump base. The water table depth and vadose zone thickness range from approximately 20 to 35 feet below the ground surface. During average storm events water ponds in the sump; water may pond on the road surface during large precipitation events. The site is located within a City of Missoula street right-of-way.

Figure 3.4. Hillsdale Cedar study site (light blue circle) showing the street drainage area.

Two environmental sites that underwent extensive geological and hydrogeological characterization are located south of the HC across the Clark Fork River (Swierc and Woessner, 2006). The 2nd-Oak (2O) site is located on the floodplain of the Clark Fork in the central part of the valley (Figure 3.5). The site is located in a mixed commercial/industrial area that was developed during the early 1900s. Based on drilling results of this work the vadose zone is dominated by very coarse gained sand, gravel and cobbles. No fine-grained lenses are present in the stratigraphy at the site. The water table depth and vadose zone thickness ranges from approximately 50 to 60 feet below the ground surface. The site, located directly north of the HC site is also north of two environmental sites on the southern side of the Clark Fork River (Swierc and Woessner, 2006). These sites provide geologic data to interpolate the site conditions from the 2O site to the HC site. The site is located in a cul-de-sac within a city of Missoula street right-of-way.

Figure 3.5. 2nd and Oak study site (light blue circle) showing the street drainage area.

The Turner Street (TS) site is located in the northern part of the valley in a mixed commercial/industrial area developed during the early to mid 1900s (Figure 3.6). The site is located south of the main railroad tracks that cross the Missoula Valley. Based on drilling results of this work the vadose zone is dominated by very coarse gained sand, gravel and cobbles. A thin laminated silt clay layer is present approximately 50 feet below ground surface. This layer can be correlated to a similar stratigraphic unit documented at an environmental site located to the northeast across the railroad tracks. The water table depth and vadose zone thickness range from approximately 50 to 65 feet below the ground surface. The site is located in a cul-de-sac within a city of Missoula street right-of-way.

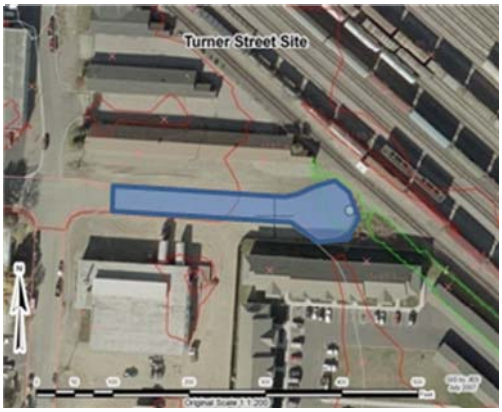

Figure 3.6. Hillsdale Cedar study site (light blue circle) showing the street drainage area.

The University of Montana (UM) site is located in a parking lot at the University along the eastern margin of the valley (Figure 3.7). The site was not developed until it was paved some time after 1960. The water table depth and vadose zone thickness is estimated at 70 to 80 feet below ground surface. The site vadose zone has several thin silt clay and fine grained layers.

Figure 3.7. UM study site (light blue circle) showing the street drainage area.

METHODS TO CHARACTERIZE THE PHYSICAL PROCESSES INFLUENCING THE TRANSPORT OF STORM WATER RUNOFF TO THE WATER TABLE

The research goals are accomplished through a comprehensive laboratory and field research program developed to obtain data to characterize the physical hydrologic and geochemical properties of the unsaturated zone. This section presents methods used to characterize storm water runoff volume and timing, infiltration rates for runoff into storm sump bases, percolation rates for infiltrating storm waters through the vadose zone, and the physical response of the receiving water table aquifer. A variety of field methods were implemented at the five study sites. The level of instrumentation varied depending on site conditions. A flow chart showing the data requirements as they relate to the physical drivers of storm water is shown in Figure 3.8.

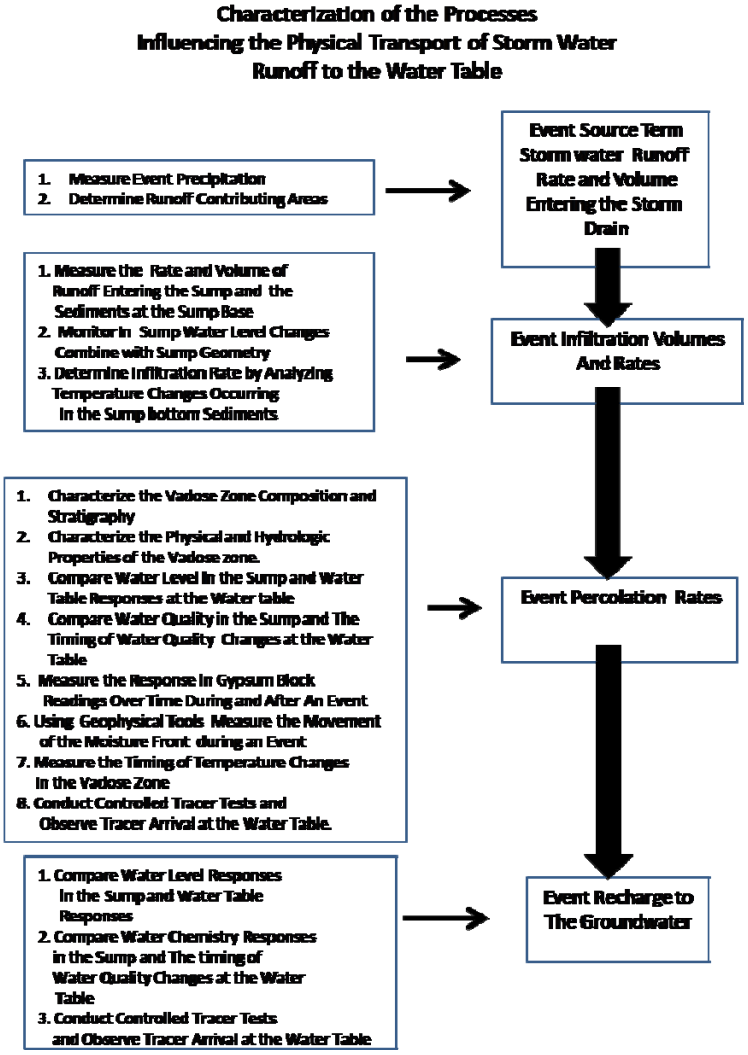

Figure 3.8. Flowchart for characterization of processes influencing the physical transport of storm water runoff to the water table.

Storm Water Source Characterization

Precipitation data were collected during the project using tipping bucket rain gauges (Novlaynx Rain Collector Model 260-7852 with data logger Model 260-2101 Rain Logger), with an event resolution of 0.01 inches, installed at the KQ, 2O and UM sites (Figure 3.2). Total daily precipitation data for the Missoula Airport NOAA station located approximately five miles west by northwest of the main urban area, were obtained for comparison with total event data from the site gauges. Gauge data provides total event precipitation and intensity for each precipitation event, allowing for calculation of storm drain runoff timing and volume.

The surface runoff contributing areas or catchments were mapped using GIS methods for each of the five sites. The primary contributing areas were interpreted as the paved areas up gradient of each selected storm sump that extended to a local hydrologic (topographic) divide (Figures 3.3 to 3.7). Elevation control was obtained using base maps obtained via the internet from the City of Missoula Public Works Department (<ftp://ftp.ci.missoula.mt.us/Maps%20and%20Graphics/Mapping/1999/>). The base maps were developed and checked by the city in 1999 and have a contour interval of two feet.

Infiltration Rate and Volume Characterization

The volume of storm water runoff that enters a sump is required for the calibration of infiltration models. Three separate methods were used to estimate the volume of runoff from a precipitation event. The first used an engineering approach to compute runoff timing using surface water hydrology methods applied to paved areas. A second method computed runoff volume and infiltration rates using sump water levels and dimensions. A third approach measured changes in temperature with depth below the sump base to derive infiltration velocities.

Engineering Estimates of Surface Runoff

Traditional methods in surface water hydrology can be used to estimate the timing and volume of storm water entering a sump for a rain event. The relationship between rainfall intensity and duration to the storm runoff volume was evaluated for each site, leading to the generation of site-specific synthetic unit hydrographs (Linsley et al., 1992). Field runoff monitoring data sets are then used as calibrate data.

The peak flow is the maximum height of the flow hydrograph and represents the maximum flow rate when all areas of the catchment are contributing to runoff. Peak flows are determined using the relationship:

$$Q_p = i\, A_d$$

Where: Q_p is the peak runoff rate
i is the rainfall intensity for duration of t_c (time of concentration)
A_d is the area of the catchment

For runoff from small paved surface areas without defined channels (assuming that runoff exclusively occurs as laminar overland flow), the time to equilibrium flow (t_e) represents the amount of time required to reach peak flows. For a rain event of a duration that exceeds the time

to equilibrium, t_e represents the time of the peak flow for the storm hydrograph. The time to equilibrium can be estimated using the following equation (Izzard, 1946 in Linsley et al., 1992):

$$t_e = \frac{41\ b\ L_0^{1/3}}{i^{2/3}}$$

Where: L_0 is the length of overland flow in feet, and
The coefficient b is determined by the following equation

$$b = \frac{0.0007\ i + c_r}{S_0^{1/3}}$$

Where: S_0 is the slope of the surface
c_r is the retardance coefficient (from a look-up table)

These calculated source inputs were compared to individual field determined values.

Monitoring of Sump Ponding during Runoff

The sumps at the five study sites were instrumented to measure the stage and timing of water ponding in the sumps. A schematic of sump general instrumentation is shown in Figure 3.9. With the dimensions of each sump known, the rates of stage rise and fall provided infiltration data sets (Figure 2.5).

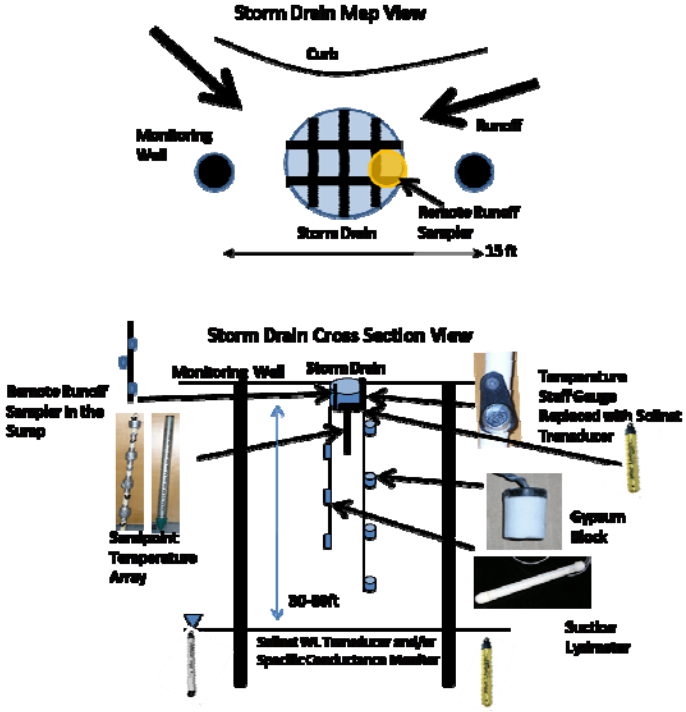

Figure 3.9. A map and cross sectional view showing general research site instrumentation.

To measure the height of the water in the sumps and its duration, an inexpensive temperature-based recording stage gauge was designed and deployed at each study site. iButton data logging thermistors were placed at regular vertical intervals on a length of three-quarter inch diameter PVC pipe (Johnson et al., 2006). The PVC pipe was filled with sand, capped, lowered into the sump, and secured to the surface grate. To retrieve the data, the temperature staff gauge was removed and individual loggers downloaded. Use of this method for stream gauging typically shows a relatively uniform temperature of submerged thermistors, with a large variation in temperature recorded by thermistors exposed only to the atmosphere. Unfortunately, this method did not successfully delineate stage height in sumps. The temperature data from all of the iButtons on the column showed little variation, thus the delineation of ponding events was not possible. Due to the poor resolution of the method, it was discontinued after the initial few months of operation.

Sump ponding water level stage data were then collected using Solinst™ leveloggers. The loggers were initially placed on the bottom of the sump. Initially an accumulation of mud in the sump base covered the transducers and corrupted the initial data set. In order to mitigate this problem, the loggers were inserted into 1.25 inch inner diameter PVC tube shields placed at the sump bottom. The shield was constructed using a 2.5 ft length of PVC monitoring well screen (0.020 slot) placed on the sump bottom and secured to a blank casing riser pipe that extended to the base of the drain grate. The logger was accessed by removing the shield and riser pipe, and then reinstalling it through the surface drain grate. Water level data from the Solinst™ leveloggers were corrected for changes in barometric pressure using a Solinst™ barologger.

Infiltration Rate Estimates from Sump Geometry and Declining Water Levels

The observed rate of the decline in the sump water level was used to compute infiltration rates. Since not all storm events routinely provided sufficient runoff to create ponding in sumps, only those data sets that showed ponding were analyzed for infiltration rates. Methods outlined in Fetter (2004) were used to compute infiltration rates.

A second approach used to determine infiltration rates was to artificially introduce "runoff" water under controlled rates and volumes. Controlled infiltration tests were performed at the KQ, 2O, HC and TS sites during the summer of 2007. Tests were not performed at the UM site. The initial test was conducted at the KQ site using a water truck provided by the City of Missoula. All subsequent tests were completed by releasing water from the closest fire hydrant or water line access point at a rate sufficient to fill the drain and create ponding at the surface. While the primary goal of these tests was to assess the efficacy of installed subsurface instrumentation, a secondary objective was to use the falling head data from the ponding to obtain estimates of the hydraulic conductivity of the receiving materials (Fetter, 2004). A mass balance of water through the system provided a method to estimate the infiltration rate when water was ponded at the surface. The infiltration rate was also determined by calculating the change in volume of water in the sump with time as the ponded surface moved downward in the sump. These data were processed and a curve was generated to estimate the infiltration rate variation with ponding height for each sump site.

Infiltration Rate Estimates from Temperature Changes in Sediments at the Base of the Sump

An analytical approach to quantifying infiltration rates utilized heat transport theory and the monitoring of changes in temperature within the bottom sediments of the sump during an infiltration event. This method was developed based on studies of stream loss flux rates and thermal gradients within the hyporheic zone (Johnson et al., 2006). For this study, the system is considered analogous to stream loss in ephemeral systems (Blasch et al., 2007). At the five study sites, a 4 ft long, 1.25 inch inner diameter galvanized steel sandpoint well point (gravel point Midwest Industries) was driven into the base of each sump, leaving the top few inches of the pipe extending above the drain floor. This was accomplished from the street surface with a 5400 Geoprobe direct push drilling rig using standard methods. Once installed, a threaded section of PVC riser pipe was connected to the top of the sandpoint to allow access at the road surface (in the sump). The top of the PVC pipe was covered with a watertight cap. The sandpoint wells were instrumented with a series of iButton data logging thermistors separated by baffles that allowed an independent vertical temperature profile to be obtained during infiltration events (Johnson et al., 2006). Thermistors were placed into the sandpoint wells at approximately 9 inch intervals, separated by baffles constructed of closed celled foam insulation wrapped with duct tape (creating a friction seal between monitoring devices). A total of five thermistors were placed into each sandpoint. Prior to installation, the thermistors were calibrated in the laboratory (Johnson et al. 2006). The 5 minute recording interval provided approximately one week of recording time, with oldest data being overwritten if there was insufficient space for a measurement; this was sufficient as the devices were retrieved after each runoff event. These data sets were analyzed using both analytical solutions presented by Hatch et al. (2006) and heat flow modeling software VS2DI (Healy and Ronan, 1996).

Methods to Characterize Percolation Rates

This work attempts to distinguish between the infiltration rate, the rate at which water enters the sump base, the percolation rate, and the rate at which water moves through the vadose zone. Percolation of water through a coarse-grained vadose zone was anticipated to be difficult to measure directly, as installation of instrumentation to detect variations in moisture conditions is challenging in coarse grain materials. The data collection program included installation of soil moisture monitors, application of geophysical cross-borehole tomography techniques, and an assessment of the response of the water table to specific surface runoff events. It was recognized that to assess possible differences in percolation rates, a detailed analyses of the sediment types, stratigraphies, and physical and hydraulic characteristics would be needed. The geological analysis methods and laboratory characterizations of both physical and hydrological site characteristics are described first; additional field methodologies are then presented.

Vadose Zone Stratigraphy

Characterizations of the sediment types and stratigraphy at each site were obtained by coring the vadose zone. The rotary sonic drilling method was selected for use in this project (Barrow, 1994). The method uses a dual tube diamond bit process that allows collection of 4 in. diameter sediment cores. The coring program was designed to obtain 10 ft continuous cores of

unconsolidated materials from land surface to 5 to 10 ft above the water table. The 10 ft long sediment cores were collected during drilling and placed into plastic core sample bags.

At the drilling sites, groundwater monitoring wells were completed inside the outer six inch diameter rotary sonic drill rod using 3 in inner diameter schedule 40 PVC well materials. Two soil borings were completed at the KQ, TS and HC sites, located approximately eight feet on each side of the center of the storm sumps (Figure 3.1). At the KQ and HC site, each boring was completed as a geophysical/monitoring well. At the TS site, the drilling subcontractor lost a segment of six-inch casing at the base of the second borehole, resulting in only a single monitoring well at that site. The construction of the monitoring wells was different from standard methods because they needed to accommodate borehole tomography geophysical tools in addition to providing measurements of water table position, response, and quality. The wells were not completed with a sand pack or long bentonite seal since this would dampen the geophysical signal between wells. The wells were completed with 10 feet of screen (slot 0.020 in) at the base, with PVC risers to the surface. The wells were finished with a neat-cement grout around the upper 3 ft, and at street level with a flush-mounted waterproof cover. Locking expansion caps were used to secure the wells. At the UM site, the completion of the boring as a monitoring well was not permitted.

The cores were described in the field and then transported to the Department of Geosciences laboratory where they were logged and photographed. The cores were opened and carefully examined in the sample bags to record fine scale sedimentological properties such as grain size gradations. Based on this initial assessment, core sections representing general sediment characteristics, including fine grained layers, were selected for hydrologic property and soil chemical analyses. Samples were placed into ziplock bags that were labeled with the drill hole location and depth. After the initial examination and sample collection, the sediment was carefully removed from the core bag, placed into a 4 in. diameter PVC pipe sample holder, and split length-wise where the sample was distributed evenly over the recorded sample interval. Once approximately 20 ft of sample was in place the entire interval was examined, logged and photographed. After the photographs were taken, additional samples for total organic carbon analysis were collected and placed in clean ziplock bags. The sediments were then re-bagged for storage in new core bags and relabeled.

Physical Properties. The primary mineralogy of the vadose zone core sediments was determined by visual examination during logging procedures. In order to obtain additional mineralogical data, grain point counts were performed on a total of 22 samples selected to represent dominant vadose zone sediment types (Folk 1974). These analyses used one hundred grains from both the fine fraction ($\leq$ 2 mm) and coarse fractions ($>$ 2 mm). The mineralogy of the samples representing identified zones of silt and clay intervals was determined using x-ray diffraction methods under the direction of Dr. Peter C. Ryan at Middlebury College, in Middlebury, Vermont (Moore and Reynolds 1997).

Core sub-samples selected to represent common stratigraphic intervals were further described by determining grain size distributions using a modified ASTM Method D 422 (ASTM, 2007). The grain size distribution for the $<$ 0.5 mm interval was determined separately using laser diffractrometry (Sperazza et al., 2004). Approximately 1.5 to 2 kilograms of sediment were separated from the cores after logging. Prior to sieving, the sub-sample was placed into a clean, stainless steel baking pan and placed in a drying oven (105°C) overnight. All sample sieving was completed by hand using standard soil sieves, to a final grain size of $<$

0.5 mm. Portions of the sediment fractions from grain sizes of < 2 mm were sub-sampled and composited for future geochemical analyses. The grain size distribution curves were plotted, and the uniformity coefficient and coefficient of gradation were computed for sampled intervals using standard techniques (Das, 1994).

Hydrologic Properties. The hydrologic properties of the unsaturated zone sediments were determined using a combination of controlled laboratory techniques. A total of eleven columns were constructed. Three were filled with sediments representing conditions at KQ and two columns were packed with sediment samples representative of dominant sediment types from each of the other four sites.

The columns were constructed of 2 ft long, 4 in diameter PVC pipe (Figure 3.10). Samples were packed by tapping and shaking in their recorded stratigraphic sequence. The sediments were disturbed to some degree as they were placed by hand into the columns. Large cobbles exceeding 2 in diameter were generally removed from the sediment sample as they were considered too large for the column. This may have biased column testing results; however, as the material is coarse grained this was unavoidable. Recognizing that this methodology resulted in the re-compaction of the original sample, testing results are considered to represent measurements of the upper limits of the sediment hydrologic properties. Grain size distributions of column specific samples were determined after all tests were completed.

Figure 3.10. Sediment filled columns and permeameter design. The instruments were suspended to allow determination of column weights during various stages in the lab experiments.

Values of saturated hydraulic conductivities were obtained using the following method. The columns were modified into constant head permeameters (Fetter 2004). Each column was modified by the installation of caps and PVC shutoff valves on both the upper and lower flow lines that allowed for easy movement of the influent and effluent lines. As each column test was initiated, the influent water line from an elevated recharge tank was connected to the input at the base, a permeameter, and an effluent line at the top of the permeameter. The permeameters were saturated from the bottom to minimize the amount of air trapped in the system. To test for short circuiting of water along the column sides a slug sodium chloride tracer was introduced, and specific conductance probe breakthrough curves were evaluated. The amount of water discharged through the permeameters was determined by monitoring the time required to fill a one-liter graduated cylinder. For each permeameter test, the rate was measured a minimum of five times to establish measurement uncertainty. The measurement of saturated flow conditions

for each column was conducted three times, with gravity drainage tests used to determine the specific yield of the sediments after each saturated flow experiment. The gravity drainage tests were completed by measuring the mass of water drained over specific time intervals. The gravity drainage was allowed to continue for a minimum of several weeks until no drainage was observed in the collectors.

The saturated hydraulic conductivity of column sediments was determined using the equation (Das, 1994)

$$K = \frac{VL}{Aht}$$

Where: V is the total volume of water moving through the permeameter over a time interval t
L is the sediment saturated length
A is the sample cross sectional area
h is the head difference between the constant head and outflow

A second method used to estimate the saturated hydraulic conductivity of the sediments applied an empirical relation between grain size and hydraulic conductivity developed for sand dominated samples, referred to as the Hazen method (Das, 1994). It is recognized that this methodology, though commonly used in hydrogeological studies, may not be appropriate to this study since the samples are not dominated by sand-sized material. It does, however, provide a second approach and may prove useful for estimating hydrologic properties where direct hydraulic testing is not available.

Modeling of vadose zone processes requires the derivation of the hydraulic function, a relationship between matric (pore) pressure, moisture content, and the unsaturated hydraulic conductivity. The hydraulic function can be approximated using scaling functions derived from the saturated field, or using laboratory hydraulic conductivity values (e.g. van Genuchten, 1980; Brooks and Corey, 1964; Millington and Quirck, 1961). Simunek et. al. (2003) present a review of the different types of models for characterizing unsaturated flow that compares these functions and the conditions where they are applicable. The saturated hydraulic conductivities derived from the column test were used to determine site-specific hydraulic function values.

After completing the last gravity drainage test, the sediments from each column were removed into a stainless steel pan and placed into a drying oven at 105°C for 24 hours. The bulk density was determined by dividing the dry mass of the soils by the total volume. The porosity of the sediments was determined by subtracting the mass of the dry sediments from the mass of the saturated sample, with the mass of water assumed as representative of void space. The saturated sample mass was determined by subtracting the dry mass of each column from the total mass of the column under saturation. The specific yield of the sediment was determined from the difference in mass between the saturated column and the column after completion of the gravity drainage tests. The field capacity was determined from the difference in the mass of the sediments after the initial gravity drainage and the dry mass of the soils.

A relationship between the sediment moisture content and the negative pressure head (matric potential) was evaluated during gravity drainage and drying of a representative sediment sample from the Kent Queen site. Mini tensiometers (Soil Moisture Corporation) were installed

directly into a permeameter through 0.25 inch diameter holes drilled through the walls of the PVC pipe. The 0.25 inch diameter porous bulbs were connected to 0.125 inch inner diameter flexible polyethylene tubing and inserted into one inch long depressions in the sample created by the drill bit. A small amount of silica flour was placed in these depressions. The annulus around the entry point in the PVC was sealed with aquarium cement. The tubing that extended from the column was attached to a water filled cylinder with a pressure gauge (Figure 3.11). Readings were monitored over time to establish negative pore water pressures. At the time of the data collection, the column weight was determined and the moisture content computed.

0.6 mm diameter porous bulb

Pressure gauges

Installation

Figure 3.11. Mini-tensiometers, presure gauges and set up in a PVC column.

Water Table Response. Storm water infiltration has the potential to induce mounding of the saturated zone of the receiving aquifers (Nimmer et al., 2009; Sumner and Bradner, 1996; Hantush, 1967). Water levels in both sumps and associated site monitoring wells were measured using Solinst datalogging pressure transducers (Solinst Inc.). The rate of percolation and its distribution over time was assessed by comparing sump water level changes during infiltration events with water level fluctuations in the underlying regional unconfined aquifer. Percolation rates were inferred from the thickness of the vadose zone beneath a sump base and the time between sump activation and the water table response.

Natural Water Quality as a Tracer. An additional approach to quantify the timing and rates of percolation used the observed natural changes in runoff water quality and groundwater chemistry. The collection of runoff specific conductance data and general ionic chemistry and changes in these components observed by sampling the underlying groundwater were evaluated. The methods used to collect water samples and characterize water quality are described in the Geochemistry part of the methods chapter in this report.

Surface runoff water chemistry was anticipated to generally reflect both the water quality of precipitation and street related influences during the May through October period. It was anticipated that runoff would contain low levels of constituents and that a “freshing”, or a reduction in specific conductance, of the groundwater quality would be observable as runoff reached the water table. Precipitation, street related influences, and runoff impacted by winter de-icing compounds were anticipated to dominate winter and early spring (November though May) storm water runoff. A measurable increase in the specific conductance of winter melt runoff was anticipated, as a magnesium chloride de-icer is used on the Missoula streets from

November through March. Schlumberger conductivity loggers were deployed during the winter period in selected sumps and associated monitoring wells to examine conductivity signals from winter melt/runoff events. In addition, in spring 2009, a set of Solinst LTC leveloggers that recorded specific conductance, water level changes and water temperature were installed at sumps and monitoring wells at KQ, HC and 2O to examine trends in specific conductance. These data were analyzed by comparing first arrival and breakthrough of specific conductance at the water table with the timing and specific conductance values of infiltrating water.

Gypsum Block Monitoring of Moisture Content. Seasonal and individual changes in ambient vadose sediment moisture profiles were attempted to be monitored qualitatively using standard gypsum blocks placed at multiple depths below the sump bases (Smith and Mullins, 2001; Ruprecht and Schofield, 1989; Williams, 1980). The gypsum block sensors were obtained from Soil Moisture Corporation, and were installed following manufacturer's instructions. These instruments are typically installed in agricultural settings to monitor moisture conditions in fine soils; thus, it was realized that they might not perform under the study site conditions.

The sensors were installed into the subsurface inside a 1.2 in. inner diameter flush coupled hollow two inch diameter steel drill pipe that was driven to depth using a Model 6600 Geoprobe subcontracted from MSE Technology, Inc., in Butte, Montana. The Geoprobe drill rod was installed through the sump base to depths greater than 15 ft. The drill pipe end was sealed during drilling with a disposable steel tip that was left at the bottom of the hole once the pipe was extracted. The drill pipe was driven to the desired depth and then pulled up about 6 in. Prior to installation, the gypsum block sensors were soaked in deionized water for approximately one hour. The sensors were placed into the borehole with approximately 250 cm^3 of dry silica powder installed by pouring it down the dry hollow drill pipe. The lead wires of the gypsum block were placed inside a continuous section of three-fourths inch outer diameter PVC pipe that extended to the surface. Once the block was in place, the drill pipe was extracted and natural materials were allowed to collapse around both the sensor and the small diameter PVC pipe. The annulus between the soils and the PVC pipe was filled with granular bentonite and hydrated to create a seal as the PVC pipe exited the sump bottom. Wire leads extended to the sump grate and were accessible from the street.

Gypsum block data sets were collected at regular intervals (Ruprecht & Schofield 1989, Williams 1980) using a Delmhorst Gypsum Block Reader which provided a relative measure of the soil moisture (a scale of 0 (dry) to 100 (wet)). Reader calibration data were collected each time field measurements were obtained to assure that results were within acceptable limits (Delmhorst Company, 2003). The readings were examined to identify variations in soil moisture readings. Percolation rates were to be estimated by computing the timing of moisture changes in sensor values and the vertical spacing of the sensors. The Delmhorst manual (2003) provides a general table used to convert readings to soil moisture tension.

Cross Borehole Geophysics. Geophysical borehole tomography was utilized to assess moisture front movement of artificially introduced percolation water. The geophysics program was implemented with support from Dr. William Clement with the Center for Geophysical Investigations of the Shallow Subsurface (CGISS) at Boise State University, Idaho. Dr. Clement has experience using ground penetrating radar methods (GPR) to obtain vertical borehole zero-offset profiles of soil moisture content in the vadose zone (Binley et al., 2001; Binley et al., 2002a; Binley et al., 2002b; Binley et al., 2002c; Deiana et al., 2008). For this study, the method

allowed imaging of the movement of the moisture front vertically downward with time at the HC and KQ sites during April 2008 and August 2008.

Data were acquired at the sites with paired monitoring wells by simultaneously lowering antennae into the two wells. One antenna sent the signal, and the second antenna acted as a receiver (Figure 3.12). The antennas were lowered in 0.25 m (0.8 ft) increments, maintaining the same vertical elevation for each to establish the zero-offset profile (ZOP). The first step was to record air wave traces to determine the starting time (T0) of the internal GPR clock. With a known distance, and a known signal velocity in air (~0.3 m/ns), the time necessary for waves to travel in air was determined. The starting time, T0, represents the delay time for the trigger, which is subtracted from each trace run to correctly position the arrival time. After the air T0 was determined for each simulated rainfall event (artificially created runoff event (or tracer test)), five ZOP traces were collected to establish a baseline prior to infiltration. The transmitter and receiver antennae were lowered down the well in 0.25m steps to the bottom of the well. The GPR used a 100 MHz signal, an 800 picosecond sampling rate, and a transmitter voltage of 400 V. The program stacked 32 traces in the field per recorded trace, with 312 samples collected per trace for a recording time window of 250 nanoseconds.

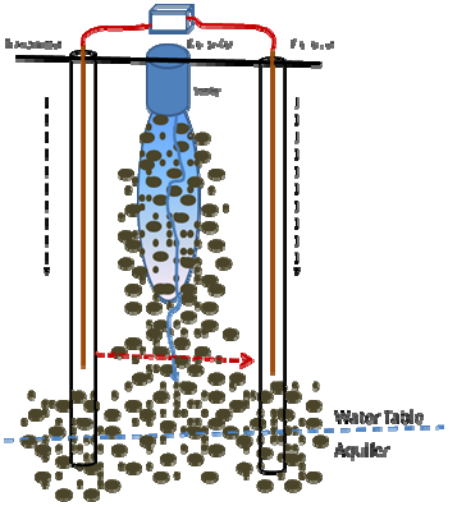

Figure 3.12. A schematic of ground penetrating radar instrumentation and site setup showing the lowering of transmitter and receiver sensors during an infiltration event. The process is repeated a number of times to examine the response of the signals to changing moisture conditions.

The data were recorded using a PulseEKKO system, which starts recording before the trigger pulse to ensure that the first arriving energy is recorded. Data results are compensated for the early start by shifting the data to the previously determined T0. For each trace in the ZOP, the peak of the first arriving energy was picked, then the time was shifted by ¼ wavelength based on the average frequency of the traces (89 MHz). The ¼ wavelength shift compensates for picking the peak of the arrival, which is easier to accurately identify, instead of the first arriving energy. Electromagnetic velocities in the subsurface correspond with the moisture content of the soils. The dielectric constant represents a property of the materials used, and is related to EM velocity by the equation

$$K = \frac{c}{}$$

$$K = \frac{c^2}{v^2}$$

Where: K is the dielectric constant
c is the speed of light in air, and
v is the velocity.

In the ZOP profiles, the travel time is measured and used to calculate the velocity, which is then used to determine the dielectric constant. The dielectric constant can be used to estimate the soil moisture content (Θ) using Topp's equation (Topp et al., 1980)

$$\Theta = -5.3\text{x}10^{-2} + 2.92\text{x}10^{-2} K - 5.5\text{x}10^{-4} K^2 + 4.3\text{x}10^{-6} K^3$$

Another method to evaluate moisture content utilized the CRIM equation (Chan and Knight, 2001)

$$K_m = \varphi(1-S_w) K_a^{½} + \varphi S_w K_w^{½} + (1-\varphi) K_s^{½}$$

Where: S_w is water saturation
φ is porosity
K_m is the determined dielectric constant
K_a is the dielectric constant of air (1)
K_w is the dielectric constant of water (80)
K_s is the dielectric constant of sediments (~4.5).

Vadose Zone Thermal Profiling. In-situ percolation rates through the vadose zone at study sites were evaluated by monitoring changes in the vadose zone temperature. Data logging thermistors (iButtons) were affixed to a 2 in diameter PVC casing that was placed inside available three inch diameter monitoring wells (Figure 3.13). Thermal monitoring was tested to a depth below land surface of approximately 40 ft. Temperature buttons were affixed to PVC pipe at 4 ft intervals. Each button was isolated from the adjacent instrument by creating a friction baffle constructed of closed cell thermal insulation and duct tape that was placed approximately 6 in above and below each sensor. Data were collected during early 2008. Changes in temperature during and after infiltration events were interpreted to be related to infiltrating storm water passing through the monitored area. Rates of percolation were computed from timing and sensor spacing information.

Figure 3.13. The design of a vadose zone temperature profile monitoring system installed in the monitoring well at the KQ site.

Artificial Tracer Testing. In an attempt to control the source water timing, volume, and quality, it was decided to conduct a number of controlled infiltration tests. Source water was obtained using Missoula Aquifer groundwater delivered from a municipal source to the site (water truck, fire hydrant or water line access port). The specific conductance of percolating artificial source water during these events was enhanced by adding sodium chloride as a tracer. Once again head, temperature, and specific conductance were logged in the sump and at the water table. During July and August 2009, a relatively dry period of the summer, such controlled infiltration tests were completed at the KQ, HC and 2O sites. The tests were conducted by first adding source water (tracer absent) to the sump to initiate and stabilize percolation through the system. After the initial volume of water had infiltrated, a second volume was added with a sodium chloride tracer. These tests were conducted twice at each of the three locations. For the HC site, where infiltration was relatively slow compared to the other sites, granular sodium chloride was added directly into and mixed in the sump, to obtain a relatively uniform concentration. For the KQ and 2O sites, sodium chloride was added as a concentrated solution to the infiltrating water using a peristaltic pump, as depicted in Figure 3.14. All site data loggers included in these tests, including the sandpont infiltration thermistor temperature buttons, were set to record at a two-minute sampling interval. Percolation rates were calculated using the distance to the water table, the timing of the first arrival, and the timing of the maximum specific conductance concentration. The timing of water level changes at the water table were also compared to the timing of the start of the testing.

Discharge of water to the 2O sump from a water line access port.

Water from hydrant flowing to the KQ sump

Peristaltic pump adding concentrated saline solution

Monitoring specific

Water ponded to the surface at

conductivity in sump recharge KQ sump

Figure 3.14. Artifical tracer testing at 20 and KQ.

METHODS TO CHARACTERIZE THE PROCESSES IMPACTING THE WATER QUALITY OF STORM WATER RECHARGING THE WATER TABLE

In order to investigate how the water quality of storm runoff is impacted by infiltration and percolation through a coarse grained vadose zone, data were collected to characterize the chemistry of the runoff "source" water, any observable or modeled transformations as it passes through the vadose zone, and its final quality as it enters the receiving groundwater system (Figure 3.15). Sampling both storm runoff events and the receiving groundwater quality at the water table are one approach that can be used to assess how transport through the vadose zone impacts recharge water quality. Ideal research settings would allow sampling of the water quality of percolating source water at various vertical intervals as it passes through the vadose zone. When in-situ vadose zone water quality data are not available, forecasting final groundwater recharge water quality requires a modeling approach. This approach uses the source water chemistry, geochemical properties of the vadose zone sediments through which the water passes, and the geochemical conditions within the vadose zone.

The water sampling program included collection of samples from storm water runoff, storm water ponded in sumps, vadose zone lysimeters, and groundwater monitoring wells. All samples were collected and placed into clean, acid-washed 250 ml polyethylene bottles. Samples were identified with a location code, date and type of sample. Immediately after collection, the samples were placed into an ice-packed cooler and transported to The University of Montana Department of Geosciences Environmental Geochemistry Laboratory for analyses. After each sampling event, a summary table of samples was prepared from field notes and forwarded to lab personnel as a chain of custody record to verify that samples had been transferred to laboratory personnel for analyses. Samples were filtered in the laboratory using a 0.45 μm filter and a peristaltic pump, with portions of the main sample transferred to smaller containers for laboratory analyses. The filtered metals samples were preserved with trace metals grade nitric acid to pH < 2. Specific analytical methods are referenced in this section.

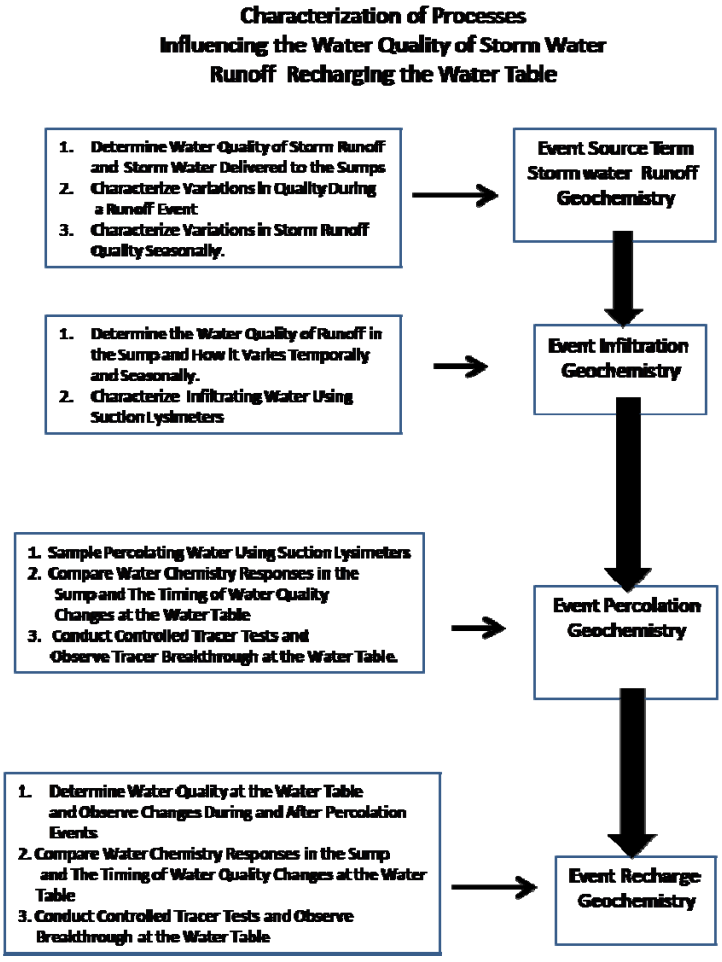

Figure 3.15. Flow chart of the steps used to characterize the processes influencing the geochemistry of storm water runoff as it infiltrates, and percolates to the water table.

Runoff, sump samples, and groundwater samples were generally analyzed for common ions, alkalinity and trace metals in order to characterize water type. Alkalinity was utilized to determine the bicarbonate concentration in the water. In addition to analyzing for standard chemical components of water, trace metals and arsenic concentrations for most samples were also reported. A limited number of water samples were analyzed for dissolved organic carbon, a proxy to evaluate the fate and transport of organic molecules during percolation. A limited number of water samples were collected and analyzed for volatile organic compounds to evaluate the presence of chemicals in storm water runoff and groundwater.

All geochemical analyses were completed at the University of Montana Environmental Geochemistry Laboratory at the Department of Geosciences, with the exception of sediment Total Organic Carbon and aqueous Volatile Organic Compound analyses conducted by Energy Laboratory in Helena, Montana. The applicable standard analytical methods are listed in Table 3.2. Quality assurance was conducted by UM Laboratory and Energy Laboratory staff in accordance with their respective Quality Assurance Plans. Both laboratory quality assurance programs include standard duplicate analyses, method blank analyses, and surrogate spikes to

assess the accuracy and precision of specific sets of analyses. When applicable, data qualifiers have been added to the data result tables presented in the following sections (EPA, 2000).

Table 3.2. Standard Analytical Methods Used for Field and Laboratory Water and Sediment Samples.

Media	Analyte	Method
Water	Anions	EPA 300.0
	Major Cations	EPA 200.7
	Trace Metals	EPA 200.7
	Alkalinity	EPA 310.1
	Total Organic Carbon	EPA 415.1
	Volatile Organic Compounds	EPA 8260
Soils	Extraction for Metals	EPA 3050
	Trace Metals	EPA 6010
	Cation Exchange Capacity	Barium Replacement Method
	Total Organic Carbon	Walkely Black Method

Though appropriate analytical procedures were used in all laboratory geochemical analyses, occasionally field samples did not meet holding times and as a result some alkalinity analyses were not performed. These samples were marked as screening level results. Alkalinity values were estimated and bicarbonate concentrations computed using ionic balance techniques (solving for alkalinity and bicarbonate concentrations assuming an ion balance of 1). Details are provided in appendices containing geochemical results.

Storm Water Runoff Source Water Quality

Runoff samples were collected both as grab samples and using a runoff sampler hanging from the surface grate. The grab samples were collected from ponded surface water by first rinsing a new, clean container, and then submerging it in a runoff puddle near the drain. Grab samples of runoff as it entered the sumps were collected by placing the sample container below the top of the sump grate in the runoff stream as it entered the sump.

The initial design of an in-situ runoff sampler used a disposable 1.5 in diameter polyethylene bailer sealed at the bottom. The open end was hung under the grate near the edge of the cover. Following an event, samples were either retrieved immediately or during the next day. Collected water was poured into labeled clean sample bottles, placed on ice, and transported to the appropriate laboratory.

After the first few months of attempting to sample runoff, a second version of the in-situ runoff sampler replaced the bailer (Figures 3.9 and 3.16). It was designed to provide more efficient collection of the first runoff waters from a storm event, including low flow events. The samplers were constructed using polyethylene funnels originally designed for filling gasoline tanks on lawn mowers. The central part of the funnels had air-filled catches which rise to the top to stop flow into the sampler once it is full. The sample container lid was attached to the funnel with aquarium cement, allowing for quick attachment and removal of new sample bottles. Plastic ties were used to secure the sample bottle to the funnel and to hang the sampler. The event sampler funnel and cap were thoroughly rinsed with deionized water after sample retrieval

and prior to placement of a new clean sample bottle. When samplers became noticeably soiled, they were taken back to the laboratory and washed with an alconox detergent bath, followed with a deionized water rinse.

Runoff sampler with attached sample bottle

Runoff sampler deployed in storm drain.

Figure 3.16. Runoff event sampler that was suspended from the drain grate. It includes an airfilled float that raises to the bottle top once full to limit further sample collection.

Water in the sump was also sampled by either a direct grab sample or an in-sump sampler located near the sump bottom. Event sampler data, direct runoff samples, and in-sump sampling data sets were used to represent the general character of the runoff and infiltrating water. Grab samples were collected by securing an open, new sample bottle to the base of a PVC staff using duct tape. The sample bottle was lowered into the ponded sump water to collect the sample. The first water retrieved was used as rinse water and discarded. A second sample was collected, capped, placed on ice and transported to the analytical lab. In an attempt to remotely sample water ponding in the sump during the initial rise in sump water level, clean sample bottles were taped to the vertical PVC pipe housing the sump stage transducer (Figure 3.9). The capped 250 ml sample bottles were modified by drilling several 5 mm diameter holes around the top of the sample bottle cap. The sample bottles filled as the sump water level rose above the bottle cap elevation. Once the bottle was full, no additional water entered. The samplers were retrieved within a day after any runoff event and the sample water was poured into a clean sample bottle. Because this was assumed to be screening-level water quality data, the samplers were cleaned and thoroughly rinsed with deionized water prior to replacement. During the winter, snow and ice cover frequently limited direct access to storm drains. When these conditions occurred, water samples were mostly collected from ponded water adjacent to a sump.

In order to characterize changes in runoff water quality during a storm event, runoff samples were collected during storm durations for a few events. Because storm intensities and durations are often difficult to predict and study sites are located over a wide area, it was difficult to sample a large number of events. For two storms in June 2009, regular hourly sampling intervals were obtained at the HC site. Seasonal changes in runoff water quality were evaluated by comparing runoff sample water chemistry results from winter and summer periods.

Volatile Organic Compound (VOC) analysis of runoff associated with a summer storm event was completed in 2009. In addition, the shallow groundwater was repeatedly sampled over a number of days following the storm event and analyzed for a suite of VOC. These samples were collected using standard 40 ml glass vials with Teflon septum lids supplied by Energy Laboratories of Helena, Montana. After collection, the samples were placed into an ice-packed cooler and shipped to the laboratory overnight with proper chain of custody documentation. The

analyses were completed using EPA Method SW846-8260 for the standard suite of volatile organic chemicals.

The geochemistry of percolating waters was evaluated by collecting water samples from lysimeters installed in the vadose zone, and using water quality samples collected from a well installed into a perched water-bearing interval above the water table at the KQ site. Lysimeters were installed at two depths at HC (12 and 20 feet bgs), and at single depths at TS (14 feet), KQ (14 feet) and 2O (16 feet). The lysimeters were small diameter (1.1 in) single chamber instruments constructed using 1 bar porous bulbs obtained from Soil Moisture Corp. The lysimeters were constructed using epoxy to bond the porous bulb to the end of a 1.6 ft length of 1.1 in diameter PVC pipe. The sample access tubes were 0.2 in diameter polyethylene tubing. The lysimeters were prepared for use by soaking them in a dilute nitric acid solution to clean the ceramic cups, and were continually flushed with deionized water using a vacuum until neutral conditions (pH) were achieved. Lysimeter installation during summer 2007 utilized a direct push Model 5400 Geoprobe. Emplacement of the lysimeters was accomplished by driving a flush coupled 2 in. diameter hollow drill rod equipped with an expendable drive point to the desired depth. The drill rod was pulled back approximately 6 in to allow the formation to collapse at the base of the borehole. A blank open-ended 1.2 in PVC pipe was installed to temporarily keep the hole from collapsing and the drill pipe was removed. A lysimeter was installed by lowering it to the bottom of the PVC pipe. As the larger diameter PVC pipe was pulled/extracted, the porous ceramic bulb was exposed to the formation material. During the beginning of this process approximately 250 cm^3 of dry silica powder (Soil Moisture Corporation) was poured down the dry PVC pipe followed by about 250 ml of deionized water as recommended by the vendor. The PVC access tube was left in place after exposing the instrument to protect the sampling tubing that extended to surface. After installation was complete, granular bentonite was placed around the outside of the PVC pipe at the sump base and hydrated to create a surface seal. The PVC and sampler tubing extended to the drain grate. The top of the PVC pipe was sealed with a water tight PVC cap at the sump grate.

In response to difficulties associated with the operation of lysimeters installed during the initial phase, a second phase of instrumentation was attempted during late Spring 2009. This phase used larger diameter and commercially available 1.5 in outer diameter PVC lysimeters (Soil Moisture Corp). Drilling was completed using a larger contracted Geoprobe rig. The larger lysimeters were installed using 3 in inner diameter hollow drive rods. Lysimeters were installed at KQ and 2O using this method. Unfortunately, during this process the subcontracted drill rig malfunctioned and installation activities were terminated.

Sampling was conducted utilizing both a standard vacuum pump (Soil Moisture, 2008) and a peristaltic pump. Because of the nature of coarse grained samples, the vacuum applied to the lysimeters was monitored to maintain a low level in order to allow for film flow on gravels to match the rate of water movement through the porous bulbs. Collected samples were placed in clean bottles, stored in an ice packed cooler, and delivered to the University of Montana Analytical lab for processing.

Vadose Zone Sediment Geochemistry

In an effort to indirectly examine how percolating water might be impacted as it passes through the vadose zone, the surface geochemistry of the sediments and their sorption properties

were determined. The fine fraction (< 2mm) of sediment samples for HC and KQ were selected for analyses of extractable compounds using several methods as follows:

- EPA 3050 extraction, utilizing a strong nitric acid solution to remove/dissolve readily available metals on mineral grain surfaces;
- Weak HCl extraction, to remove weakly sorbed metals on mineral grains, possibly associated with amorphous oxy-hydroxide minerals;
- Extractions with a barium chloride solution to determine the total amount of available sites for cation exchange (Cation Exchange Capacity);

Sediment samples were also evaluated to establish the percentage of organic carbon content by Energy Laboratory in Helena, Montana.

The potential for sorption of storm water constituents on vadose sediment surfaces was evaluated using standard batch tests methods. Once again, the same fine fraction samples (<2 mm) were used. Four representative core sections from two cores (KQ and HC), and a background sand (collected from a construction excavation), were combined with a deionized water control, a solution of sodium chloride (used in tracer tests), a solution of dissolved metal standards, and a solution of road de-icer. Additionally, one of the sediment samples and the background quartz sand sample were carried through the procedure with the above solutions prepared in collected rain water. The ASTM 4646D Standard Test Method for 24h Batch Type Measurement of Contaminant Sorption by Soils and Sediments with modifications that included a higher sediment to solute ratio and a longer mixing time (Limousin et al. 2006, Porro et al. 2000, University of Waterloo 2006) were used. The ratio of sediment to solute was 2:3 and concentrations of each solute were selected to bracket observed field concentrations. The batch tests were performed by placing 12 g portions of sediment in clean 30 ml wide mouth bottles which were then filled to 20 ml with the batch solution. Samples of sediment and the prescribed solution were shaken for 24 hours. Aliquots were drawn from each sample using a micro liter syringe and filtered (0.45 micron) into the appropriate vessel for each analysis, preserved according to standard procedures, and refrigerated. Anions were evaluated by Ion Chromatograph. Major and trace elements were evaluated by ICP at the University of Montana Environmental Geochemical Laboratory in the Department of Geosciences, using the methods listed above.

Plots of the solution concentration versus the amount of solute sorbed on the sediments were plotted and analyzed to compute sorption coefficients (Kd) and retardation factors using methods presented by Fetter (1999).

Water Quality of Groundwater Recharge

Groundwater samples were collected from monitoring wells following EPA guidelines for environmental water sampling (EPA method 1669, USEPA 1983). Monitoring well purging was completed using either a new clean disposable bailer, or a cleaned electronic pump. Typically three bore volumes of groundwater were removed and groundwater electrical conductivity was allowed to stabilize before samples were collected. The purge pump, only used at the HC site, was prepared for use with new polyethylene discharge tubing. The pump was thoroughly rinsed with distilled water between uses. All samples were collected using new clean disposable bailers.

Artificial Tracer Testing

As described in the previous section on examining the physical processes affecting the movement through the vadose zone, a series of artificial tracer tests were conducted at the KQ, HC, and 2O sites. The physical percolation of water was described by observing changes in the water table elevations, and the arrival of the first and peak concentrations of the tracer. The timing and distribution of the sodium chloride tracer during each test was also evaluated using breakthrough curves and mass balance analyses to assess both how the physical properties of the vadose zone effected tracer concentrations, and if geochemical processes impacted the observed magnitude and timing of observed concentrations (Fetter 1999). These data sets were then used in conjunction with laboratory determined sorption coefficients and ion exchange capacity results to model likely changes in the chemistry of percolating storm water runoff.

CHARACTERIZATION OF PHYSICAL AND GEOCHEMICAL PROCESSES INFLUENCING THE TRANSPORT AND FATE OF PERCOLATING STORM WATER

The results of the efforts to characterize the nature and quality of storm water runoff, and processes influencing percolating water, and groundwater recharge were first reviewed with respect to the proposed conceptual models presented in the introductory section of this report (Figures 1.1 and 1.2). The rapid transport and minor observable changes in groundwater quality at research sites suggest the vadose zone in this geological setting has allowed for rapid transport and limited impact to the quality of percolating water. In an attempt to examine and better quantify the physical and geochemical parameters influencing the recharge of storm water to the underlying aquifer, conceptual models were translated into vertical two dimensional cross sectional models. These models were used to represent the vadose zone conditions underlying valley CVIW sites.

The flow and transport process was numerically simulated at each site using Variably Saturated Two-dimensional Flow and Transport modeling package (VS2DI), a modeling suite created by the United States Geological Survey (Healy, 2007). VS2DI is composed of two components: VS2DH to simulate flow and energy (temperature) transport, and VS2DT, to simulate flow and solute transport (Healy, 2007; Healy and Ronan, 1996). It is recognized that unsaturated fluid flow and geochemical processes occur in three-dimensional space, however, since the dominant flow and transport component is vertical, a less complex (2D) unsaturated flow model representation of the percolation processes was used.

VS2DI iteratively solves the Richard's equation to generate the unsaturated flow field conditions for each model time step. The Richard's equation and other vadose zone governing flow equations use relationships between moisture content, pressure head and relative hydraulic conductivity (hydrologic function) to obtain unsaturated parameters. Boundary conditions in VS2DI allow for the specification of head, pressure or flux, evaporation, infiltration with ponding, plant transpiration, and seepage faces. Solute transport simulations in the VS2DT module are capable of simulating solute advection, dispersion, first-order decay, and ion exchange processes. Heat transport is simulated in the VS2DH module by modifying the solute transport parameters to represent heat properties and flux conditions.

The modeling process requires defining the geometry of the modeled setting (vertical profile dimensions and grid), vadose zone flow parameters (functions of pressure head vs. relative hydraulic conductivity and moisture content, and saturated hydraulic conductivity),

transport parameters (molecular diffusion and mechanical dispersion), heat capacities of water and sediment, and thermal conductivity), and initial conditions (pressure heads or moisture contents, and concentrations and temperatures) (Figure 3.17). Simulation results include moisture content, degree of saturation, pressure head, velocity or flux, and temperature and concentration distributions.

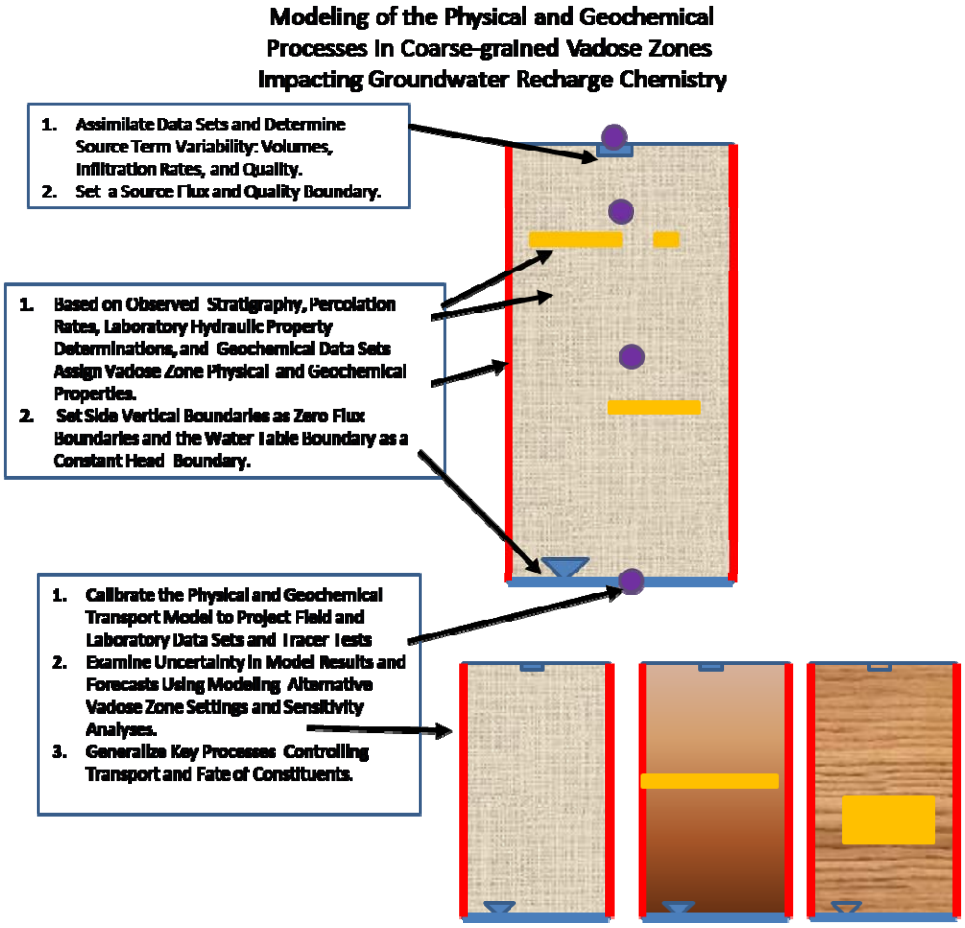

Figure 3.17. Flow chart of the vadose zone modeling process.

The modeling efforts used field and laboratory data for the KQ site to represent general valley vadose zone settings. Field and laboratory data were used to calibrate models to observed vadose zone flow conditions. Once the models were adequately calibrated the input water source conditions were varied to examine the behavior of flow and transport under varying geologic conditions. In order to develop a more generalized understanding of the properties and processes that dictate transport and fate of storm water in coarse grained vadose zone settings, additional simulations were conducted using general parameters to represent other typical geological settings. Results of this work were used to suggest how geological and vadose zone properties (in particular sediment coarseness) may impact the storm water percolation processes.

RESULTS

The study results are organized by first presenting the physical response of the vadose zone to natural storm water runoff events and controlled tracer tests. This is followed by observations of solute transport during natural runoff events as well as the controlled tracer tests. Next the geochemical characterization of the vadose sediments and the likely effect these properties have on infiltrating storm water are presented. Finally, results of site specific and generic numerical modeling of the transport and geochemical processes occurring during percolation are described.

STORM WATER RUNOFF SOURCES

A number of methods were used to quantify the volume of water entering the study site sumps. These methods included using precipitation data and paved runoff areas to compute runoff volumes, monitoring of water levels in sumps during runoff events, and variations in temperature within the bottom sediments to compute infiltration rates.

Precipitation data were collected during the project using tipping bucket rain gauges with an event resolution of 0.01 in that were installed at the KQ, 2O and UM sites (Figure 4.1). The rain gauges operated continuously through the project, from Spring 2007 to Summer 2009, with the exception of the winter months of late 2008-early 2009 when the batteries for the data loggers failed.

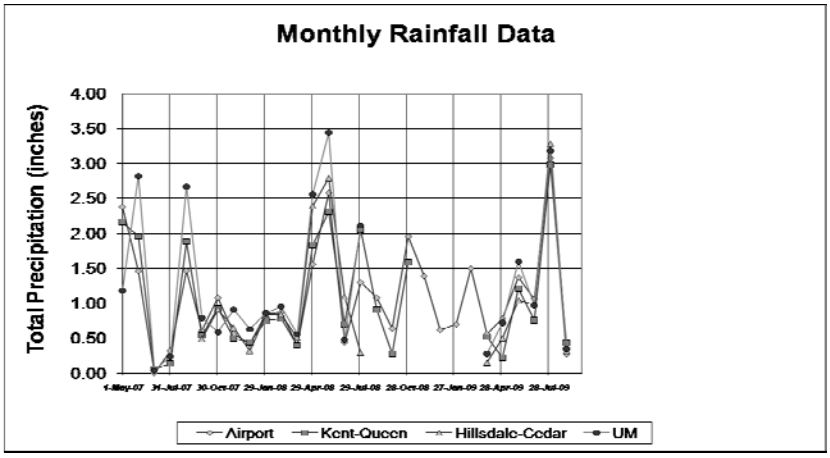

Figure 4.1. Monthly rainfall totals from the three project gauge sites and the Missoula County Airport located in the valley about 5 mi west of downtown Missoula. Airport data are considered representative for conditions at sites when data gaps occurred.

Low rainfall rates and volumes, and high rainfall rates and volumes were difficult to capture. Runoff water quality was not monitored at all sites for all storms (Figure 4.2). Winter precipitation was not usually recorded at most project gauges as most fell in the form of snow. Winter snows were often partially removed in various stages by street clearing processes, and/or

melted to varying degrees during warmer periods. Winter conditions also often limited data collection as sumps and equipment were often inaccessible

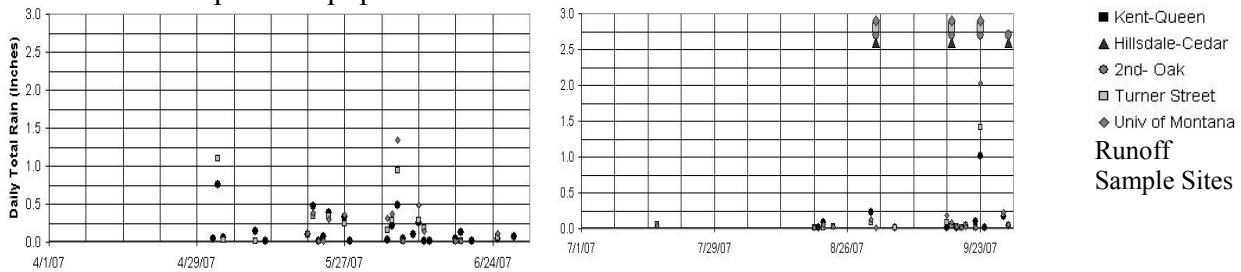

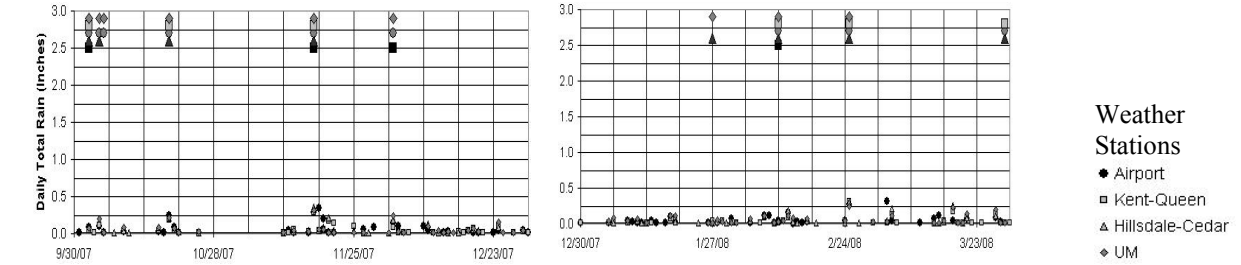

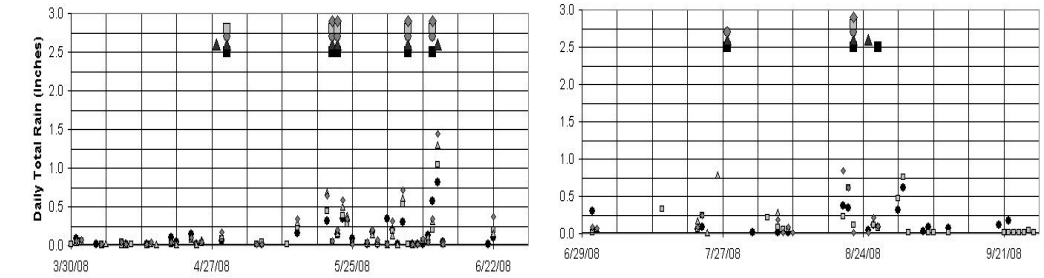

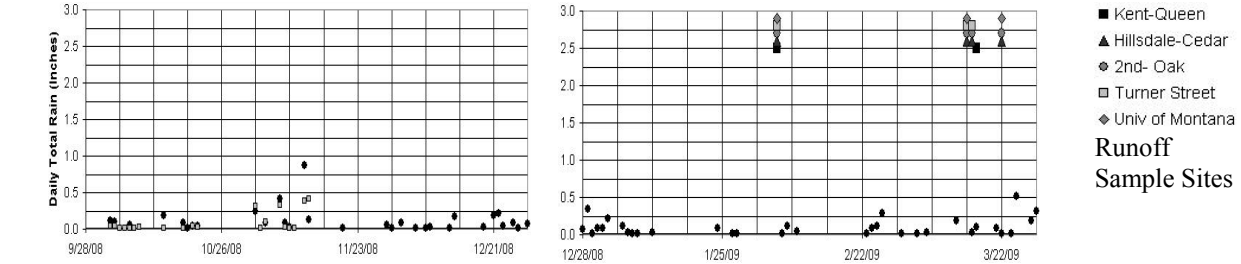

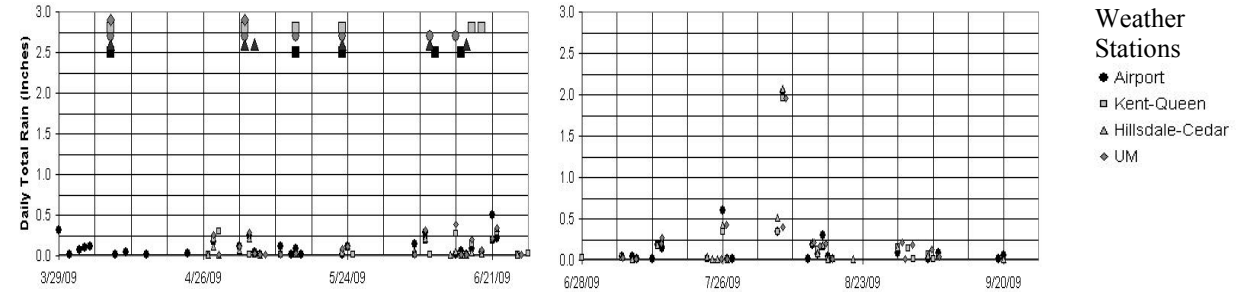

Figure 4.2. Plot of precipitation event totals (in) measured at the 4 precipitation gauge stations plotted using small symbols in relation to the y axes. The larger symbols along the top graph axes are indications of a surface water quality sampling at a specific site.

Results of the Precipitation-area Approach

For each of the five sites, the surface runoff contributing areas, or catchment, were mapped using GIS methods. The primary contributing areas were interpreted as the paved areas up gradient of each selected storm sump that extended to a local hydrologic (topographic) divide (Figures 3.3 to 3.7; Table 4.1).

Table 4.1. Physical Conditions at Each Research Site.

Site	Catchment Area	Runoff Slope	Sump Depth		Sump Volume	VZ Thickness	Depth to WT High	Depth to WT Low	Water Table Variation
	(ft2)	(avg.)	ft	ft3	gal	ft	ft bgs	ft bgs	ft
Kent-Queen	12460	0.003	4	12	90	42*	44	>48	>4
Hillsdale-Cedar	5800	0.005	3.5	14	105	26	17	29	12
2nd-Oak	9500	0.005	8	64	479	45	45	57	12
	5000	0.007	8	64	479	42	44	56	12
	18700	0.005	9	77	576	70**			

* Receiving groundwater is perched, above water table at approximately 65 ft bgs

** No well was installed at the UM site

The initial approach to computing runoff that entered the storm drain at research sites during the study period simply took the computed paved contribution area and multiplied it by the storm recorded precipitation (Figure 4.3). This approach assumes all water hitting the paved areas contributing to a drain would flow to and then enter the sump. These values are impacted by evaporation and a loss of water needed to wet pavement surfaces, however in this analyses these reductions were ignored. These processes most likely had a larger influence on events that were of small volume and low intensity in contrast to short term high intensity runoff events (that often dominated runoff contributions at sites). As a result, computed runoff values are estimates that represent maximum runoff values.

Monthly combined runoff at the five sites ranges from a low of about 1,700 gallons in July 2007 to 101,700 gallons in September 2009. Over the 29 months of monitoring a total of 1,064,000 gallons of water was available to enter the vadose zone at the five research sites. Using data for a winter period defined as November 2007 through April 2008, and a summer

period of May 2008 through October 2008, 40% of the precipitation/runoff was available to become runoff during the winter period and 60% in the summer. Some storm runoff occurs during each month with summer and fall periods contributing the largest quantities. These data also show the runoff to the UM site is greater than for other sites because it has the largest contributing area and a higher quantity of precipitation.

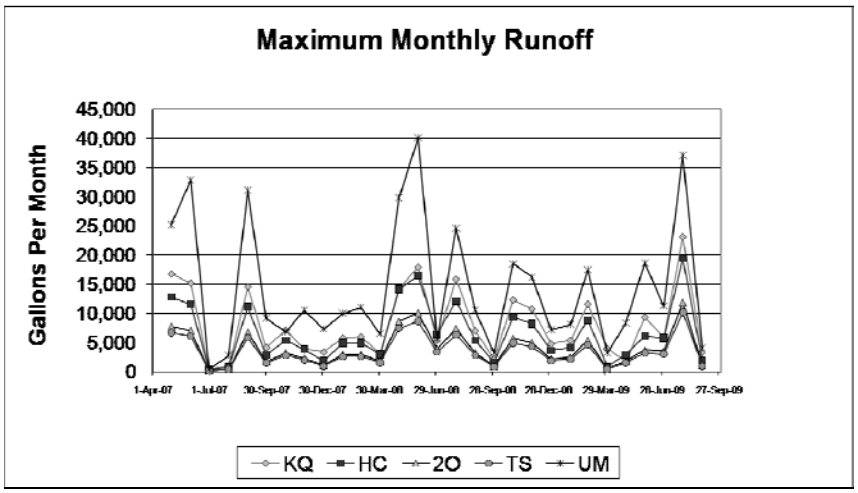

Figure 4.3. Computed monthly runoff assuming all precipitation falling on paved contribution area (Table 4.1) flows into the associated sump.

The timing of runoff and its relationship to storm intensity was examined using site specific synthetic unit hydrographs (Linsley et al., 1992). The synthetic hydrographs were developed for each site based on the size of the contributing catchment area and were treated as preliminary unit hydrographs (Linsley et al., 1992) (Table 4.2). They were scaled to match recorded rainfall and compared to actual runoff ponding data from the sumps. A triangular shape for the hydrograph was used as a simplification of the actual curve. The hydrograph assumes that the portion of the hydrograph related to the rise of peak flows occurs at 3/8 of the total base time. The receding part of the curve accounts for 5/8 of the base time. The storm duration is assumed to be less than 0.25 of the time for the rising part of the hydrograph. For this study, the peak flows for a storm event of constant rainfall intensity are estimated to occur at the time of equilibrium as presented in Table 4.2. A mass balance is used to account for all runoff from the catchment, based on the total rainfall amount.

Table 4.2. Estimates of Peak Flows at Study Sites Based on a Rate of 1 in/h.

Site	Flow Length	Gradient	Catchment Area	Constant	Time of Equilibrium	Peak Flows		
	L (ft)	S	A_d (ft^2)	b	min	cf/hr	cfs	Gal/h
KQ – Kent Ave	370	0.0044	7150	0.0773	22.76	596	0.17	4,460
KQ Queen St pt 1	125	0.0031	2450	0.0871	25.64	204	0.06	1,500
KQ Queen St pt 2	135	0.0013	2860	0.1179	34.70	238	0.07	1,800
Kent Queen – Total						1038	0.29	7,800

2nd - Oak	60	0.005	5800	0.0743	11.92	483	0.13	3,600
Hillsdale Cedar	175	0.005	9500	0.0743	14.13	792	0.22	5,900
Turner Street	100	0.0075	5000	0.0649	12.35	417	0.12	3,100
Univ of Montana	450	0.005	18700	0.0743	23.33	1558	0.43	11,700

An example of a runoff hydrograph for a 0.15 in storm event at the Hillsdale-Cedar site is depicted in Figure 4.4. The correlation of synthetic hydrographs to actual runoff events was used to investigate if this approach provided necessary information. It is recognized that Unit hydrographs can be scaled to reflect different rainfall amounts, and can be added to simulate different event durations.

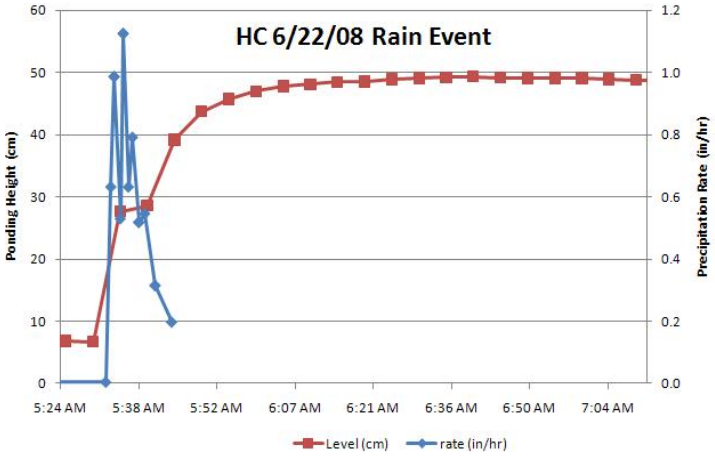

Ponding levels in HC sump in response to a short duration, high intensity rain event. During peak flows, the runoff rate into the sump corresponds to the rate estimated for the ponding level from infiltration tests, approximately 15 gpm.

HC	
Date & Time	rate (in/hr)
6/22/2008 2:43	0.0005
6/22/2008 5:32	0.0036
6/22/2008 5:33	0.6316
6/22/2008 5:33	0.9863
6/22/2008 5:33	0.9863
6/22/2008 5:35	0.5294
6/22/2008 5:35	1.1250
6/22/2008 5:35	1.1250
6/22/2008 5:36	0.6316
6/22/2008 5:37	0.7912
6/22/2008 5:38	0.5180
6/22/2008 5:38	0.5180
6/22/2008 5:39	0.5455
6/22/2008 5:41	0.3144
6/22/2008 5:41	0.3144
6/22/2008 5:44	0.1967

Rainfall rate data from HC rain gauge, for a total rainfall amount of 0.15 inches.

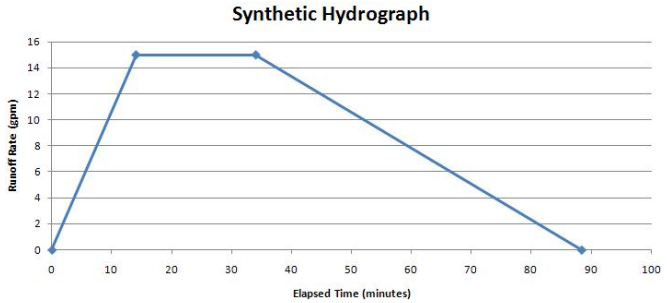

Synthetic hydrograph simulating runoff from rain event. Time to peak flow estimated at 14 minutes (Table 4.2). Peak flow rate is estimated from 1 in/hr rate of 18 gpm. With rainfall rate information above, peak flow for this event was estimated at 15 gpm

Interval (min)	Elapsed Time (min)	Runoff Rate GPM	Runoff Volume Gallons
0	0	0	0
14	14	15	105
20	34	15	300
54.4	88.4	0	408
	total runoff (gallons)		813

Endpoint data and mass balance for rain event. Total runoff estimated from catchment area size (9,500 ft2) and total rainfall (0.15 inches), 888 gallons.

Figure 4.4. Development of synthetic storm hydrograph for the HC site.

Another approach to computing the volume and timing of storm water entering sumps was derived by examining records of the rate and duration of water ponding (water level data) during an event and combining these data with sump dimension information (Table 4.1). To generate these data, the sump water level changes and timing were initially monitored using a vertical rod that was outfitted with a number of individual temperature sensors. However, these temperature staff gauges were discontinued because of resolution issues and replaced with recording transducers. An example of the temperature stage gauge approach collected at the UM site during a 2 day period in June 2007 is illustrated in Figure 4.5.

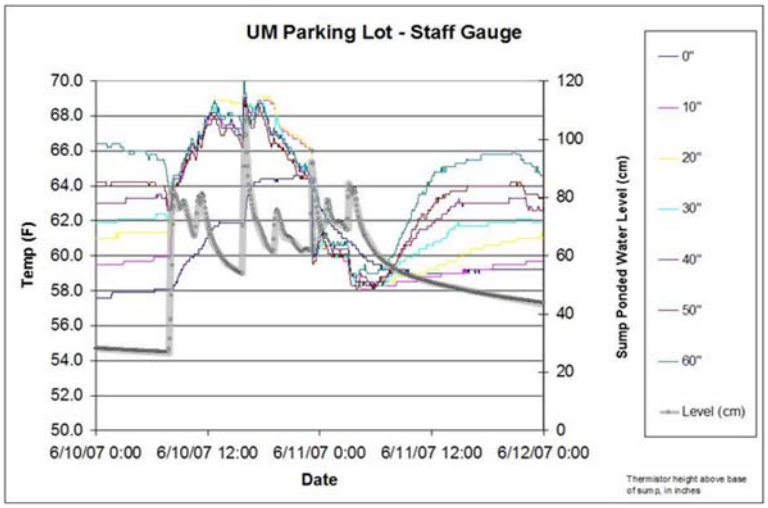

Figure 4.5. Sample sump thermistor staff gauge results compared with ponding levels in the sump (as inches from the sump base 1in= 2.5cm) over a two day period at the UM site. Water levels in the sump (in cm above the sump base) were at 30 cm above the sump base prior to the 6/10/07 event.

The water level data for Figure 4.5 was collected by a transducer placed at the base of the sump (Level = 0 cm). The air temperature distribution in the sump prior to the start of the storm event (that occurred about 10:00 AM on 6/10/07) ranged from 58.0 F near the bottom to 66.5 F 60 inches (152 cm) above the sump base (a difference of 8.5 F). At the initiation of the runoff event, the two highest thermistors cooled while the remaining instruments recorded an increase in temperature; thermistors located at the bottom of the sump concurrently registered the same temperature increase as they were submerged. It appears the water remained ponded until the mid morning of 6/11/07. As the water level began falling, the highest to lowest thermistors were successively exposed to the sump air temperature resulting in the pattern of rising temperatures shown in Figure 4.5.

Recording transducer instruments replaced the temperature staff gauges. Transducers simultaneously record the stage, temperature and time, thereby allowing the direct measurement of water levels during ponding events. Transducers were placed on the floor of the sump and water levels were recorded as depth below street level (below surface), or the level above the sump bottom. When runoff events were of sufficient duration and intensity, and in some cases when sump sediments were at high moisture contents (as related to antecedent conditions), infiltration rates were exceeded and sump water levels rose allowing the recording of sump stage.

An example of transducer sump water levels for a portion of the late summer period (a period mostly impacted by short duration storm events) is illustrated in Figure 4.6. A portion of the winter transducer data shows events were dominated by periods of melting of ice and snow (Figure 4.7).

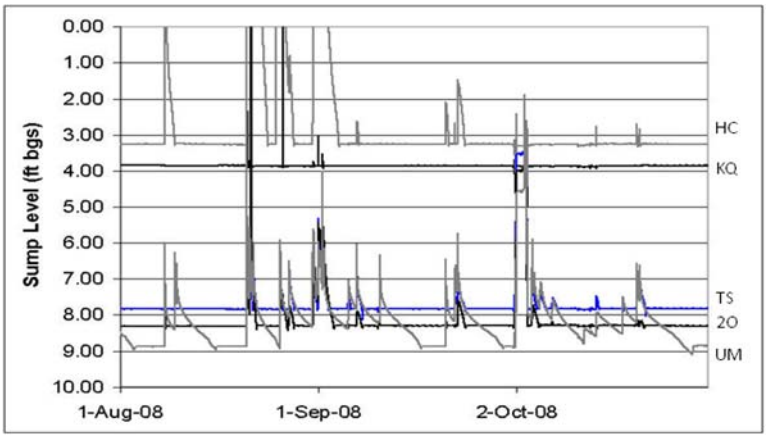

Figure 4.6. Late summer period sump level transducer data at all 5 sites. Levels are reported as above the base of the sump (e.g. KQ sump is 4 ft deep). Levels shown to reach zero indicate street ponding occurred.

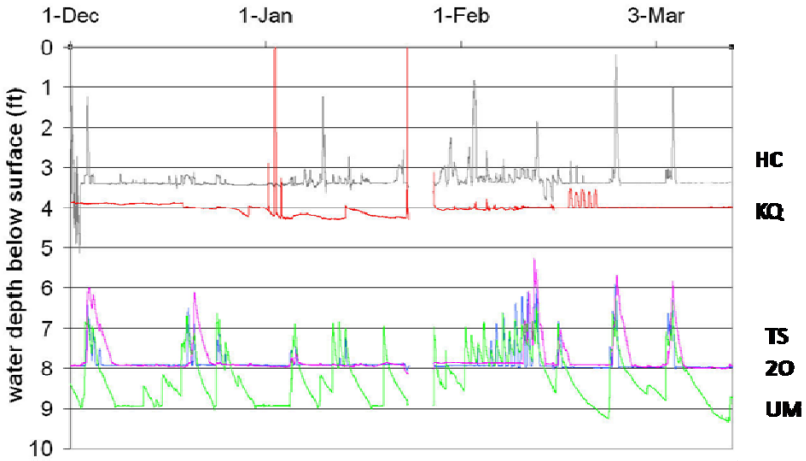

Figure 4.7. Sump water levels reflecting winter storm and snow melt events. Levels are reported as above the base of the sump (e.g. KQ the sump is 4 ft deep). Levels shown to reach zero indicate water levels reached the street elevalation and ponding occurred.

The winter record indicates that ponding only occurred at KQ in response to winter events. This is interesting as ponding events during the summer period were rarely observed. Two possible reasons for this are either runoff quantities were greater in the winter, or, sump infiltration rates were affected by periods of freezing conditions. The winter period record shows that runoff is a result of above freezing rain events and periods of warming that melted snow and ice cover. Significant warming and snowmelt occurred at the beginning of February

2008, with diurnal fluctuations in sump levels. The runoff pattern was not observed at KQ site until late February because apparently the high infiltration capacity at this site limited ponding.

INFILTRATION RATE ESTIMATES

Quantification of the source water infiltration rates under a number of different runoff conditions was developed to understand possible ranges and likely controls on sump infiltration capacities. Four approaches were use to bracket field conditions.

Stage and Sump Geometry Analyses

The first involved analyses of the temperature staff gauge and water level transducer data at each site combined with event duration and volume data. These data sets were used to evaluate under what conditions precipitation events (e.g. at < 0.01 in/hr no ponding was observed to occur) caused storm water runoff to enter site sumps (Table 4.3). The relationships between ponding height and storm intensity, and ponding height and total rainfall for the three sites instrumented with precipitation gauges are presented in Figure 4.8 through 4.10.

Table 4.3 The Precipitation Threshold at which Measurable Sump Stages Occur. Local Site Precipitation Gauge Data Used for the Three Instrumented Sites.

Site	Precipitation Intensity Threshold ➢ in/h	Precipitation Intensity Threshold Total Storm Volume ➢ in
KQ	0.02	0.1
TS	0.01	0.05
2O	0.01	0.05

At each site the relationship between rainfall volume and ponding height, though not necessarily linear, shows a general increasing trend as expected. The relationship between rainfall rate and ponding height seems to increase more rapidly for lower rainfall rates than higher ones, though few high intensity storms were monitored during the study.

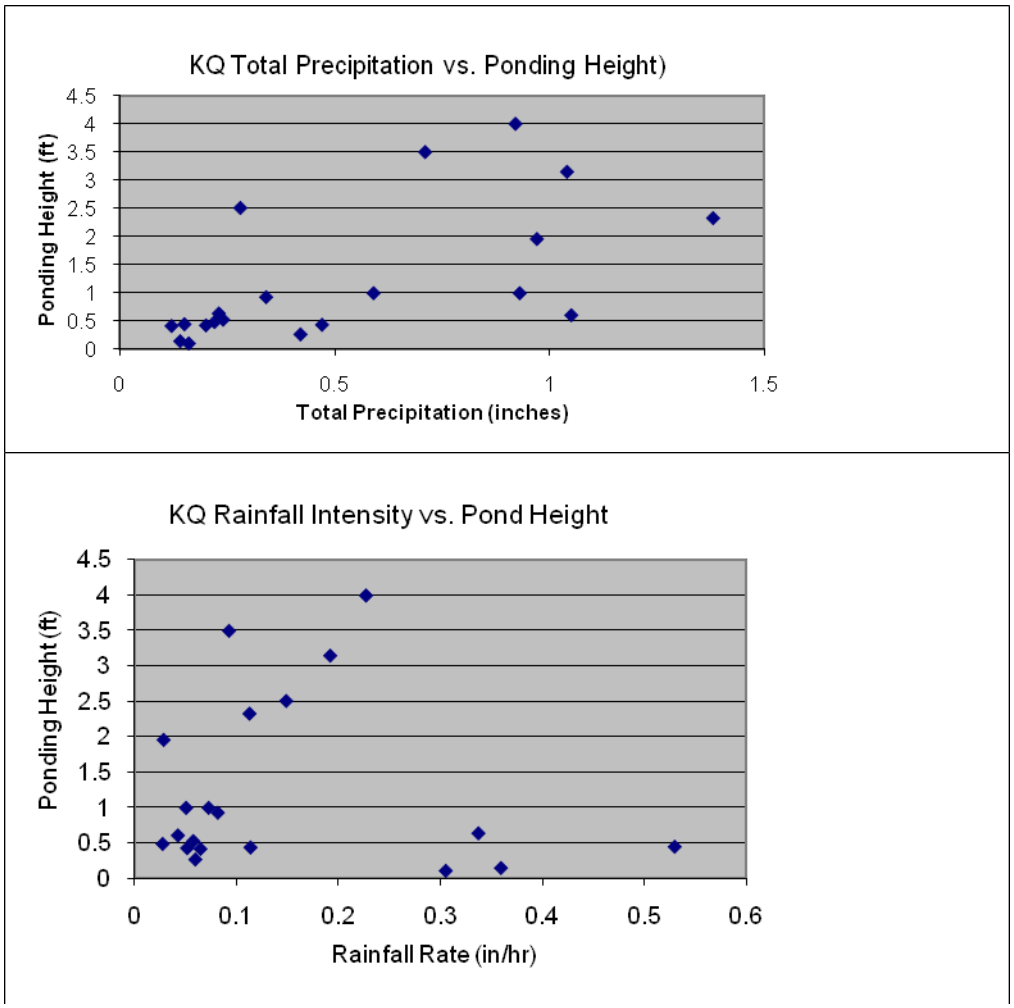

Figure 4.8. KQ relationships of total event precipitation and rainfall rate with ponding height (sump stage measured from the bottom of the sump). Ponding occurs at 4 ft above the sump base (0 ft).

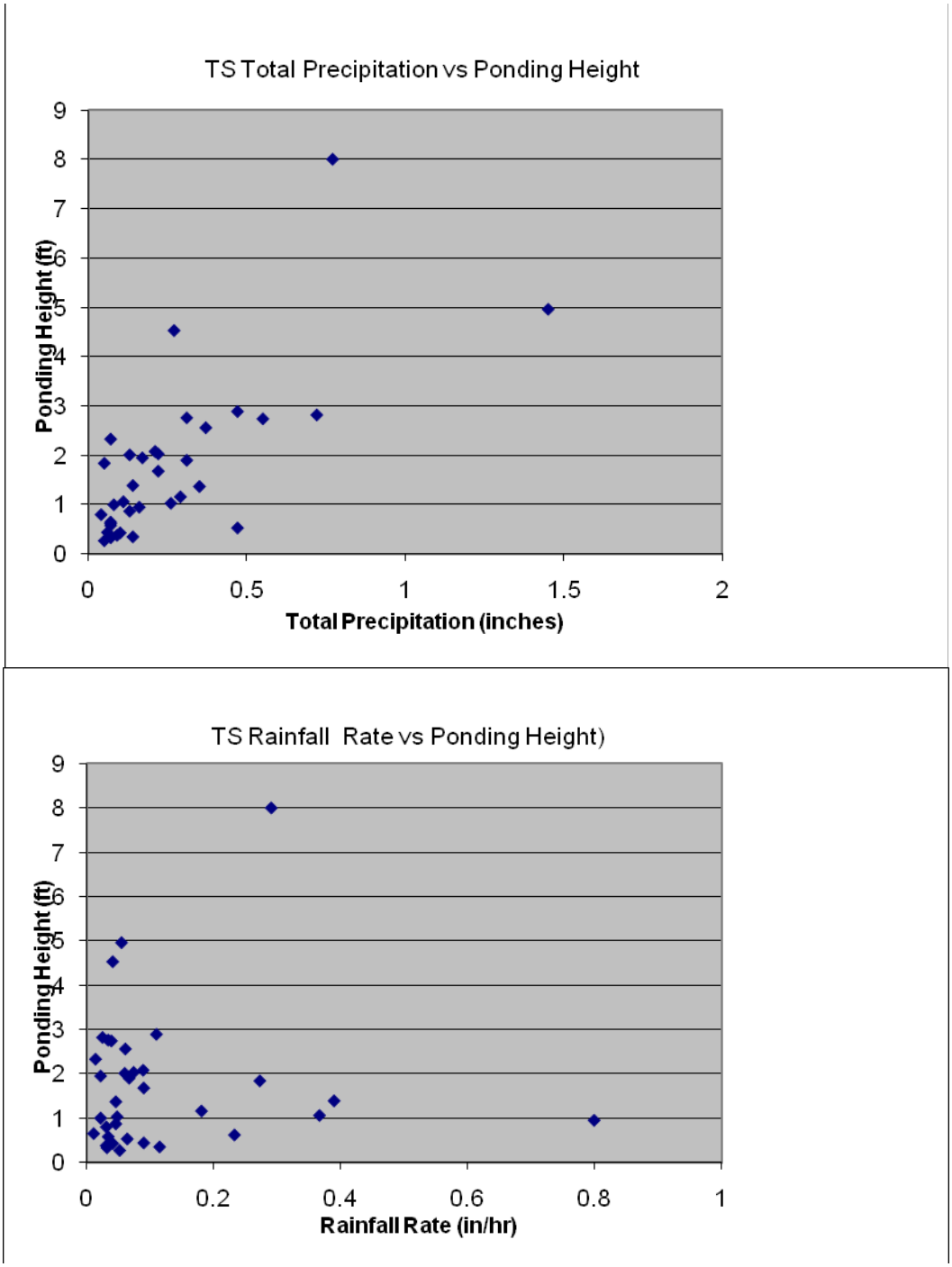

Figure 4.9. TS relationships of total event precipitation and rainfall rate with ponding height (sump stage measured from the bottom of the sump). Ponding occurs at 8 ft above the sump base (0 ft).

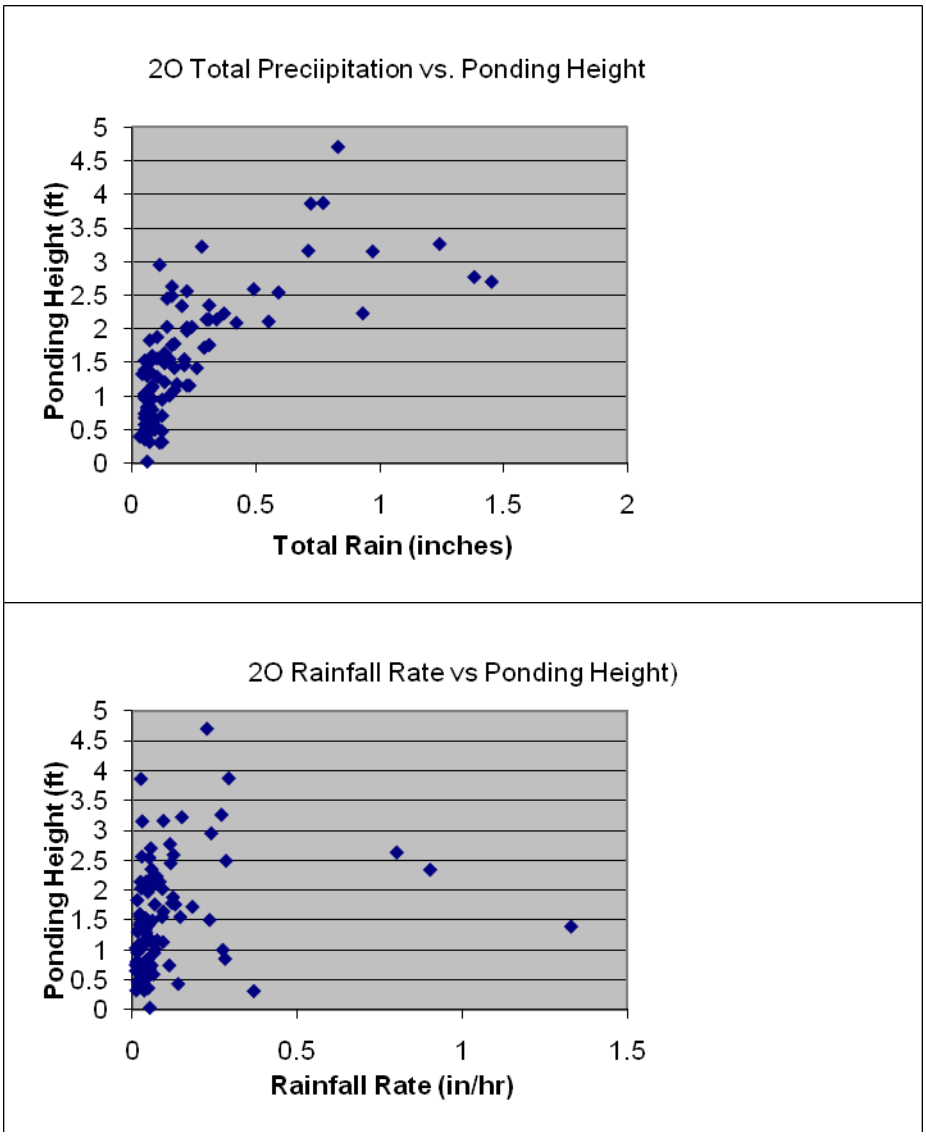

Figure 4.10. 2O relationships of total event precipitation and rainfall rate with ponding height (sump stage measured from the bottom of the sump). Ponding occurs at 8 ft above the sump base (0 ft).

Natural Infiltration Events

The second approach to determining infiltration rates used field observed changes in sump stages and sump geometry. Infiltration rates under these conditions were estimated by analyzing the rate of fall of the water levels in the sumps. This information was then used to calculate time variant infiltration rates (Fetter, 2004). An example of these data are depicted in Figure 4.11. The slopes of these infiltration curves can be used to estimate average infiltration rates, as listed in Table 4.4.

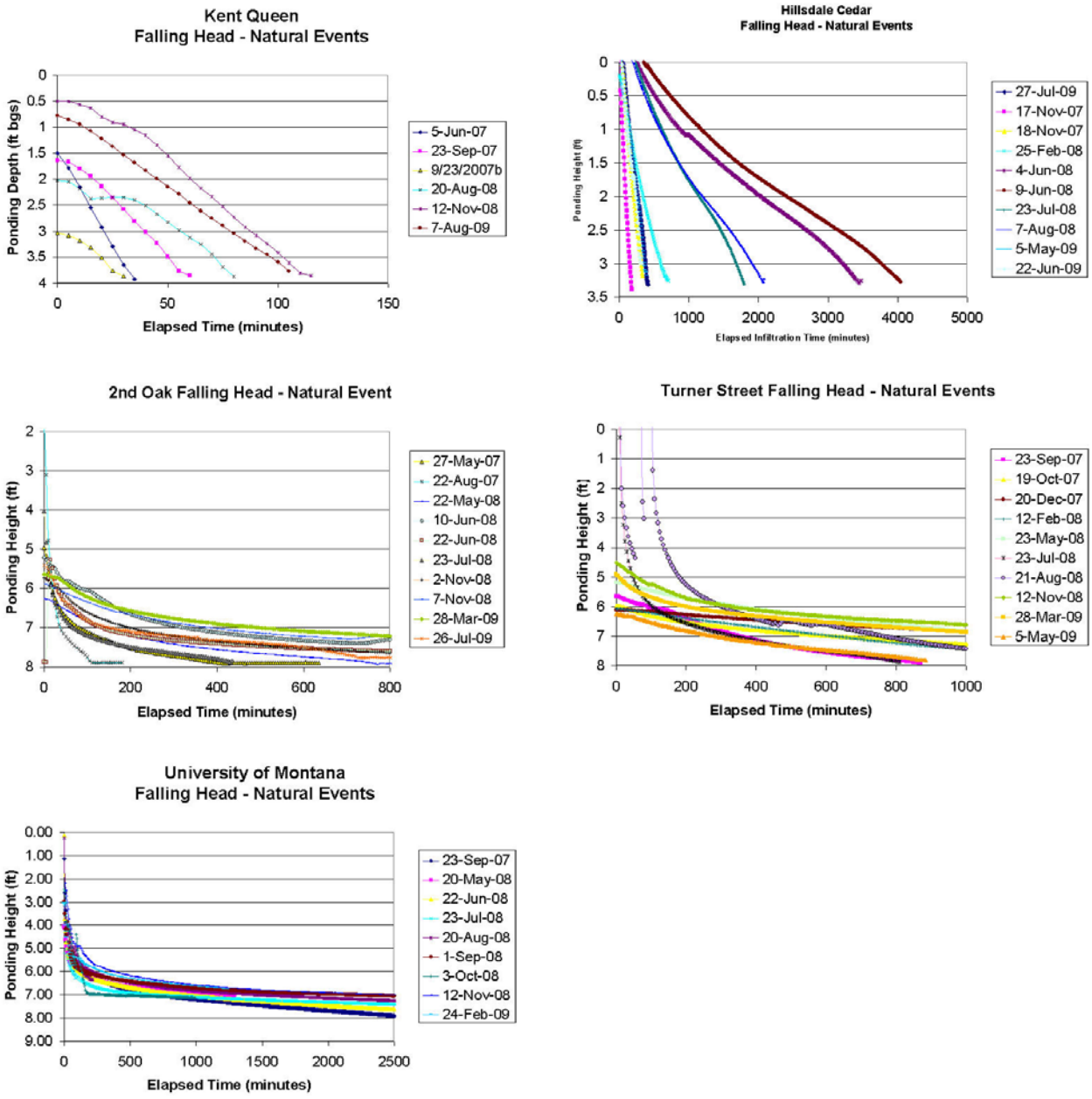

Figure 4.11. Falling head curves for rain events with ponding at study sites. The plot for Kent Queen shows all natural events where more than one foot of ponding occurred. The plots for the remainder of sites include representative curves showing the variability in infiltration rates at the sites.

These analyses show that there is a wide range of variability between site-specific event infiltration rates. At KQ and HC infiltration averaged 2.4 and 0.4 ft/h, respectively. A large number of events were evaluated at the other sites; they were classified as slow, intermediate and rapid. At 2O lower rates averaged 0.06 ft/h, intermediate 0.7 ft/h, and rapid 15.3 ft/h. Rates

recorded at TC ranged from 0.08 ft/h, 2.7 ft/h and 25.5 ft/h, respectively. At UM they were 0.02 ft/h, 2.3 ft/h and 25 ft/h.

Table 4.4. Infiltration Rates when Ponding Conditions Occur in Sumps (not including rates where ponding is present to surface)

KQ Natural Event

Slope ft/hr	Rate gpm
1.75	2.74
1.79	2.80
2.05	3.21
2.06	3.23
2.74	4.29
4.16	6.52
n 6	6
avg 2.43	3.80
med 2.06	3.22
st dev 0.92	1.44

HC Natural Event

Slope ft/hr	Rate gpm
0.05	0.08
0.06	0.09
0.10	0.16
0.13	0.20
0.26	0.41
0.53	0.83
0.56	0.88
0.66	1.03
0.66	1.03
1.07	1.68
n 10	10
avg 0.41	0.64
med 0.40	0.62
st dev 0.34	0.53

TS Natural Event

Slow Slope ft/hr	Slow Rate gpm	Intermediate Slope ft/hr	Intermediate Rate gpm	Rapid Slope ft/hr	Rapid Rate gpm
0.043	0.07	1.74	2.73	17.69	27.71
0.056	0.09	2.72	4.27	20.25	31.72
0.062	0.10	3.72	5.83	28.76	45.06
0.064	0.10			35.42	55.50
0.080	0.12				
0.083	0.13				
0.084	0.13				
0.114	0.18				
0.118	0.18				
0.125	0.20				
n 10	10	3	3	4	4
avg 0.08	0.13	2.73	4.28	25.53	40.00
med 0.08	0.13	2.72	4.27	24.51	38.39
st dev 0.03	0.04	0.99	1.55	8.12	12.72

2O Natural Event

Slow Slope ft/hr	Slow Rate gpm	Intermediate Slope ft/hr	Intermediate Rate gpm	Rapid Slope ft/hr	Rapid Rate gpm
0.036	0.06	0.758	1.19	15.31	23.98
0.064	0.10	0.547	0.86		
0.075	0.12				
0.039	0.06				
0.06	0.09				
0.069	0.11				
0.064	0.10				
0.056	0.09				
n 8	8	2	2	1	1
avg 0.06	0.09	0.65	1.02	15.31	23.98
med 0.06	0.10	0.65	1.02	15.31	23.98
st dev 0.01	0.02	0.15	0.23		

UM Natural Event

Slow Slope ft/hr	Slow Rate gpm	Intermediate Slope ft/hr	Intermediate Rate gpm	Rapid Slope ft/hr	Rapid Rate gpm
0.012	0.02	0.35	0.55	12.97	20.32
0.013	0.02	1.32	2.07	14.93	23.38
0.014	0.02	1.53	2.40	17.76	27.82
0.017	0.03	1.70	2.66	36.18	56.69
0.017	0.03	1.83	2.86	43.09	67.50
0.017	0.03	1.89	2.96		
0.024	0.04	2.13	3.33		
0.028	0.04	2.44	3.83		
0.030	0.05	3.11	4.87		
		3.39	5.32		
		5.43	8.50		
n 9	9	11	11	5	5
avg 0.02	0.03	2.28	3.58	24.99	39.14
med 0.02	0.03	1.89	2.96	17.76	27.82
st dev 0.01	0.01	1.33	2.09	13.70	21.47

Artificial Event Analyses

A third approach to establishing infiltration rates involved the artificial introduction of water to the sump under conditions that the total volume of water was known. The first set of infiltration experiments were conducted in August 2007. Additional controlled experiments included the geophysical experiments in April and August 2008, and tracer tests conducted during July-August 2009.

The first set of experiments was conducted partly because few large runoff events occurred during the summer 2007. These experiments were designed to test installed subsurface instrumentation and to obtain infiltration rate data for the sumps. Experiments were completed

at all sites except UM. The UM sump was evaluated using natural event data, as previously discussed. Water was introduced to the sumps using a water truck. Hydrographs of the ponding level in the sumps are shown in Figure 4.12. The falling head portions of the hydrographs were separated to evaluate infiltration rates, as shown in Figure 4.13 and 4.14. These curves were further divided into steep and low slope segments, reflecting rapid infiltration at high stage conditions, and slower infiltration rates as the ponding levels receded. A range of infiltration rates were estimated for each time interval, with maximum and minimum rates listed in Table 4.5.

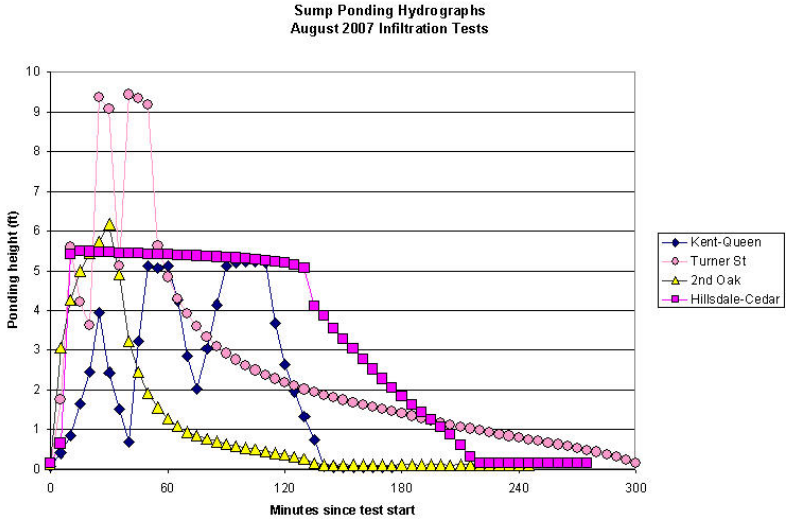

Figure 4.12. Hydrographs showing ponding height in sumps at each site during August 2007 infiltration tests. Multiple peaks represent separate discharges from the water truck.

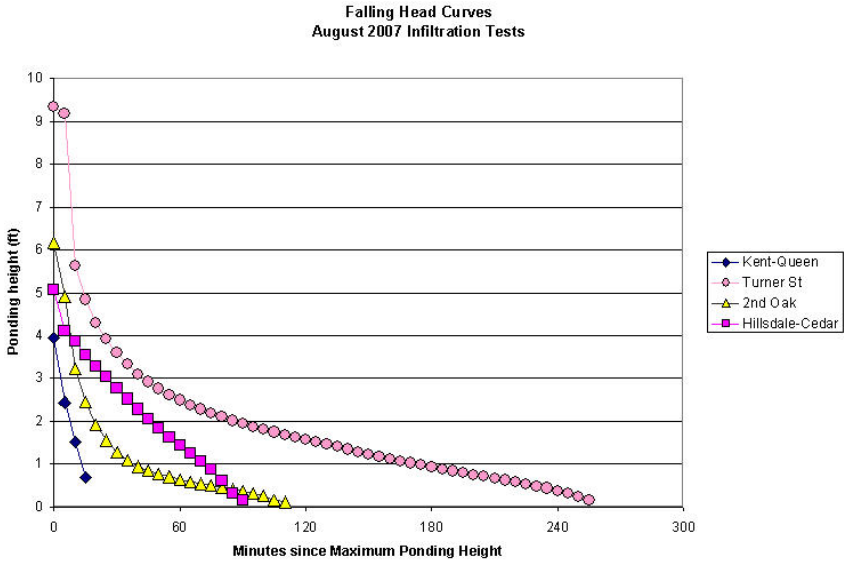

Figure 4.13. The declining portions of the artifical tests at each sump used for the falling head analyses.

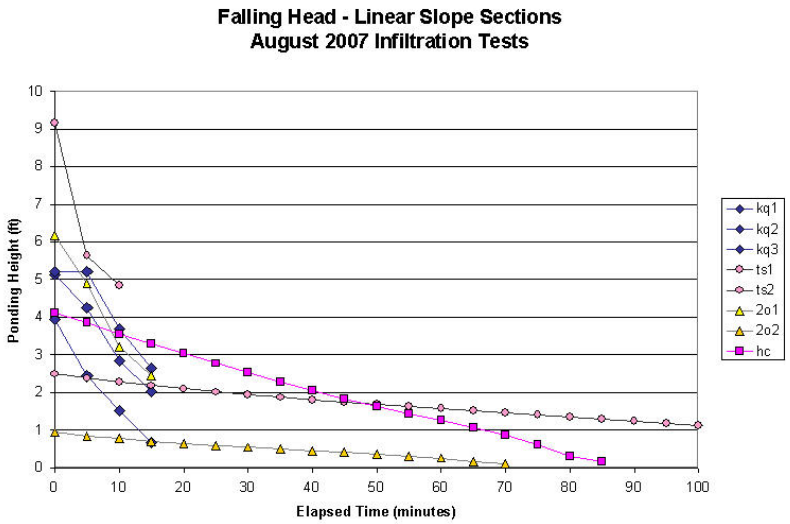

Estimated Infiltration Rates for Slope Segments

	ft/hr	gpm
kq1	13.05	20.45
kq2	12.39	19.41
kq3	10.30	16.14
ts1	17.32	27.13
ts2	0.71	1.11
2o1	14.90	23.35
2o2	0.71	1.11
hc	2.78	4.36

Figure 4.14. Separation of falling head hydrographs to upper and lower linear components representing rapid infiltration when ponding approaches the surface (e.g. kq1), and rates during lower ponding levels (e.g. kq2).

The results of the controlled infiltration tests for the KQ, HC and 2O sites conducted in 2008 and 2009 are depicted in Figure 4.15. These curves show generally consistent slopes during infiltration, with the exception of the curves for the August 2008 geophysics infiltration event at HC. The reduced infiltration rate for this experiment is attributed to a large rain event which occurred prior to this experiment, resulting in high saturation conditions that may have impacted infiltration rates. The slope for the two 2O experiments was divided into rapid, intermediate and slow components. The slope analyses from these tests are listed in Table 4.5.

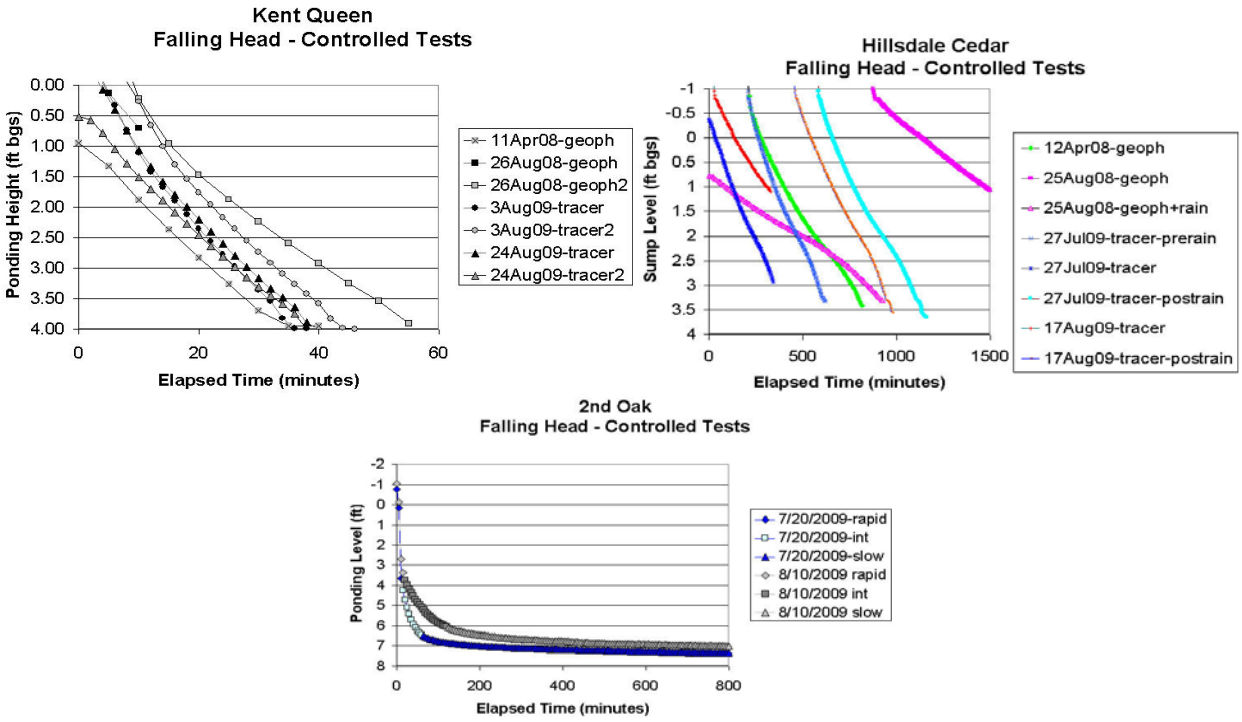

Figure 4.15. Ponding height in the sumps at KQ, HC and 2O duirng multiple periods of artifical infiltration tests (April 2008 and August 2009). Geoph represents water infiltration testing performed during geophysical data colletion, and tracer represents a water and salt infiltraiton tests. Test were repreated hence the numbers 2 and 3. Rain, pre-rain, and post-rain document if a significant rain event occurred within the measurment period. Tests with varying inflow are listed as initial, rapid and slow. Zero feet is the street surface.

Table 4.5. Slope Analysis from Controlled Infiltration Tests

	KQ		HC			2O	
	Controlled Event Slope	Infiltration Rate	Controlled Event Slope	Infiltration Rate		Controlled Event Slope	Infiltration Rate
	ft/hr	gpm	ft/hr	gpm		ft/hr	gpm
	4.19	6.56	0.16	0.25	Rapid	26.45	41.44
	5.45	8.54	0.16	0.25	Int	2.86	4.47
	5.50	8.62	0.34	0.53	Slow	0.04	0.06
	5.74	8.99	0.38	0.60			
	5.92	9.27	0.44	0.69	Rapid	19.33	30.28
	6.8	10.65	0.49	0.77	Int	1.34	2.11
			0.56	0.88	Slow	0.05	0.08
			0.56	0.88			
n	6	6	8	8			
avg	5.60	8.77	0.39	0.61			
med	5.62	8.80	0.41	0.64			
st dev	0.85	1.33	0.16	0.25			

A fourth approach used to compute infiltration rates analyzed the vertical temperature array data collected from the sandpoint instrument installed in the sump base sediments. This data set was collected but not analyzed and reported here.

PERCOLATION RATES

The rates and processes impacting percolating water were assessed by both insitu measurements and indirect evidence, such as the timing of infiltration and responses at the water table. Both natural runoff events and controlled infiltration experiments were completed and analyzed. The project conceptual model relates the vadose zone geology and the sediment physical properties to the percolation process. This section will begin by providing the results the vadose zone sediment characterization at each site.

Characterization of the Vadose Zone Composition and Stratigraphy

Rotary Sonic drilling methods were used to sample the coarse-grained vadose zone. The drilling rig was supplied by Western Environmental of Spokane, Washington. The sediment coring program obtained continuous 4 in diameter cores of unconsolidated materials from land surface to the upper 5 to 10 ft (estimated depth) of the water table (Figure 4.16).

Rotary sonic drilling rig with core barrel

Extrusion of core sample into plastic bag

Management of cores from soil boring

Soil cores managed at laboratory facility

Figure 4.16. Photographs of the rotary sonic drilling operation, core collection, and storage.

Core samples were described by visual inspection and photographed in a split PVC 4 in diameter pipe (Figure 4.17). Geologic logs were prepared for each site. A schematic fence diagram showing the generalized geology of the borings and their relative location is presented in Figure 4.18.

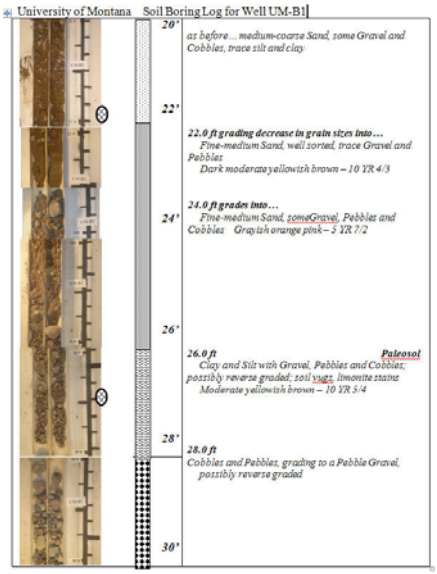

Figure 4.17. Example of a geologic boring log and core pictures for an interval of the UM boring.

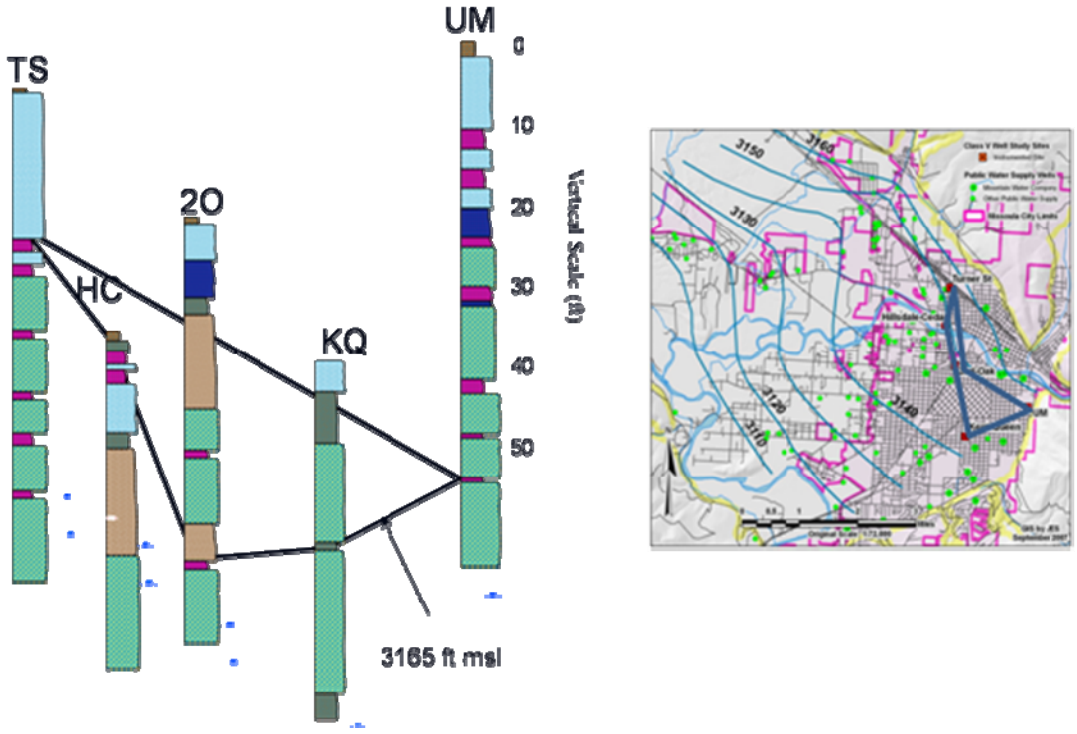

Figure 4.18. Geologic Logs for each of the study sites showing the general lithology as well as the local position of the water table. Geologic units are represented by the following colors and demarcations: Solid brown- asphalt and fill; stippled light blue- medium to coarse sand and gravel with cobbles and a trace of silt and clay; purple- silty clay with cobbles; solid dark blue- fine to medium sand , some gravel, pebbles and cobbles; light green stippled-cobbles and pebbles, grading to a pebble gravel; solid green- cobbles, gravel, clay and silt with a trace of sand; light brown- clay and silt with sand, gravel, pebbles and cobbles. The blue lines represent high and low water table positions and the black line shows the location of a common elevation.

The primary mineralogy of the sediments was determined by visual examination during the core logging procedures (Figure 4.17). In order to obtain more quantitative description of the grain mineralogy, after sieving portions of grain size, the separates were counted. The 100 grain point count procedure was performed on a total of 22 samples; both the fine fraction (≤ 2 mm) and coarse fractions (> 2 mm) were assessed. The results show that the mineralogy of both the fine and coarse fractions were both predominantly comprised of weathered grains of purple, red and green quartz siltstone. This composition is consistent with bedrock mineralogy in the region, which is dominated by a sequence of Proterozoic metasedimentary siltstone and sandstone rocks comprised predominantly of quartz. While some igneous rocks are present in the headwaters of the Clark Fork River and its tributaries, they were not frequently observed in point count samples. A single weathered igneous rock, approximately 7 cm in diameter, was collected at a depth of approximately 40 ft in the University of Montana boring.

The fine-grained portion of the samples, comprised of silt particles with a diameter of 63 microns (0.063 mm) and smaller clay sized particles (< 4 microns) represent less than 5% of the

total mass of the soils in the core samples (Table 4.6). The mineralogy of the fine grained particles was determined using X-ray diffraction methods. These bulk samples primarily contained silt sized particles and were found to be predominantly composed of quartz.

Table 4.6. Mineralogy of the Fine Grain-Size Fraction of Selected Core Samples. (Sample sites are listed as 2O11, a 2O sample form a depth of 11 ft is indicated; analyses conducted by Dr. Peter C. Ryan at Middlebury College, Middlebury, Vermont)

Mineral abundances (wt%) in < 2 micron fraction, normalized*

						~Mineralogical Signal	
Site-Depth	Illite	Smectite	Chlorite	Kaolin	SUM	Belt	~Tertiary
2011	71.4	13.6	7.7	7.4	100	x	
2014	73.9	9.6	7.5	9.0	100	x	
2034	56.8	33.9	4.7	4.6	100		x
HC5	46.8	41.8	6.6	4.8	100		x
HC19	48.7	40.9	6.2	4.2	100		x
HC25	75.6	9.4	7.7	7.3	100	x	
HC29	57.0	32.8	6.2	4.0	100		x
HC36	72.2	13.3	6.9	7.5	100	x	
HC43	70.5	21.3	3.1	5.0	100		
KQ9	67.5	17.3	9.5	5.7	100		
KQ21	72.6	11.1	9.6	6.6	100	x	
KQ27	62.8	22.2	9.3	5.7	100		
KQ37	71.4	13.6	6.1	8.9	100	x	
KQ46	70.0	12.7	7.4	9.9	100	x	
T10	76.1	11.5	4.8	7.6	100	x	
T36	79.2	8.1	5.0	7.7	100	x	
T47	75.2	13.9	4.3	6.6	100	x	
T55	71.8	18.8	3.5	6.0	100		
UM12	65.9	20.2	4.3	9.6	100		
UM19	70.1	14.9	5.6	9.4	100	x	
UM31.5	73.4	13.4	5.2	8.0	100	x	
UM43	73.2	12.8	5.9	8.1	100	x	
UM51	58.7	20.8	7.6	12.9	100		
UM65	65.9	22.2	6.3	5.7	100		

"Belt" = >75% I+C, <15% smectite.
"~Tertiary" = >30% smectite. (If seds were entirely derived from Tertiary sediments they should be close to 100% smectite +/- kaolin).
Glacial Lk Msla seds are typically dominated by Illite with smaller amounts of chlorite and smectite.
Tertiary seds in the Missoula, Mission and Bitterroot valleys are usually dominated by smectite but locally also have kaolin.

* Minerals were quantified by measuring integrated peak areas from XRD data (oriented mounts) and normalized to 100% given a clay assemblage of illite, chlorite, smectite and kaolin.

Standard grain size analyses were performed in order to characterize the grain size distribution of sediment grains found in the vadose zone core samples. Grain size analyses of KQ core intervals show that the vadose zone stratigraphy is dominated by coarse grained sediments (Figure 4.19). The median grain size is in the pebble range and the majority of the intervals are dominated by sand and gravel, pebbles and cobbles. Uniformity coefficients of sampled intervals ranged from 44 (at 16 ft bgs) to 4.5 (42 ft bgs). No clear grain size trends with depth were apparent.

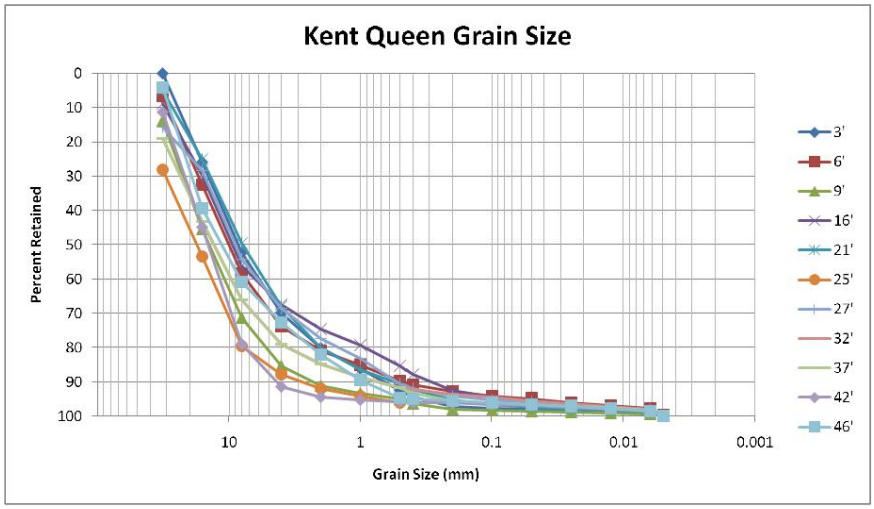

Figure 4.19. Cumulative percent retrained grain size analyses for core intervals at KQ. Sample intervals in ft below ground surface (bgs) are presented.

The sediment at HC is also dominated by coarse-grained sediments (Figure 4.20). Median grain sizes range in the pebble to cobble size class. The uniformity coefficients ranged from 21 (11 ft bgs) to 4 (19 ft bgs). As observed at KQ, the majority of the intervals were dominated by sand and gravel, pebbles and cobbles. No clear grain size trends with depth were apparent.

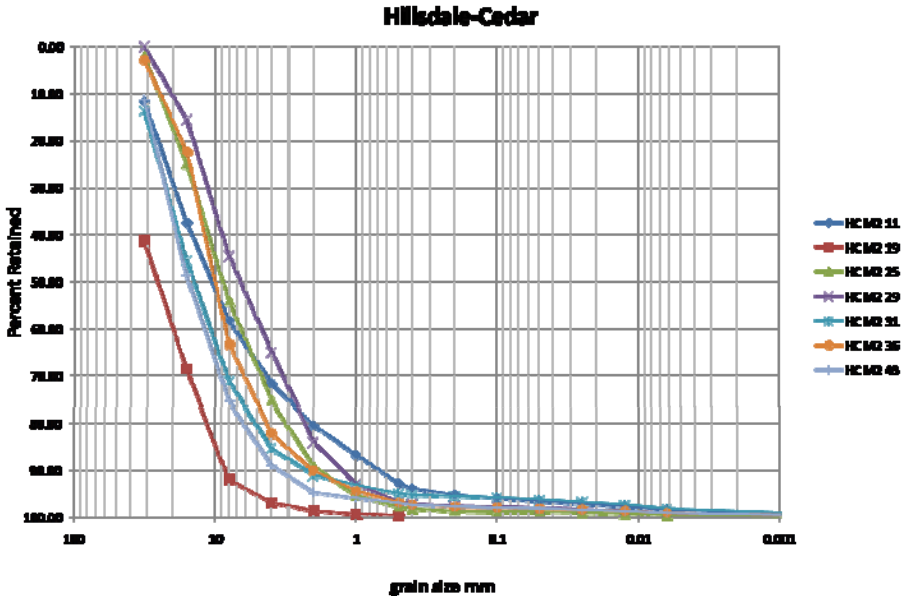

Figure 4.20. Cumulative percent retrained grain size analyses for core intervals at HC. Samples for analyses were selected from the second core M2. The sample interval is listed last and is in feet below ground surface (HC M2 36 ft).

The sediment core grain size analyses for 2O is also dominated by coarse-grained sediments (Figure 4.21). Median grain sizes range in the pebble to coarse grained sand class. The uniformity coefficients ranged from 111 (27 ft bgs) to 1.5 (11 ft bgs). Finer sediment is noted at two locations in the near surface (8 ft bgs and 11 ft bgs), a third zone with some fine

sediment is located at 21 ft bgs. As observed at KQ the majority of the sample intervals were dominated by sand and gravel, pebbles and cobbles. No clear grain size trends with depth were apparent.

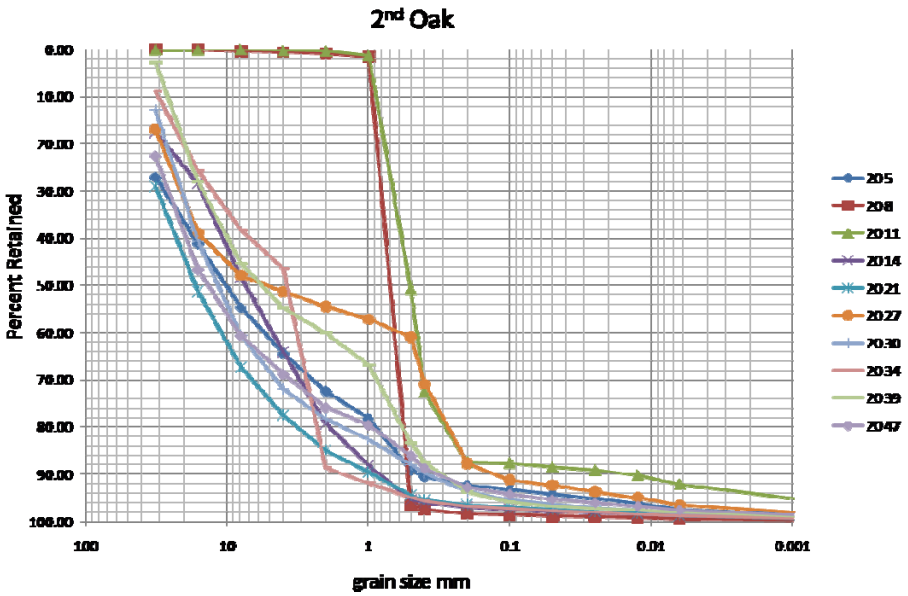

Figure 4.21. Cumulative percent retrained grain size analyses for core intervals at 2O. The interval is listed last and is in feet below ground surface (2O 39 ft).

The sediment core grain size analyses for TS are also dominated by coarse-grained sediments (Figure 4.22). Median grain sizes range from pebbles to medium sand. Uniformity coefficients ranged from 32 (10 ft bgs) to 4.3 (47 ft bgs). The majority of the sample intervals were dominated by sand and gravel, pebbles and cobbles. A finer interval was observed at 27 ft bgs with the coarsest material found near the surface. Unlike the previous sites, there is a correlation between grain size and depth with finer grained sediments located closer to the surface and coarse grained sediments at depth (below 27 ft bgs).

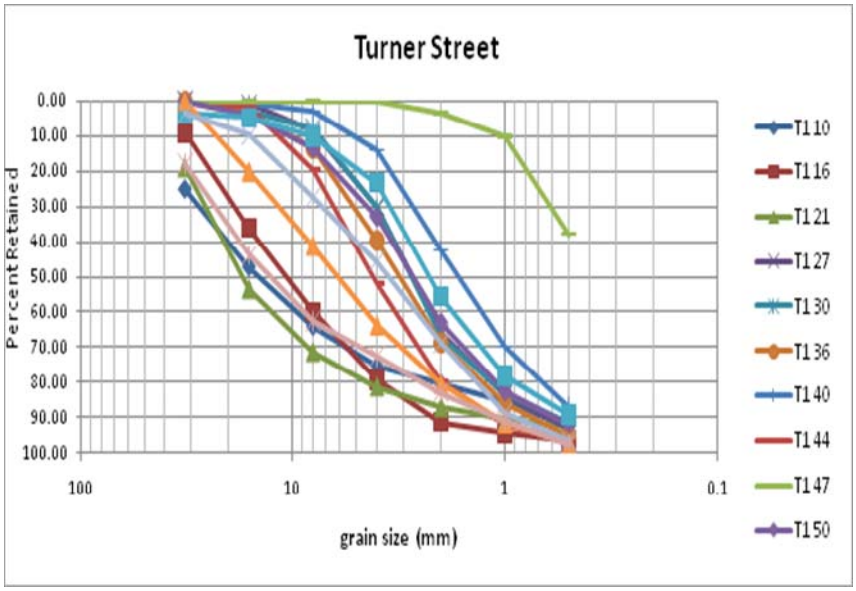

Figure 4.22. Cumulative percent retrained grain size analyses for core intervals at TS. The interval is listed last and is in feet below ground surface (T1 60 ft).

The sediment core grain size analyses for UM are also dominated by coarse-grained sediments (Figure 4.23). Median grain sizes are spread over a larger grain size distribution from pebbles and cobbles to coarse sand. Uniformity coefficients ranged from 84 (19 ft bgs) to 3 (30.5 ft bgs). The majority of the intervals are dominated by sand and gravel, pebbles, and cobbles. Layers of finer sediments were observed at 19 ft bgs to 22 ft bgs, and at 34 ft bgs. The coarsest sediments were found near the land surface and at about 30 ft bgs. No clear trend in grain size distribution with depth was apparent.

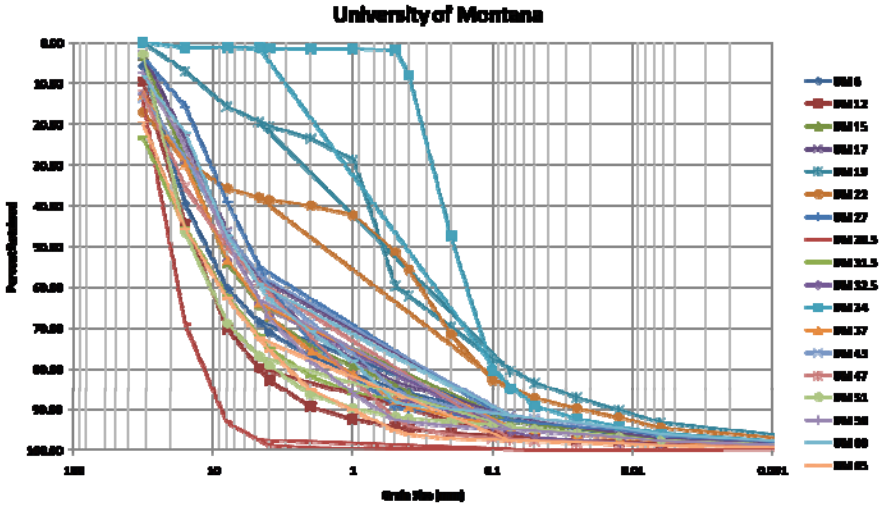

Figure 4.23. Cumulative percent retrained grain size analyses for core intervals at UM. The interval is listed last and is in feet below ground surface (UM 60 ft).

The study of the cores and other data sets, including well logs for nearby and valley wide sites, provided insight as to the depositional character of the Missoula vadose zone and aquifer sediments (e.g. Tallman, 2005). The vadose zone is dominated by sand, gravel, pebbles and cobbles in what appear to be deposits associated with gravel dominated braided rivers. The stratigraphically cohesive fine-grained (silt and/or clay) layers were limited in occurrence and extent, and primarily occur as lenses. Recovered core sample sections dominated by cobbles were generally washed clean of any fine-grained materials suggesting they were deposited as open framework deposits. In most cores, cored sections of cobbles were logged suggesting that the vadose zone deposits include large cobbles and boulders (>4 in diameter).

Hydrologic Property Determination

Additional characterization of the vadose zone sediments utilized column experiments. Eleven core sample intervals were selected to represent dominant vadose zone coarse grain intervals and a few finer-grained segments (Table 4.7). Columns were filled and drained multiple times to generate bulk and hydrologic properties. Porosity values ranging from 0.22 to 0.54 are most likely higher than in situ values as columns were repacked with sediment and large clasts removed. Gravity drainage data for the soil columns shows rapid drainage of the majority of sediment water from coarse grain dominated samples (Figure 4.24). Field capacities were generally larger proportionally for the samples dominated by finer grain size material.

Table 4.7. Results of General Hydrologic Characteristics Determinations From Core Sediments. Note: KQ 25-27 Represents the Sample Interval in ft Below Land Surface.

	Column 1	Column 2	Column 3	Column 4	Column 5	Column 6	Column 7	Column 8	Column 9	Column 10	Column 11
	KQ 25-27	HC 24-26	KQ 15-17	KQ 35-37	TS 34-36	2O 44-46	2O 10-12	HC 6-8	UM 10-12	TS 28-30	UM 40-42
Dominate Sediment	Fine-Med	Pebbles Cobbles	Med-Coarse	Gravel and Cobbles	Coarse Sand and Gravel	Med. Coarse Sand	Med. Coarse Sand	Silt with Clay	Silt and Clay with	Coarse Sand and Gravel	Med. Coarse Sand
Type	Sand, Gravel Cobbles	Clay and Silt Matrix	Sand and Gravel	Some Silt	Some Pebbles	Gravel, trace Clay a and Silt	Trace of Gravel	Trace of Gravel	Cobbles Pebbles and Gravel	Trace Pebbles Silt and Clay	and Gravel, Trace Silt and Clay
Porosity	0.42	0.54	0.29	0.38	0.46	0.30	0.38	0.22	0.30	0.35	0.37
Specific Yield	0.30	0.31	0.09	0.27	0.29	0.20	0.09	0.13	0.17	0.23	0.10
Field Capacity	0.12	0.23	0.10	0.11	0.17	0.10	0.29	0.09	0.13	0.12	0.27
Residual Moisture Cont.	0.09	0.10	0.09	0.10	0.08	0.09	0.28	0.08	0.12	0.11	0.08
Bulk Density (g/cm3)	1.93	1.84	1.95	1.87	1.68	2	1.48	1.81	1.91	1.76	1.76

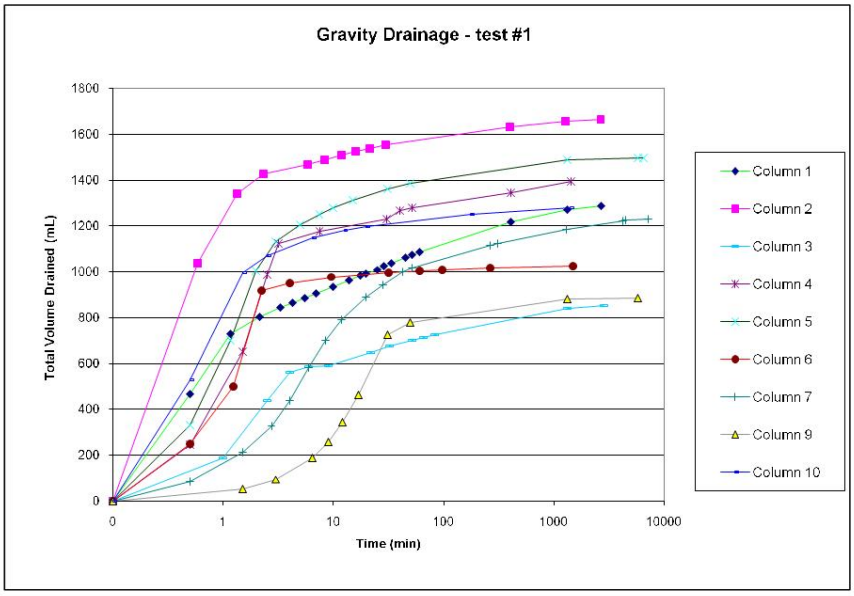

Figure 4.24. Column drainage showing the rapid response to gravity drainage and longer times to reach residual moisture contents (Table 4.7).

The same samples used for column experiments were also set up as constant head permeameters in order to determine saturated hydraulic conductivities (Fetter, 2004). Experiments were repeated three times. During the first phase, flow through three of the columns was limited, and further experiments were discontinued. Results of saturated hydraulic conductivity determinations are presented in Table 4.8.

Table 4.8. Results of Saturated Vertical Hydraulic Conductivity Determinations Of Sediments In Saturated Columns.

Summary Values ft/d								
	KQ Column 1	KQ Column 3	KQ Column 4	HC Column 2	2O Column 6	TS Column 5	Ts Column 10	UM Column 9
Average	1002	964	1050	1182	954	694	914	461
Median	951	963	1014	1194	954	694	914	461
St Dev	154	87	85	96	7	19	8	468
Number	3	3	3	3	2	2	2	2

The grain size distribution curves for 49 borehole intervals (presented previously as cumulative retained grain size distributions) were analyzed to determine estimates of hydraulic conductivity using the Hazen approximation. Values are reported as averages for the entire borehole and ranges are presented in Table 4.9. These estimates should be regarded with caution as the Hazen empirical correlation was originally developed for uniformly graded sand size

sediments. The applicability of the Hazen correlation to less uniform sediments dominated by gravel, pebbles and cobbles has not been explored in the literature.

Table 4.9. Average Saturated Horizontal Hydraulic Conductivity Values (ft/d) Computed from Grain Size Analyses of Borehole Samples (n = number of intervals examined) using the Hazen Approximation for Sands (C = 100).

Site	n	Median	Mean	STD	Range
KQ	11	1,500	8,100	14,600	240-47600
HC	7	11,700	41,600	75,300	1500-210,400
2O	10	500	1,400	2,100	0.8-7,000
TS	13	1,800	3,000	3,600	5-14, 100
UM	17	200	15,300	56,500	5-234,000

The saturated hydraulic conductivity of vadose zone sediments varied widely depending upon the methodology used. Saturated hydraulic conductivity values for column tested intervals ranged from 400 to 1200 ft/d with lower values associated with the presence of finer sediments. The column values represent an approximation of the vertical saturated hydraulic conductivity that is often approximated as 0.1 times the horizontal value. The average values computed solely from grain size data are similar to results derived from large scale aquifer testing of the Missoula Aquifer and likely best represent horizontal properties (Tallman 2005). These magnitudes of computed values are representative of very coarse grain sediments. The large ranges and standard deviations of hydraulic conductivity values documents the heterogeneous nature of the vadose zone .

An attempt to quantify the relationship between moisture content and negative pore water pressure (matric potential) of a draining column was examined by instrumenting one of the sediment columns. Mini tensiometers were installed in Column 1 that was filled with KQ sediments. They were zeroed, and observed over a ten month period during which time the column was allowed to slowly dry (Figure 4.25). This experiment was designed to assess if the drying curve data could be obtained for samples of the coarse grained vadose zone sediments. The tensiometers generally showed a poor response to changes in soil moisture during gravity drainage, consistent with the matric pressures that would be expected for coarse grained materials (Tokanaga et al., 2004). Additional columns were not instrumented.

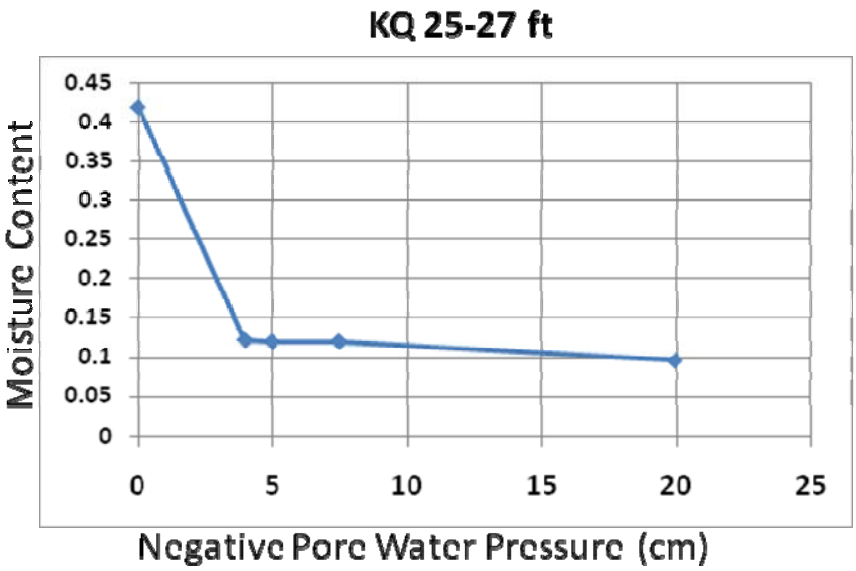

Figure 4.25. Plot of moisture content for the coarse grained sediment in column 1, KQ 25-27 ft generated by readings of mini-tensiometers and moisture content over time.

The measurement of in situ soil moisture content in the vadose zone was attempted by installing gypsum blocks at each site (Table 4.10). This was completed with the realization that such instruments are not designed to work well in coarse grained settings. Data were collected for the period from spring 2007 to spring 2008 or 2009 depending on the site (Figure 4.26-4.30). All readings indicated soil moisture at the instrument site remained high throughout the investigation. Two interpretations are possible: either the instruments were not working properly, or vadose zone sediments held a high water content through most of the year.

The soil moisture readings at KQ suggested the site stayed near maximum moisture content to depths of 35 ft during most of the study (Figure 4.26). All instrumented depths experienced a decline in readings during the summer of 2007 that may have been caused by a drying trend or the instrument adjusting conditions related to installation. This decline was most pronounced at the instrument located at 20 ft bgs, a depth interval with medium to coarse sand and gravel with some cobbles and a trace of silt (Table 4.10).

Table 4.10. Gypsum Block Installations.

Location	Gypsum Block bls (ft)	Dominant Sediment
KQ	6	Medium to coarse sand, gravel and cobbles with silt and clay
	14	Medium to coarse sand, gravel and cobbles with a trace of silt and clay, with boulders (4")
	20	Medium to coarse sand, gravel with some cobbles with a trace of silt and clay
	35	Silt, cobbles, gravel, trace of clay, large boulders
	50**	Cobbles, gravel , clay and silt, a trace of sand
HC	9	Medium-coarse sand and gravel, with pebbles and cobbles, a trace of silt and clay, boulders (4")
	15	Medium-coarse sand , gravel and clay, with pebbles, a trace cobbles
	25	Pebbles and cobbles with clay and silt
2O	12	Medium to coarse sand and gravel, trace of silt and clay
	16	Clay and silt with sand, gravel, pebbles and cobbles
	50	Cobbles and pebbles, open framework
TS	12	Medium to coarse sand and gravel, pebble and cobbles, some boulders
	16	Medium to coarse sand and gravel, pebbles and cobbles, some boulders
UM	14	Medium to coarse sand and gravel with cobbles, a trace of silt and clay

** instrument did not function properly after installation

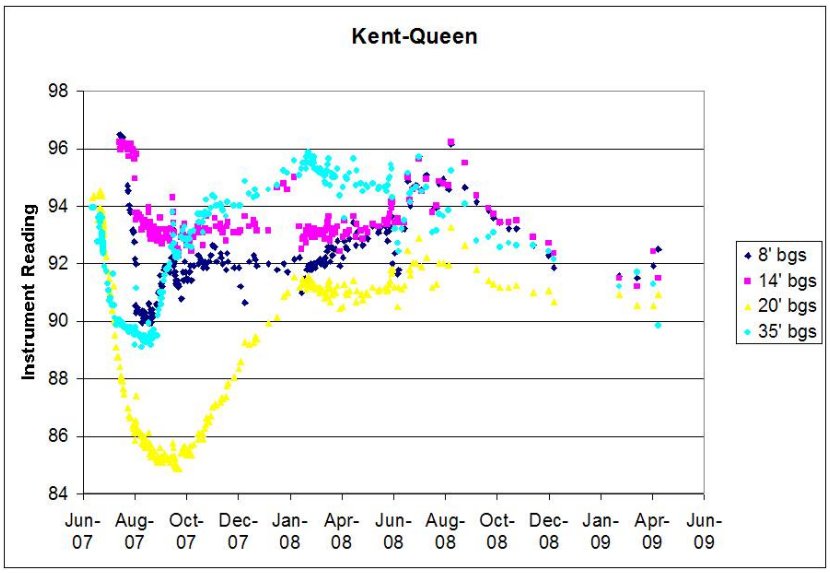

Figure 4.26. Gypsum block readings at the KQ site from June 2007 through May 2009. An instrument reading of 100 suggests sediments were fully saturated.

Instrument readings at HC showed an apparent drying response in the late summer of 2007 (Figure 4.27). The apparent sediment drying was most pronounced at depths of 15 ft bgs and 25 ft bgs. Both depths are dominated by coarse grained sediments (Table 4.10). The shallowest instrument (located at 9 ft bgs) showed the most variability during winter months. Overall, the instrument readings at HC suggest sediments stayed relatively wet during this period of study.

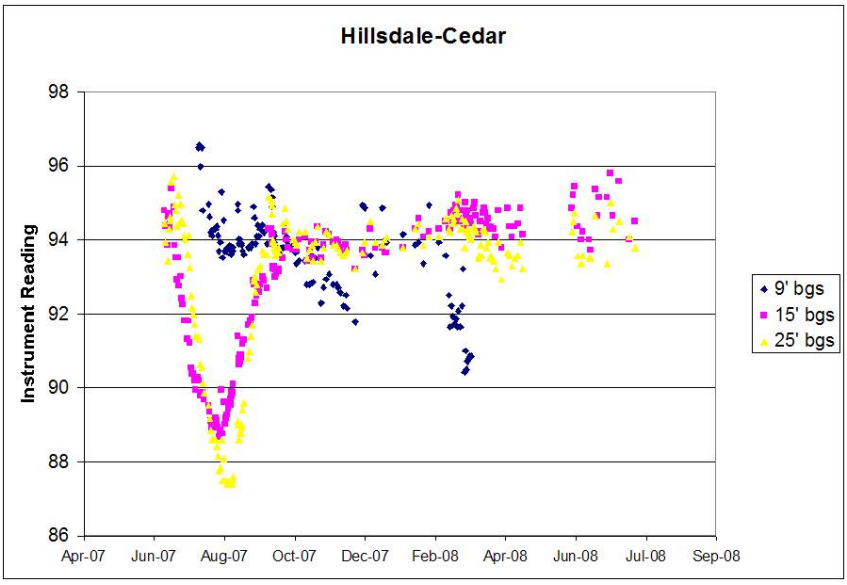

Figure 4.27. Gypsum block readings at the HC site from June 2007 through July 2008. An instrument reading of 100 suggests sediments were fully saturated.

Instrument readings at 2O generally indicated conditions remained wet at all depths with a possible drying period starting in the fall of 2008 (Figure 4.28).

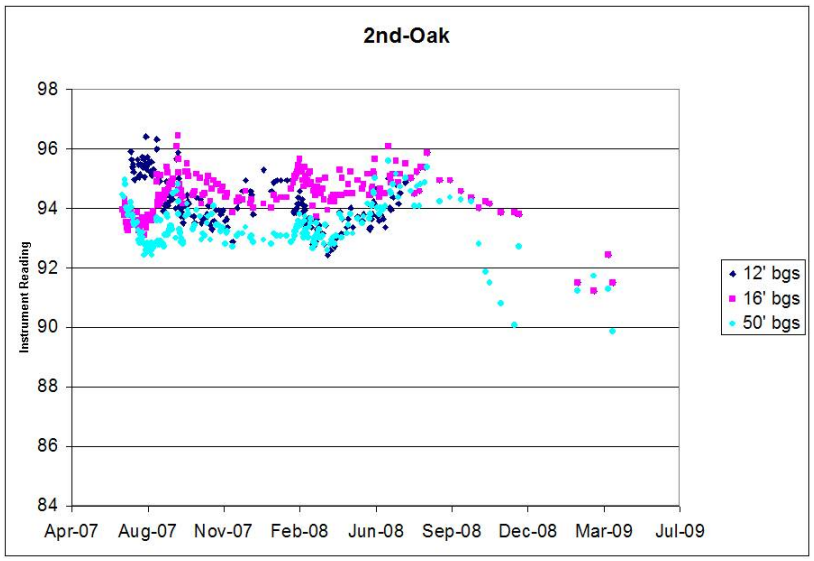

Figure 4.28. Gypsum block readings at the 2O site from April 2007 through July 2009. An instrument reading of 100 suggests sediments were fully saturated.

Instrument readings at TS showed an apparent drying response in the late summer of 2007 (Figure 4.29). The apparent sediment drying was most pronounced at 16 ft bgs. Both instrument depths are dominated by coarse grained sediments (Table 4.10). Overall, the instrument readings at TS suggest sediments stayed relatively wet during this period of study.

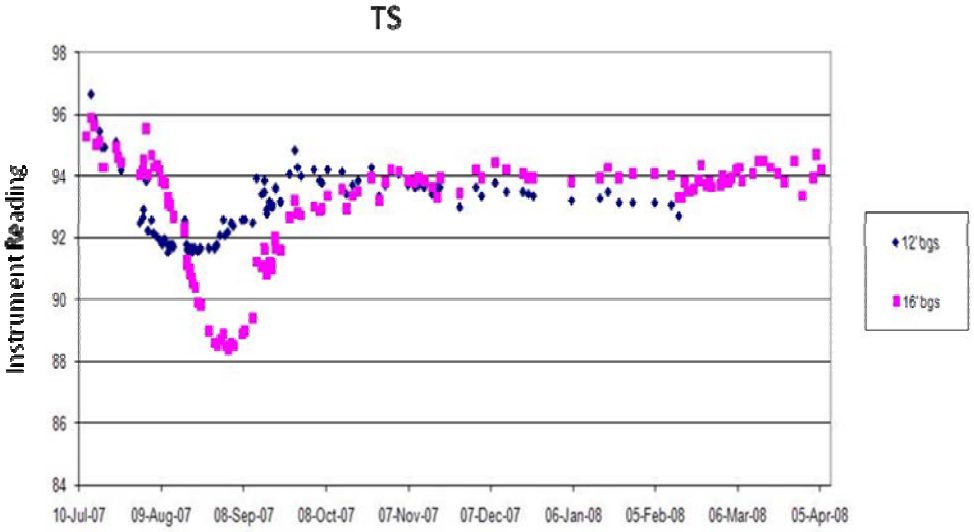

Figure 4.29. Gypsum block readings at the TS site from April 2007 through June 2008. An instrument reading of 100 suggests sediments were fully saturated.

Instrument readings at UM recorded an apparent drying trend in the late summer of 2007; similar concurrent trends were also observed in KQ and HC. The drying was most pronounced at 16 ft bgs, but was also recorded at 12 ft bgs (Figure 4.30). Both depths are dominated by

coarse grained sediments. Overall, the instrument readings suggest sediments stayed relatively wet during this period of study.

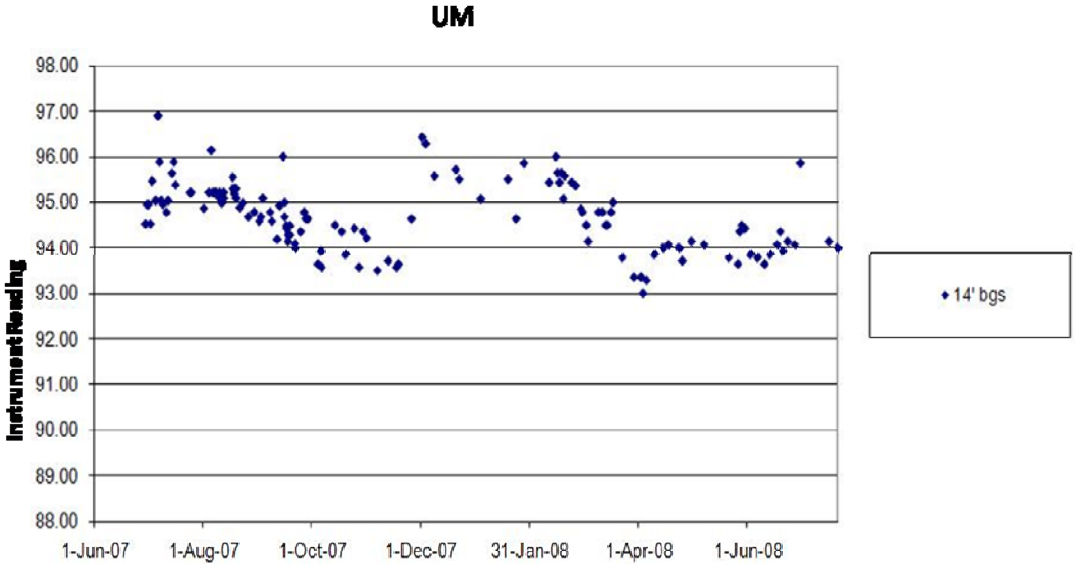

Figure 4.30. Gypsum block readings at the UM site from June 2007 through November 2008. An instrument reading of 100 suggests sediments were fully saturated.

At some sites gypsum block readings were repeated after storm events to determine if the moisture front moving through the vadose zone could be detected. Once again, conditions at all depths appeared to remain wet and clear indications of wetting fronts passing instrument depths were not evident. An example of pre and post storm water infiltration data sets at HC are presented in Figure 4.31.

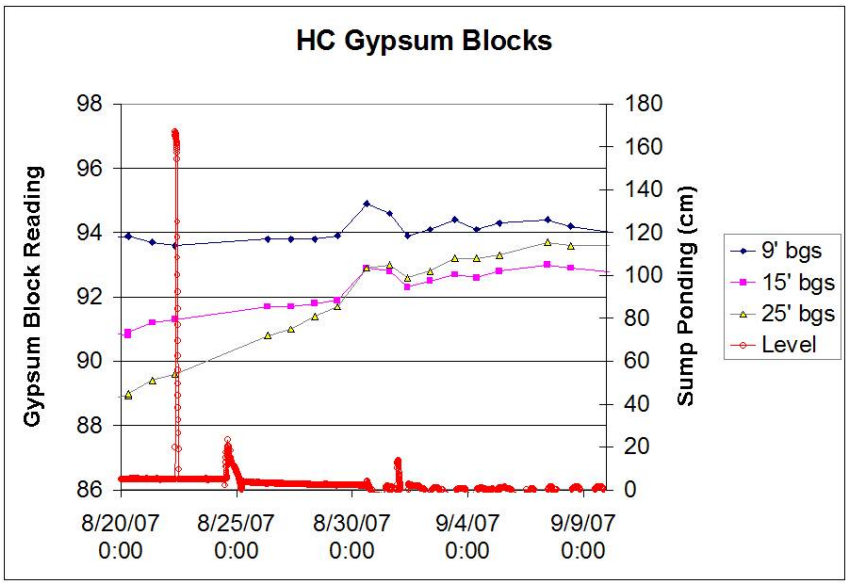

Figure 4.31. Pre and post runoff (Level) gypsum block readings at the HC site from 8/20/07 to 9/9/07. Instrument readings of 100 represent saturated conditions. Sump ponding (Level) is shown as cm measured above the sump base.

Thermal Profiling

Monitoring vadose zone temperature changes as water percolated through the sump base to the water table was assessed during the winter/spring period of 2008 using site monitoring wells. Individual thermistors were placed on the outside of a 2 in diameter PVC casing that was packed off isolating vertical sections of the 3 in diameter well casing. The data collection program was discontinued after results did not provide sufficient resolution to correlate temperature changes with infiltration events. The technique could potentially provide useful data if temperature monitors with a resolution higher than +/-0.5C are employed in future field studies.

One data set from the HC site did show some interesting trends that were not analyzed further as part of this study (Figure 4.32). The data set in Figure 4.32 corresponds to a winter thaw in late January through February 2008. During this period some storm events combined with daily melt water periods provided percolation water at near freezing temperatures. As a result, vadose zone temperatures beneath the 3.5 ft depth of the HC sump appear to have responded by cooling during this time period at all depths (maximum of 28 ft) over the one month period. The overall step changes in temperature (partly a function of instrument resolution, 0.5 C) are lagged from the 8 ft bgs to the 28 ft bgs. It is likely that further data analyses may allow computation of percolation rate estimates; however, the source term is complex and may limit the applicability of such computations.

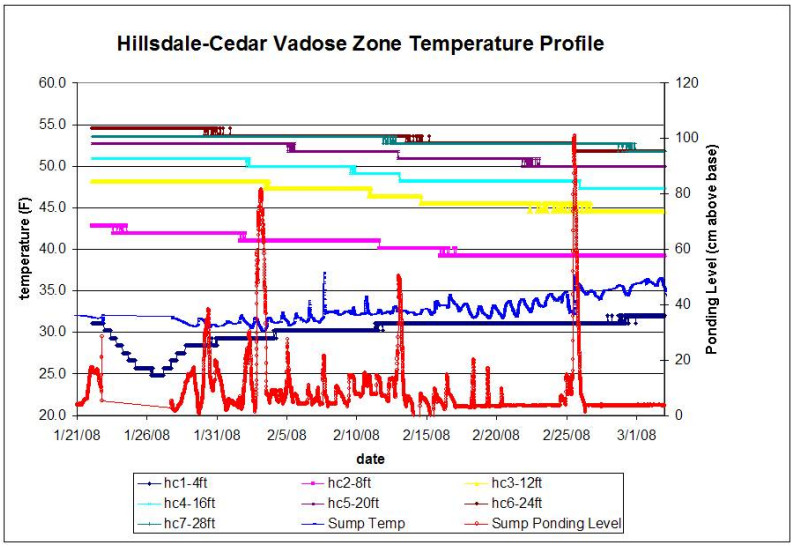

Figure 4.32. Thermal profiling of the vadose zone at HC. Temperatures were measured in baffled zones within the 3 in diameter monitoring well. Ponding levels are represented as cm above the bottom of the sump (3ft bgs).

Geophysics – Cross Borehole Tomography

Difficulties applying traditional in situ vadose zone monitoring methods to the coarse grained sediments of Missoula Valley were anticipated in the initial planning of this research. The application of geophysical borehole tomography using Ground Penetrating Radar (GPR) was selected as an alternative method to examine the variations in the rate of vertical downward movement of water during percolation. Ground penetrating radar (GPR) is a geophysical method that measures the velocity of radar pulses from a vertical well mounted transmitting antenna to a nearby set of vertical well mounted receivers. Due to the fact that radar velocity is higher in air than in water, radar velocity in unsaturated porous media is retarded by the presence of moisture.

GPR was applied at the two sites instrumented with pairs of monitoring wells, KQ and HC (well construction details are presented in Table 4.11). Monitoring natural runoff events would have been preferable, however, the scheduling of equipment use with Boise State University limited project accessibility and necessitated the use of controlled infiltration and percolation tests.

Table 4.11. Monitoring and Geophysical Well Design, and Approximate Low and High Water Table Positions (ft bgs ** Wells at KQ Site are installed in perched zone, above regional water table)

Site	Well Diameter	Screen Interval	Approximate Water Table (ft bgs)	
		(20 Slot Screen)	Low	High
KQ**	3 in		>48	44
Well KQ-M1		38-48 ft bgs		
Well KQ-M2		38-48 ft bgs		
HC	3 in		32	17
Well HC-M1		38-48 ft bgs		
Well HC-M2		28-38 ft bgs		
2O	3 in		>58	45
Well 2O-M1		48-58 ft bgs		
TS	3 in		56	43
Well TS-M1		58-68 ft bgs		

The transducer and receiver sets were first used to establish baseline conditions. The results of the initial five baseline datasets were used to estimate the velocity of the radar signal between boreholes under ambient moisture conditions. Once the initial datasets were collected, the contributing street area received a controlled volume of water from a fire hydrant or a water-line access point. The source water was obtained from Mountain Water Company, ground water derived from their supply well network. The quantity and timing of the added water during the test was recorded (Table 4.12). Once the source water began to enter the sump, the vertical geophysical profiling was repeated numerous times to obtain time dependant vertical profiles between boreholes located on either side of the sump.

Table 4.12. Water Source Term for Geophysical Tomography Data Collection

Site	Date	Initial Pre-Test Volume (gal)	2nd Water Input (gal)	Total Volume (gal)
KQ				
	4/11/08	1000	2,000 (200 gpm for 10 minutes)	3000
	8/26/08	1400	1200	2600
HC				
	4/12/08	1000		1000
	8/25/08	1700		1700

The velocity profiles with depth for each successive data run are compared with the background velocity profile determined at the beginning of each test (Peretti et al.,1999). In general, soil pores are interpreted to have been filled with water when the run velocity record is shifted from the background profile.

The profiles for the two tests at the KQ site are depicted in Figure 4.33. These profiles show a geophysical response indicative of an increase in moisture content, a slowing of the wave velocity with depth over time. The signal response dissipates at a depth of approximately 20 feet bgs in a zone that is known to contain a higher fraction of fine grained sediments.

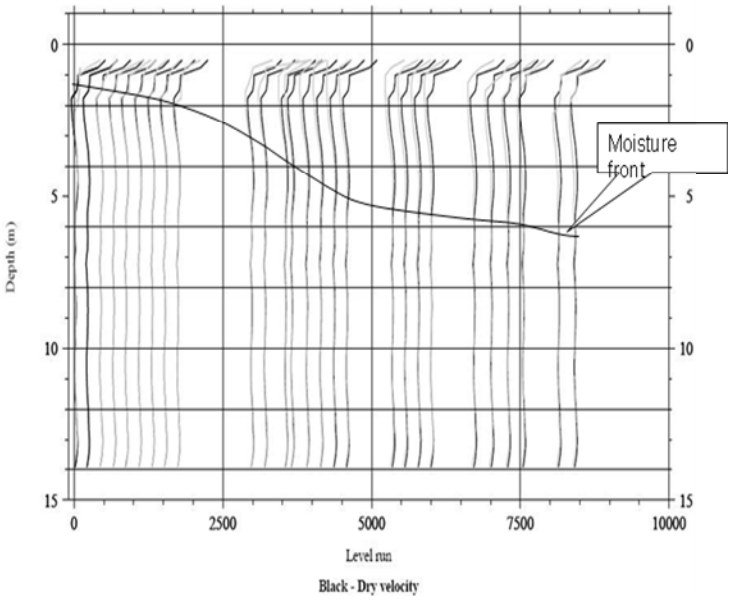

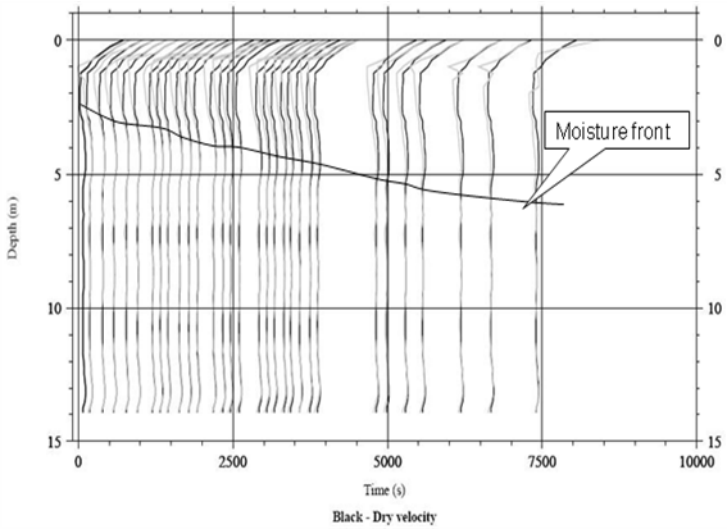

Figure 4.33. KQ borehole tomography results showing the progression of the movement of the wetting front, April 11, 2008 (upper diagram). The lower figure presents the results of the experiment repreated in August, 2008. The depth is in meters. By the end of the test the front was interpreted to have moved about 20 ft below the sump base.

The interpreted progression of the moisture fronts to a depth of about 20 ft bgs for the KQ experiments was used to estimate a percolation rate 6.5 ft/hr for the April experiment, and 6.3 ft/hr for the August experiment (Figure 4.34). The total volume of sediment occupied by the percolating water can be estimated if the following assumptions are made: the infiltration rate is 90 gpm when water is ponded in the sump at the surface, the in situ sediment porosity is 30% (column values ranged from 29-42%), and lastly the percolation rate is uniform. The radius of sediments impacted by the infiltrating water reaches a relatively constant value of approximately five feet (Figure 4.35). This suggests that during a percolation event, the volume of saturated sediments impacted by the infiltrating water can be estimated as a vertical cylinder with a diameter of approximately 10 ft.

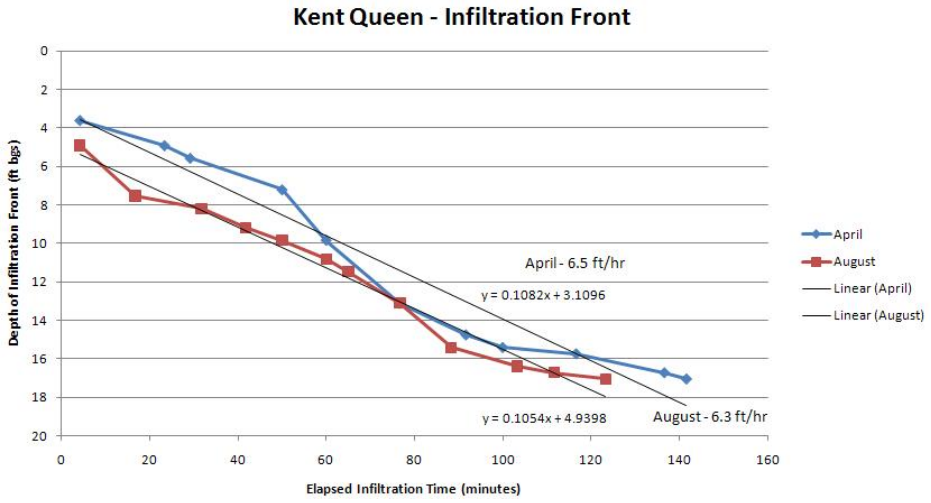

Figure 4.34. A plot of time verse depth (ft) representing the moisture front position interpreted from borehole tomography data analyses at the KQ site (April and August 2008 tests).

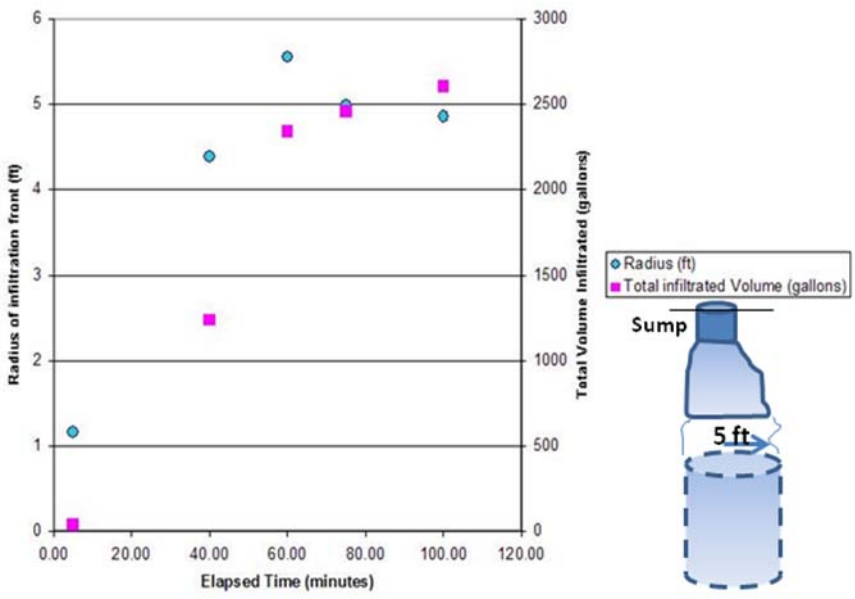

Figure 4.35. Calculation of the theoretical equivalent cylinder radius occupied by infiltrating water beneath the sump at KQ during the August 2008 artificial infiltration test. The plateau at a radius of 5 ft suggests additional lateral spreading of the percolating water may be limited by hydrodynamic dispersion properties of the sediments as long as the geological material encountered remains similar to that found near surface.

Review of the data sets collected from the geophysical experiments at the HC site suggest that a deposit of fine-grained material (described as a silt) located near the sump base controls the overall infiltration rate in the system (Figure 4.36). The percolation front can be imaged for several feet beneath the base of the silt before the signal shifts. The source of water for this percolation front is interpreted as pore waters released from the silt as additional water infiltrates into the system from the sump. The interpretation of these data suggests a percolation rate of 1.2 ft/h in the upper 20 ft sediment (Figure 4.37

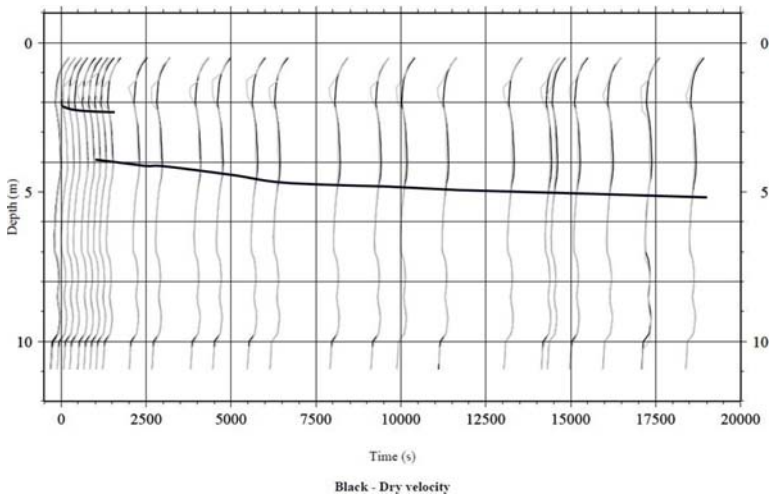

Figure 4.36. Borehole tomography at HC (April 2008). By the end of the test the front was interpreted to have moved about 20 ft below the sump base.

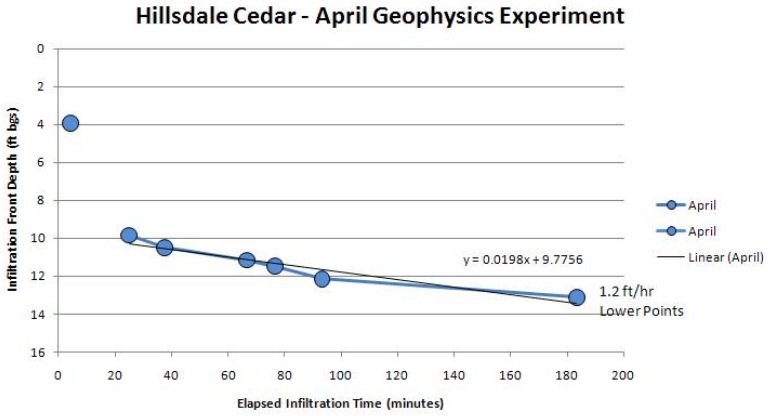

Figure 4.37. A plot of time verse depth (ft) representing the moisture front position interpreted from borehole tomography data analyses at the HC site (April 2008).

Interpretation of borehole tomography results suggests that the addition of water did not significantly alter the moisture content of sediments located in the lower vadose zone at KQ and HC. A side–by-side comparison of velocity profiles with site stratigraphy at both sites is presented in Figure 4.38. This observation is consistent with the gypsum block data results, which do not appear to show any significant changes in the moisture content with time.

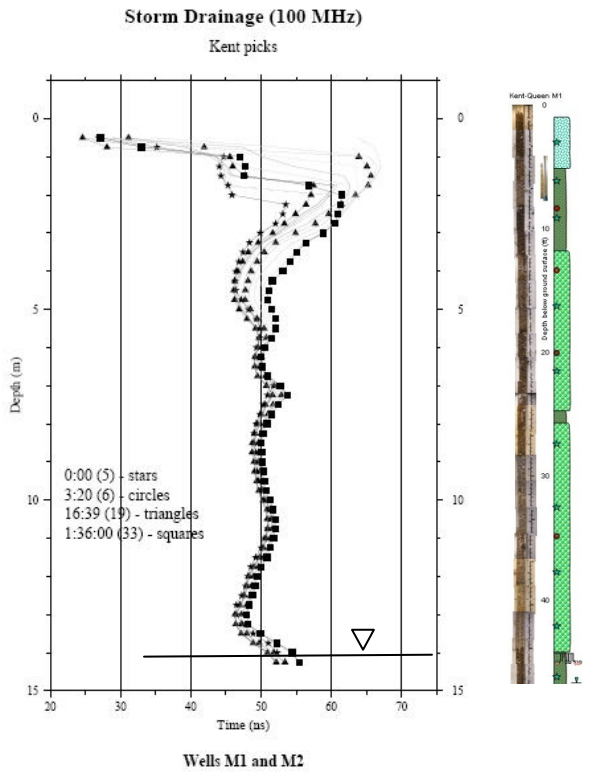

Kent-Queen site geology compared with geophysical signals

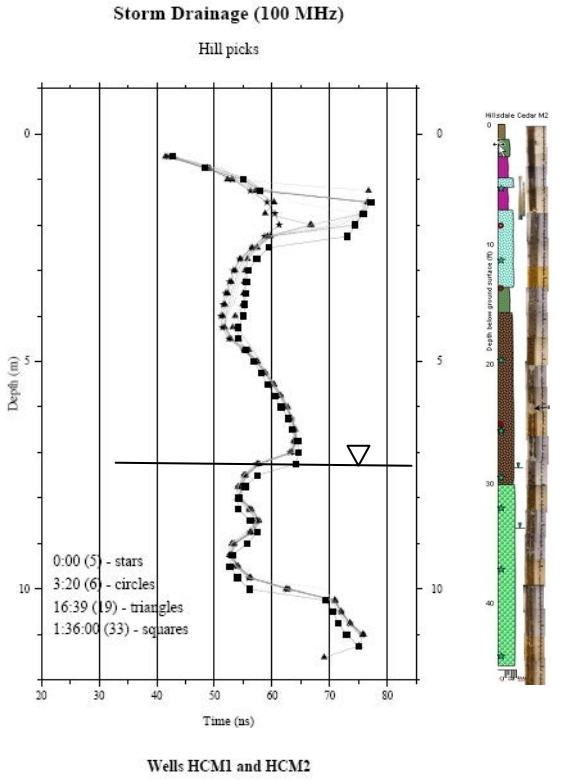

Hillsdale-Cedar site geology compared with geophysical signals

Figure 4.38. Results of borehole tomography measurements compared to site geology at KQ and HC. Artificial source water was used. Depths are in meters (April 2008).

Interpretation of Percolation Rates from Observed Response of the Underlying Water Table

Event Driven Water Table Responses. In an attempt to examine a range of conditions influencing percolation rates at the four sites with monitoring wells, the relationship between runoff entering the sump and the timing of an observable water level response at the site monitoring well, and/or a change in probe-monitored groundwater specific conductance were evaluated. Unfortunately, in most cases the high saturated hydraulic conductivity values of the sediments located immediately below the water table in the Missoula valley (6,400 ft/d to15,850 ft/d, Tallman 2005) combined with an anticipated diffuse delivery of recharge water rarely resulted in detectable storm water induced changes (mounding) in the water table position. After plotting and comparing both hydrographs and specific conductivity probe results, no percolation rates could be computed from these data sets.

Artificial Runoff Tracer Testing. During July and August 2009, a relatively dry period of the summer, controlled infiltration tests were completed at the KQ, HC and 2O sites. The tests were conducted by first adding source water (tracer absent) to the sump to initiate and stabilize percolation through the system. After the initial volume of water had infiltrated, a second volume was added with a sodium chloride tracer. These tests were conducted twice at

each of the three locations. Source water was obtained using Missoula Aquifer groundwater delivered from a municipal source to the site (water truck, fire hydrant or water line access port). The distance to the water table, and the timing of the first arrival water level response and the maximum specific conductance concentration were used to calculate percolation rates. Data interpretations are presented in Table 4.13. Graphs of test data including sump observations, groundwater water level, and conductivity responses are presented in Figures 4.39 to 4.41.

Table 4.13. Computed Percolation Rates Based on Artificial Water Tracer Tests for August 2009 (Peak Specific Conductivity)

Site	Sump Specific conductance uS/cm	Sump Cl mg/l	Groundwater Specific conductance uS/cm	Receiving Ground Water Cl mg/l	Peak Ground Water Cl mg/l	Dilution Factor	Time to peak (h)	Water Table Level (ft)	Sump Base (ft)	Travel Distance (ft)	Percolation Rate (ft/hr)
2009											
HC	3,300	960	161	52	58	0.007	10.5	25	4	21	2
KQ	2,000	645	240	140	280	0.277	3.2	46	5	41	13
2O	1,000	300		60	105	0.188	4.5	51	8	43	10

Tracer test results consistently showed that groundwater levels responded earlier than the specific conductivity values. This behavior is attributed to the displacement of vadose zone water with lower specific conductivity that was released from pore spaces during the initial stages of the test and moved to the water table during percolation. The existing vadose zone water arrived just ahead of the tracer water. Note in Figure 4.39 the groundwater conductivity becomes slightly lower just prior to the arrival of the highly conductive tracer solution.

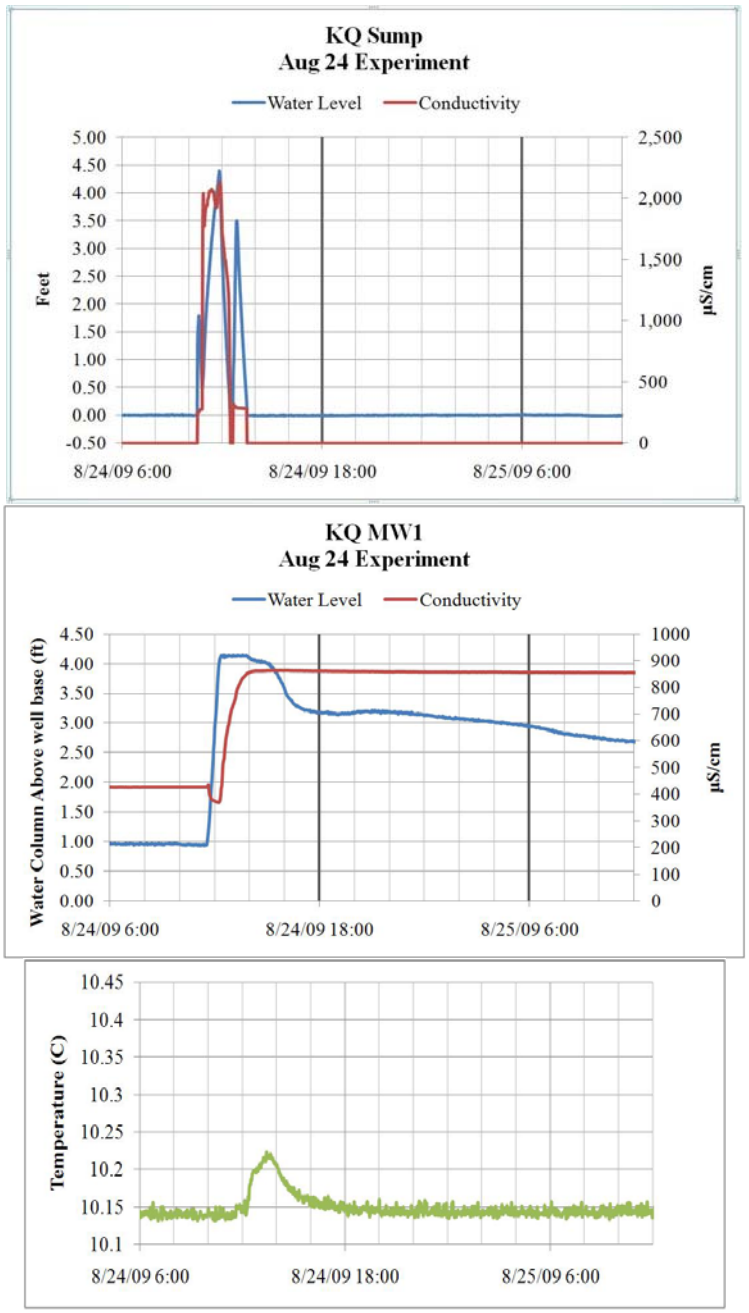

Figure 4.39. Results of artificial tracer (runoff) test at KQ 2009. Water levels and specific conductance were measured at the sump and at the water table in well KQ MW1. The temperature data were collected at the water table during the test.

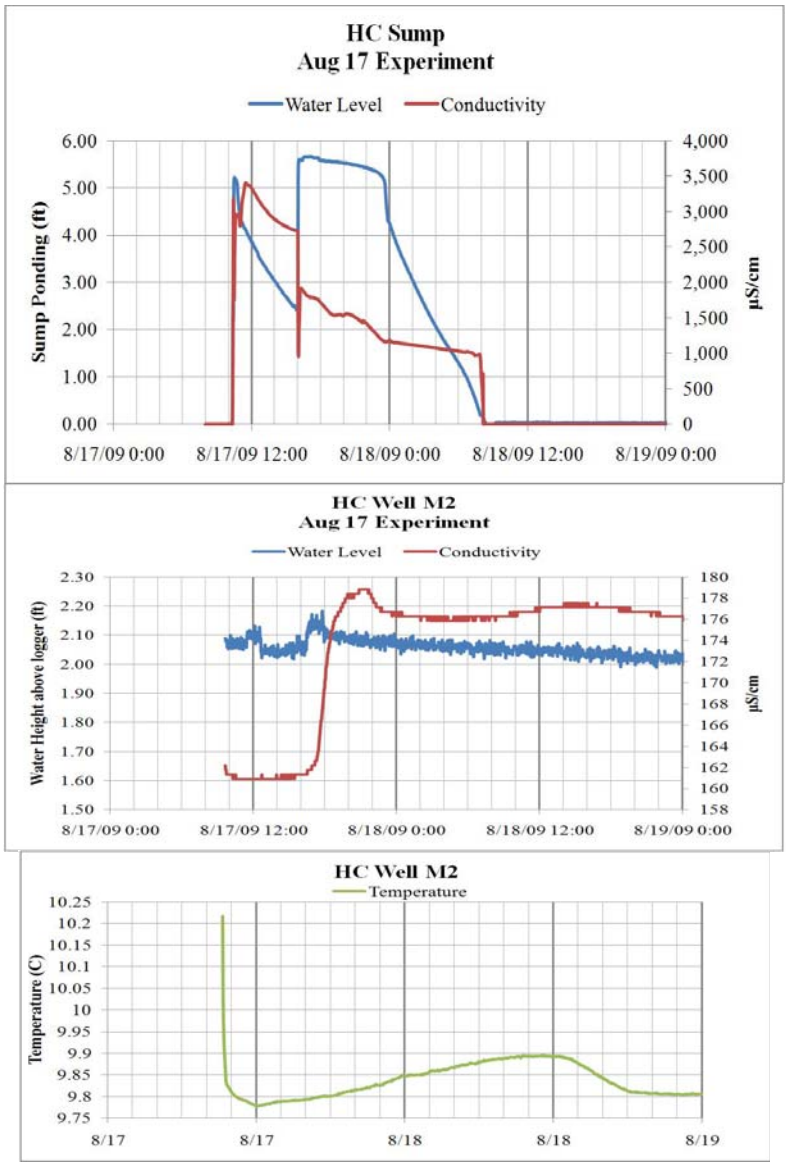

Figure 4.40. Results of artificial tracer (runoff) test at HC 2009. Water levels and specific conductance were measured at the sump and at the water table in well HC MW2. The temperature data were collected at the water table during the test.

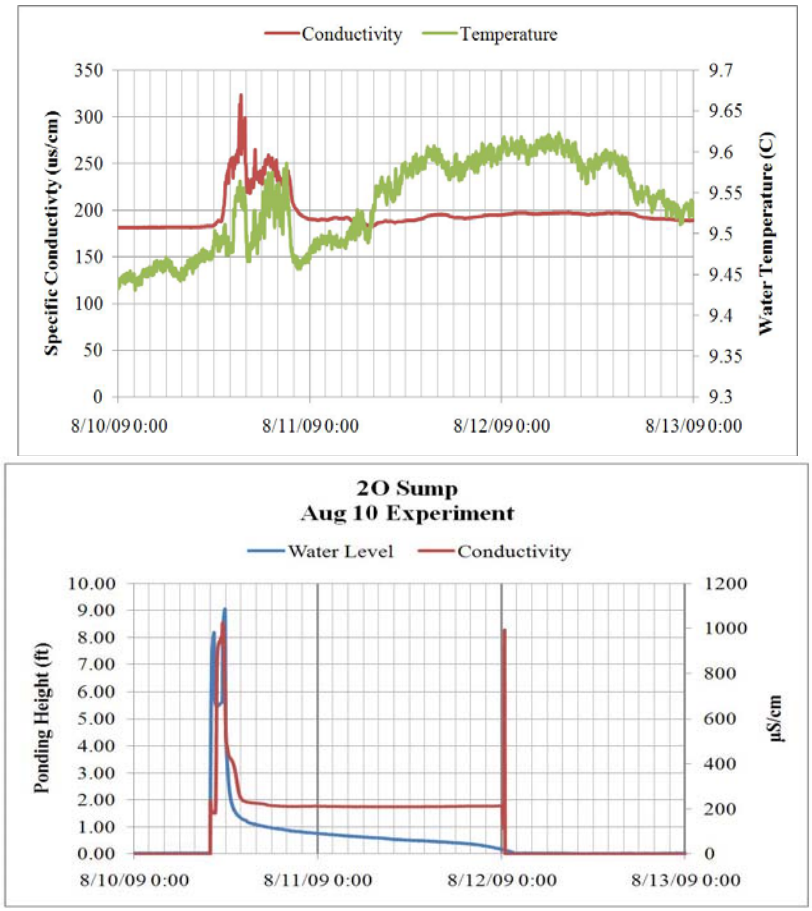

Figure 4.41. Results of artificial tracer (runoff) tracer test at 2O 2009. Water levels and specific conductance measured at the sump, and a record of the temperature and specific conductance at the water table in well 2O MW1.

The water level and conductivity responses of the groundwater to water injected at KQ and HC during the August 2008 borehole tomography testing were also evaluated. The responses at the KQ site showed no measurable change in the specific conductance of the groundwater but did show a rise in the water table (Figure 4.42). The percolation rates at KQ appear to be very fast, with water arriving at the water table (40 plus ft) in a few hours.

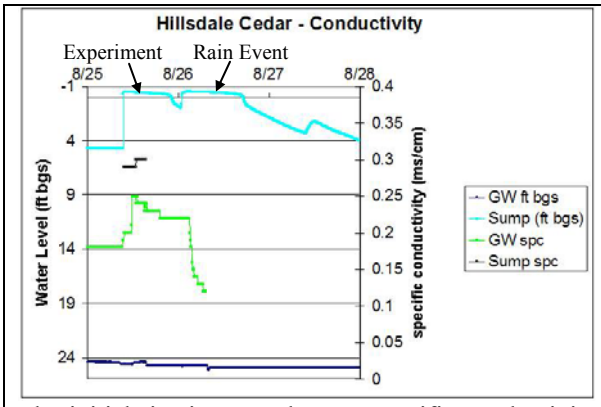

The initial rise in ground water specific conductivity in ground water interpreted to occur from piston flow residual vadose zone waters. With no precipitation, water had time to equilibrate with soils

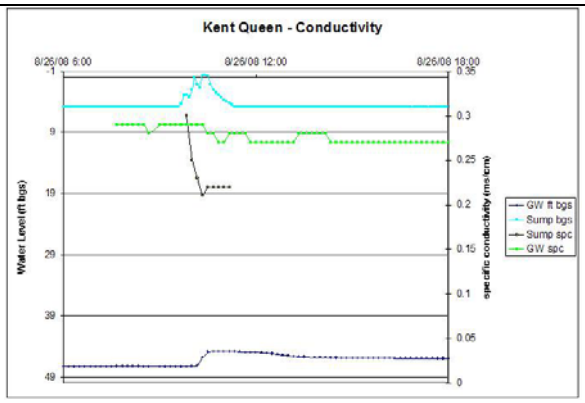

No significant response pattern noted in conductivity. Precipitation event occurred the night before test

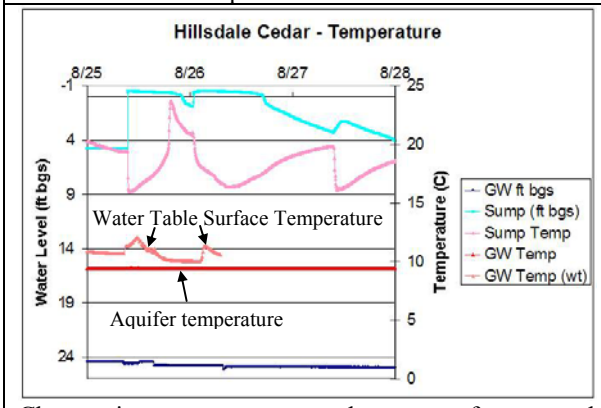

Change in temperature noted at top of water table. Water ponded at HC site with test, followed by precipitation re-filling sump. Temperature spikes at water table surface interpreted to be piston flow of water from within unsaturated zone

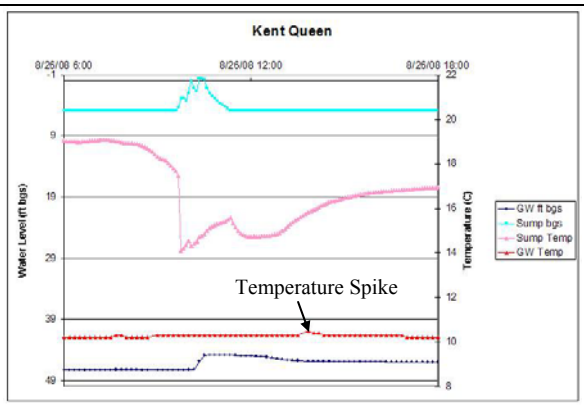

Very small temperature spike noted in ground water in perched aquifer. Timing is consistent with arrival of near surface waters from piston flow in ponded infiltration waters. The infiltration rate corresponds with the rate estimated with geophysics experiment.

Figure 4.42. Specific conductance and water level data for KQ and HC sumps and monitoring wells recordered during the August, 2008, borehole tomography tests. Water was obtained from fire hydrants; no salt tracers were added. Specific conductance values are in mS/cm (previous plots uS/cm).

GEOCHEMISTRY OF SOURCE WATER, PERCOLATING STORM WATER AND RECEIVING GROUNDWATER

The potential for the vadose zone to affect the quality of percolating water is dependent on the nature of the source water, the rates of infiltration, and the reactivity and attenuation potential the vadose zone sediments (Figure 4.43). Study results define the natural storm runoff quality, composition of the infiltrating waters, geochemical character of the vadose zone materials, potential for the vadose zone to alter the chemistry of the infiltrating water, and the observable impacts to the water quality of the shallow groundwater. The geochemical interaction

of percolating waters with unconsolidated vadose zone sediments represents the main processes available to alter percolating water quality.

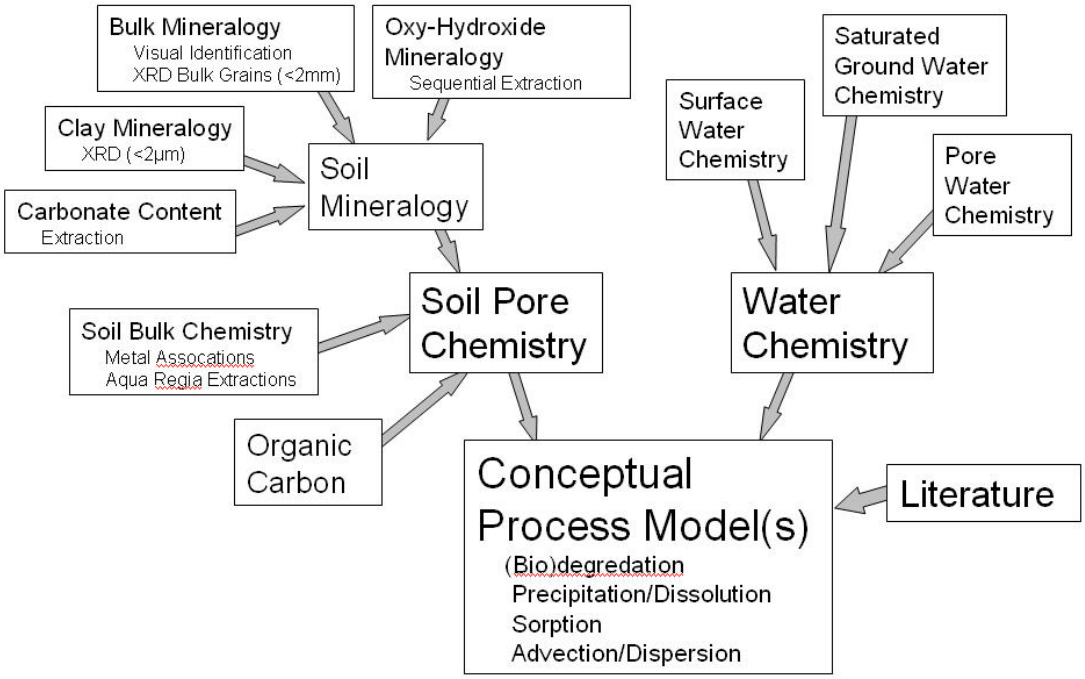

Figure 4.43. Geochemical conceptual process model development.

Source Water

The storm water runoff originates as rain and snow fall throughout the year. Though no precipitation chemistry samples were collected as part of this investigation, the literature notes that samples of precipitation are typically slightly acidic, are low in total dissolved solids, and have a low specific conductivity (Blatchley and Thompson, 1998).

In this study, the storm water runoff was characterized as the water that entered and/or ponded at each specific storm drain site (sump) under investigation. Water quality reflects the original composition of the precipitation and the interaction of this water with the land and road surface of the contributing areas. Generally, the rainfall events in the non-snow period, defined for this study as May through October, resulted in runoff that is directly associated with the timing of the rainfall event. However, during the winter period (November through April) snow and ice accumulate, and direct storm runoff does not occur during intervals of sub-freezing temperatures. Runoff water only enters the storm drains during melt and winter rain events. Winter and early spring runoff entering a storm drain are impacted by the use of de-icer on the roads during this period. The City of Missoula applies a commercial liquid magnesium chloride de-icer under the brand name of FreezGard (North American Salt Company) to melt ice and snow on the streets (Table 4.14). These de-icers have the general composition indicated in Table 4.14. The annual formulation of this de-icer varies. The Colorado Transportation Department compiled analyses for comparable de-icers by the same manufacturer; these results are presented in Table 4.15.

Table 4.14. General Formulation of FreezGard CL Plus Deicer Provided By the Manufacturer

	Percentage	Concentration mg/l
MgCl	30	300,000
K	0.3	3,000
Ca	0.2	2,000
SO4	0.4	4,000
Cl plus inhibitor	0.2	
Water	67	

Table 4.15. Additional Deicer Composition Reported By Colorado Department of Transportation (2000).

Chemicals (ppm)	Magnesium Chloride (FreezGard Zero w/Shield LS)
Arsenic	0.001
Barium	0.0013
Cadmium	0.00001
Chromium	0.0003
Copper	0.0047
Lead	0.0009
Mercury	<0.0004
Selenium	<0.0008
Zinc	0.007
Total Cyanide	<0.0003
Total Phosphorus, ppm (1% solution)	1.02
pH (1:4 Solution)	NA
Sulfate (% by wt)	NA
Ammonia-nitrogen	0.505
Nitrate-nitrogen	0.0681
Biochemical Oxygen Demand (BOD)	<200
Corrosion Inhibitor	1-2% (organic)

A sample of FreezGard Cl Plus De-icer obtained from the City of Missoula street department was analyzed for cations and trace elements (Table 4.16). The lab noted that concentrations of organics in the sample were too high to successfully determine the anions using standard IC analytical techniques (ion chromatography).

Table 4.16. Elemental Analysis of Concentrated FreezGard Cl Plus (North American Salt Company) Solution Used on Missoula Streets Diluted One Hundred to One.

Deicer solution diluted 100X	As	B	Ca	K	Li	Mg	Mn	Na	P	S
mg/l	0.05	5.4	2.7	8.4	7.9	653	0.007	14.6	0.6	20.4

The use of de-icer has increased since its introduction in the fall and winter of 1990 and 1991. Over the course of this study (2006-2009), the City of Missoula applied a cumulative total of over 770,000 gallons of liquid de-icer, along with 12,000 tons of sand that contained 5% NaCl. In the 2008/2009 winter, an additional 318 tons of NaCl were directly applied to the streets as de-icer (Table 4.17)

Table 4.17. Weights and Volumes of Deicers used on Missoula Streets, 2006-2007.

Year	Sand (tons)	MgCl (gal)	NaCl (tons)
2006/07	2000	268519	
2007/08	6379	355850	
2008/09	3904	155362	318.27

Over 170 source water quality samples were collected during the study period (2007 to 2009) (Table 4.19). These samples were collected by both hanging remote samplers (first flush) and by grab sampling. Remote water samplers hung beneath the drain grate and placed near the bottom of the sumps were collected, usually within 24 hours of a runoff event. Grab samples were taken from gutters or from the sump, though not at uniform time intervals from the start of the event. Usually, collection of a complete set of samples from every study site during an event was impossible due to the brevity of the events. Researchers responding to the initiation of a precipitation event would also often find that the quantity of rainfall was insufficient to generate runoff.

The following discussion addresses source water data sets collected at each of the five research sites. Sampling results will be discussed both generally and will also be related to summer (May through October) and winter (November through April) time periods. Generally, the water quality sampling and analysis plan was closely followed. For some samples the alkalinity was not determined within recommended holding times because of sample scheduling and personnel availability, and values were not initially reported. During the study it was noted that some ion balances for surface water samples exceed a 20% criteria. This is attributed to the presence of organics and particulates that occurred in these low total dissolved solid samples along with errors associated with missing holding times for some alkalinity analyses. As a result, these measurements were considered screening level data. The near neutral pH of the runoff water suggests all alkalinity occurs as bicarbonate. In order to generate a data set that is as complete as possible, bicarbonate concentrations were estimated from the alkalinity data. If an alkalinity analysis was missing, the bicarbonate concentration was estimated by setting the ion

balance for the sample equal to one, and then computing the equivalent bicarbonate concentration. Groundwater sample data sets generally have fewer data gaps and meet ion balance criteria. The number of samples collected at each site is summarized in Table 4.18.

Table 4.18. Number of Storm Water and Groundwater Samples Collected at Research Sites.

Site	Total # of Samples	Winter (Nov.-April)	Summer (May-October)
KQ			
Storm Runoff	15	5	10
Groundwater	12	0	12
HC			
Storm Runoff	49	15	34
Groundwater	32	1	31
2O			
Storm Runoff	38	12	26
Groundwater	22	1	21
TS			
Storm Runoff	34	14	20
Groundwater	15	0	15
UM			
Storm Runoff	31	15	16
Groundwater	0	0	0

KQ Source Water Quality

The site at KQ received runoff from an area of about 17,460 square feet. However, ponding at the storm drain was rarely observed. Fifteen samples of runoff were obtained, ten of which were from the remote grate water sampler (catch sample) and five of which were grab samples. Four were collected during the winter and 10 represent conditions during the summer period. One sample had incomplete data. Fourteen percent of the samples were considered screening level data. Two samples had only partial analyses.

The general source water chemistry at KQ grouped by seasonal periods and major ions is presented in the box and whisker plots (Figure 4.44 and 4.45). These show that the runoff water quality during the summer period is dominated by Ca-HCO_3, and concentrations of common ions are low. The ion chemistry during the winter period is dominated by Na-Mg–Cl, and the concentrations of dominant ions are elevated above summer concentrations. Measurable concentrations of lithium were observed in the winter period runoff. Concentrations of dissolved organic carbon are lower in winter runoff than the summer period runoff. Measurable concentrations of iron were observed in 9 of 15 samples. Manganese concentrations were detectable in all samples. Phosphate was detected sporadically in both summer and winter samples (n=4). Nitrate was only detected in two late summer samples. Water quality trends related to first flush versus later storm runoff are not clearly evident in the data set, though for one event (5/5/09) the measured cations appeared to be elevated in the catch sample. Samples

collected in samplers under the grate and in the sump showed no clear difference in water quality.

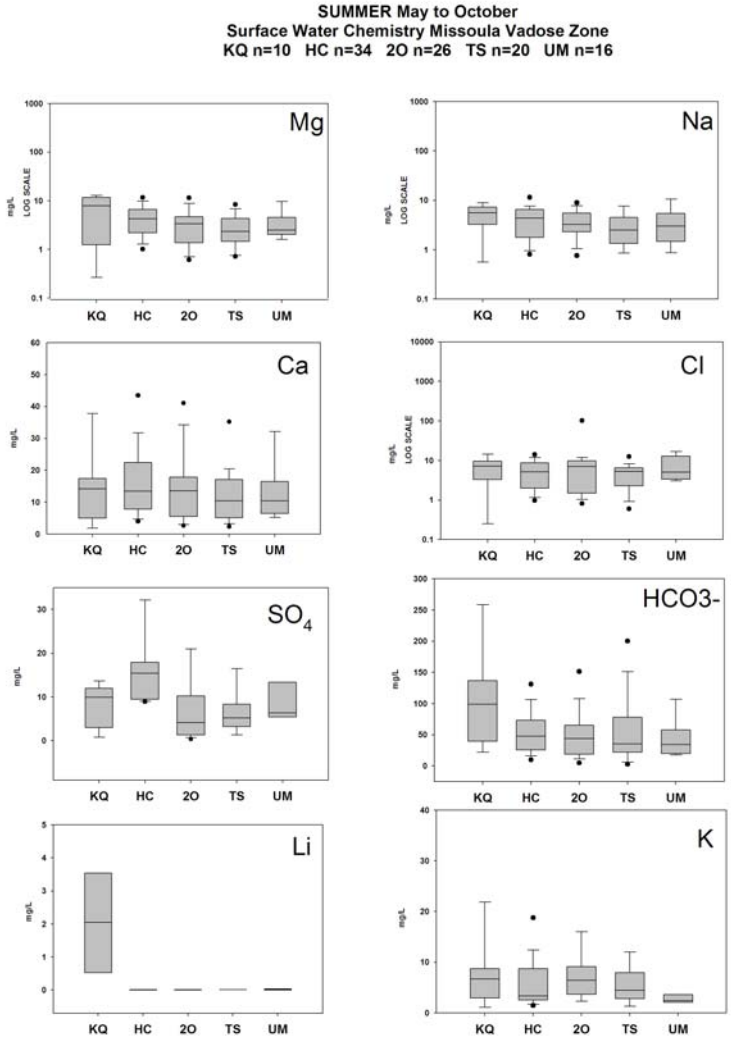

Figure 4.44. Box and whisker plots of major ions and selected trace components of runoff samples collected during the Summer period (May through October). Shaded boxes terminate at the 25 and 75 quartile of values, the horizontal line is the median value and the lines and bars represent maximum and minimum values. Outliers are indicated by solid black dots.

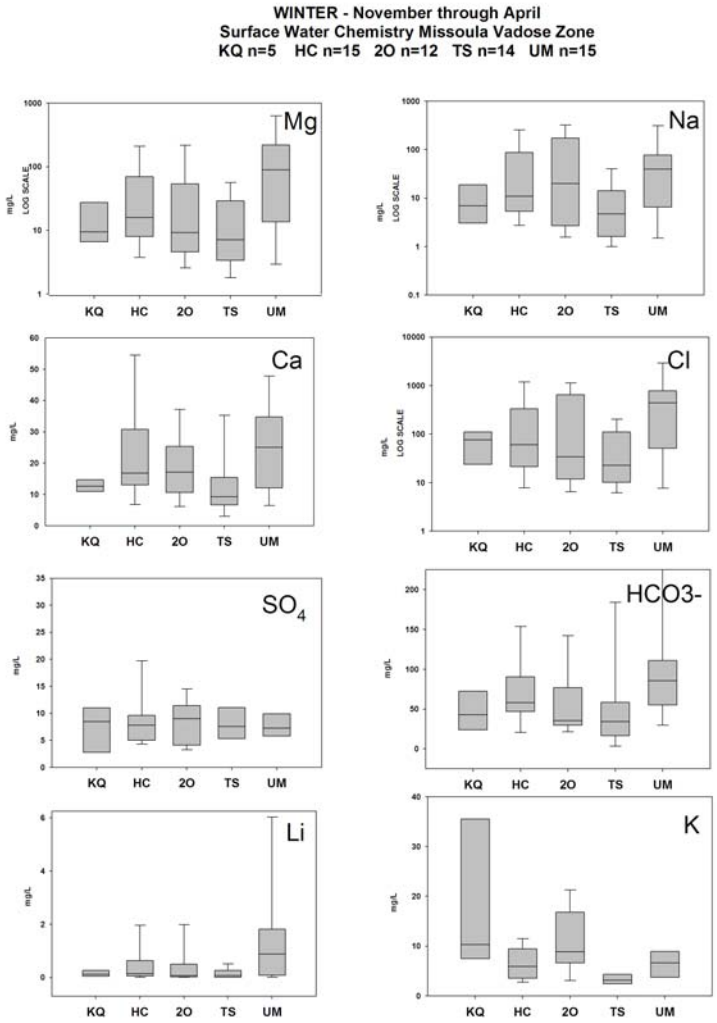

Figure 4.45. Box and whisker plots of major ions and selected trace components of runoff samples collected during the Winter period (November through April). Shaded boxes terminate at the 25 and 75 quartile of values, the horizontal line is the median value and the lines and bars represent maximum and minimum values. Outliers are indicated by solid black dots.

HC Source Water Quality

The site at HC received runoff from an area of about 5,800 square feet. Ponding at the storm drain was commonly observed. Forty nine samples of runoff were collected, 32 of which were obtained from the remote grate water sampler (catch sample) and 17 of which were grab samples. Fifteen were collected during the winter period (2007-2008 and 2008-2009) and 34 represent conditions during the summer period. One sample in the summer (5/5/09) has only a partial analysis. Thirty four percent of the sample results were considered screening level data.

General source water chemistry at HC grouped by seasonal periods and major ions is presented in the box and whisker plots (Figure 4.44 and 4.45). Seasonal trends noted at KQ were also seen at HC.

Water quality of first catch versus later samples from the sumps (same dates of sampling) doesn't show a clear difference in water quality during the summer period. Winter grab samples were typically very elevated in magnesium, sodium and chloride compared to summer period samples. Lithium was detectable above 0.1 mg/L in most winter samples. Nitrate and phosphate in summer samples were detected sporadically and rarely found at concentrations exceeding 1 mg/L. Both winter (n=10) and summer (n=6) sampling found total dissolved organic carbon concentrations ranging between 6 and 75 mg/L, with the higher concentrations occurring in the winter.

2O Source Water Quality

The site at 2O received runoff from an area of about 9,500 square feet. Ponding at the storm drain was occasionally observed. Thirty eight samples of runoff were collected, 23 of which were obtained from the remote grate water sampler (catch sample) and 15 of which were grab samples. Twelve were collected during the winter period (2007-2008 and 2008-2009) and 26 represent conditions during the summer period. Two samples have only partial analyses. Eighteen percent of the sample results were considered screening level data.

General source water chemistry at 2O grouped by seasonal periods and major ions is presented in box and whisker plots (Figure 4.44 and 4.45). Seasonal trends noted at KQ and HC were also seen at 2O. Water quality results of first catch versus later samples from the sumps (same dates of sampling) generally doesn't show a clear difference in water quality during the summer period, suggesting that the first flush effect is minimal. For the event sampled on 9/17/07, the first catch sample data contained higher concentrations of cations and lower concentrations of anions than a later grab sample. Winter grab samples collected after the beginning of the application of street de-icers are typically very elevated in magnesium, sodium and chloride when compared to summer period samples. Lithium was detectable above 0.1 mg/L in most winter samples. Nitrate and phosphate were detected sporadically, and rarely at concentrations exceeding 1 mg/L in summer samples. Both winter (n= 10) and summer (n=2) sampling found total dissolved organic carbon concentrations ranging between 6 and 80 mg/L, with the higher concentrations occurring in the winter.

TS Source Water Quality

The site at TS received runoff from an area of about 5,000 square feet. Ponding at the storm drain was occasionally observed. Thirty four samples of runoff were collected, 28 of which were obtained from the remote grate water sampler (catch sample) and 6 were grab samples. Fourteen were collected during the winter period (2007-2008 and 2008-2009) and 20 represent conditions during the summer period. Thirty two percent of the sample results were considered screening level data.

General source water chemistry at TS grouped by seasonal periods and major ions is presented in box and whisker plots (Figure 4.44 and 4.45). Seasonal trends noted at KQ, HC and 2O were also seen at TS. Water quality of first catch versus later samples from the sumps (same dates of sampling) generally doesn't show a clear difference in water quality during the summer

period. Winter grab samples collected after the beginning of the application of street de-icers are typically very elevated in magnesium, sodium and chloride when compared to summer period samples. Lithium was detectable above 0.1 mg/L in most winter samples. Nitrate and phosphate were detected sporadically, and were rarely at concentrations exceeding 1 mg/L in summer samples (n=2 and n=3 respectively). Both winter (n=9) and summer (n=4) sampling found total dissolved organic carbon concentrations ranging between 5 and 88 mg/L, with the higher concentrations occurring in May.

UM Source Water Quality

The site at UM received runoff generated in an area of about 18,700 square feet. Ponding at the storm drain was occasionally observed. Thirty one samples of runoff were collected, 20 of which were obtained from the remote grate water sampler (catch sample) and 11 ere grab samples. Sixteen were collected during the winter period (2007-2008 and 2008-2009) and 15 represent conditions during the summer period. Two samples have only partial analyses. Thirty three percent of the sample results were considered screening level data.

General source water chemistry at UM grouped by seasonal periods and major ions is presented in box and whisker plots (Figure 4.44 and 4.45). Seasonal trends noted at KQ, HC, 2O, and TS were also seen at UM. Water quality of first catch versus later samples from the sumps (same dates of sampling) generally doesn't show a clear difference in water quality during the summer period. However, for a sample collected during an event on 11/17/07, the grab sample was elevated in all constituents. Winter grab samples collected after the beginning of the application of street de-icers were typically very elevated in calcium, magnesium, sodium and chloride as compared to summer period samples. Lithium was detectable above 0.1 mg/L in 6 winter samples. Nitrate exceeding 1 mg/L was detected in one sample. Other nutrients were not detected above analytical minimums. Both winter (n=9) and summer (n=4) sampling found total organic carbon concentrations ranging between 8 and 80 mg/L, with the higher concentrations occurring in the winter months.

De-icer Impacts on the Winter Period Runoff Chemistry

As presented previously, the City of Missoula applies a liquid de-icer to the streets from mid to late fall and continuing until early spring. This solution is composed of an organic-rich magnesium chloride solution with a high percentage of other cations including potassium (Table 4.17 and 4.18). Trace metal chemistry includes up to 7 mg/L of lithium, a constituent not commonly found in precipitation or local groundwater. As reported in the discussion above, winter runoff samples often contain measurable and even elevated concentrations of the dominant components of the de-icer. The impact of de-icer on runoff chemistry is illustrated by water quality data collected in January 2008 (Table 4.20).

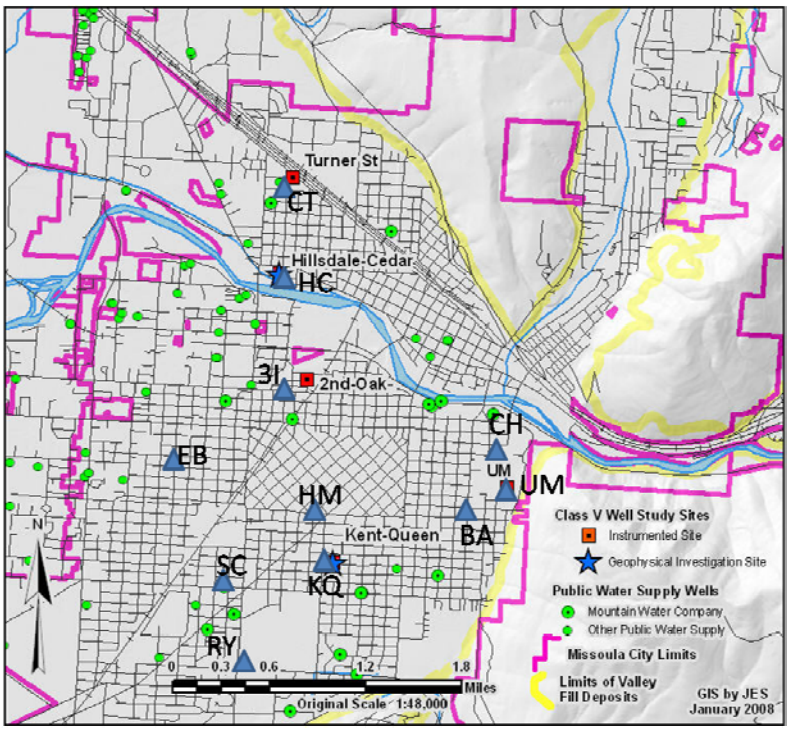

Figure 4.46. Location of sumps and runoff samples (blue triangles) collected to characterize winter melt water quality on January 9, 2008.

On January 9, 2008, accumulated ice and snow began to melt and runoff flowed to city sumps. Grab samples were collected at 11 sites, including KQ, HC, and UM (Figure 4.46). Sampling results are presented in Table 4.19.

The results of sampling winter runoff generated by this event clearly demonstrate that the water at all sites contained anions and cations that are significantly elevated above median summer runoff values. Na, Mg and Cl dominated the water composition. The measurable occurrence of Li (a de-icer component) is also observed. Some sites, such as KQ, appear to be more dominated by Na and Cl, possibly because runoff during the time of sampling was influenced by residential use of NaCl de-icers on driveways and walks. There were no samples during the winter period that were not impacted by either commercial or residential de-icer.

Table 4.19. January 9, 2008 One Day Sampling of Winter Runoff at 11 Storm Drains During a Melt Event.

					m/l								
Sampling Site		Runoff	Na	K	Ca	Mg	Cl	SO4	HCO3*	Li	Zn	Sr	Mn
KQ-0109	1/9/2008	sw	25.9	10.3	14.8	9.5	76.6	<6	49.5	0.08	0.01	0.04	0.005
HM-0109	1/9/2008	sw	84.9	7.3	11.2	46.6	309.6	6.2	41.2	0.44	0.20	0.03	0.111
3I-0109	1/9/2008	sw	274.8	11.1	29.9	113.2	1046.4	11.7	64.3	1.18	0.12	0.19	0.162
CT-0109	1/9/2008	sw	50.3	6.5	9.4	14.7	133.7	<6	37.1	0.12	0.04	0.03	0.035
HC-0109	1/9/2008	sw	88.0	3.6	16.1	49.1	341.4	7.0	45.2	0.48	0.19	0.05	0.125

RY-0109	1/9/2008	sw	113.7	4.4	27.5	110.9	704.4	18.6	81.1	1.09	0.07	0.06	0.254
SC-0109	1/9/2008	sw	112.4	10.7	8.3	39.7	341.0	7.3	311.7	0.39	0.02	0.03	0.038
EB-0109	1/9/2008	sw	21.5	2.1	9.5	38.8	159.8	<6	36.4	0.36	0.08	0.02	0.119
CH-0109	1/9/2008	sw	68.7	9.0	17.4	99.3	467.3	8.5	81.1	0.98	0.04	0.04	0.104
UM-0109	1/9/2008	sw	73.3	3.5	14.2	89.5	439.5	6.7	55.6	0.88	0.03	0.03	0.061
BA-0109	1/9/2008	sw	70.8	10.0	21.1	97.7	475.6	10.5	96.5	0.96	0.18	0.05	0.237
Corresponding Trace Elements			Al	As	Cd	Cr	Cu	S	P	Pb	Fe	F	
KQ-0109	1/9/2008		0.05853	<0.015	<0.004	<0.010	<0.010	0.802	0.405	<.0.08	0.082	<0.7	
HM-0109	1/9/2008		<0.2	<0.015	<0.004	<0.010	0.012	2.200	0.115	<.0.08	<0.100	1.38	
3I-0109	1/9/2008		<0.2	<0.015	<0.004	<0.010	0.006	4.072	<.0.060	<.0.08	<0.100	<0.7	
CT-0109	1/9/2008		<0.2	<0.015	<0.004	<0.010	<0.010	1.319	0.324	<.0.08	<0.100	<0.7	
HC-0109	1/9/2008		<0.2	<0.015	<0.004	<0.010	0.010	2.589	<.0.060	<.0.08	<0.100	<0.7	
RY-0109	1/9/2008		<0.2	<0.015	<0.004	<0.010	0.009	6.000	<.0.060	<.0.08	<0.100	<0.7	
SC-0109	1/9/2008		0.1204	<0.015	<0.004	<0.010	0.017	2.616	0.286	<.0.08	0.125	1.18	
EB-0109	1/9/2008		<0.2	<0.015	<0.004	<0.010	<0.010	1.581	<.0.060	<.0.08	<0.100	1.21	
CH-0109	1/9/2008		<0.2	<0.015	<0.004	<0.010	0.008	2.971	0.208	<.0.08	<0.100	<0.7	
UM-0109	1/9/2008		<0.2	<0.015	<0.004	<0.010	<0.010	2.502	<.0.060	<.0.08	<0.100	<0.7	
BA-0109	1/9/2008		<0.2	<0.015	<0.004	<0.010	0.021	3.702	0.087	<.0.08	<0.100	<0.7	

- *Computed from Alkalinity

Volatile Organic Compounds.

The Turner Street site (TS) runoff was evaluated for volatile organic compounds during sequential storm events beginning the 17th of June 2009. A catch sample was collected during the initial rain event, and the well was sampled intermittently over the next five days. Eight samples were submitted to Energy Laboratories for analysis under EPA SW-846 Method 8260 for Volatile Organic Compounds. The analyte list of fifty one compounds includes all detectable organic compounds of concern, including benzene, toluene, ethyl benzene and xylenes (BTEX). These analyses showed no volatile organic compounds present above 0.5 ug/L.

Percolating Water Quality

At each site, lysimeter sampling was attempted to characterize percolating water quality. Instruments were accessed during infiltration events, when water was ponded at the surface, as well as during likely high sediment moisture periods associated with spring runoff. In some cases, identified non-functioning lysimeters and access tubes were moved to shallower depths. As with the deeper locations, sampling was unsuccessful. Lysimeter sampling was attempted using either a hand pump as a vacuum source or a peristaltic pump when conditions were favorable for its use. The initial sampling protocol used the hand vacuum pump to apply a moderate vacuum onto the lysimeter to maintain low-velocity film flow from the coarse grained materials into the smaller pores of the lysimeter. Sampling was also attempted immediately after and during both controlled and natural infiltration events. During infiltration events when

ponded water was present in the sumps, the peristaltic pump was utilized to maintain a constant vacuum. At 2O, the lysimeter vacuum access tube was cut within the vadose zone by the drilling operator while retrieving the drive rods from the ground and was unusable.

Despite repeated attempts during specific infiltration events, only two lysimeter samples were obtained from the HC instrument placed at 20 ft bgs. Because of the limited sample volume collected complete geochemical characterization was only realized on the 7/2/08 sample. Cations and trace constituents were completed for the 5/5/09 sample (Table 4.20).

Table 4.20. Results of Lysimeter Sampling at HC (7/2/08).

					m/l								
Sampling Site		**Sample**	**Na**	**K**	**Ca**	**Mg**	**Cl**	**SO4**	**HCO3***	**Li**	**Zn**	**Sr**	**Mn**
HC	**7/2/08**	**SW**	**1.13**	**3.26**	**8.47**	**2.17**	**<5**	**<6**	**33**	**<0.005**	**0.090**	**0.020**	**0.072**
		L	**4.31**	**2.64**	**18.08**	**5.86**	**22.52**	**<6**	**85**	**0.037**	**0.016**	**0.027**	**0.593**
	5/5/09	**SW**	**7.13**	**<2.00**	**52.4**	**12.96**	**7.8**	**<6**	**73**	**0.005**	**<0.004**	**0.093**	**0.004**
		L	**5.20**	**<2.00**	**35.24**	**10.31**				**<0.005**	**<0.004**	**0.113**	**<0.004**
Corresponding Trace Elements			**Al**	**As**	**Cd**	**Cr**	**Cu**	**S**	**P**	**Pb**	**Fe**	**F**	
HC	7/2/08	SW	<0.2	<0.015	<0.004	<0.010	<0.010	0.83	<0.060	<0.080	<0.100	<0.5	
		L	**<0.2**	**<0.015**	**<0.004**	**<0.010**	**<0.010**	**0.11**	**<0.060**	**<0.080**	**0.17**	**<0.5**	
	5/5/09	**SW**	**<0.2**	**<0.015**	**<0.004**	**<0.010**	**<0.010**	**4.73**	**<0.060**	**<0.080**	**<0.100**	**<0.4**	
		L	**<0.2**	**<0.015**	**<0.004**	**<0.010**	**<0.010**	**6.27**	**<0.060**	**<0.080**	**<0.100**	**<0.5**	

- * SW Storm Water at the sump, L Lysimeter at 20 ft bls

Recognizing that the number of lysimeter samples is small, the results of the July 2008 storm runoff and vadose zone water sampling would suggest that values for major ions found in the percolating water increased slightly, with calcium concentrations more than doubling. Chloride in the lysimeter sample was 3 to 4 times higher than the runoff, and bicarbonate was about 2.5 times higher. Both iron and manganese were higher in the percolating water sample. Other trace metals concentrations were mostly below detection limits. The sampling in May 2009 generally found the percolating water to be lower in concentrations of cations than the infiltrating storm water. Unfortunately, insufficient sample volume was available for anion analyses.

Characterization of Vadose Zone Geochemical Conditions.

In an effort to indirectly examine how percolating water might be impacted as it passes through the vadose zone, the surface geochemistry of the sediments and their sorption properties were determined. The fine fraction (< 2 mm) of nine sediment samples from the borings at HC and KQ were selected for analyses of extractable compounds using several methods. The first two approaches used a weak HCl acid and a strong acid extraction (Table 4.21).

Table 4.21. Average Elemental Values in a Weak Acid (HCl) and Strong Acid Sediment (n=11 KQ and n=9 HC) Extraction. Values are in mg/Kg.

	Al	Ca	Fe	K	Mg	Mn	Na	P	S	Si	Ba
HCL	327.0	6002.8	1333.8	173.8	1211.3	117.4	21.1	166.8	81.7	269.7	85.4
Strong Acid	5995.5	7768.1	11740.5	1473.3	6154.6	282.6	70.8	396.2	166.8	496.9	206.8
	Ti	As	B	Be	Cd	Co	Cr	Cu	Li	Mo	Ni
HCL	3.0	0.622	0.2	0.1	0.1	0.8	0.7	10.7	0.6	0.0	0.7
Strong Acid	114.7	4.886	1.0	0.2	0.1	4.7	8.1	24.8	0.2	0.1	8.8
	Pb	Sb	Se	Sn	Sr	Tl	V	Zn			
HCL	3.3	-0.1	-0.3	1.1	8.3	0.1	0.8	3.2			
Strong Acid	6.8	-0.3	-4.3	1.8	13.0	-1.2	11.2	26.8			

*Values listed as negative were, on the average below analytical detection limits.

The weak HCl acid extraction was intended to target the surface sorbed elements. The top row of the table contains the elements that were found in the highest concentrations for this extract (HCl). The strong acid extracts removed both the sorbed and reactive compounds at the grain surface. The elements with the highest concentrations are on the second row. When the HCl extract data for KQ are plotted with depth, values at or below 30 ft appear to become more variable, either increasing or decreasing. At HC, however, trends are less clear. Both iron and manganese appear to increase significantly at 31 ft bgs, and then decrease. Review of the boring logs did not identify a lithologic change that correlates with the extraction data trends.

The sediment samples from KQ and HC were also examined for organic carbon content (Figure 4.47). TOC at HC decreased with depth from about 1% at 5ft bgs to less than 0.5% at 18 ft bgs. Concentrations remained low to the final sampling depth of 30 ft bgs. At KQ, TOC values showed little variation from the near surface value of <0.5% to a depth of 45 ft bgs.

Sediment samples of borings at HC and KQ were also examined to determine the cation exchange capacity (CEC) of sediments (Figure 4.48.). The CEC varies between 2 and 5 to a depth of about 20 ft at HC, then decreases to values slightly less than 3 beyond 35 ft. At KQ the CEC shows less variation with depth, declining from about 3.5 to 2 within the first 5 ft bls. The value then stabilizes at approximately 3.

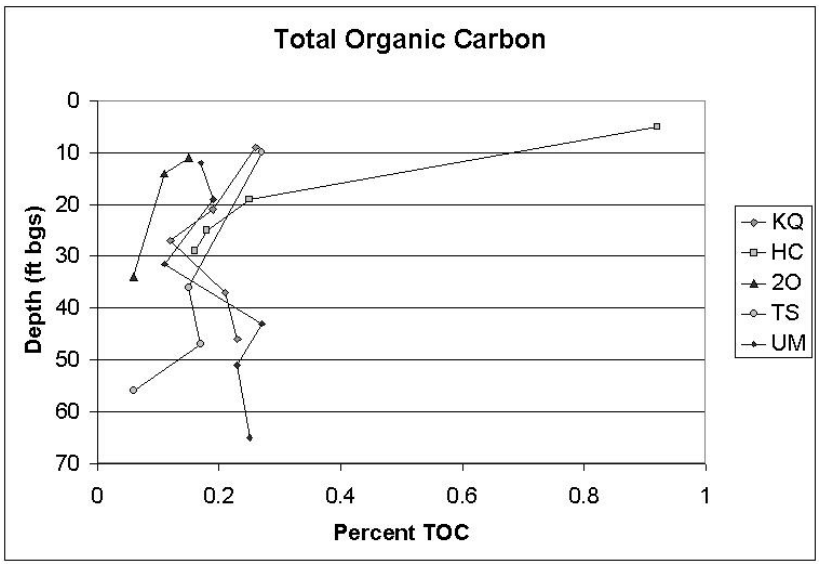

Figure 4.47. Sediment organic carbon content verses depth below land surface at the HC and KQ site.

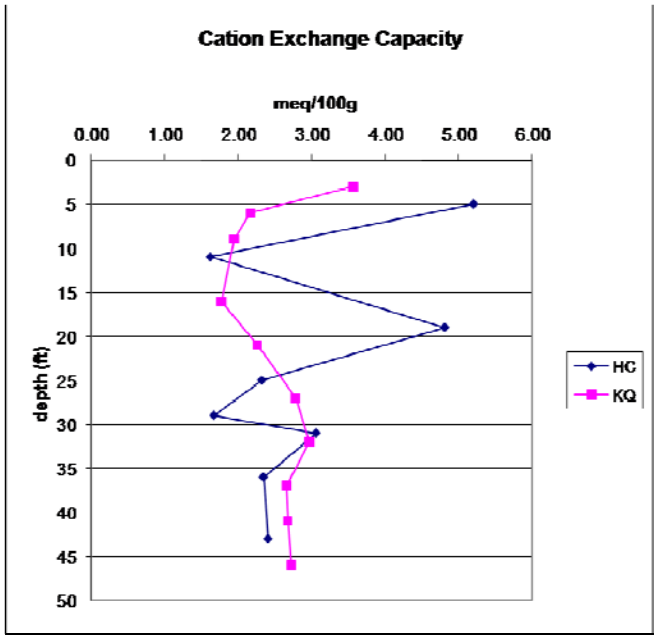

Figure 4.48. Cation exchanges capacity with depth at HC and KQ.

The potential for sorption of storm water constituents on vadose sediment surfaces was evaluated using standard batch tests methods. Four representative core sections from two cores (KQ and HC), and a background sand (collected from a construction excavation containing sediments un-impacted by infiltrating storm water runoff), were placed in a number of different solutions containing different concentrations of dissolved constituents (EPA, 1999a). The solutions included a deionized water (blank), deionized water with a sodium chloride solution (Tracer, T), deionized water with a pH adjusted analytical trace metal standard solution (trace metal, M), and deionized water with a FreezGard deicer solution (deicer, D). A rainwater

(catch) sample was also used as the solute. The rainwater source batch tests were performed using one sediment sample each for the HC and KQ borings, and a control sand sample. At the initiation of the batch tests the five sediment samples were placed in deionized water and three in rainfall catch water to establish nominal values for test parameters. Concentrations of the test constituents were formulated by developing a stock solution and then diluting it to obtain 6 batch solutions (e.g. concentrations 5, 25, 50, 100, 500, and 1000 mg/l) (Table 4.22). The highest concentrations were chosen to represent, in most cases, observed concentrations of the constituents in runoff during the study (e.g. Mg in winter runoff samples ~800 mg/l and Mg in the batch test deicer solution ~650 mg/l).

Table 4.22. Range of Concentrations of Constituents Used in Batch Tests (mg/L).

Na (T)	Na (M)	Na (D)	Cl (T)	Mg (D)	Li (D)	Ba (D)	K (D)	Ca (D)
2-340	5-110	0.7-15	3-700	3-650	0.4-8	<0.03	0.4-8	0.05-3

T= NaCl Artificial Tracer Tests
M= Na in metals standard
D= Deicer solution

Batch tests were completed and the concentrations of initial and final solutions were corrected for blanks. The mass of solute sorbed per unit weight of the solid was then computed as mg/Kg, C*. The final concentration of solute in equilibrium with the sediment, C, was then plotted versus C* to derive the distribution coefficient, Kd (L/Kg) (determined as the slope of the best fit line through zero, Fetter, 2006). In each case, a linear sorption isotherm was interpreted. Once the Kd values were computed, a retardation factor Rf was derived, assuming reversible sorption, using the following equation:

$$Rf = 1 + \frac{BdKd}{n}$$

Where: Rf = retardation factor
Bd= Bulk Density (Kg/m3)
Kd= distribution coefficient (L/Kg)
n= porosity

Examples of the plotted results of the batch experiments are presented in Figures 4.49, 4.50 and 4.51.

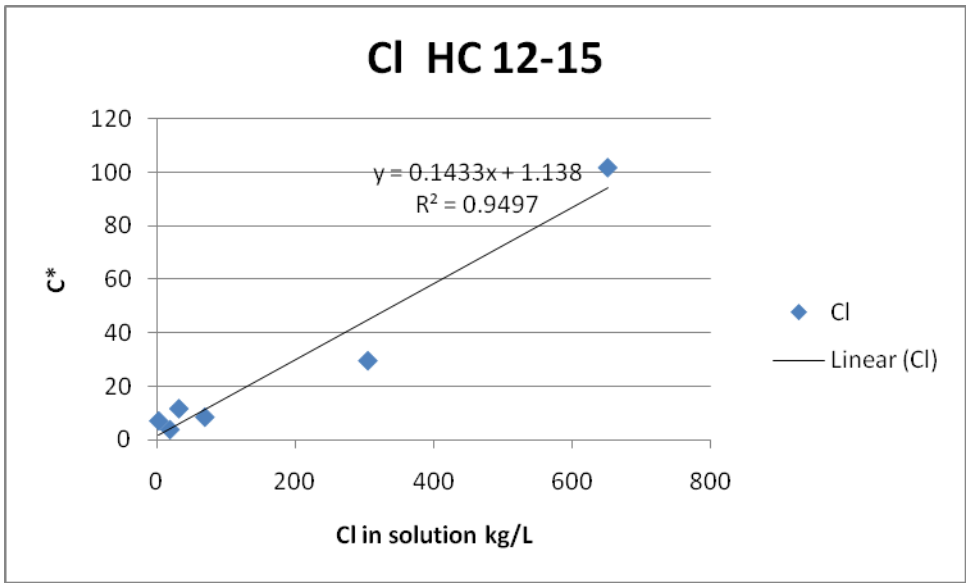

Figure 4.49. Batch test results for chloride (NaCl tracer solution) showing the relationship of the equilibrium solution chemistry (C mg/L) to the mass of solute sorbed per dry unit weight of solid (C* (mg/Kg) for the sediment representing the 12 to 15 ft interval at HC. The Kd is the slope of the line, 0.1433 L/Kg.

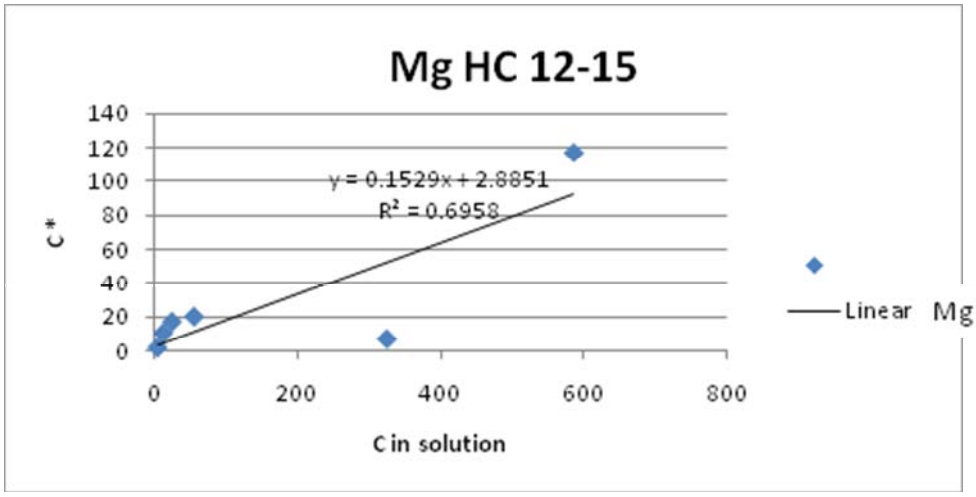

Figure 4.50. Batch test results for magnesium (deicer solution) showing the relationship of the equilibrium solution chemistry (C mg/L) to the mass of solute sorbed per dry unit weight of solid (C* (mg/Kg) for the sediment representing the 12 to 15 ft interval at HC. The Kd is the slope of the line, 0.1529 L/Kg.

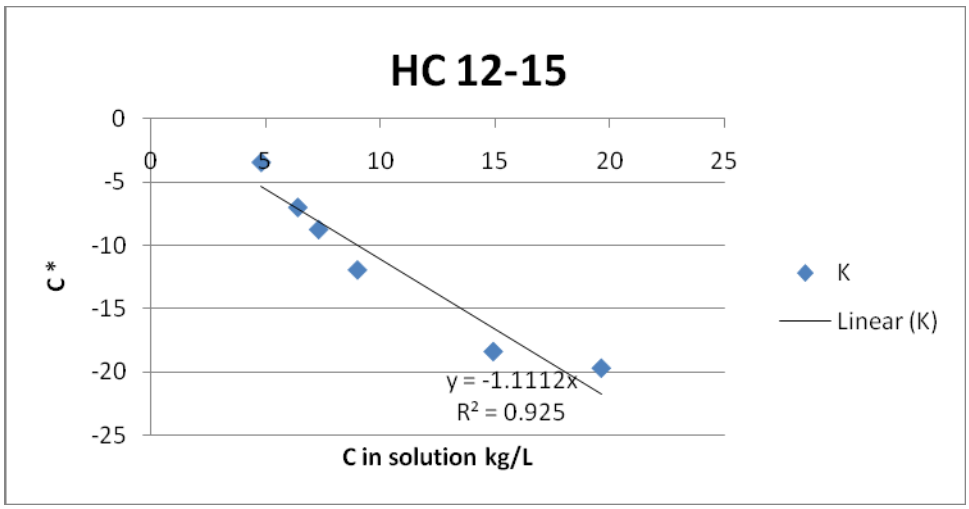

Figure 4.51. Batch test results for potassium (deicer solution) showing the relationship of the equilibrium solution chemistry (C mg/L) to the mass of solute sorbed per dry unit weight of solid (C* (mg/Kg) for the sediment representing the 12 to 15 ft interval at HC. The Kd is the slope of the line, -1.1 L/Kg. The results show potassium is being released into solution from the sediments (negative slope).

Computed Kd and Rf values are reported in Table 4.23. Because the KQ and HC sediments were similar in character, average values of bulk density and porosity were generated from the eleven values of these parameters derived during the physical and hydrologic characterization of the column samples described previously. The same parameters were used to represent the character of the control sand sample in all cases. In each case, in situ vadose zone sediments are likely to have lower porosities than assigned, as well as slightly higher bulk densities. As a result, computed Rf values may be as much as 40% larger than reported values.

The magnitude of the Rf values suggest how the transport of elements found in percolating water would move through the vadose zone under near-saturated or saturated conditions. A Rf value of 1.0 indicates that no sorption occurs. Under these conditions the transport of the constituent is conservative, meaning no loss of mass or concentration occurs during transport and the solutes move with the average percolation rate. The sorption process is assumed to be temporary and totally reversible. When the Rf is greater than 1.0, transport is retarded. For example, during the batch test using deionized water, if Li in the de-icer solution is moving through the sediment type represented by KQ at 18-22 ft, the rate of transport will be slower than the water by 0.5 (Rf = 2.01). When Rf values are less than 1.0, or negative mass is being added to the solution via desorption during transport, and the concentration found in the percolating water will increase. Under these conditions the average rate of transport is not impacted. Additional factors complicating predictions of the degree of surface reactions that will take place for a particular constituent are the nature of the exposed mineral surfaces and the geochemical matrix of the water.

Table 4.23. Batch Test Computed Kd (L/kg) and Rf Values for Sediment Samples from Borings at KQ and HC, and a Control Sand. Solutions were Formulated with Deionize Water and a Field Collected Rainwater Sample.

Note that negative Kd and Rf values indicate elements are being added to the initial batch fluid in contrast to positive values that suggest sorption is occurring to varying degrees.

	KQ18-22		KQ38-42		HC12-15		HC 15-18		Sand Control	
Deionized	**Kd**	**Rf**	**Kd**	**Rf**	**Kd**	**Rf**	**Kd**	**Rf**	**Kd**	**Rf**
Na (T)										
Na (M)	**0.092**	**1.44**	**0.08**	**1.40**	**0.094**	**1.24**	**0.080**	**1.41**	**0.085**	**1.43**
Na (D)	0.026	1.13	-0.077	0.61	0.087	1.44	-0.87	-3.40	-0.06	0.70
Cl (T)										
Mg (D)	0.18	1.91	0.261	2.32	0.153	1.77	0.204	2.03	0.121	1.61
Li (D)	**0.2**	**2.01**	**0.16**	**1.81**	**0.177**	**1.89**	**0.205**	**2.04**	**0.064**	**1.32**
As (D)	1.365	7.90	1.092	6.52	1.039	6.25	1.092	6.52	0.345	2.74
K (D)	**-0.919**	**-3.85**	**-1.806**	**-8.13**	**-1.11**	**-4.81**	**-1.52**	**-6.88**	**-0.05**	**0.75**
Ba (D)	-2.5	-11.64	-2.5	-11.64	-2.5	-11.64	-2.5	-11.64	-0.484	-1.45
Ca (D)	**-2.26**	**-10.43**			**-2.22**	**-10.22**	**-2.29**	**-10.58**	**-2.39**	**-11.08**
Rain Water										
Na (T)					0.27	2.37			0.18	1.91
Cl (T)					**0.14**	**1.71**			**0.07**	**1.35**
Mg (D)					0.227	2.15			0.208	2.05
Li (D)					**0.376**	**2.90**			**0.287**	**2.45**
As (D)					1.615	9.16			0.89	5.50
Average porosity, n=0.36 (n=11)										
Average bulk density, Bd= 1.82 (n=11). Data from column experiments										

Examination of the deionized water based batch test results suggests that Na in the metals standard matrix behaved similarly in all 5 samples, with an Rf about 1.4. However, the Rf of Na in the de-icer matrix was more dependent on the specific sediment sample used. Rf values greater than 1 were found for samples KQ 18-22 and HC 12-15, but values of less than 1 were observed for the other three samples. Magnesium in the deicer matrix sorbed to all samples, as did Li and As. Arsenic had the highest observed Rf of all of the samples. Evaluation of the sorption potential for K, Ba and Ca all show that sediments released those elements into solution. Chloride sorption for the sodium chloride tracer matrix was also noted to occur. This is quite interesting as anions are assumed to act conservatively in most settings.

Water Quality of Ground Water Recharge

Over 70 groundwater quality samples were collected during the study period (2007 to 2009) (Table 4.20). These samples were from monitoring wells at four of the sites: KQ, HC, 2O and TC. The UM site did not have a monitoring well. The construction of these wells was completed after the rotary sonic coring process. The final screen interval for each well and the low and high water table position at each site is indicated in Table 4.11. During the well construction, the depth of the water table was estimated from available historic data, and the coring advanced to 10 to 15 ft below this depth. In some cases the monitoring well screened interval ended up being positioned further below the water table than ideal. As a result, some samples of groundwater may not fully represent the direct impact of storm water as it induced changes in groundwater quality. This is most likely at times of the year when the top of the screened interval was located 10 to 15 ft below the water table. The number of samples collected at each site is summarized in Table 4.19. A discussion of groundwater quality at each research site follows.

KQ Groundwater Quality

At KQ 12 groundwater samples were collected. All samples represented the summer period. Eight samples were collected from well M1 in the perched aquifer and four from M3 in the regional aquifer. One sample had only a partial analysis and one was considered screening level data. Two samples were duplicates.

The general major ion groundwater chemistry at KQ is presented in the box and whisker plots presented in Figure 4.52. These show that the groundwater quality during the summer period is dominated by Ca-HCO_3 and by concentrations of common ions, which results in a specific conductance of 200 to 300 µS/cm. Measurable concentrations of lithium were observed at less than 0.1 mg/L for one sample, and detectable phosphorous was only found in one sample. Nitrate concentrations occurred more frequently, with eight samples containing

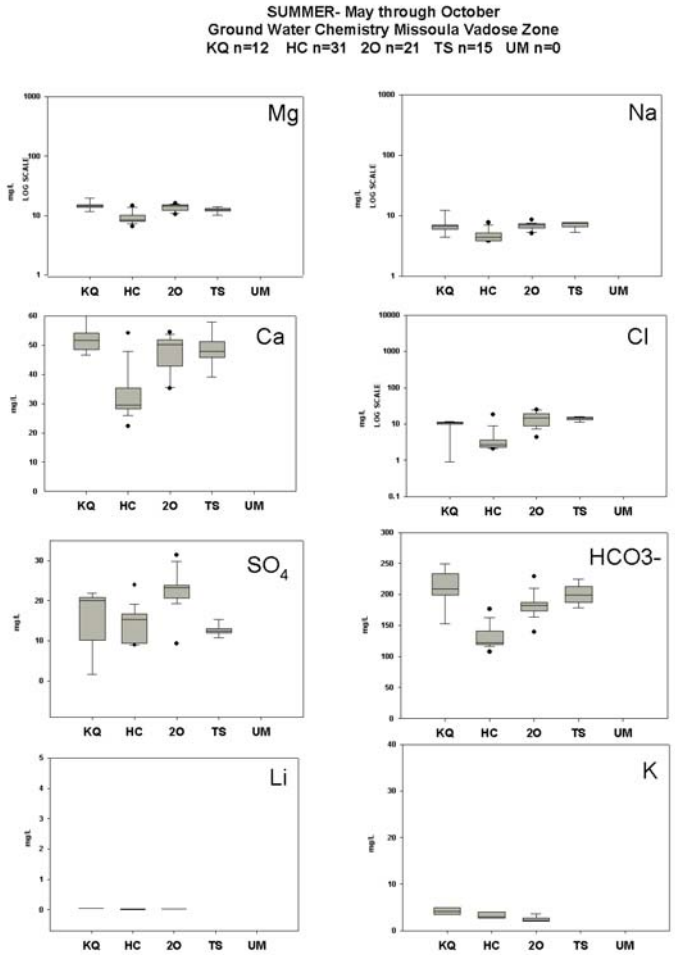

Figure 4.52. Box and whisker plots of major ions and selected trace components of groundwater. Shaded boxes terminate at the 25 and 75 quartile of values, the horizontal line is the median value and the lines and bars represent maximum and minimum values. Outliers are indicated by solid black dots.

detectable nitrate, seven of which were in 1 to 2 mg/L NO_3-N range. Two dissolved organic carbon samples (May and June 2008) ranged from 4 to 13 mg/L.

HC Groundwater Quality

A total of 32 groundwater samples were collected from HC. Thirty one samples represented the summer period and one the winter period. Twenty nine samples were collected from well HC M2 and 3 samples were collected from M1. Two samples had only a partial analysis.

The general major ion groundwater chemistry at HC is presented in the box and whisker plots (Figure 4.52). These show that the groundwater quality during the summer period is dominated by Ca-HCO_3 and by measurable concentrations of common ions, which result in a specific conductance of 200 to 300 µS/cm. Measurable concentrations of lithium were observed at less than 0.1 mg/L for two samples and phosphorous was not detectable. Measurable nitrate concentrations were less than 0.7 mg/L NO_3-N for12 samples and one was 2.0 mg/L. Two samples for dissolved organic carbon were 4 and 6 mg/L.

2O Groundwater Quality

A total of 22 groundwater samples were collected at 20. Twenty one samples represented the summer period and one the winter period. One sample was considered screening level data.

The general major ion groundwater chemistry at 2O is presented in the box and whisker plots (Figure 4.52). These show that the groundwater quality during the summer period is dominated by Ca-HCO_3 and by measurable concentrations of common ions, which result in a specific conductance of 200 to 300 µS/cm. Measurable concentrations of lithium were observed at less than 0.1 mg/L for two samples, and phosphorous was not detectable. Measurable nitrate concentrations were detected in all but one sample. Values range from 0.4 to 5.0 mg/L NO_3-N. Two samples for dissolved organic carbon were 4 and 6 mg/L.

TS Groundwater Quality

Fifteen groundwater samples were collected and they all represented the summer period. All were collected from well M1. One sample had only a partial analysis.

The general major ion groundwater chemistry at TC is presented in the box and whisker plots (Figure 4.52). These show that the groundwater quality during the summer period is dominated by Ca-HCO_3 and measurable concentrations of common ions, which result in a specific conductance of 200 to 300 µS/cm. Measurable concentrations of lithium and phosphorous were not detectable. Measurable nitrate concentrations were detectable in each sample and ranged from 1.3 to 4.0 mg/L NO_3-N. One sample for dissolved organic carbon reported 2.5 mg/L.

Groundwater VOC Analyses

The Turner Street site (TS) was evaluated for volatile organic compounds during sequential storm events beginning on the 17th of June 2009. A catch sample was collected during the initial rain event and the well was sampled intermittently over the next five days. Eight samples were submitted to Energy Laboratories for analysis under EPA SW-846 Method 8260

for Volatile Organic Compounds. The analyte list of 51 compounds includes all detectable organic compounds of concern including benzene, toluene, ethylbenzene and xylenes (BTEX). Results for these analyses showed no volatile organic compounds present above 0.5 µg/L.

Groundwater Quality Change after a Runoff Event

In an attempt to determine if impacts to the groundwater from runoff events were observable by sampling the underlying groundwater, a 5 day storm event was sampled at KQ in May 2009 (Figure 4.53). Groundwater from the monitoring wells was sampled daily and weekly after this period of storm water infiltration (Figure 4.54). The groundwater results suggest no clear impacts to the water quality occurred as no significant changes in water quality were observed after the event had ended.

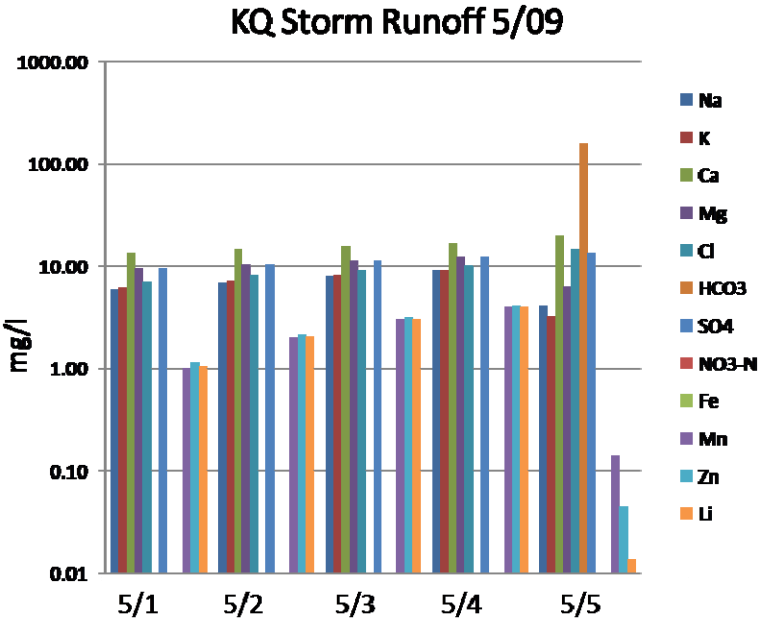

Figure 4.53. Water quality of storm water entering the sump at KQ in the first 5 days of May 2009. Runoff was of similar quality during the period.

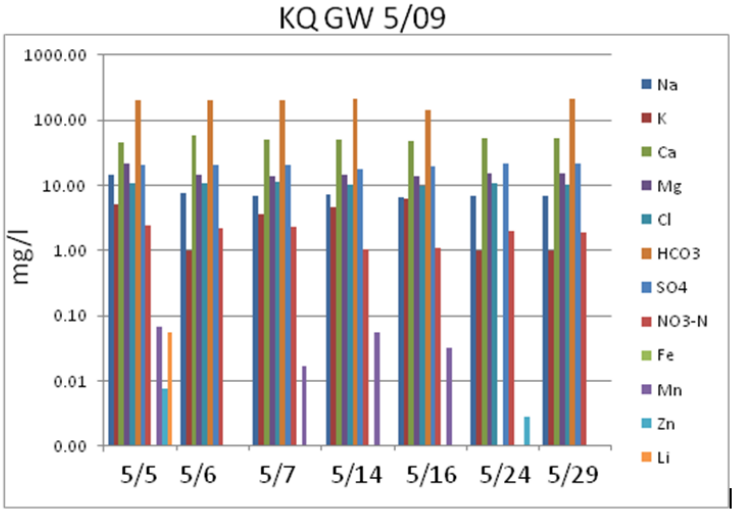

Figure 4.54. Quality of groundwater at KQ at the end of the 5 day runoff event and for the next 2 days and 2 weeks.

CONCEPTUAL AND NUMERICAL MODELING

The conceptual model formulated at the initiation of this work was used to design and execute this research. The conceptual behavior of storm water as it moves into and through the vadose zone was proposed in Figure 1.1. This basic model was supported by the observed behavior of storm water recorded during this work (Figure 4.55 A). Sediment data from the rotary sonic corings indicate that fine grained deposits are only minor components of the vadose zone stratigraphy and, most likely, act locally to retard downward movement of percolating water (Figure 4.55 B). The only minor deviation observed from the conceptual model is that water table responses to percolation events were generally subdued by the diffuse arrival of the recharge and the high hydraulic conductivities of the receiving aquifer. Numerical simulations were developed to further investigate physical controls on percolation.

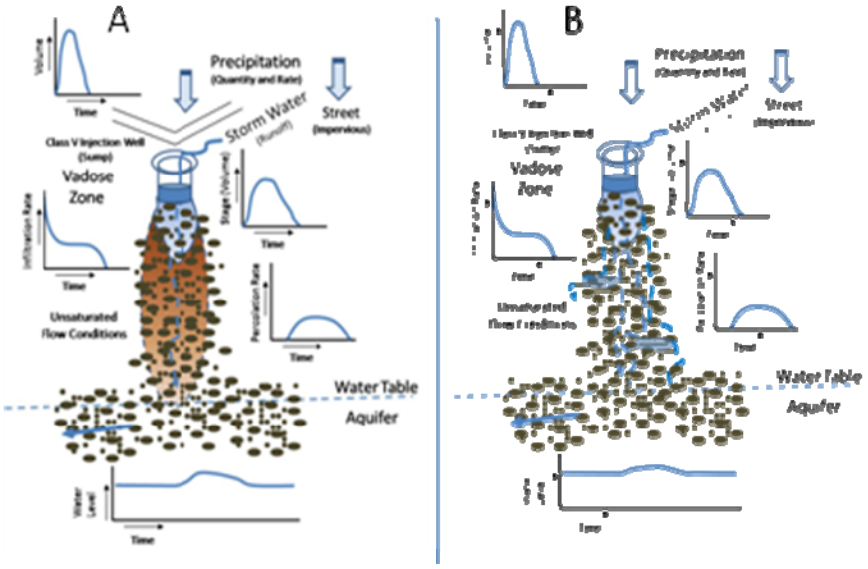

Figure 4.55. Conceptual model of factors controlling the physical movement of water through the vadose zone. A. The original model. B. The revised model based on study results.

The geochemical conceptual model originally presented suggested that the quality of infiltrating water would show measurable differences in the first flush and later runoff samples (Figure 1.2). In addition, as water was transported through the vadose zone, reactions would reduce percolating water constituent concentrations (as specific conductance) resulting in an overall reduction in the dissolved constituents in the water, and thus groundwater recharge (Figure 4.56 A). Based on limited vadose zone water quality samples and extensive geochemical investigation of the sediment composition and properties, it appears that both the reduction of some compounds, and addition of others occur as water percolates downward (Figure 4.56 B).

The processes affecting the fate of storm runoff constituents during percolation is elaborated upon in the discussion section of this report and is not simulated directly in this work.

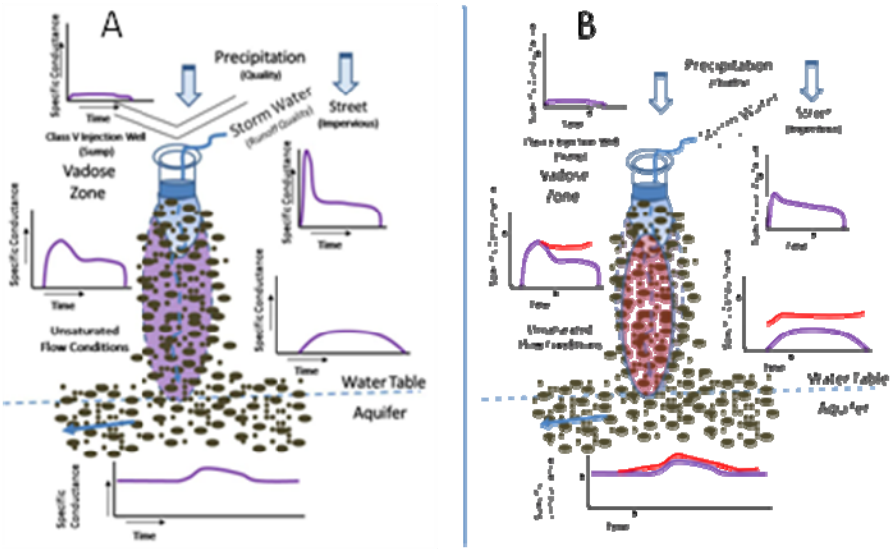

Figure 4.56. Conceptual model of the water quality changes (represented as specific conductance) that occur during storm water percolation. A. The original conceptual model that assumes vadose processes reduce constituents in a storm water source during percolation. B. The revised conceptual model that suggests that infiltrating and percolating water both loses some constituents during percolation (purple line) and reacts with the sediment gaining other constituents (red line).

To simulate the observed physical percolation process the modeling program VS2DT was utilized. It was used to simulate the general physical conditions found at KQ. Detailed geological data, extensive geochemical information, and physical and hydrological property data were available to formulate the vadose zone model. In addition, two percolation data sets were available to use for model calibration: the geophysics cross borehole tomography results (for first 25 ft of transport), and the saline tracer tests results that provide overall percolation rates to a depth of about 50ft.

Modeling Phase 1. Geophysical Results Calibration of Near Surface Percolation

The initial model was developed assuming isotropic and homogenous conditions in a single type of coarse-grained geologic materials. The model was structured as a two dimensional cross section of the vadose zone underlying the KQ site (Figure 4.57). The base model run was developed using three time periods. The first period allowed the model domain to equilibrate within initial moisture conditions. The second period introduced water into the system using a constant flux rate from the base of the sump. A rate of 0.005 m/s was used to approximate an infiltration rate of 90 gpm across the 4-foot diameter sump base for a 30 minute period. The third time sequence represented an additional hour to observe the movement of the infiltrating

water body. Additional simulations utilized this input boundary approach, however, as needed the second and third periods were expanded to simulate longer percolation times.

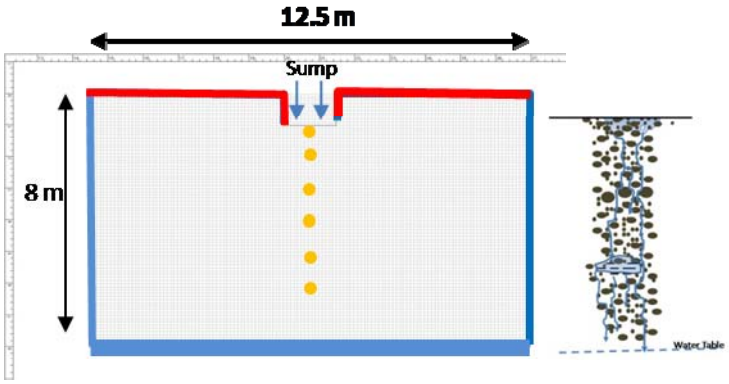

Figure 4.57. Cross sectional model formulation for the general setting at KQ. The boundaries shown in blue are flux boundaries that allow water to exit the model if it reaches the boundary. The top red boundary is a no flow. The blue arrows at the sump base represent a specific flux boundary where "infiltrating storm water" enters the model. The model grid is 10 cm by 10 cm. Orange dots are the locations where model results are compared to field observations (geophysical tomography results).

The hydraulic parameters assigned to the geologic unit as initial conditions are listed in Table 4.24. Once these conditions were input, the model was initiated using discrete two minute time steps to avoid numerical stability issues. Results were evaluated after a simulation was completed. If simulated conditions did not reasonably match the observed conditions, the parameters were manually changed within observed ranges and the model was re-executed. This process was repeated until the model was judged calibrated.

Table 4.24. Model Parameters Use in the VS2DHT Simulations.

Parameter	Discussion
Saturated Hydraulic Conductivity	The saturated hydraulic conductivity (Ks) is the sediment property that controls the rate of fluid movement in the subsurface. The unsaturated hydraulic conductivity varies with moisture content and pore pressure (matric potential); however, modeling functions for unsaturated hydraulic conductivity are based on the saturated hydraulic conductivity. The initial value used for the modeling program was 0.0035 m/s, determined from the results of the permeameter tests.
Ratio, vertical to horizontal, conductivity	Sediments deposited by flowing water will align themselves in a preferred direction, with the long axis generally horizontal. This structure in sediments, imbrication, results in horizontal permeabilities greater than vertical permeability. The initial value for this parameter was estimated at 0.1, where the horizontal permeability is an order of magnitude greater than the vertical hydraulic conductivity.
Specific Storage	Specific storage represents the amount of water released from sediments during gravity drainage from saturated conditions. The specific storage value was estimated at 0.1 for the soils

Porosity	Porosity represents the amount of void or open space in a material, presented as a percent of total volume in a material. The porosity for the soils was estimated at 40%, based on the results of the permeameters
Residual Moisture Content	The residual moisture content represents the amount of water retained in soil pores after gravity drainage has occurred. For this study, the residual moisture content was estimated at 9%, based on the results of column experiments.
Van Genuchten Parameters	The Van Genuchten parameters represent the numerical values applied to curves empirically fit to soil retention data characterizing the relationship between saturated hydraulic conductivity, moisture content and pore (matric) pressure. Alpha is a multiplier for the pressure head, and beta helps fit exponential curves. The initial Van Genuchten parameters for this study were set at 4.5 for alpha, and 4 for beta; based on parameters for medium sand as provide by the VS2DH model.

Percolation rates for each simulation were estimated by examining graphs of the arrival of saturation levels with time at model observation points. The time correlating with conditions approaching maximum saturation was selected to represent percolating water arrival (Figure 4.58).

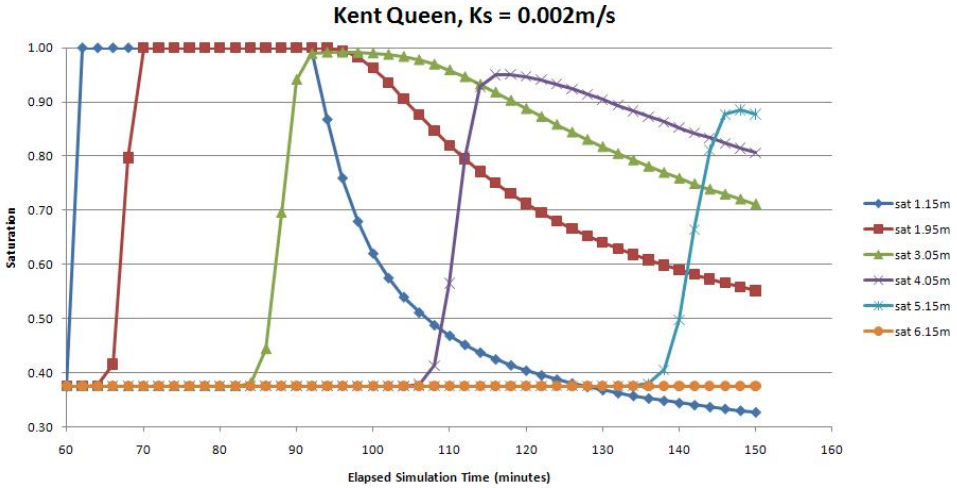

Figure 4.58. Sample simulation results for determination of maximum saturation at different depths with time as the simulation progressed. Water was introduced into the system at 60 minutes. The ledgen represent model output at that depth below the sump base.

Model calibration required refining the initial parameter values, primarily the saturated hydraulic conductivity value and the van Genuchten parameters. The van Genuchten parameters represent the most difficult part of the modeling program to define as coarse grain sediments. The van Genuchten parameters are poorly represented in vadose zone models because they are often based on limited data sets of moisture content and matric potentials relationships. Studies to define these parameters for specific soils and sediments require an extensive laboratory investigation and are difficult to complete for coarse grained conditions as seen in this work.

The observed column drainage results completed as part of this project, mirrored the expected behavior of coarse grained sediments,. Little change was observed in matric potential (negative pore water pressure) until the sediment moisture content approached the field capacity (Figure 4.25).

Due to difficulties encountered in laboratory analysis of the van Genuchten parameters, literature values by Ippisch et al. (2006) were used as parameters for this modeling approach. Changes in the van Genuchten parameters for the simulations completed here show the position of the percolation front is fairly insensitive to parameter uncertainty (Figure 4.59). Lowering the parameter numbers generally results in increased water retention properties for the soils.

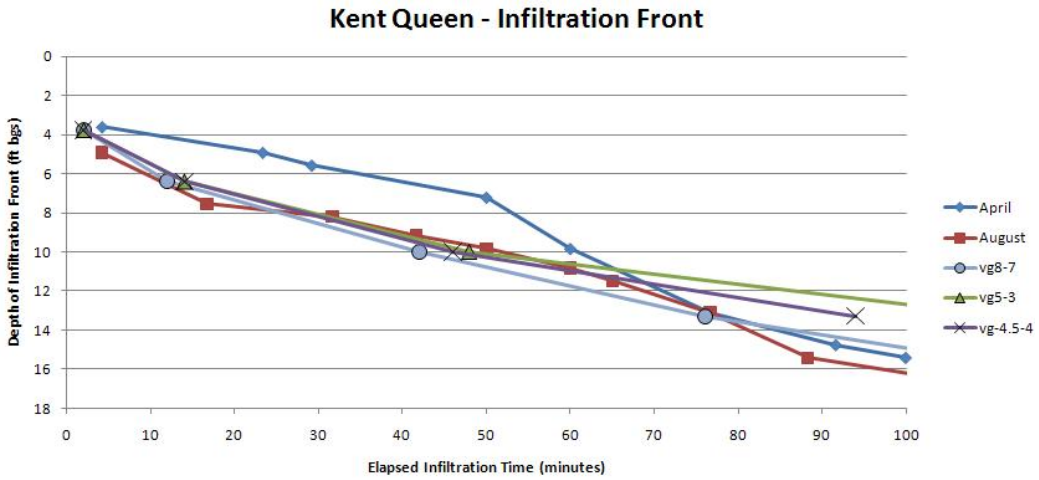

Figure 4.59. Changes in percolation rates with variations in van Genuchten parameters. Three curves were derived from varying the van Genuchten parameters, and compared percolation front simulated for the April and August tracer test data. The first curve has alpha at 7.97 and beta at 6.97 (vg8-7). The other curves use alpha at 5 and 4.5, and beta at 3 and 4, respectvively (vg5-3 and vg4.5-4).

With the base van Genuchten parameters held constant, the model was executed with different saturated hydraulic conductivity values in an attempt to calibrate the simulation to field observations. A saturated hydraulic conductivity value of 0.0015 m/s (425 ft/d) was found to provide the most acceptable match of simulated percolation rates with observed (Figure 4.60). This value of saturated hydraulic conductivity is approximately half of the value predicted from the laboratory permeameter results (Table 4.8). While the estimated permeability is lower than column measured values, it is likely that natural insitu values are lower than the disturbed sample lab values. In addition, the coarse nature of the sediments may have permitted some infilling with storm water sediments and or partial clogging by biological activity. With all other parameters treated as constants, the saturated hydraulic conductivity becomes the principle parameter controlling the percolation rate.

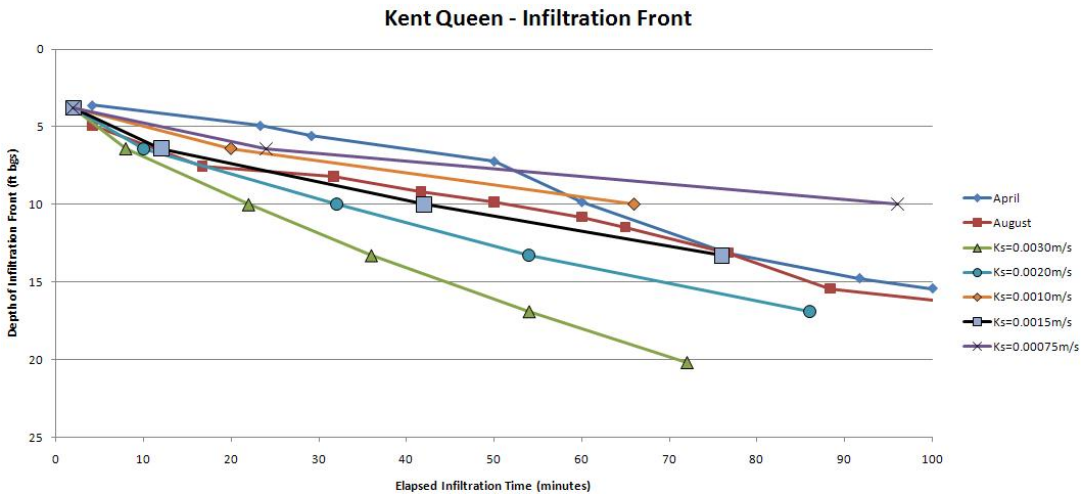

Figure 4.60. Comparison of model generated depth of percolation front data sets using different hydraulic conductivity values. The computed percolation front behavior from the April and August geophysical artificial tracer tests were compared with model results.

This first phase of modeling resulted in simulating percolation at shallow depths. The calibrated simulated percolation rate was 7.7 ft/h, slightly more than the average rate of 6.4 ft/h percolation rate interpreted from the geophysics experiments. Interestingly, under the modeled conditions, the percolation rate appears to be relatively insensitive to the actual storm water infiltration rate (Figure 4.61).

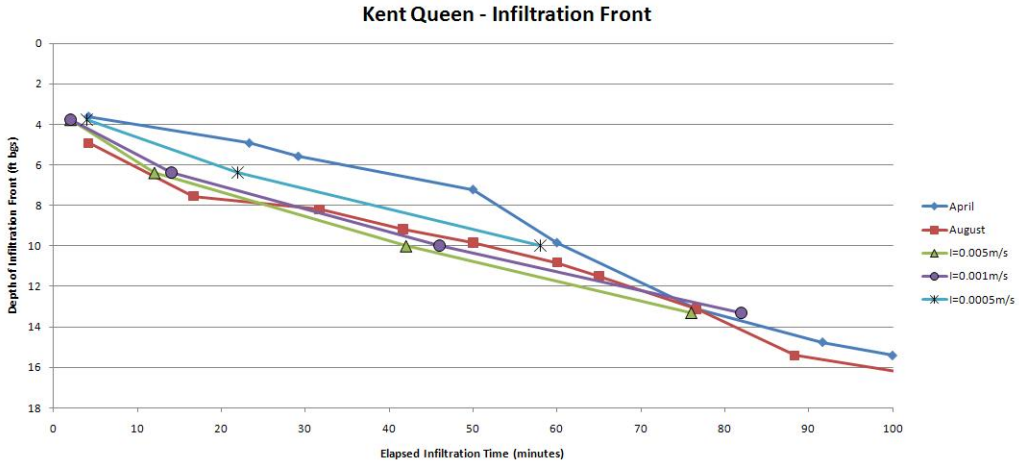

Figure 4.61. Changes in the percolation rate with variations in the infiltration rate from the sump base.

Modeling Phase 2. Tracer Test Based Calibration of the Full Unsaturated Zone

The second phase of modeling utilized the full thickness of the vadose zone. Tracer test results and observations of water table responses from a natural runoff event were used for calibration (August 2009). Both events showed a delay of approximately one hour between the

time that storm water entered the sump and the detection of a water level response in monitoring well KQ-M1 (total depth of 48 ft). Hydrographs of water levels in the sump and in KQ-M1 are shown in Figure 4.62. The expanded model required the modeling of both shallow and deep percolation fronts

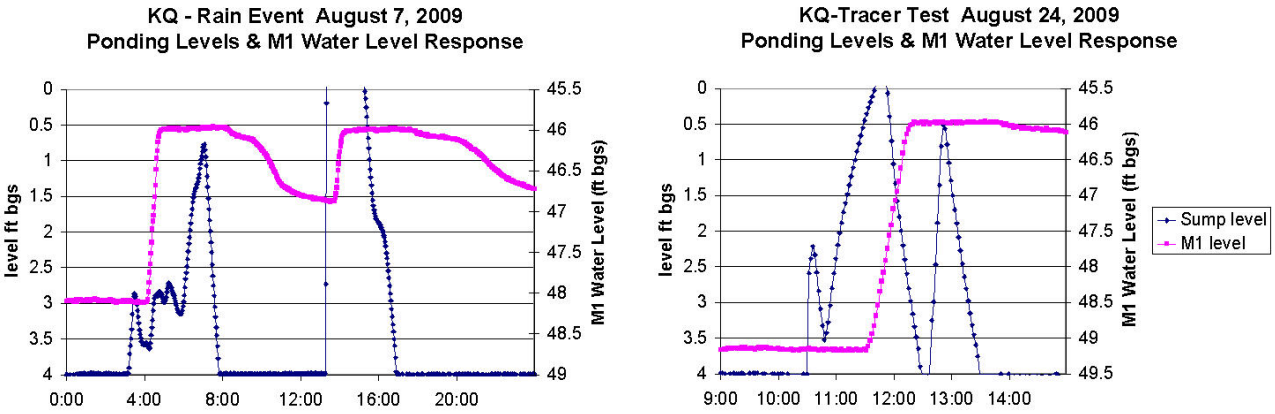

Figure 4.62. Responses of the perched water table (M1) to a surface water ponding (August 7, 2009), and artifical tracer test event(August 24, 2009) at the KQ. The time delay from introduction of water into the sump to a rise in water level in the well is approximately one hour.

The expanded model was developed by increasing the model domain to double the dimensions and grid size (Figure 4.63). The original model depth of 8 m (26 ft) was increased to 16 m (52 ft) bgs. The width of the domain was increased from 12.5 m (41 ft) to 25 m (82 ft). The grid size was expanded from 10 cm^2 to 20 cm^2. The model used an infiltration rate of 0.005 m/s, approximately equal to 90 gpm, that was input through a circular area with a two-foot radius. The model includes three recharge periods consistent with the first modeling phase. The active recharge period, the second time period was expanded from 30 minutes to 60 minutes, and the third period allowed for equilibrium to develop and was extended to several hours.

The ratio of vertical to horizontal hydraulic conductivity was changed from 0.1 to 0.3 to account for the increased percolation rate through the system. The hydraulic parameters of the lower coarse grained unit were the same as the upper layer except for saturated hydraulic conductivity was estimated to be 0.03 m/s, more than an order of magnitude greater than the upper unit. The ratio of horizontal to vertical hydraulic conductivity was changed to one for the lower unit.

Based on geological logs and the wetting front behavior interpreted from the geophysical test results two finer grained lenses of material were included in the model domain. One zone was placed at the contact between the primary upper and lower coarse grained facies. In addition, a lower hydraulic conductivity layer was also placed at the depth of well M1 that appears to be completed in a perching layer (Figure 4.63). Parameter values were assigned based on observed and geologic descriptions provided by the VS2DT user interface.

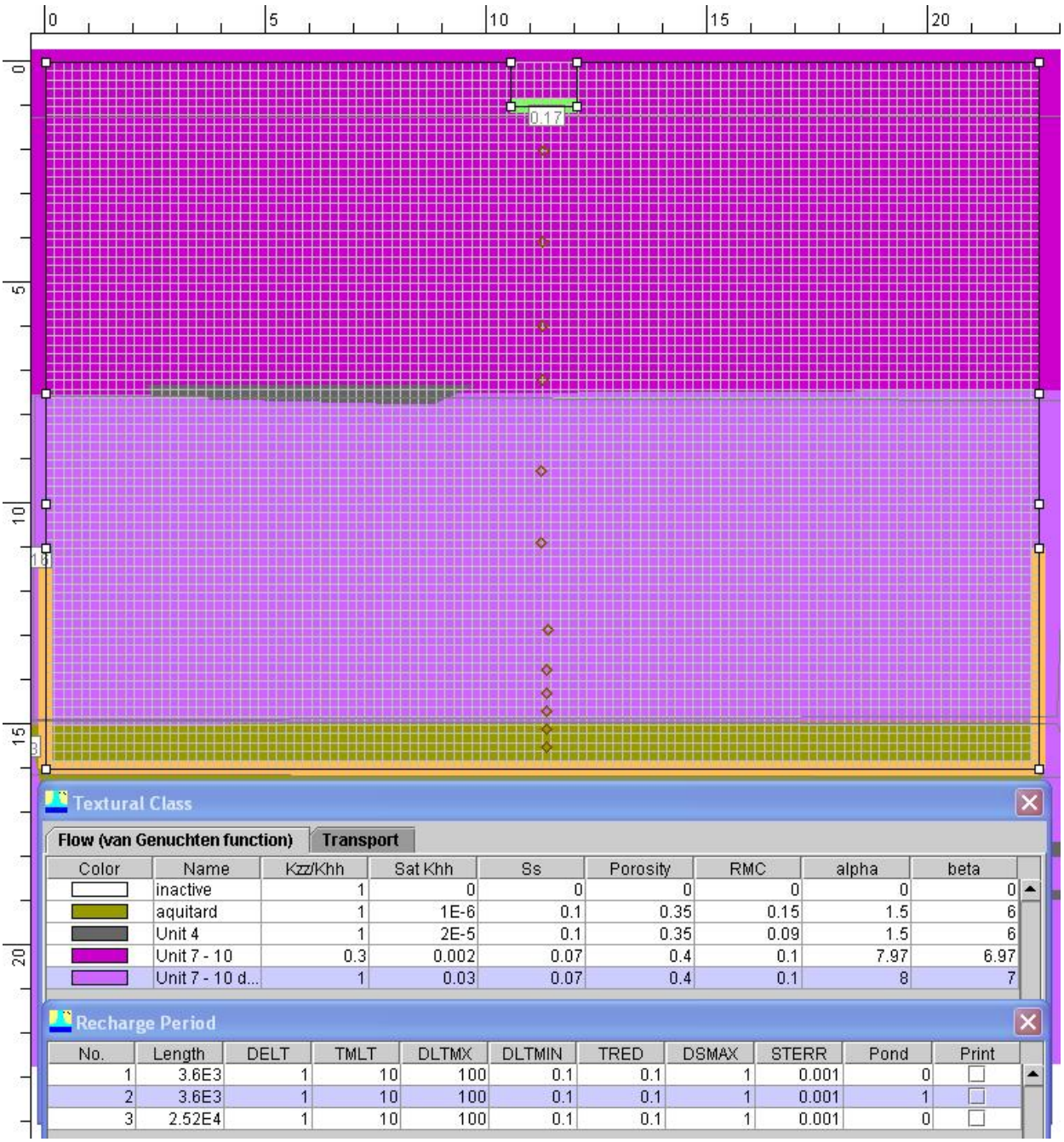

Figure 4.63. VS2DT Model domain and lithology map for Kent-Queen site. The vertical and horizontal scale units are in meters. This model was expanded from the initial model with the addition of a lower coarse grained unit, an aquitard at the base where a perched water lens occurs, and a discontinuous finer-grained layer between the two upper units. The physical transport parameters and recharge periods from the model are shown. The observation points for the model are indicated by the dots. The initial moisture content is shown by boxes around the lower two units, and a line near the surface.

Results of phase 2 modeling efforts appropriately matched observed water level responses. Model calibration required the assignment of a higher hydraulic conductivity zone (0.03 m/s (8,500 ft/d)) below the phase 1 modeling layer to account for the percolation rate (Figure 4.64). Simulations yielded a 68 minute lag between the introduction water to the system and the percolation front arrival.

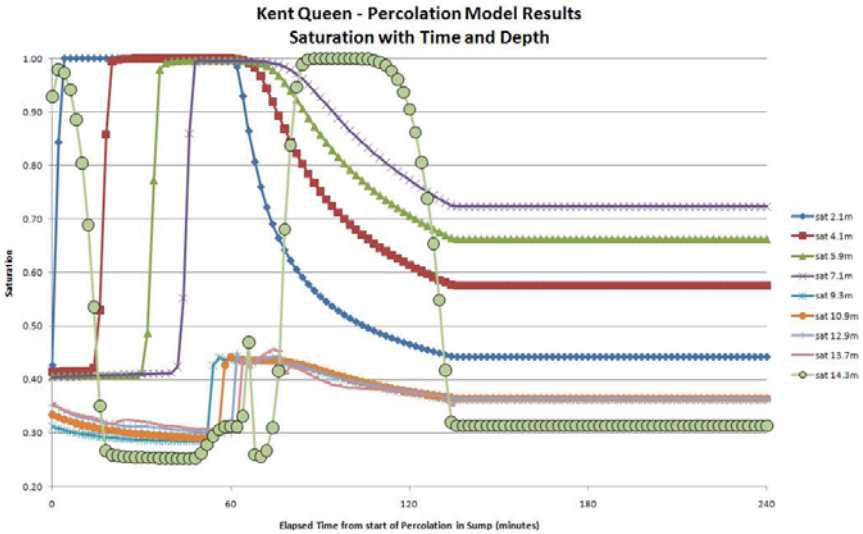

Figure 4.64. Changes in saturation with time and depth for KQ vadose zone simulation. The relative saturation at the 14.3 m bgs position, above the top of the aquitard at 15 m bgs, depicts the accumulation and ponding of water in the perched aquifer. The observation points below this level show constant saturation levels within the aquitard unit. The saturation levels observed at observation points from 9.3 m to 13.7 m bgs indicate that the rapid infiltration occurs primarily as unsaturated flow through the highly conductive part of the system.

Snap shots of phase 2 modeling results after 332 minutes are presented in Figure 4.65. The halo of a higher degree of saturation in the upper sediments is visible. After this water crossed into the lower, highly conductive material, the percolation occurred as vertical unsaturated flow with little observable lateral dispersion. A finer grained lens (mid model) intercepts a portion of the percolating water and provides a degree of lateral dispersion. The lower hydraulic conductivity unit at the base of the domain results in percolating water ponding on the sediments.

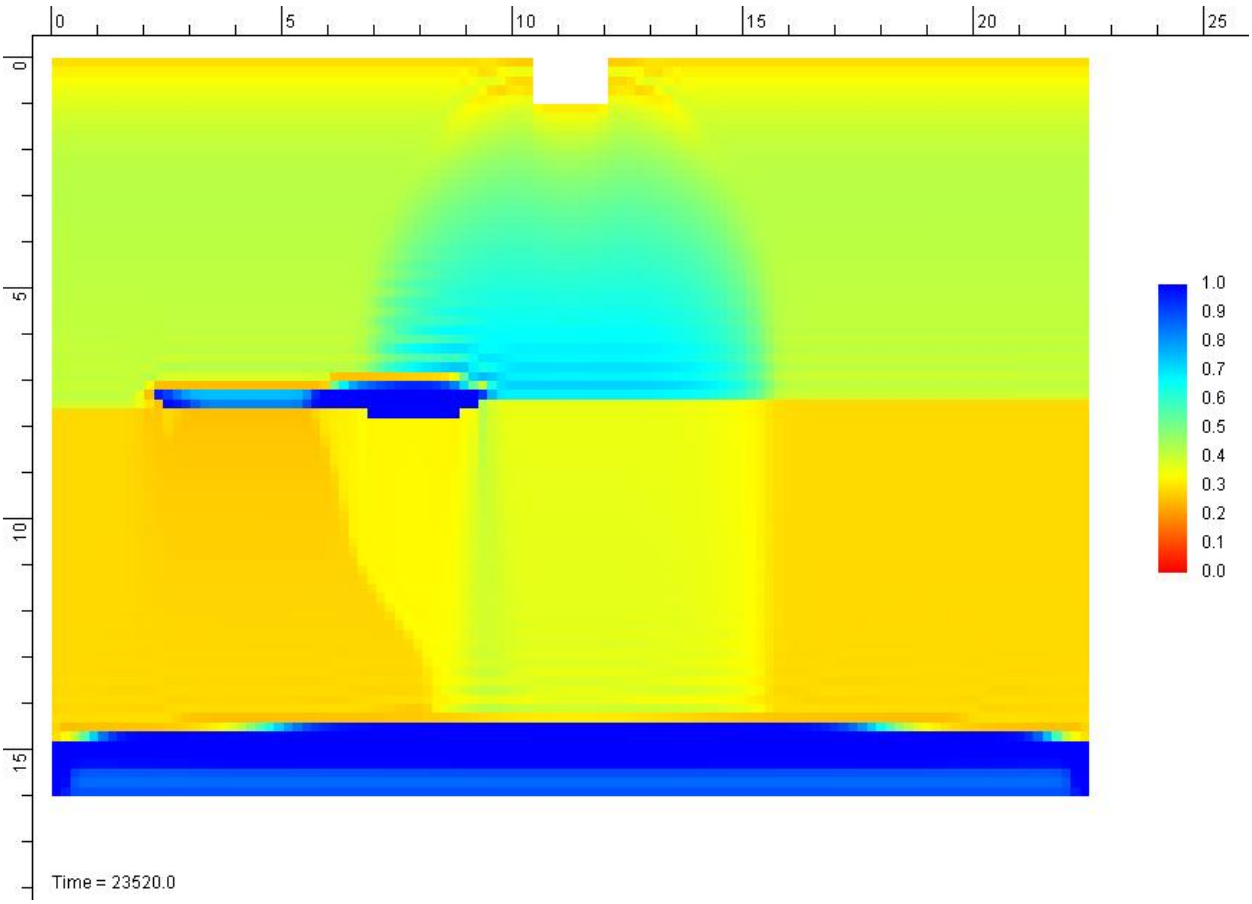

Figure 4.65. Cross section of numerical model results showing sediment saturation percentage 330 minutes after the introduction of sump water. The color coding shows the level of saturation, red-dry and dark blue-fully saturated. The area occupied by the percolation water is observable as locations with higher moisture contents. The horizontal line ,dividing the light green from the yellow, is the boundary between the upper lower hydrualic conductivity zone and the deeper higher hydraulic conductivity zone.

Calibrating a 2D vadose zone model that represent coarse grained conditions. such as those observed in the Missoula valley is feasable as shown by this work. The general shape of the percolating water front as a result of a 30 minute water input is depicted in Figure 4.66. The addition of the lower layer, with a hydraulic conductivity an order of magnitude greater than the upper layer, results in downward flow under conditions of about 50% saturation that is predominantly vertical.

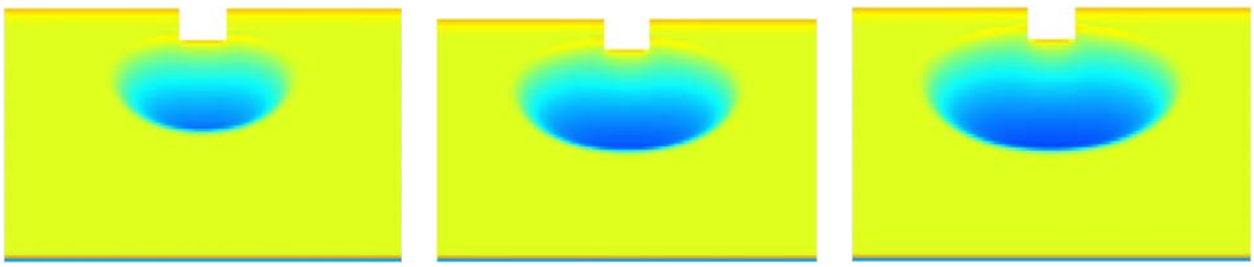

Figure 4.66. Development of the percolating envolope after a 30 minute infiltration period. Colors show relative saturation, with blue indicating near saturated conditions. Note that the lateral expansion of percolating water, and near saturated conditions in central part of water body occur as percolation proceeds.

Generic Simulations of Coarse Grain Systems with Variable Stratigraphy

While the stratigraphy encountered at the five drilling locations was dominated by coarse grained facies, a small number of fine-grained layers were observed. These fine grained lenses are conceptualized as features that would act to reduce overall percolation rates as their frequency and thickness in a vertical profile increased. In order to investigate the influence of fine grained lenses on percolation rates in coarse grained settings, a set of simulations was performed using the final site calibrated KQ numerical model.

The revised model incorporated a large lens representing finer sediment located directly beneath the sump (Figure 4.67). For the first simulation, the hydraulic conductivity of the lens was set at 0.00015 m/s (4 ft/d), an order of magnitude lower permeability than the upper vadose zone unit. Once again a 30 minute period of infiltration was simulated. During this simulation, ponding temporarily occurred on top of the lens as the percolating water moved through the material (Figure 4.68). For the second simulation, the permeability of the perching layer was decreased by an additional order of magnitude, 0.000015 m/s (0.4 ft/d). Results of this simulation showed ponding occurred on the lens, and the percolating water was delayed until the ponding level on the lens was sufficient to allow water to spill over the edges of the lens (Figure 4.69).

Plots of the saturation profiles at locations both above and below the finer grained lens represented in the calibrated KQ simulation and the two hydraulic conductivity representations of the finer grained layer are presented in Figure 4.70. Results of this analysis show the front movement over time is delayed proportionally to the reductions in layer hydraulic conductivity. The one order of magnitude delays the arrival of the percolating water to the 14.3 m depth, as compared to the calibrated KQ model by more than 30 minutes. Whereas when the lens properties are reduced to a two order of magnitude difference, the simulated percolation front does not arrive within the 180 minute time period.

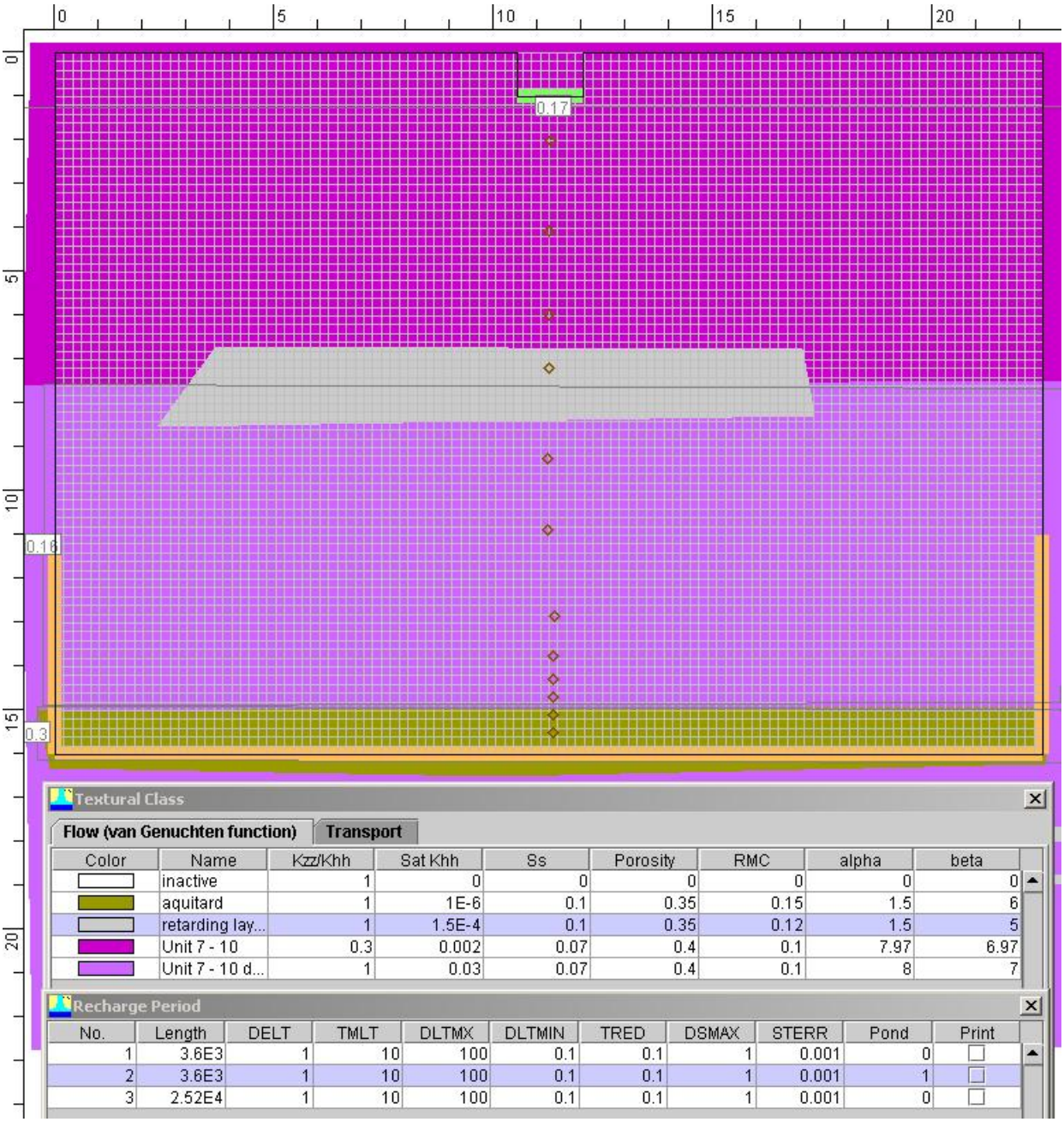

Figure 4.67. A cross section of the model domain including a lens of finer grained material between the sump and model base. The lens is located at the interface between the two primary coarse grained facies (KQ phase 2 modeling). The hydraulic conductivity of the lens was initiated as 0.00015 m/s in the first set of simulations, and then changed to 0.000015 m/s for an additional set of simulations. The horizontal and vertical axes are in meters.

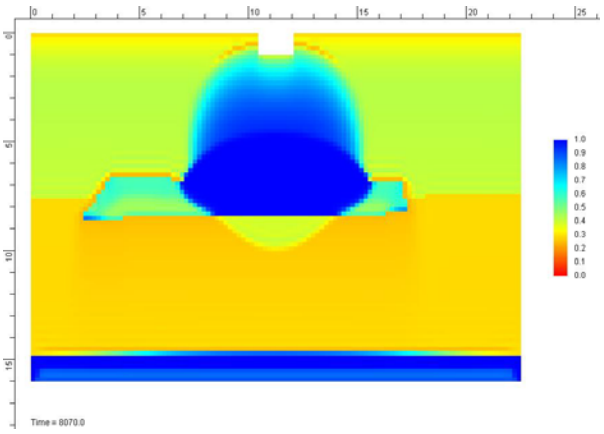

75 minutes after initiation of water into sump

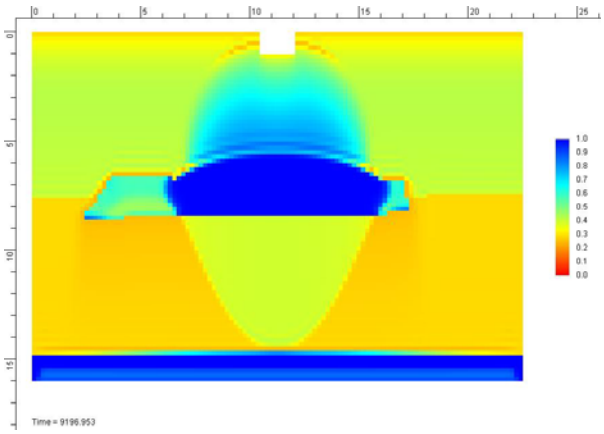

93 minutes after initiation of water into sump

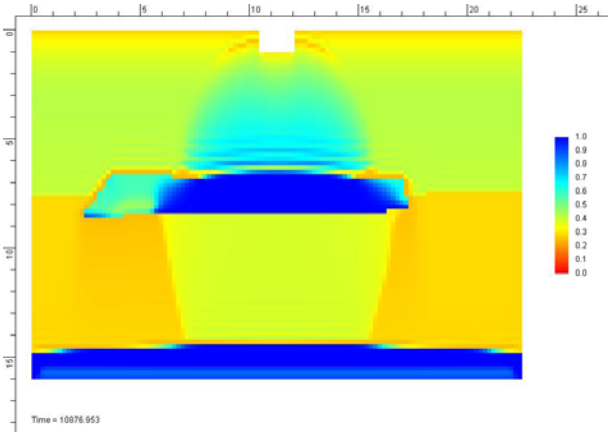

120 minutes after initiation of water into sump

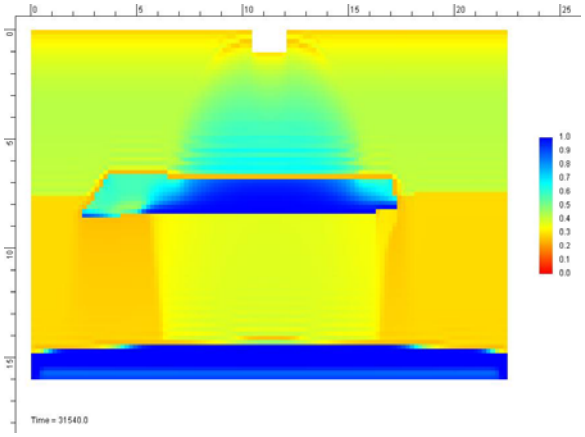

465 minutes after initiation of water into sump

Figure 4.68. Simulations including the lower hydraulic conductivity layer that was assigned a value equal to one order of magnitude less than upper layer. The color scale is saturation with dark blue =1.0. Scales are in meters.

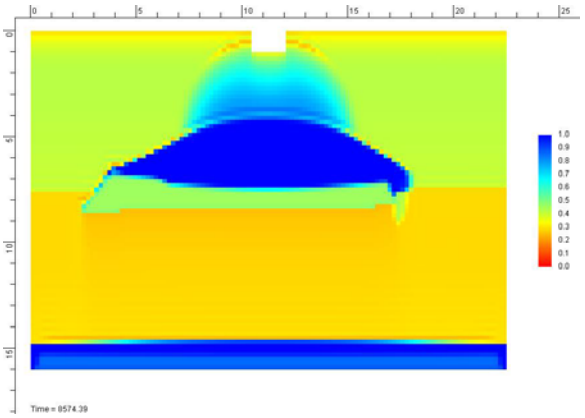

83 minutes after initiation of water into sump

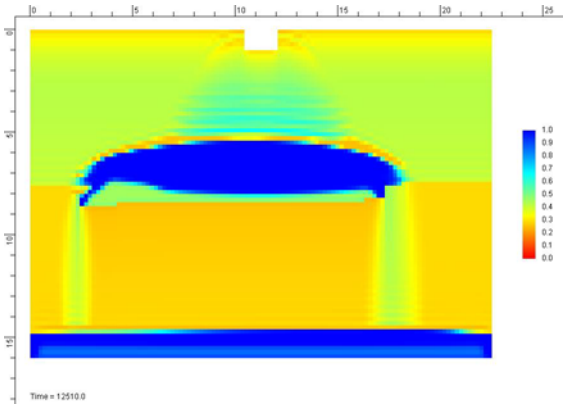

150 minutes after initiation of water into sump

Figure 4.69. A simulation that has a fine grained layer assigned a hydraulic conductivity that was two orders of magnitude lower than the upper layer (green area). The percolating water downward movement is slowed. The color scale is saturation with dark blue =1.0. Scales are in meters.

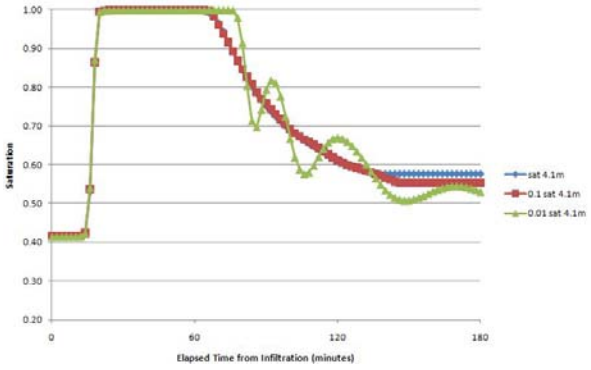

Saturation with time at 4.1m (above the fine grained layer). Saturation profile is similar for all hydraulic conductivity scenarios

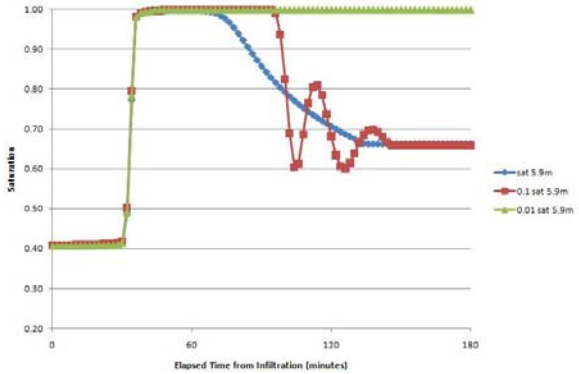

Saturation with time at 5.9m (about 1 m above the layer), with temporary ponding and total ponding for two hydraulic conductivity scenarios

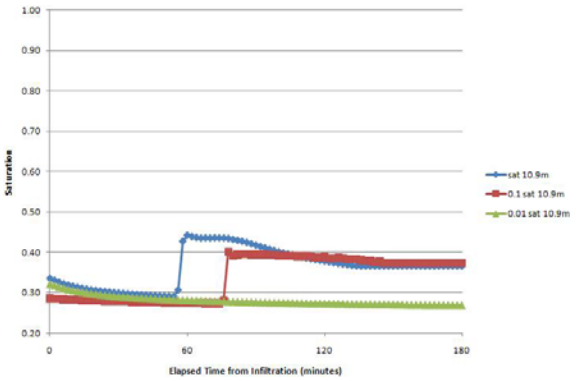

Saturation with time at 10.9 m (about 3 m below the layer). A higher moisture content and earlier arrival time is associated with base model calibrated run. Water does not percolate through this location position during second hydraulic conductivity scenario.

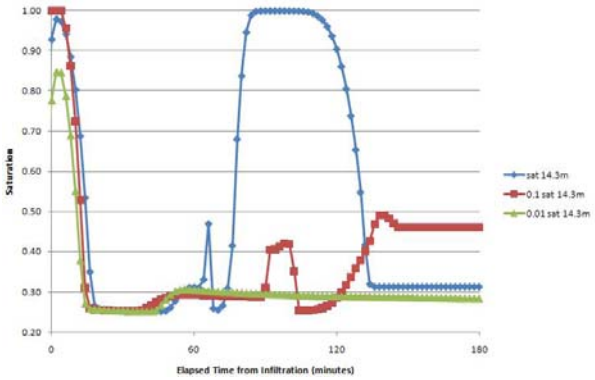

Saturation with time at 14.3 m (about 6 m below the layer). Ponding occurs in original modeling simulation. An increase in moisture content, with no ponding, occurs during first simulation; and no effects of percolating water is noted in second simulation

Figure 4.70. Changes in saturation with time at four observation points located vertically below the sump input (Figure 4.66). The top and bottom position of the simulated fine grained layer are located at about 6.5 and 8.5 m, respectively. The total simulation time is for a period of 180 minutes after the introduction of water to the system from the sump base. The plots compare data from the original calibrated KQ simulation (two layers and no extensive fine grained layer), and simulations with the hydraulic conductivity of the lens one order of maganiture (red) and two orders of magnitude (green) lower than the hydraulic conductivity of the original upper layer of the KQ model.

DISCUSSION

This work was proposed and designed to identify key processes controlling the rates of movement and impacts to the quality of water through sand and gravel, cobble, and boulder dominated vadose zones commonly encountered in the intermountain basins of the Northern Rocky Mountains. To accomplish this goal, a field and laboratory based approach was developed that relied heavily on characterizing source water and vadose zone sediment properties, and used generic vadose models to investigate how a variety of physical and geochemical settings would impact groundwater recharge rates and quality. Characterization of these systems is challenging and was frequently unsuccessful. Interpretation and evaluation of the methods used in this work, analysis and comparison of results produced in this work with other related research, and project limitations are presented in this section of the report.

First, a discussion of the application and usefulness of field and laboratory methodologies will be presented. Second, a discussion of the identified vadose zone characteristics impacting the runoff volume, infiltration rates and the vadose zone percolation rates is presented. Third, the factors controlling the quality of the water reaching the shallow aquifer with analyses of the treatment capacity of the sediments will be addressed. The fourth section will suggest how study results could be used by water utilities providing potable groundwater recharged partly from vadose zone infiltration of natural and artificial source water. Finally, limitations of this research will be presented.

EVALUATION OF THE APPROACHES USED TO CHARACTERIZE SOURCE WATER AND VADOSE ZONE HYDROGEOLOGY

As was stated in the introductory and methods sections, characterization of source water and vadose zone hydrology in a setting with rapid infiltration and coarse grained sediments is challenging. Developing methods to examine the quality of storm water runoff entering a particular sump relied heavily upon the physical sampling of events by grab sample, or the collection of runoff in simple passive samplers positioned under the grate, and/or at the sump bottom. Both of these samplers were inexpensive to construct, but they required site visits and sample collection within approximately 24 h of a runoff event. Other types of samplers, such as automatic event samplers, were evaluated at the start of the project. These systems were considered impractical due to high probability of damage by traffic, total flooding, and vandalism. The inexpensive catch samplers appeared to work well unless events were very small and storm runoff volumes did not reach or fill samplers.

Characterization of both water volume generated by storm events and the local infiltration rate were approached using in-sump water level (stage) loggers that recorded water level changes and temperature with time. These data were then paired with site specific sump dimension data. In an effort to avoid the costs of traditional transducers or other stage measuring devices, the described temperature staff gauge was installed and operated at sites. This proved inadequate, as contrasts in sump air temperatures and runoff water were often un-differentiable. After about the first 6 months of the project these were replaced with Solinst Levellogger instruments that measured time, temperature and pressure head above the instrument (corrections for barometric pressure are made by simultaneously operating a Solinst Barologger). These instruments worked well even after long dry periods and in periods of below freezing

temperatures. Infiltration was computed from rates of in sump water level changes and sump dimensions. As another check/approach, a 4 ft long steel sandpoint was driven into the sump bottom and fitted with a baffled temperature button array that recorded temperature and time. Conceptually, this instrumentation would record a front of infiltrating water moving vertically downward as a lagged change in temperature between individual sensors. The temperature lags are typically evaluated using either analytical solutions or numerical methods. This methodology has been reported to work well in river systems, where in-bed and river temperatures vary seasonally. However, responses were too rapid in the highly conductive sediments found at the sump base, and infiltration rates were not computed from these instruments.

The most difficult data to acquire in this investigation were the physical and geochemical conditions occurring within the vadose zone. The basic approach was to both install traditional soil moisture and soil water sampling devices, and to apply more experimental approaches. Because of the coarse nature of the vadose zone, it was anticipated that traditional tensiometers, gypsum blocks and/or lysimeters would likely not provide meaningful data sets. Previous work investigating Class V Injection Wells in Missoula by Wogsland (1988) successfully installed a conventional suction lysimeter to 13 ft bgs at two sites. Gypsum blocks and lysimeters were installed as part of this work and data collection attempted. The installation of gypsum blocks and suction lysimeters was initially performed using a model 5400 Geoprobe direct push drilling rig. This allowed only the shallowest of instrumentations, less than 20 ft below the drain bottom. The Geoprobe model 6400 was then contracted for use, and instruments were placed to 50 ft. For the sand, gravel, pebble and cobble dominated vadose zone, the large direct push rig was able to place instruments at the desired depths using 2.1 in outer diameter hollow drill rods as conductor casing. Gypsum block readings were collected at sites during most of the study period. However, they consistently indicated wet conditions, suggesting that the vadose zone sediment in the vicinity of a block was near saturation. This seems unlikely, as the coarse nature of the sediments would gravity drain quite readily as suggested by the column testing of boring sediments; field capacities ranged from 0.10 to 0.29 (Table 4.7). It is possible the instruments were impacted by the saturated silica flour installed with the gypsum blocks, or were not working properly. Suction lysimeters (1.1 in diameter) were also installed using the hollow 2.1 in diameter Geoprobe drill rod. These were installed at various depths, however, using standard methods samples were only successfully collected from one lysimeter for two events. The requirement that instruments are in continuous contact with water films in the vadose zone was most likely negated by the coarse nature of the sediment. In the spring of 2009 the Geoprobe model 6400 was contracted to use a 3.2 in outer diameter hollow drill rod to place 1.5 in diameter instruments at depths just above identified sediment zones containing silts and clays. However, this work was unsuccessful, as drilling and installation efforts were hampered by the coarse grained sediments (penetration depths). From the initiation of the project it was anticipated that both gypsum block and lysimeters installations were likely to perform poorly, which was the case, so additional methodologies, both direct and indirect, were developed and implemented.

Vadose sediment sampling and monitoring well installation were not attempted using traditional auger or forward rotary drilling methods. As it was desirable to both obtain a detailed record of the stratigraphy and to have “continuous” samples of the vadose zone sediments, the rotary sonic drilling method was used to core the sediments and provide a cased hole for monitoring well construction. This methodology worked well, though some equipment failures

resulted in only one of the planned two holes at the TS site to be completed. For some intervals core recovery was limited, however, in most cases, good core recovery was achieved. Monitoring wells were designed (3 in diameter schedule 40 PVC casing and 10 ft of 20 slot screen) and paired at two (three sites were planned) sites about 15 ft apart (located on either side of a sump). These were used for borehole tomography sediment characterization and percolation front monitoring during controlled percolation testing. The borehole tomography appeared to work well in the coarse grained vadose zone. However, its resolution to detect the position of a wetting front at KQ and HC was limited to about 20 ft. It is unclear that if a longer on-site recording time was implemented, further movement of the front would have been observed. The loss of resolution below 20 ft was attributed to the occurrence of finer material at that depth. Results are encouraging and were used, along with other field data, to calibrate site specific and generic numerical models simulating the percolation process in coarse grained vadose zone sediments.

The coring methodology also allowed for a more holistic sampling of the vadose zone sediments, and provided the opportunity to conduct detailed physical descriptions and characterization. The core samples also preserved finer sample fractions and allowed for column testing of more representative sediment interval samples. Besides standard hydraulic conductivity testing and the derivation of other hydrologic properties, one column was instrumented with mini tensiometers in an attempt to develop soil moisture/pore water pressure relationships. This approach produced some data; however, it is unclear how representative this information is of field conditions. The data did provide some insight of matric potentials associated with residual moisture contents. Core samples were sub-sampled to determine mineralogical characteristics of finer sediment fractions. The geochemical properties of selected core fractions were also examined for sorption, leachabilty and ion exchange capacities. Total organic carbon analyses were performed on selected intervals of the core. Overall, the collection of vadose zone cores at each site provided important data regarding the physical, geochemical, and hydrological character of the vadose zone. Generating a similar data set using samples of drill cuttings produced by conventional drilling methods would have resulted in a much less detailed description of the vadose zone. The rotary sonic drilling method worked well in this coarse grained setting.

IDENTIFYING CONTROLS ON THE SOURCE WATER VOLUME, INFILTRATION RATES, AND THE VADOSE ZONE PERCOLATION RATES

Within the two year research window (extended to three years because of the limited rainfall in 2007), storm water characterization required estimates of storm event volumes and water quality. The five areas chosen for characterization represented a range of contributing areas from 3000 ft^2 at TS to 18,700 ft^2 at the UM site (Table 4.1). As a result, not all local storm events generated measurable runoff, although storm volume thresholds at which measurable responses in sump transducers were observed, and ranged from 0.01 to 0.05 in (site data KQ, TS and 2O). Ponding heights in the sumps generally increased with storm intensity and event volumes (Figure 4.10). Estimated monthly maximum volumes of storm water runoff (local precipitation multiplied by the catchment area) were highest at the UM site followed by KQ, HC, 2O and TS, as were the estimated peak storm flow rates (Figure 4.3, Table 4.8). These five sites contributed over 1,000,000 gal of water to the vadose zone over the 29 month period of this investigation, with over 60% of this volume associated with the summer period (May-October)

and about 40% with the winter period. For 2008, the computed total maximum runoff at all five sites was approximately 500,000 gallons. In Missoula, there are well over 7,000 storm drains; assuming the average conditions at the five research sites are representative of average conditions at the valley sumps, over 700 million gallons of storm runoff likely enters the vadose zone annually. This estimate compares favorably with the work of Wogsland (1988) who estimated about 2000 storm drains contributed 119 million gals/y of water to the aquifer.

This work separates the infiltration process occurring at the sump base from the physical transport of water through the vadose zone, which is the percolation process. Sump infiltration rates are controlled by the saturated hydraulic conductivity of the sump base and underlying fill material. The coarse nature of the backfill material and underlying natural vadose zone sediment provides large interconnected pore spaces (and their resulting high hydraulic conductivity) that directs water into the vadose zone. When the rate of water discharging into a sump is less than the combined saturated hydraulic conductivity of the fill and natural underlying material, the water will infiltrate without ponding. As the runoff rate into a sump increases during an event, water continues to infiltrate (being added to vadose zone storage with some downward flow). As long as the inflow rate is less than the saturated conductivity of the sediments, all water entering the drain will be moving downward and into the vadose zone. Once the inflow rate exceeds the saturated hydraulic conductivity of the sediments, water will begin to pond. As the water rises in the sump, additional infiltration will occur as the ponding level results in a large hydraulic gradient. The infiltration rate is also enhanced in these settings by the presence of macro pores (large open interconnected pores created in the cobble and boulder drain backfill). Macro pores tend to redirect and enhance infiltration until full saturation is reached. Typically, the infiltration rate in a dry setting starts out as a large value, and then declines and levels off at a lower rate, if the rate of infiltrating water fully saturates the near surface sediments.

Infiltration rates at the research sites computed from natural storm events and controlled artificial injection tests associated with borehole tomography experiments (2008) and summer tracer tests (2009 ranged from 1 gpm to over 40 gpm. These observations were conducted under saturated sediment conditions and with sump ponding. High rates are not surprising as it was observed that when storm water enters the drains it does not commonly pond at research sites during most runoff events. When ponding does occur at the street surface it is usually associated with spring and fall rains (frontal storms) and high intensity summer thunder storm events (Figure 4.6). During the winter, at the 5 research sites, thaw events were more likely to cause water ponding at KQ and HC than other sites (Figure 4.7). These two sites have the shallowest sumps, and are the most vulnerable to freezing temperatures; ice buildup can alter the character of the sump base by reducing the quantity of interconnected open space.

It should be noted that once the runoff water infiltrates into the vadose zone it does not always become immediate or observable groundwater recharge. The water moving vertically downward through the vadose zone sediments is impacted by tensional forces and partially enters into storage, increasing local moisture contents. Saturated infiltration fronts generally move vertically downward. This occurs when certain preexisting conditions in the vadose zone are met, such as a near saturation moisture content. When vadose zone moisture contents are low, infiltrating water migration is inhibited because water is initially redistributed to form water films on grain surfaces, which in turn causes otherwise saturated pore channels to become unsaturated. In some cases evaporation of vadose zone water occurs, reducing water available for groundwater recharge.

Clearly, the relationship between infiltration rates and groundwater recharge rates is not straight forward, thus, under most circumstances, infiltration rates alone cannot be used to predict either percolation rates or the timing and volume of local groundwater recharge. Thus, additional information about how water moves through the vadose zone is needed to identify key factors controlling percolation.

It was recognized that in addition to the rates and duration of infiltrating storm water, it is the geologic nature of the vadose zone, its lithology and stratigraphy, and its physical, hydrological and geochemical properties ultimately control the behavior of the percolating water within the vadose zone. Thus, to decipher likely principle controls on percolation rates and processes, rotary sonic drilling was used to obtain continuous 4 in diameter cores of the vadose zone at each site.

The vadose zone sediments in this research area were deposited in a high energy fluvial environment where transported sediment included sand, gravel, pebbles, cobbles and boulders. The sediments are dominated by clasts of the rocks composed of material that makes up the local and regional mountains (Proterozoic metasedimentary siltsone and sandstone), weathered grains of purple, red and green quartz argillites (Belt Super Group). The stratigraphy at each site is dominated by clearly visible gravel or larger size particles in layers of a few feet to 10+ ft in thickness. Common descriptions of the sediment include fine to medium sand, gravel and cobbles with pebbles; cobbles with clay and silt matrix; medium course sand and gravel, and gravel and cobbles, with some silt. Median grain sizes of sediment layers are often recorded as gravel to pebble. Uniformity coefficients vary widely and commonly range from 3 to 30. Values at KQ had the smallest range, 4 to 21, and 2O values included the largest range, 1.5 to 111. Few fine grained layers, dominated by silt and clay, were observed. Silt and clay sized particles made up less than 5% of the total sample mass in most cases. When clays are present they are dominated by illite, although some smectites were seen in a few samples. Generally, one or two thin fine grained layers were recorded in most cores. They commonly varied from 1 to 3 ft in thickness. These zones may represent a period of soil development and erosion, remnants of lake sediments and/or river overbank deposits. In most of the sites they appear to be lenses and cannot be correlated between research sites. Previous work that utilized hundreds of environmental borings and drillers logs to map the presence of fine gained layers in the valley vadose and aquifer found local discontinuous areas could only be identified north of the river and that they were discontinuous (Swierc and Woessner 2006) (Figure 5.1). HC was the only study site located in an area where fine grained units had been previously mapped. Within the 48 ft boring at this site, clay and silt dominated sediments were present only from 0 to 2 ft and 4 to 8 ft bgs. HC is commonly observed to pond water during larger runoff events. This ponding is probably caused by the presence of these finer sediments. The measured infiltration rate at this site was lower than others, about 2.5 ft/h.

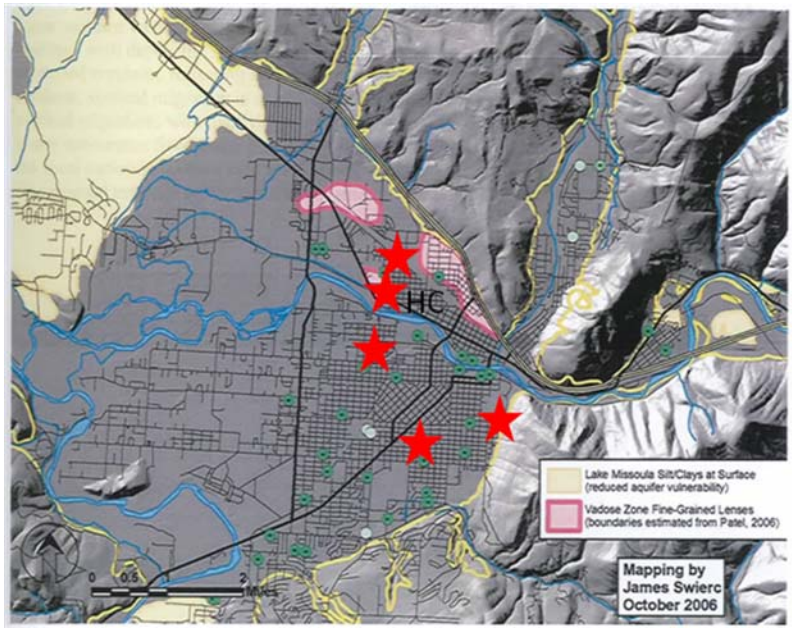

Figure 5.1. Map of identified fine grained deposits reported on boring and well logs (Swierc and Woessner 2006). Red stars represent research site locations.

Laboratory sediment bulk densities based on packed column experiments ranged from 1.76 to 2.0 grams per cubic centimeter. Field capacities ranged from 0.09 to 0.29. Average saturated vertical hydraulic conductivity values derived from sediment permeameter tests ranged from 460 to 1,200 ft/d. Estimates of average saturated horizontal hydraulic conductivities derived from grain size data for 58 boring intervals, ranged from 1,200 to 41,600 ft/d. Standard deviations were large, suggesting the vadose zone is highly heterogeneous. Both the column tests of single intervals and the grain size derived values are similar to computed saturated horizontal hydraulic conductivity values determined for the underlying Missoula Aquifer throughout the valley (e.g. Tallman, 2005). Analyses of cores did not show clear hydraulic conductivity trends with sampling depths. The vadose zone characterized as part of this study is principally composed of coarse fluvial derived sediments and contains some deposits of silt dominated matrix supported gravels and cobbles. The vadose zone sediments also contained only thin and a limited number of fine grained layers composed of silts and clay as noted earlier. This suggests that networks of large diameter interconnected pore spaces are present in the vadose zone and that they form preferential pathways directing infiltrating water downward.

Site percolation rates were derived by tracing the movement of infiltrating water through the vadose zone, observing the associated water table response, and simulating percolation using local conditions. Gypsum blocks located at one or more intervals beneath the sumps were placed with the purpose of developing information on how the moisture content changes during infiltration and percolation events, and to characterize antecedent conditions (both wet and dry). The readings obtained throughout the year (Figures 4.26 to 4.30), during and after infiltration events (Figure 4.31), suggest moisture contents remained high. The reduction in readings at instruments located to depths of 8 to 25 ft at KQ, HC and TS in the fall of 2007 could be interpreted as the instruments recording a sediment drying period (below normal precipitation occurred that summer). However, this interpretation is clouded by the often different response

(less variation) of instruments placed at shallower depths at these sites. There is the possibility that gypsum block readings are in fact recording site conditions, however, the results were not confirmed using other techniques. Previous attempts to characterize moisture contents at a commercial and residual sump site using neutron access tube readings to depths of about 30 ft found moisture profile trends constant even after precipitation events (Wogsland, 1988). The interpreted moisture content varied between 5.5 and 14.5 volume percent. Wogsland (1988) attributed the lack of recorded moisture profile change after runoff events to the disturbed zone created during tube installation, and the location of the monitoring tube possibly being too far from the drain to record changes in the moisture profile.

A second approach used to determine the movement of percolating water involved monitoring changes in vadose zone temperature. It was hoped that summer storms would produce warmer runoff temperatures (heated air and pavement surface) and winter melt out events would percolate water with colder temperatures than those found in the vadose zone. Unfortunately, this methodology proved insensitive to site percolation processes. The technique looks promising, however, as some over-all changes in vadose zone temperature were recorded at HC during a winter thaw event (Figure 4.32). Possibly, higher resolution temperature monitors are required to capture subtle temperature changes. The third methodology applied was the use of downhole GPR tomography. This method was effective in providing a profile over time of the percolating water front. The variations in saturated and unsaturated conditions were successfully interpreted and percolation rates calculated at KQ (6.7 ft/h) and HC (7.2 ft/h). These rates represent movement through the first 20 to 25 ft of the vadose zone. The tomography data sets did not resolve percolation beyond these depths. It is unclear if the occurrence of a zone of sediments with some fine grained matrix reported at these depths slowed the percolation process, or if the wetting front became too diffuse to detect. The methodology is promising and may need further development to be more successfully applied in coarse grain settings.

It is interesting that the percolation rates computed from artificial tracer tests ranged from 1.2 to 20 ft/h. The geophysical profiling shows that actual percolation of the wetting front was less than the infiltration rate at KQ and higher than the rate at HC. The observed changing rates at KQ are most likely attributed to the spread of the volume of water entering the drain bottom both horizontally and vertically as it encountered a variety of sediments and hydraulic conditions, slowing the rate of downward movement. At HC, it appears that once infiltrating water passed through the sump bottom, it moved more rapidly downward. This may suggest a finer sediment layer is present and is discontinuous and localized, so the infiltrating water displaced pore water, moving the displaced water into the large pore spaces below the sump bottom. Another possibility is that large interconnected pore spaces are present, and persist from the sump bottom to the observation depth (20 ft). Unfortunately, variations in percolation rates could not be observed in the deeper vadose zone regions of these sites.

Artificial infiltration tests were conducted in the summer of 2009. Known rates and volumes of water containing a salt tracer were released into four of the five storm drains while conditions in the sump and at the water table were continuously monitored. These experiments found percolation rates of 13 ft/h through the 21 ft thick vadose zone at KQ, 2 ft/h as the overall percolation rate through 41 ft of unsaturated zone at HC, and 10 ft/h through the 43 ft thick vadose zone at 2O. Rates are dependent on input (volume and rate) conditions as well as the vadose zone properties and antecedent conditions. For these tests, a non tracer slug of water was added until street ponding occurred and then it was followed by an additional volume of water

containing the tracer. So these computed percolation rates should be considered maximum or worst case values, as field conditions were near saturation before the salt tracer water was added and volumes of water added to the sump were large compared to natural recorded runoff.

IDENTIFYING CONTROLS ON THE WATER QUALITY OF THE VADOSE ZONE DERIVED GROUNDWATER RECHARGE

The recharge water quality recharging the shallow aquifer is dependent on the nature of the initial storm water source, its quality at the time of infiltration, and geochemical processes impacting the percolating water. The over 170 storm water runoff samples collected during both the summer and winter periods provided source water characterization (Figures 4.44 and 4.45)

Summer runoff at all sites was relatively low in total dissolved solids, and dominated by a mixture of common cations and bicarbonate. Mean values for manganese were about 8 mg/l, sodium 6 mg/l, calcium 12 mg/l, chloride 7 mg/l, sulfate 10 mg/l, bicarbonate 60 mg/l and potassium 5 mg/l. Lithium, an exclusive component of winter de-icer solutions, was <0.005 mg/l at all sites except at KQ, where a series of storm events in the first week of May 2008 contributed to runoff (mean 2.5 mg/l). This possibly reflects the flushing of residual de-icer compounds into the sump as the summer period began. Sampling of runoff for total dissolved organic carbon found a wide range in concentrations, from 5 to 50 mg/l. One set of VOC samples collected at TS and analyzed for 51 compounds found no compound above the analytical detection limits. Previous work by Wogsland (1988) reported three storm water runoff samples that were analyzed for EPA priority pollutants during her work, and all parameters were also below detection limits.

Winter runoff samples contained higher mean concentrations of magnesium, sodium, calcium, potassium, and chloride than did summer runoff. Concentrations of total dissolved organic carbon ranged from 6 to 85 mg/l; winter samples consistently had higher concentrations than summer samples. Lithium concentrations were detectable at all sites with a mean of about 0.5 mg/l. These higher winter concentrations of constituents are linked to the chemistry of the liquid deicer, salted (NaCl) sand, and in 2008/2009 the direct application of NaCl used on the Missoula streets. Sampling runoff during a winter melt event at 11 sumps clearly showed elevated cations and chloride, and measurable lithium in the melt water entering sumps at all sites. At KQ the presence of higher concentrations of Na and Cl in winter samples suggest local residential deicers and our city use of NaCl may also be influencing runoff quality.

A number of summer and winter storm water runoff samples were obtained from samplers hung under the sump grate, thus they may represent “first flush” runoff samples. Only a few comparison samples were taken to examine how first flush samples may differ from samples of runoff generated later in a storm event, thus, flow weighted event mean concentrations were not computed (e.g Wogsland, 1988). Generally, when multiple samples were collected during a runoff event during this work, results did not clearly suggest storm water quality varied significantly. Generally, the early part of summer period runoff is dominated by low levels of common ions; however, some samples may have reflected the presence of constituents associated with winter deicer use. Winter runoff is influenced by the use of liquid street deicers that elevate concentrations of major cations, anions and total organic carbon. Measurable concentrations of dissolved lithium are also present in winter runoff. Similar trends have been reported previously by Wogsland (1988) and Perine (1999). One challenge, when comparing previous work to this study, is that the de-icers used in the past are different

formulations from those currently being applied. Wosgland (1988) instrumented two sumps, one in a commercial and industrial area and one in a residential area. She then collected runoff from parking lots, as well as a storm sewer that collected runoff from 2 blocks of residential areas (Figure 5.2). The principle deicer was a NaCl mixed with gravel (Figure 5.3). She noted impacts to storm water quality during winter melt periods, as this work documented. Woggland (1988) found low concentrations of iron, copper, manganese and zinc in runoff. Manganese concentrations were often below detection limits in runoff samples collected as part of this study. The Missoula City-County Health Department and the Missoula Valley Water Quality District (1997) evaluated the impact of MgCl deicer and sodium chloride sanding on winter storm water quality at eight sites including composite sampling of storm sewer outfalls and individual storm drains. The de-icers most commonly applied by the city Public Works Department during a 7 year analyses period were Freezegard/PCI and CG-90. They found winter runoff quality was dominated by sodium, magnesium, and chloride, with concentrations in runoff increasing as the total volume of de-icer used increased throughout the winter. In addition, the Public Works Department detected measurable concentrations of arsenic and copper in some runoff samples.

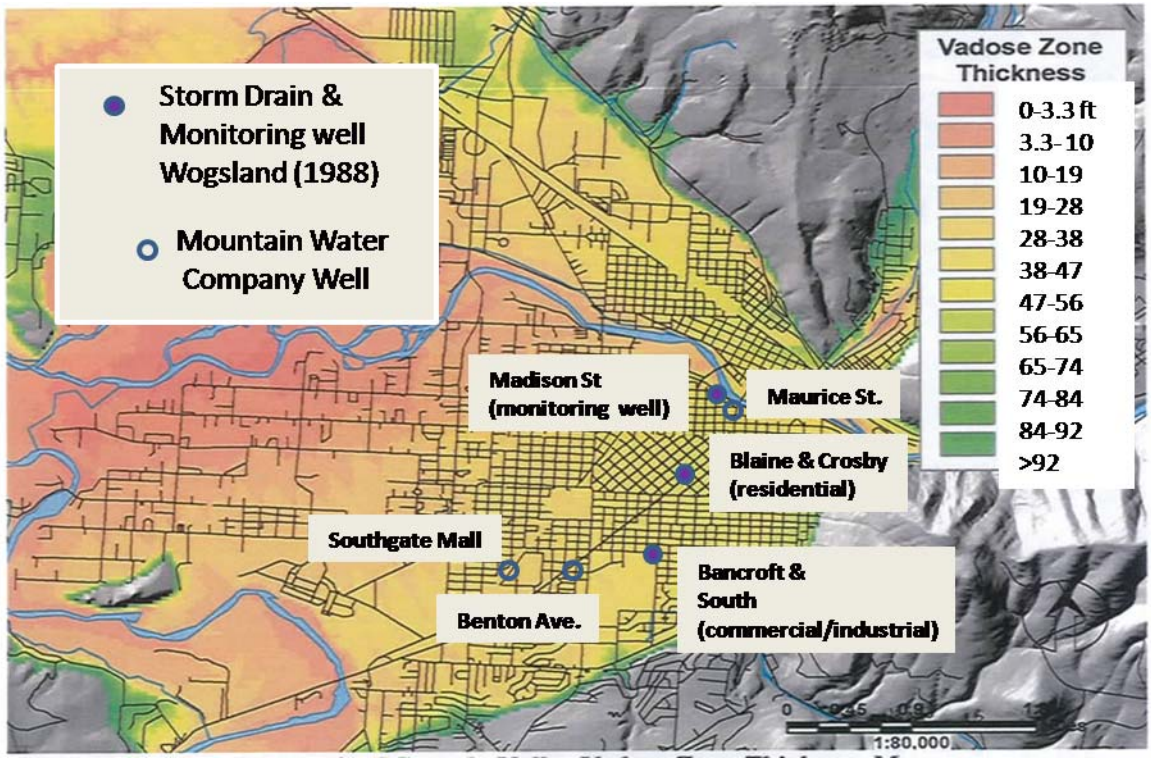

Figure 5.2. Map of the vadose zone thickness showing the location of monitoring wells and sumps referenced by Wogsland (1988) and Missoula Water Quality District (1997). Selected Mountain Water Company Wells are also shown.

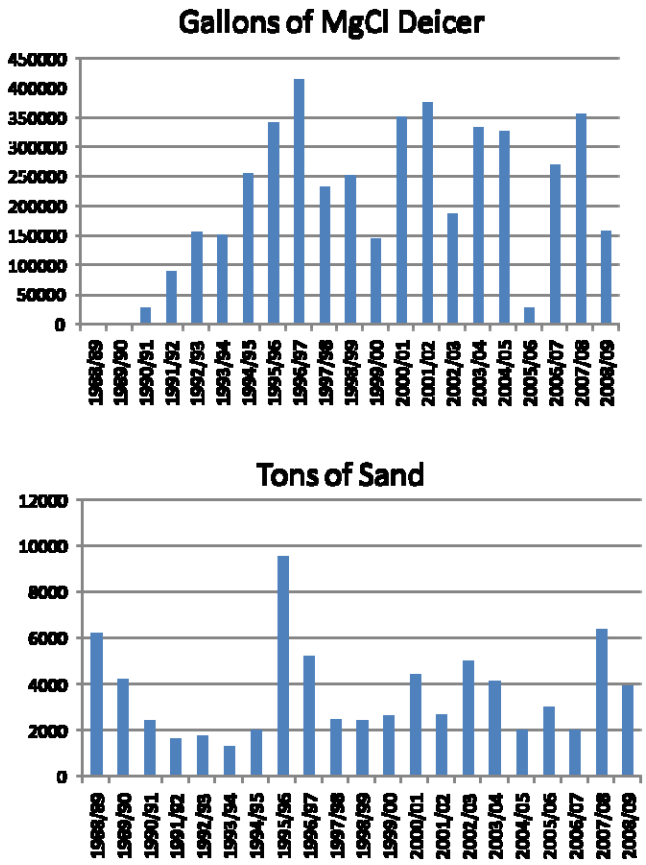

Figure 5.3. Deicer use by the City of Missoula Public Works Department 1988 through the winter of 2009. Sand is mixed with 5% NaCl by weight (e.g. 6000 tons of sand use correlates with 300 tons of salt) (Missoula Water Quality District, personal communication, 2010).

This work's approach to determine if street sampled versus in-sump sampled runoff differed in water quality compared the results of grab or grate samples, and bottle samplers placed in the sump. Results found the composition of these samples was similar. This suggests that the runoff water chemistry entering the vadose zone through the bottom of the sump is represented by the runoff water samples. In an earlier study, Perine (1999) sampled the sediments (upper 10 cm) in 15 storm drains to determine if metals were accumulating in these sediments. He found As, Cd, Cr, Cu, Mn, Pb, and Zn elevated in the sediments over background values. Li and Ni concentrations were referred to as "close to background". The near neutral pH and oxidizing conditions in runoff water were anticipated to limit the transport of metals into the vadose zone. Perine's work suggests that finer grained material present in a number of the study's sumps were capable of removing some trace metals from the infiltrating water. Though he presented evidence that this process does occur, it is also possible that when infiltration rates are high, at some sites insufficient reaction times may occur. His work did not explore the possibility that water quality changed immediately beneath the sump bottom sediments.

The water quality of water passing through the vadose zone will be impacted by a number of geochemical processes, including: precipitation, dissolution, reversible and

irreversible sorption, and ion exchange. This work addressed the geochemical conditions and likely impacts to percolation water. The approach included the placement of one or more vadose zone sampling instruments (suction lysimeters) between the sump bottom and the water table at each site to directly characterize percolating water. However, only two samples of percolating water were obtained. Both samples were collected from HC at a 20 ft bgs (16 ft below sump base) during the summer period, May, 2009 and July, 2008. When the chemistry of the July runoff grab sample is compared to the lysimeter sample, major ion concentrations in the lysimeter sample were higher than the run-off grab samples. Chloride concentrations were 3 to 4 times higher and bicarbonate about 2.5 times higher than the runoff sample. Iron, manganese, and lithium were also elevated in the percolating water. These data suggest that percolating water was acquiring additional constituents as it moved downward and interacted with the sediments. At the same site one year later (May), comparison of the lysimeter and runoff sample for an event showed contrasting results, as major ion concentrations in the lysimeter sample were less than those reported for the runoff (chloride, sulfate and bicarbonate were not reported for the lysimeter sample). In addition, metal concentrations were below detection in both the runoff and lysimeter sample. One exception was the presence of strontium in both samples. These results are insufficient to reach a conclusion regarding the likely reactions that take place in the upper portion of the vadose zone at HC, other than to report that the vadose zone was a source and a sink to major ions and metals. Wogsland (1988) was able to obtain lysimeter samples at her two instrumented sumps and reported that the vadose zone was a source of bicarbonate, sulfate, chloride, nitrate, calcium, magnesium, sodium and potassium when low TDS storm water infiltrates the vadose zone (Figure 5.2). Wogsland (1988) also noted that trace metal concentrations decreased. However, during the winter percolating water increased in concentrations of chloride, copper, iron, manganese and zinc, and sodium was partially attenuated (it should be noted that Wogsland's research involved winter runoff dominated by high concentrations of sodium chloride).

As this work anticipated that lysimeters may not provide percolating water samples, sediment geochemistry and laboratory testing to determine the nature of geochemical interplay between vadose zone sediment and selected ions was investigated. The dominant siliceous nature of sediment clasts and the absence of a high percentage of silt and clay (fine gained sediment <5%) suggested that it was unlikely that percolating water quality would be impacted as it passed through the vadose zone. Finer grained portions of the sediments have large surface areas and thus many sites for exchanges and reactions. Organic carbon can also provide potential reaction sites in sediments. Total organic carbon analyses of borehole sediments found concentrations were low, all less than about 0.3% (one sample at HC at 5 ft bls was about 1%) (Figure 4.46) These low concentrations suggest that organic carbon's role in altering the chemistry of percolating water is small to insignificant. The cation exchange capacities of the vadose zone sediments to depth to 45ft bgs at HC and KQ were also very low, about 3.0 meq/100g (Figure 4.48). Thus, the capacity of sediments to release and take on cations is small. This is in line with the site conditions: the siliceous nature of the sediments, the low percentage of clay and silt, the fact that the clay minerals present are dominated by illite, and the sediments contain a small percentage of organic matter.

As an additional examination of the geochemical reactivity of the sediments, borehole samples were treated with a strong acid to identify readily available reactive or sorbed elements at sediment surfaces. A second sub set of samples was treated with a weak HCL solution to examine the elements attached to the grain surfaces primarily by sorption. Under these sets of

conditions Al, Ca, K, Mg, NA, Fe, Mn, Si, P, S and Ba were extractable and where found at the highest levels (Table 4.21). The HCL extract results (sorbed values) were lower than the total reactive values (strong acid) as expected. These results suggest sediment surfaces could both contribute, and retain constituents, depending on the local geochemical conditions. Further assessment of the reactivity and sorption potential of the sediments was examined by conducting batch tests that placed known weights of sediment to a volume of water containing a known concentration of a particular ion. This approach was used specifically to examine if components of the liquid deicer (FreezGard CL, mixed in deionized and rain water) were likely to react with the vadose sediment. The examination of how storm water with low concentrations of constituents interacts with vadose zone sediment was also addressed by conducting batch experiments using both deionized water and rain water as the solute. Results are expressed in terms of retardation factors (Rf= the degree of impact to the transport velocity of a constituent as a result of sorption onto the sediment surface). Usually, computed values are 1 (no sorption, constituent acts conservatively) or greater than 1, where transport though the porous media is slowed and concentrations reduced by sorption to sediment surfaces. When retardation factors are less than one, this suggests that mass is being contributed from the solid surfaces to the test solution. When this occurs, the constituent concentration in the batch solution increases. Results show that Na , Mg, Li and As present at various concentrations in the deicer are all potentially sorbed at varying degrees to sediments (ions listed in order of increasing Rf values). Chloride data were not available for the de-icer solution, however, Cl sorption did appear be effected under some conditions (Rf value of 1.7 for rainwater and NaCl batch tests). It can be assumed that Cl in the deicer solution would behave in a similar fashion. Sodium also was noted to sorb using the same rainwater solution. Additional results of the batch tests showed that when deicer solutions were placed in contact with sediment, K, Ba and Ca concentrations in the solute increased. For these components the sediments were sources of these compounds.

These geochemical characterizations of vadose zone sediment reactivity suggest that these sediments do have some sorption properties and could act as a source of dissolved constituents. The limited lysimeter data show both of these trends. Site history may also influence the geochemistry of percolating water. For example, at a site where winter de-icer runoff has entered and been stored in the vadose zone, it may be remobilized when low concentration spring and summer runoff water enters the sediment (July lysimeter sample). In contrast, at sites that typically receive little winter runoff impacted with deicer, percolating storm water may become more mineralized as it reacts with the vadose zone sediments. Previous work by Wogsland (1988) observed that percolating water that started as runoff containing low concentrations of major cations and anions increased in dissolved constituents by several hundred to several thousand percent after percolating through 13 ft of vadose zone. She noted that percolating water also contained increased trace metal concentrations. She also reported the presence of oil and grease in 13 winter runoff samples (average concentration 7.3 mg/l). Six late winter vadose zone water samples collected as part of her work averaged 1 mg/l or less suggesting these types of compounds were attenuated at her two study sites. Clearly, characterization of the geochemistry of the vadose zone sediments and their capacity to remove or add constituents to infiltrating water are needed to predict the composition of the recharge entering the groundwater beneath storm sumps.

As a further measure of the effect of the vadose zone sediments and geochemical conditions on the quality of water that discharges from this zone to the groundwater system, the chemistry of the receiving groundwater was evaluated. Major ion groundwater chemistry, based

on 70 summer period samples collected at the four sites with monitoring wells, is dominated by calcium and bicarbonate. No discernable influences of summer storm runoff events on the quality of the underlying groundwater chemistry were observed. Sampling of groundwater at the same time as a runoff event and/or multiple days after a infiltration event, found no direct relationship between the runoff events and changes in groundwater quality based on major ion and trace metal chemistry (Figure 4.5). In addition to major ions, groundwater commonly contains from 4 to 13 mg/l dissolved organic carbon and low concentrations of trace metals. At KQ, HC, 2O and TC all groundwater samples contained nitrate-N in measurable quantities with a number of samples containing concentrations ranging from 1 to 5 mg/l-N. These concentrations suggest that to some degree an anthropogenic impact to the local groundwater is occurring.

Another indication of the impact storm water has on the shallow groundwater quality was further evaluated by examining the results of twice a year (March and June) shallow monitoring well water quality sampling collected by the Missoula Water Quality District (Jon Harvala, Missoula Water Quality District, personal communication, 2010). The Missoula Water Quality District has been collecting shallow groundwater data in the Missoula urban area for over 20 years. Their data show the background (un-impacted by storm water) concentrations of major constituents, sodium, magnesium and chloride, have mean values of 6, 12 and 5 mg/l, respectively (#U121922C, Madison Street River Bowl) (Figure 5.2). A plot of a monitoring well adjacent to a street storm sump at the corner of a busy four lane intersection (Bancroft and South) shows groundwater quality in the winter sample being lower in Mg, Ca and Cl than samples taken in early June (Figure 5.4). As de-icer is usually not needed after April, the higher concentrations of these constituents in June samples suggest winter deicer applications impact water quality into early summer. A groundwater evaluation examining the effects of de-icer use on groundwater conducted by the water quality district in 1997, using data from Wogsland's work and sampling from 1994 to 1997, found increases in deicer related ions occurred in the Bancroft and South well in the spring and they decreased as the summer progressed as well as into the fall. Wogsland (1988) installed and monitored this same well and she found vadose zone chloride concentrations increased as low TDS storm water infiltrated at the site. A second site located in a residential area was monitored by the water quality district from 1998 to 2002 and only once, June 1999, was the chloride concentration twice what was observed at other times, as other constituents remained the same. These data combined with the results of this study, the Missoula water quality district's earlier work (1997), and Wogsland's research (1988) suggest that major ions and dissolved metals including arsenic, cadmium, chromium and lead are not clearly increasing in shallow groundwater as water flows (along a flow line) beneath the urban area served by storm drains. It is more likely that street areas where extensive de-icer use is exercised create local areas or zones of impacted groundwater, whereas residential areas show less or no measurable change in groundwater quality. Wogsland (1988) also investigated shallow commercial and domestic wells in the vicinity of a mall parking lot and concluded observed measureable changes in major ion chemistry were likely the result of winter deicer use.

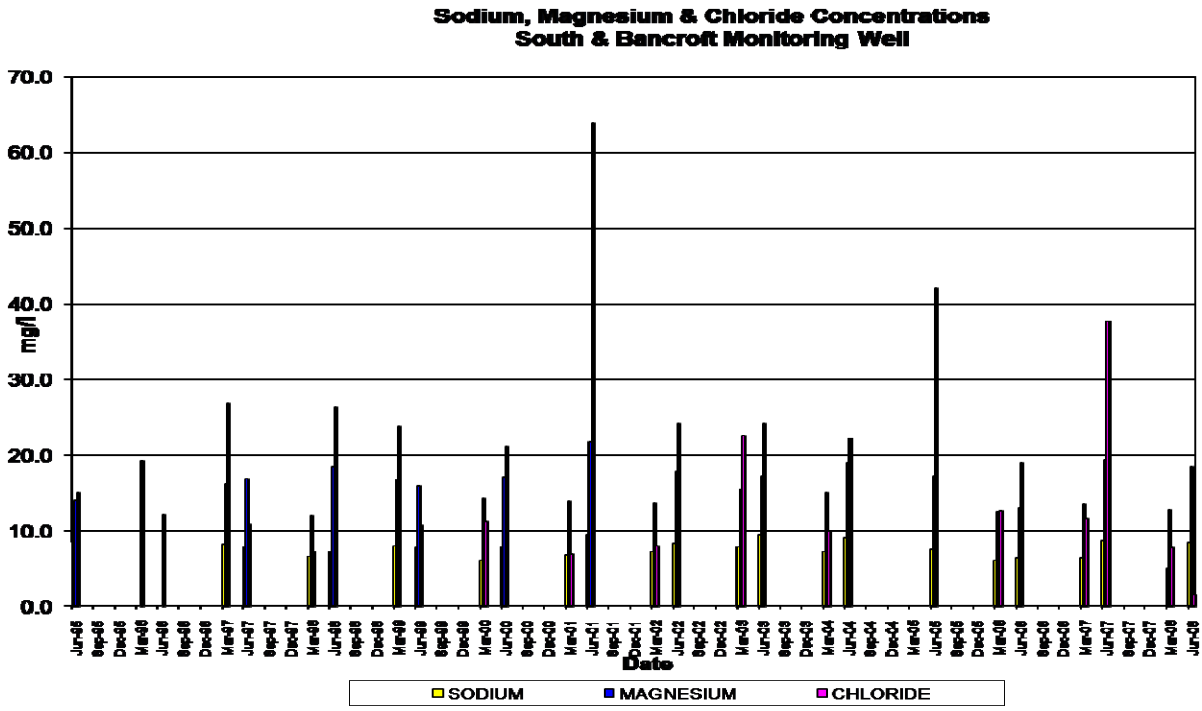

Figure 5.4. Sodium, magnesium and chloride concentrations from 1995 to 2008 plotted against time in shallow groundwater from a Missoula Water Quality District monitoring well located on the southside of the intersection of Bancroft and South Avenue, Missoula. (Jon Harvala, personal communication 2010).

Though the focus of this last discussion was on the negative impact that winter deicer use may or may not have on the shallow groundwater system, it is of interest to examine if indicators of storm water runoff and percolating water quality are observed in the discharge of large municipal water supply wells providing potable water to the city residents. A1997 study conducted by the Missoula Water Quality District reviewed Mountain Water Company well water quality records and concluded that impacts to groundwater quality caused by storm water sources were not detectable. They attributed this observation to the high flow rate in the aquifer and the fact that most supply wells access deeper portions of the aquifer. Cook (2005) sampled selected Mountain Water Company and monitoring wells as part of a valley wide geochemical study. Her data included seasonal water quality results that did not reflect a wide variation in chloride, sodium and magnesium.

IMPLICATIONS TO WATER UTILITIES

Study results and conclusions are of importance to both local municipal water providers and local and state governments, as this work has attempted to provide information regarding the fate of storm water and its constituents as they percolate to underlying aquifers. Source water protection efforts require hydrogeological assessments, including the identification of barriers that will reduce relative vulnerability of aquifers to contamination (Swierc and Woessner, 2006). Thus, quantifying the effectiveness of thick, coarse grained vadose zones to mitigate storm water quality, water that eventually becomes groundwater recharge, is of value to water managers.

The results of this work suggest that storm water quality in an urban intermountain valley area (>60,000 population) generated during May through October is commonly characterized by low concentrations of major ions and minor constituents. This general observation is like somewhat biased by the choice and location of the study sites. In contrast, winter runoff (November through April) was commonly found to contain significantly higher values of major and minor constituents, with the chemistry dominated by the composition of street de-icers used during this period. Thus, in regions with similar climatic conditions, winter road treatments will clearly impact infiltrating water quality. Additional human activities associated with particular categories of land and street use, especially high traffic areas and industrial/commercial land use areas, are also likely to negatively impact runoff water quality (Wogsland, 1988).

It is well known by both the city street departments and water purveyors utilizing unconfined sand and gravel aquifers, that infiltration rates are high in geologic settings with coarse grained sediments exposed at the surface. Storm drains operating in these settings act as conduits to the vadose zone and are usually quite effective in handling storm water. It is logical that in these settings both infiltration and percolation are rapid, conditions found in this work. Because of high downward migration rates of water and the presence of only isolated deposits of fine grained sediments, it would be anticipated that the capacity of the vadose zone to reduce major chemical components found in infiltrating water would be limited. Our work and the work of others suggest that trace quantities of metals and organic compounds are likely to be partially removed during infiltration and percolation. However, both field sample results, pervious work, and geochemical sediment characterization suggest the vadose zone can both act as a source of dissolved ions, or at least provide temporary storage. The occurrence of elevated chloride in annual June samples of groundwater from a well located adjacent to a sump receiving runoff from a four lane intersection suggests de-icer related impacts to underlying groundwater may continue beyond the winter period.

Based on the results of this work, simulations of the movement of water through the vadose zone reveal transport times are rapid. In settings with a 50 ft vadose zone, the first arrival of storm water observed after controlled tracer tests was as soon as 1 hr. The average percolation rates observed as part of this work varied from a few hours to 5 or 6 hours (transport to depths of from 32 to 58 ft). Modeling results suggest that the presence of even thin layers of lower permeable material (lenses of fine grained sediment) act to slow percolation to the water table and to lengthen the time it takes to reach the water table.

The findings of this work were hardly surprising; they suggest that street and land uses impact the quality of infiltrating water, and this water will deliver some of those constituents to the underlying aquifer. In settings with very coarse gained vadose zones, like the system studied in the Missoula valley, water transport from the sump to the water table takes a matter of a few hours. This realization suggests that a rapid response to releases of either impacted storm water or a spill of chemicals will be mostly ineffective once the liquid has entered the storm drain. Water quality impacts to the underlying groundwater will be immediate, assuming the mineralogy of the vadose zone sediments have little to no treatment capacity as seen in this work. Source Water Protection Plans need to include rapid response to on-the-street spills as constituents will enter street sumps and quickly move to the water table. Similar rapid response plans should be investigated and possibly implemented in many basins in the Northern Rocky Mountains, as fluvially deposited sediments found there are often similar to those of the Missoula valley. Those basins dominated by alluvial fan coarse grain sediment may provide more capacity to impact percolating recharge, as the depositional environments may have more

fine grained deposits and reactive sediments that were preserved over wider areas. Still, the available management options to protect receiving groundwater quality are limited by the rapid percolation in course-grained vadose zones. As a result, Source Water Protection Planning, including spill response planning, is increasingly important for public water supply sources overlain by coarse grained vadose zones. The spill response planning must identify methods to shut off pumping from supply wells as soon as possible after a spill occurs. This requires identification of responsible management personnel, and providing steps for shutting down well pumps and isolating any contaminated water that may have entered the system.

It does need to be noted that this study never observed direct water quality impacts to the Missoula Aquifer quality that were related to storm water infiltration. This is most likely a result of the sampling times used, as well as the fact that relatively small volumes of water were being added to the highly prolific aquifer. As a result, measureable changes in groundwater quality were not detected. That was not the case, however, in the research of Wogsland (1988), nor is it reflected in the results of long term sampling of a well located near a sump at a busy four lane intersection (Figure 5.4). This is evidence that de-icer compounds are at least temporarily stored in the vadose zone once they enter it. Lab experiments suggest some sorption to vadose zone sediments of Mg, Na, Cl, and metals may occur, but the presence of elevated Cl in spring shallow groundwater samples suggests that non de-icer impacted storm water facilitates downward transport of contaminants as it enters the sump. Thus, it is likely that virtually all of the de-icer compounds used on Missoula streets eventually reach the underlying groundwater system. This would suggest during the last three years, over 770,000 gallons of MgCl de-icer and 900 tons of NaCl, added to street sand or applied directly, have entered the aquifer. It is recognized that other compounds are also present in the runoff and have the potential to reach the underlying aquifer.

Managers of potable unconfined aquifers receiving recharge through coarse grained vadose zones need to consider approaches that would limit the volumes and concentrations of storm water constituents that enter the aquifer. In addition, the nature of practical vadose zone barriers available to protect aquifer quality need to be assessed. It is recommended that this be accomplished using a range of approaches including:

1. The monitoring of street deicers use, including the variations in liquid deicer and salt compositions, locations and volumes of applications, and identification of which municipal wells are most likely to be impacted.
2. The evaluation of advantages and disadvantages of using multiple chambered storm drain systems to reduce storm water impacts and/or the impacts from spills to underlying groundwater systems.
3. The further analysis of the spatial distribution of vadose zone properties, including mapping of vadose zone character, seasonal thicknesses, dominant geologic material, presence and nature of fine grained deposits, and overall treatment capacity.
4. Monitoring of sump stage and conductivity, and shallow groundwater stage and quality at selected storm drain sites to further characterize timing and seasonal variations in water quality.

LIMITATIONS OF THE INVESTIGATION

The research design assumed that some of the proposed instrumentation may not function as conceptualized in the complex and challenging field conditions of Missoula valley. The characterization of factors controlling storm water movement to the water table and the resulting recharge geochemistry required application of standard approaches, as well as innovative and creative methods. In addition to meeting overall project goals, limitations of the executed research approach and analyses are presented in an effort to guide future research efforts. The following is a list of study limitations with a brief explanation of their perceived effect on this report:

1. Winter groundwater data were insufficient. Once this oversight was recognized a supplemental data collection effort was initiated beginning in January of 2010, with a focus on winter storm water and resulting groundwater quality.

2. Water quality of percolating water was not sampled at varying depths and times to further support the development of a more detailed conceptual model of the key geochemical processes impacting recharge water quality. It was anticipated that lysimeters installed at sites would not provide needed percolating water samples. Nevertheless, lysimeters were installed because no alternative sample collection method was available.
3. Direct observations of wetting fronts using borehole tomography techniques only characterized two infiltration and percolation conditions. The experiments were schedule for spring wet conditions, and summer dry conditions. Unfortunately, it rained immediately prior to the experiment planned for the summer dry period, when the greatest difference between residual and saturated moisture content was expected to provide the best resolution for the method. If the method had been sensitive enough, it would have been helpful to generate additional field data sets for different infiltration rates that could be used to further support and calibrate generic models of the vadose zone transport process.

4. The timing of percolating water reaching the water table at each site was not determined until later in the study. It would have been more appropriate to conduct artificial infiltration tracer tests to establish maximum percolation rates in the early stages of the work. This would have allowed more targeted groundwater sampling (e.g. the impact of the percolating water on groundwater quality).

5. Additional model calibration with field physical and geochemical data sets, coupled with the development of additional transport scenarios, would strengthen transferability of research results. The modeling results are more generic, and not as extensive as planned.

CONCLUSIONS

Based on the results of this work and analysis extensive data sets the following is concluded:

1. Coarse grained vadose zones act to rapidly infiltrate storm water into the underlying vadose zone and aquifer;
2. Vadose zone stratigraphy containing finer gained lenses of sediment act to slow and spread percolating water;
3. Coarse grained vadose zones typical of deposition by large rivers have limited components likely to affect percolating water quality;
4. Percolation rates are rapid, from 1 hr to over 8 h through portion of the vadose zone 32 to 58 ft thick;
5. Storm water quality varies seasonally in climates where winter de-icers are used;
6. Summer period (May through October) storm runoff is generally low in dissolved constituents;
7. Winter through Spring street runoff includes constituents associated with de-icer use;
8. Vadose zone sediment composition and surface chemistry act to both sorb some storm water constituents and react with and transport other constituents.
9. Land use, street conditions and vadose properties control final groundwater recharge quality;
10. Groundwater management in settings using storm water sumps requires vigilance in managing storm water quality.

REFERENCES

Ainsworth, C.C., F.J. Brockmand and P.M. Jardine, 2000. Biogeochemical Considerations and Complexities. Chapter 6, pp. 829-947 *in* Vadose Zone, Science and Technology Solutions, edited by B.B. Looney and R.W. Falta, Battelle Press, Columbus, Ohio. 1540 pages in 2 volumes.

American Society for Testing and Materials, 2007. Standard Practice for Particle-Size Analysis and Determination of Soil Constants.

Aquirre, C.G., and K. Haghighi, 2003. Stochastic modeling of transient contaminant transport. Journal of Hydrology, Vol. 276, Issue 1-4, pp. 14-35.

Asaf, L., Nativ, R., Shain, D., Hassan, M., and S. Geyer, 2004. Controls on the Chemical and Isotopic Compositions of Urban Stormwater in a Semiarid Zone. Journal of Hydrology, No. 294, pp. 270-293.

Barrow, J.C., 1994. The resonant sonic drilling method: an innovative technology for environmental restoration programs. Ground Water Monitoring Review, p. 153-160.

Basha, H.A., 1999. Multidimensional linearized nonsteady infiltration with prescribed boundary conditions at the soil surface. Water Resources Research, vol. 35, no. 1, pp. 75-83.

Bauters, T.W.J., Darnault, C.J.G., Steenhuis, T.S., and J.Y. Parlange, 1999. Lateral expansion of preferential flow paths in sands. Water Resources Research, vol. 35, no. 2, pp. 427-434.

Binley, A., Winship, P., Middleton, R., Pokar, M. and J. West, 2001. High-resolution characterization of vadose zone dynamics using cross-borehole radar. Water Resources Research, vol. 37, pp. 2639-2652.

Binley, A., G. Cassiani, R. Middleton, and P. Winship, 2002. Vadose zone flow model parameterization using cross-borehole radar and resistivity imaging. Journal of Hydrology, Vol. 267, pp. 147-159.

Binley, A., Cassiani, G., Middleton, R., and P. Winship, 2002a. Vadose zone model parameterisation using cross-borehole radar and resistivity imaging. Journal of Hydrology, vol., 267, pp. 147-159.

Binley, A., Cassiani, G., and P. Winship, 2002b. Characterization of heterogeneity in unsaturated sandstone using borehole logs cross-borehole tomography. In Bridge, J.S. and Hyndman, D.W., editors, *Aquifer Characterization,* pages 129-138. Society for Sedimentary Geology, Tulsa, OK. Special Publication no. 80.

Binley, A., Winship, P., West, L.J., Pokar, M. and R. Middleton, 2002c. Seasonal variation of moisture content in unsaturated sandstone inferred from borehole radar and resistivity data. Journal of Hydrology, vol. 267, pp. 160-172.

Blasch, K.W., Constantz, J., and D.A. Stonestrom, 2007. Thermal Methods for Investigating Ground Water Recharge, US Geological Survey Professional Paper 1703, Appendix 1.

Bodvarsson, G., S. Finsterle, H.H. Liu, C.M. Oldenburg, K. Pruess, E. Sonnenthal, and Y. Wu, 2000. Flow and Transport Modeling of the Vadose Zone. Chapter 5, pp. 591-827 *in* Vadose Zone, Science and Technology Solutions, edited by B.B. Looney and R.W. Falta, Battelle Press, Columbus, Ohio. 1540 pages in 2 volumes.

Borden, R.C., Black, D.C., and K.V. McBlief, 2002. MTBE and Aromatic Hydrocarbons in North Carolina Stormwater Runoff. Environmental Pollution No. 118, pp. 141-152.

Bouwer, H., and R.C. Rice, 1984. Hydraulic properties of stony vadose zones, Ground Water, vol. 22, no. 6, pp. 696-705

Brooks, R.H., and A.T. Corey, 1964. Hydraulic properties of porous media. Hydrology Paper No. 3, Colorado State University, 29 p.

Chan, C.Y., and R.J. Knight, 2001. Laboratory measurements of electromagnetic wave velocity in layered materials. Water Resources Research, vol. 37, no. 4, pp. 1099-1105.

Clark, K.W., 1986. Interactions between the Clark Fork River and Missoula Aquifer, Missoula County, Montana. 157 pp., Unpublished Masters Thesis, Department of Geology, The University of Montana.

Collinson, J.D., 2006. Alluvial Sediments, Chapter 3 in Reading, H.G (editor), Sedimentary Environments: Processes, Facies and Stratigraphy. Blackwell Publishing, Malden, MA

Cook, R., 2005. Differentiating sources of recharge and investigating the fate of arsenic in the shallow groundwater system adjacent to a losing river, western Montana. Unpublished MS thesis, Depart. Of Geology, The University of Montana.

Das, B.M., 1994. Principles of Geotechnical Engineering, 3rd edition. PWS Publishing Company, Boston MA 672 p.

Datry, T., Malard, F., and J. Gilbert, 2004. Dynamics of solutes and dissolved oxygen in shallow urban groundwater below a stormwater infiltration basin. Science of the Total Environment, vol. 329, issues 1-3, pp. 215-229.

Deiana, R., Cassiani, G., Villa, A., Bagliani, A., and V. Bruno, 2008. Calibration of a vadose zone model using water injection monitored by GPR and electrical resistance tomography. Vadose Zone Journal, Vol. 7, pp. 215-226.

DiCarlo, D.A., 2006. Quantitative network model predictions of saturation behind infiltration fronts and comparison with experiments. Water Resources Research, vol. 42, no. 7.

Dingman, S.L., 2002. Physical Hydrology, 2nd Edition. Prentice-Hall, Inc., 646 pp.

Elder, J.F., 1988. Metal Biogeochemistry in Surface-Water Systems: A Review of Principles and Concepts. USGS Circular 1013, 43 pages.

Environmental Protection Agency, 1983. Results of the Nationwide Urban Runoff Program, Volume 1 – Final Report. NTIS PB84-185552.

Environmental Protection Agency, 1986. Quality Criteria for Water. EPA 440/5-86-001

Environmental Protection Agency, 1986a. Test methods for Evaluating Solid Waste Physical/Chemical Methods, SW-846.

Environmental Protection Agency, 1994. Methods for the Determination of Metals in Environmental Samples – Supplement I. EPA/600/R-94/111

Environmental Protection Agency, 1997. State Source Water Assessment Protection Program Final Guidance. EPA 816-R-97-009

Environmental Protection Agency, 1999. Class V Underground Injection Control Study, Volume 3, Storm Water Drainage Wells. EPA/816-R-99-014c

Environmental Protection Agency, 1999a. Understanding variation in Partition Coefficients, K_d, Values. Vol. II: Geochemistry and available K_d.values for selected inorganic contaminants. EPA 402-R-99-004B.

Environmental Protection Agency, 2000. Methods for the Determination of Organic and Inorganic Compounds in Drinking Water, Volume I. EPA 815-R-00-014.

Evans, C.A., 1998. A constrained gravity model of the Central Missoula Valley and shape of the Nine Mile Fault, 69 pp., Unpublished Masters Thesis, Department of Geology, The University of Montana.

Fields, R. W., D.L. Rasmussen, A.R. Tabrum, and R. Nichols, 1985. Cenozoic rocks of intermontane basins of Western Montana and Eastern Idaho: a summary, Cenozoic paleogeography of west central United States, Rocky Mountain Section-S.E.P.M., R.M. Flores and S.S. Kaplan, editors, Denver, Colorado, 9-36.

Fetter, C.W., 1999. Contaminant Hydrogeology, 2nd Edition. Prentice-Hall.

Fetter, C.W., 2004. Applied Hydrogeology, 4th Edition. Prentice-Hall.

Folk, R.L., 1974. Petrology of Sedimentary Rocks. Austin, Hemphill Publishing Company, 170 p.

Foster, S., R. Hirate, D. Gomes, M. D'Elia and M. Paris, 2002. Groundwater Quality Protection – A guide for water utilities, municipal authorities and environment agencies. The World Bank, Washington DC, 116 pages.

Graf, C. 2010. Drywells: on country's novel approach to stormwater management and disposal. Southwest Hydrology. Univ. of Arizona. Vol 9, no. 1:22-23, 34-25.

Gallagher, J.T. and W.E. Price Jr., 1966. Hydrology of the Alluvial Deposits of the Ohio River Valley in Kentucky, USGS Water Supply Paper 1818.

Geldon, A.L. (1979). Hydrogeology and Water Resources of the Missoula Basin. An unpublished Master of Science Thesis, University of Montana, 1979.

Green, W.H., and G.A. Ampt. 1911. Studies on soil physics: 1. Flow of air and water through soils. J. Agric. Sci. 4:1–24.

Gromaire-Mertz, M.C., S. Garnaud, A. Gonzalez and G. Chebbo, 1999. Characteristics of Urban Runoff Pollution in Paris. Water Science and Technology, Vol. 39, No. 2, pp. 1-8.

Haack, E.A., and L. A. Warren, 2003. Biofilm Hydrous Manganese Oxyhydroxides and Metal Dynamics in Acid Rock Drainage. Environmental Science and Technology, Vol. 37, No. 18, pp. 4138-4147.

Hantush, M.S., 1967. Growth and decay of groundwater-mounds in response to uniform percolation, Water Resources Research, vol. 3, no. 1, pp. 227-234.

Harvala, J., 2010. Personal communcation, Missoula Valley Water Quality Protection District

Hatch, C.E., Fisher, A.T., Revenaugh, J.S., Constantz, J. and Ruehl, C., 2006. Quantifying surface water-groundwater interactions using time series analysis of streambed thermal records: Method development. Water Resources Research, 42(10).

Healy, R.W., and A.D. Ronan, 1996. Documentation of computer program VS2DH for simulation of energy transport in variably saturated porous media – Modification of the US Geological Survey's computer program VS2DT, US Geological Survey Water Resource Investigations Report 96-4230.

Healy, R.W., 2008. Simulating water, solute, and heat transport in the subsurface with the VS2DI Software package. Vadose Zone Journal, Vol., 7, pp. 632-639.

Hillel, D., 1998. *Environmental Soil Physics*, 2nd Edition. Academic Press, San Diega, California, 771 p.

Horowitz, A.J., and K.A. Elrick, 1987. The relation of stream sediment surface area, grain size and composition to trace element chemistry. Applied Geochemistry, Vol. 2, pp. 437-451.

Hutchins, S.R., M.S. Davidson, J.A. Brierley, and C.L. Brierley, 1986. Microorganisms in reclamation of metals. Annual Review of Microbiology, Vol. 40, pp. 311-336.

Ippisch, O., Vogel, H.J., and P. Bastian, 2006. Validity limits for the van Genuchten-Mualem model and implications for parameter estimation and numerical simulation. Advances in Water Resources, Vol. 29, pp. 1780-1789.

Jensen, J.R., and C.M. Eckart, 1989. The Spokane Aquifer. Bulletin – Washington Department of Natural Resources, Division of Geology and Earth Resources, Vol. 78, pp. 975-982.

Johnson, J.S., L.A. Baker, and P. Fox, 1999. Geochemical transformations during artificial groundwater recharge: soil-water interactions of inorganic constituents. Water Resources, Vol. 33, No. 1, pp. 196-206.

Johnson, A.N, Boer, B.R., Woessner, W.W., Stanford, J.A., Poole, G.C., Thomas, S.A., and S.J. O'Daniel, 2006. Evaluation of an inexpensive, small-diameter temperature logger for documenting ground water – river interactions. Ground Water Monitoring and Remediation, Vol. 25, No. 4, pp. 68-74.

Kendy , E. and R.E. Tresch, 1996. Geographic, Geologic and Hydrologic Summaries of Intermontane Basins of the Northern Rocky Mountains, Montana. U.S. Geological Survey Water-Resources Investigations Report 96-4025, 233 pp.

Konigsberger, E., Konigsberger, L.C., and H. Gamsjager, 1999. Low-temperature thermodynamic model for the system Na2CO3-MgCO3-CaCO3-H2O. Geochimica et Cosmochimica Acta, Vol. 63, No. 19/20, pp. 3105-3119.

LaFave, J.I., 2002. Tracing Ground-Water Flow in the Missoula Valley Aquifer, Southwest Montana. Montana Bureau of Mines and Geology Ground Water Assessment Open-File Report 17.

Land & Water Consulting, 2005 *Final Draft* Source Water Delineation and Assessment Report, Mountain Water Company. Unpublished Report, Missoula MT.

Linsley, R.K., Franzini, J.G., Freyberg, D.L., and G. Tchobanoglous, 1992. Water Resources Engineering. Irwin/McGraw-Hill

Lin, Z., and R.W. Puls, 2003. Potential indicators for the assessment of arsenic natural attenuation in the subsurface. Advances in Environmental Research, Vol. 7, pp. 825-834.

Marinoschi, G., 2008. The diffusive form of Richards' equation with hysteresis. Nonlinear Analysis: Real World Applications, vol. 9, no. 2, pp. 518-535

McMurtrey, R.G., R.L. Konizeski, and A. K. Brietcrietz, 1965. Geology and groundwater resources of the Missoula Basin, Montana. Montana Bureau Mines and Geology, Bulletin 47, 35 pp.

Menziani, M., Pugnaghi, S., and S. Vincenzi, 2007. Analytical solutions of the linearized Richards equation for discrete arbitrary initial and boundary conditions. Journal o fHydrology, vol. 332, pp. 214-225.

Miller, Ross. 1991. A Numerical Flow Model of the Missoula Aquifer: Interpretation of Aquifer Properties and River Interaction. Unpublished MS thesis Department of Geology, The University of Montana.

Millington, R.J., and J.P. Quirk, 1961. Permeability of porous solids. Transactions of the Faraday Society, Vol. 57, pp. 1200-1207.

Missoula City-County Health Department, 1997. Storm and ground water quality impacts of chemical deicer usages in Missoula, Montana. Environmental Health Division of MCCHD, http://www.co.missoula.mt.us/wq/FAQ/Reports/reports.htm

Moore, D.M. and R.C. Reynolds Jr., 1997. X-Ray Diffraction and the Identification and Analysis of Clay Minerals. 2nd Edition, Oxford, New York, 378 p.

Morrow, N., 2002. Characterization of the Lithostratigraphic Factors Controlling Petroleum Hydrocarbon Migration in a Portion of the Missoula Valley Aquifer, Missoula, Montana. Unpublished MS Thesis, University of Montana. 242 pp.

Mountain Water Company, 2006. Consumer Confidence – Water Quality Report for 2006, obtained at http://mtnwater.com/WaterQualityReports/2006CCR.pdf

Mualem, Y., 1976. A new model for predicting the hydraulic conductivity of unsaturated porous media. Water Resources Research, vol. 12, pp. 513-522

NOAA, 2008. Climate data for Missoula, Montana. obtained at http://www.wrh.noaa.gov/mso/climfacts.php

Nimmer, M., Thompson, A., and D. Misra, 2009. Water table mounding beneath stormwater infiltration basins. Environmental and Engineering Geoscience, vol. 15, no. 2, pp. 67-79.

Or., D., 2008. Scaling of capillary, gravity and viscous forces affecting flow morphology in unsaturated porous media. Advances in Water Resources, Vol. 31, pp. 1129-1136.

Parlange, J.Y., Barry, D.A., Parlange, M.G., Hogarth, W.L., Haverkanp, R., Ross, P.J., Ling, L., and T.S. Steenhuis, 1997. New approximate analytical technique to solve Richards' Equation for arbitrary surface boundary conditions. Water Resources Research, vol. 33, no. 4, pp. 903-906.

Patel, S. , 2006. The hydrogeology of the northeastern Missoula Valley, western Montana. Unpublished MS thesis, Depart. Of Geology, The University of Montana.

Peretti, W.R., M.D. Knoll, W.P. Clement, and W. Barrash, 1999, 3-D GPR imaging of complex fluvial stratigraphy at the Boise Hydrogeophysical Research Site: Proceedings of SAGEEP99, The Symposium on the Application of Geophysics to Engineering and Environmental Problems, March 14-18, 1999, Oakland, CA, p. 555-564.

Perrine, A.N., 1998. An investigation of potential ground and surface water contamination from stormwater discharge, City of Missoula, MT; Part I, Accumulation of arsenic and metals in storm-water injection well sediments. Unpublished Missoula Valley Water Quality District document, http://www.co.missoula.mt.us/wq/FAQ/Reports/reports.htm

Pitt, R., S. Clark, K. Parmer and R. Field, 1996. Groundwater Contamination from Stormwater Infiltration. Ann Arbor Press Inc., 219 pp.

Qafoku, N.P., C.C. Ainsworth, J. E. Szecsody and O.S. Qafoku, 2004. Transport-controlled kinetics of dissolution and precipitation in the sediments under alkaline and saline conditions. Geochemica et Cosmochimica Acta, Vol. 68, No. 14, pp. 2981-2995.

Richards, A.L., 1931. Capillary conduction of liquids through porous media. Physics, Vol. 1, pp. 313-333.

Ross, P.J., 1990. Efficient numerical methods for infiltration using Richards' equation, Water Resources Research, vol. 26, no. 2, pp. 279-290.

Ruprecht, J.K., and N.J. Schofield, 1989. Seasonal soil water dynamics in the jarrah forest, Western Australia. I: Results from a hillslope transect with coarse-textured soil profiles. Hydrological Processes, Vol. 4, No. 3, pp. 241-258.

Schaap, M.G., and M.Th. van Genuchten, 2005. A modified Mualem-van Genuchten formulation for improved description of the hydraulic conductivity near saturation. Vadose Zone Journal, Vol. 5, pp. 27-34.

Schaap, M.G., and F.J. Leij, 2000. Improved prediction of unsaturated hydraulic conductivity with the Mualem-van Genuchten Model. Soil Science Society of America Journal, Vol. 64, pp. 843-851.

Simunek, J., N.J. Jarvis, M.Th. van Genuchten, and A. Gardenas, 2003. Review and comparison of models for describing non-equilibrium and preferential flow and transport in the vadose zone. Journal of Hydrology, Vol. 272, Issue 1-4, pp. 14-35.

Smith, K.A., and C.E. Mullins, 2001. Soil and environmental analysis, physical methods, 2nd edition. Marcel Dekker, Inc.

Smullen, J.T., Shallcross, A.L., and K.A. Cave, 1999. Updating the US Nationwide Urban Runoff Quality Data Base. Water Science and Technology, Vol. 39, pp 9-16.

Sperazza, M., Moore, J.N., and M.S. Hendrix, 2004. High-resolution particle size analysis of naturally occurring very fine-grained sediment through laser diffractometry. Journal of Sedimentary Research, Vol. 74, No. 5, pp. 736-743.

Spieker, A.M., 1968. Ground-Water Hydrology and Geology of the Lower Great Miami River Valley, Ohio, USGS Professional Paper 605-A.

Stipp, S.L.S., 1999. Toward a conceptual model of the calcite surface: Hydration, hydrolysis and surface potential. Geochimica et Cosmochimica Acta, Vol. 63, No. 19/20, pp. 3121-3131.

Sumner, D.M., and L.A. Bradner, 1996. Hydraulic characteristics and nutrient transport and transformation beneath a rapid infiltration basin, Reedy Creek Improvement District, Orange County, Florida. US Geological Survey Water Resource Investigations Report 95-4281.

Stringer, C.A.,1992. A hydrogeological investigation of the former Burlington Northern fueling site, Missoula, Montana, 185 pp., Unpublished Masters Thesis, Department of Geology, The University of Montana.

Swierc, J.E., and W.W. Woessner, 2006. Vadose zone assessment; background data compilation program, Missoula Valley environmental sites, preliminary vulnerability assessment. Unpublished report for Mountain Water Company, Missoula, Montana.

Taebi, A., and R.L. Droste, 2004. Pollution Loads in Urban Runoff and Sanitary Wastewater. Science of the Total Environment, No. 327, pp. 175-184

Tallman, A. 2005. Identifying the factors controlling the sources and quantity of water captured by municipal supply wells in 5the hyightly conductive Missoula aquifer. Unpublished MS Thesis, Department of Geology, The University of Montana.

Tindall, J. A., and J.R. Kunkel, 1999. Unsaturated Zone Hydrology for Scientists and Engineers. Prentice Hall, Inc., 624 pp.

Tocci, M.D., Kelley, C.T., and C.T. Miller, 1997. Accurate and economical solution of the pressure-head form of Richards' equation by the method of lines. Advances in Water Resources, Vol. 20, no. 1, pp. 1-14.

Tokunaga, T.K., Wan, J., and K.R. Olson, 2002. Saturation-matric potential relations in gravel. Water Resources Research, Vol, 38, no. 10.

Tokunaga, T.K., Olson, K.R., and J. Wan, 2004. Conditions necessary for capillary hysteresis in porous media. Water Resources Research, Vol, 40, no. 5

Tokunaga, T.K., Olson, K.R., and J. Wan, 2005. Infiltration flux distributions in unsaturated rock deposits and their potential implications for fractured rock formations. Geophysical Research Letters, Vol, 32, no. 5, pp. 1-4.

Topp, G.C., Davis, J.L., and A.P. Annan, 1980. Electromagnetic determination of soil water content: Measurements in coaxial transmission lines. Water Resource Research, vol. 16, no. 3, pp. 574-582.

Tracy, F.T., 2007. Three-dimensional analytical solutions of Richards' equation for a box-shaped soil sample with piecewise-constant head boundary conditions on the top. Journal of Hydrology, vol. 336, no. 3-4, pp. 391-400.

Tucker, M.E., 1981 Sedimentary Petrology, Blackwell Publishing, Oxford, 262 p.

Vanderzalm, J.L., T. Schiller, S. Burn and P. Dillon, 2004. Impact of stormwater recharge on drinking water supply for Mount Gambier. Proceedings of the International. Conference on Water Sensitive Urban Design, Adelaide, Australia, November 2004.

Van Genuchten, M.T., 1980. A closed-form equation for predicting the hydraulic conductivity of unsaturated soils. Soil Science of America Journal, vol. 44, pp. 892-898.

Wang, Z., Tuli, A., and W.A. Jury. 2003. Unstable flow during redistribution in homogenous soil. Vadose Zone Journal, vol. 2, pp. 52-60.

Wentworth, C.K., 1922. A scale of grade and class terms for clastic sediments. The Journal of Geology, Vol. 30, pp. 377-392.

Wilde, F.D. 1994. Geochemistry and Factors Affecting Ground-Water Quality at Three Storm – Water-Management Sites in Maryland, Report of Investigations No. 59. Department of Natural Resources, Maryland Geological Survey. *From summary description and citation in* Pitt et. al. (1996), Groundwater Contamination from Stormwater Infiltration.

Williams, T.H.L., 1980. An automatic electrical resistance soil moisture measuring system. Journal of Hydrology, Vol. 46, No. ¾, pp. 385-390.

Woessner, W. W., 1988. *Missoula Valley Aquifer Study: Hydrogeology of the Eastern Portion of the Missoula Aquifer, Missoula County, Montana.* Prepared for Water Development Bureau, Montana Department of Natural Resources and Conservation, December 1988.

Woessner, W.W., and J.E. Swierc, 2006. Quantifying the capacity of coarse-grained vadose zones to treat Class V injected storm water that recharges aquifers managed for water supply. Unpublished research proposal to AwwaRF and Mountain Water Company

Wogsland, K. L., 1988. The Effect of Urban Storm Water Injection by Class V Wells on the Missoula Aquifer, Missoula, Montana. An unpublished Master of Science Thesis, University of Montana. June 1, 1988.

World Health Organization, 1996. Guidelines for Drinking-Water Quality – Second Edition, Volume 2 – Health Criteria and Other Supporting Information